

AN ABSTRACT OF THE THESIS OF

Scott J. Hein for the degree of Doctor of Philosophy  
in Chemistry presented on August 5, 1988

Title: THE DEVELOPMENT OF A HIGH SPECTRAL-RESOLUTION  
LASER-EXCITED MOLECULAR FLUORESCENCE SYSTEM AND ITS  
APPLICATION TO GAS CHROMATOGRAPHY AND THE DETERMINATION  
OF POLYNUCLEAR AROMATIC HYDROCARBONS

Redacted for Privacy

Abstract approved: \_\_\_\_\_  
E. H. Piepmeier

A high-spectral resolution laser-excited molecular fluorescence system was developed that utilizes a pulsed supersonic expansion to simplify the fluorescence excitation spectra of large, gas-phase aromatic molecules diluted in an excess of a monatomic gas. A microcomputer was used to control and synchronize the instrumental components, which included a Chromatix CMX-4 tunable dye laser, a novel detector/vacuum cell, and a modified automobile fuel injector that was used as the pulsed supersonic nozzle.

The spectra of two closely-related, model polynuclear aromatic hydrocarbons (PNAs), fluorene and 1-methylfluorene, were acquired and exhibited spectral bandwidths (FWHM) of 0.1 nm or less, compared to the bandwidths of 5 to 10 nm that are observed in the static gas phase. These high resolution spectra were acquired despite using only a low-volume rotary mechanical pump to maintain the supersonic expansion. The gas-pulse characteristics of the fuel injector were examined to establish proper operation of the valve. In addition, factors such as the type of diluent gas used, and the axial position that the laser intersects the expansion, were examined in terms of their influence on the observed spectra. Helium was determined to be the best diluent gas for this system since the use of argon resulted in the production of significant PNA-Ar clusters.

The laser-excited fluorescence system was then interfaced to a packed-column gas chromatograph, which provides both a means of quantitative sample introduction, and the additional selectivity required for the analysis of very complex mixtures. A theoretical model was developed to describe the interaction between the GC mass flow, which is continuous, and the mass flow through the supersonic nozzle, which is pulsed in nature. Fluorescence excitation chromatograms were acquired by monitoring the eluate fluorescence signal at a transition wavelength characteristic of one of the model compounds. A calibration curve was constructed for 1-methylfluorene, and was used to calculate a detection limit of 6 ng. In addition, the excellent selectivity provided by the system was demonstrated by acquiring fluorescence-excitation chromatograms of mixtures containing the two model compounds, using different excitation wavelengths.

Finally, the requirements for performing internal standard quantitation with highly selective detectors such as this are discussed. A versatile, programmed-excitation-wavelength scanning method was then developed that allows multiple PNA analytes to be detected in a single chromatographic elution. Relative response factors calculated for fluorene and 1-methylfluorene from replicate chromatograms, were shown to be reproducible, thereby allowing internal standard quantitation to be performed using this detection system.

The Development of a High Spectral-Resolution  
Laser-Excited Molecular Fluorescence System  
and its Application to Gas Chromatography and the  
Determination of Polynuclear Aromatic Hydrocarbons

by

Scott J. Hein

A THESIS

submitted to

Oregon State University

in partial fulfillment of  
the requirements for the  
degree of

Doctor of Philosophy

Completed August 5, 1988

Commencement June, 1989

APPROVED:

Redacted for Privacy

\_\_\_\_\_  
Professor of Chemistry in charge of major

**Redacted for Privacy**

\_\_\_\_\_  
Chairman of Department of Chemistry

Redacted for Privacy

\_\_\_\_\_  
Dean of Graduate School

Date thesis is presented \_\_\_\_\_ 5 August 1988

Typed by Scott J. Hein for \_\_\_\_\_ Scott J. Hein

## Acknowledgments

This thesis is dedicated to my family,  
Linda, Dick, Kris, and Claudia,  
and to my father, Martin Jan Hein.

I would also like to acknowledge the contributions of a variety of individuals and organizations to both my thesis research and to my development as a chemist:

Dr. Carroll Dekock and the Department of Chemistry for providing research and teaching assistantships throughout my six years at OSU.

Dr. Joe Nibler for advice concerning the construction and control of pulsed supersonic nozzles.

Dr. Mike Schuyler for advice regarding computers and computer interfacing and for understanding the importance of IU basketball.

John Archibald and Bob Boyer of the chemistry department machine shop for their expertise in the construction of a number of important instrumental components.

Dr. Doug Keszler and Dr. Jim White for providing the X-ray crystallography research assistantship, and Dr. John Westall for several consulting opportunities.

Dr. Fred Prahl and Orest Kawka of the Department of Oceanography at OSU for the generous contribution of real PNA samples from their own research.

The Bailey Foundation and N.L. Tarter Foundation for research fellowships, and the National Institutes of Health and the OSU Research Council for an important grant that allowed me to purchase crucial equipment.

The important contributions of my graduate research advisors, Dr. Larry Thomas and Dr. Edward Piepmeier, should be emphasized. I would also like to acknowledge the influence of Dr. Ron Hites, my undergraduate research advisor at Indiana University. The experiences I had in his laboratory led to my interest in environmental analytical chemistry and prepared me well for graduate school.

Finally, I would like to thank the other graduate students in the chemistry department who helped to make the road a little easier. In particular, Joe McGuire, Jay Shields, and Gerald Dodo should be thanked for being great friends throughout my graduate career.

## TABLE OF CONTENTS

I.	Introduction . . . . .	1
A.	Polynuclear Aromatic Hydrocarbons . . . . .	9
1.	Molecular Structure . . . . .	10
2.	Biological Activity . . . . .	12
3.	Sources and Distribution . . . . .	14
4.	Spectroscopic Properties . . . . .	17
a.	Liquid-Solution Phase Spectra . . . . .	25
b.	Gas-Phase Spectra . . . . .	28
B.	Supersonic Expansions . . . . .	32
1.	Theoretical Description of a Supersonic Expansion . . . . .	36
2.	Nozzles . . . . .	41
a.	Continuous-Flow Nozzles . . . . .	42
b.	Pulsed-Flow Nozzles . . . . .	43
C.	Chromatographic Interfacng Considerations . . . . .	46
1.	Carrier / Diluent Gas . . . . .	46
2.	Nozzle Interface . . . . .	47
D.	Applications of Supersonic Expansions to the Fluorescence Determination of PNAs . . . . .	48
1.	Survey of Published Spectra . . . . .	50
2.	Survey of Analytical Applications . . . . .	52
II.	Instrumentation . . . . .	56
A.	Laser System . . . . .	56
1.	Chromatix CMX-4 Dye Laser . . . . .	56
a.	Triggering Requirements . . . . .	59

b.	Laser Wavelength Selection . . . . .	59
c.	Ultraviolet Wavelength Generation . . . . .	60
d.	Wavelength Calibration of . . . . . the CMX-4 Laser	62
(1)	Etalon and Birefringent Filter . . . . .	62
(2)	UV Doubling Crystal . . . . .	65
2.	Stepper Motor Control of the CMX-4 Laser . . . . .	65
a.	Birefringent Filter and Etalon . . . . .	66
b.	Ultraviolet Doubling Crystal . . . . .	69
(1)	Stepper Motor and Translator . . . . .	70
(2)	Stepper Motor Gearing . . . . .	73
(3)	Stepper Motor Mount . . . . .	75
(4)	Reading the Stepper . . . . . Motor Position	75
3.	CMX-4 Cooling Water and . . . . . Laser Dye Pumping System	78
4.	Laser Power and Synchronization Photodiodes . . . . .	80
5.	Beam Blocker/Filter Holder . . . . .	81
B.	Optical Table Configuration . . . . .	81
C.	Measurement/Vacuum Cell . . . . .	83
1.	Detection Optics . . . . .	84
2.	Detector . . . . .	89
3.	Heated Nozzle Flange . . . . .	90
4.	Temperature Control System . . . . .	92
a.	Temperature Controllers and Heaters . . . . .	92
b.	Photomultiplier Tube Cooling Coils . . . . .	94
5.	Mounting Bracket . . . . .	94

D.	Vacuum Pumping System . . . . .	95
E.	Supersonic Nozzle . . . . .	97
1.	Driver Circuit . . . . .	100
F.	Sample Introduction System . . . . .	104
1.	Continuous Sample Introduction . . . . .	104
2.	Quantitative Sample Introduction System: Gas Chromatograph . . . . .	107
G.	Computerized Data Acquisition and Control System . . . . .	108
1.	Computer . . . . .	108
2.	Native PC Hardware Used . . . . . for Instrument Control	109
a.	Parallel Port . . . . .	109
b.	8253 Programmable Interval Timer . . . . .	111
3.	Other Data Acquisition and Control Hardware . . . . .	116
a.	MetraByte DASH-8 Data Acquisition . . . . . and Control Board	116
(1)	Analog-to-Digital Converter . . . . .	117
(2)	Digital Input/Output . . . . .	120
(3)	Programmable Interval Timer . . . . .	124
b.	Evans Associates Gated Integrator . . . . .	124
4.	Laser and Detector Timing and . . . . . Synchronization Electronics	125
a.	General Overview: Delays . . . . .	128
b.	Interface Circuitry . . . . .	129
(1)	Stepper Motor Interface . . . . .	131
(2)	Synchronization Interface . . . . .	135
5.	Acquisition and Control Software . . . . .	137
a.	General . . . . .	137



b.	Assembly Language Acquisition . . . . .	138
	and Control Subroutines	
(1)	Data Acquisition Loop . . . . .	141
	(a) DATAQ Acquisition Subroutine .	144
	(b) A2D Acquisition Subroutine . .	145
(2)	Other Important Subroutines . . . . .	146
	(a) DELAY . . . . .	146
	(b) PULSE . . . . .	147
	(c) TRAIN . . . . .	147
c.	High Level BASIC Acquisition and . . . . .	148
	Control Programs	
(1)	Overview: Master Control . . . . .	148
	Program, GPMENU	
(2)	Laser Signal Peaking Utility, PEAK	151
(3)	Laser Wavelength Calibration, CMX4CAL	153
	(a) Polynomial Fit of Birefringent	160
	Filter Data, BIFIT	
	(b) Simplex Optimization of Etalon	164
	Calibration Data, SIMPLEX	
(4)	Calibration of the . . . . .	166
	Doubling Crystal, UVCAL	
(5)	Acquisition of Fluorescence . . . . .	167
	Excitation Spectra, SPECTRUM	
(6)	Acquisition of Fluorescence . . . . .	172
	Excitation Chromatograms, CHROM	
(7)	Plotting and Analysis of Data, REPLOT	176
d.	Commercial Software Packages Used in . .	179
	This Research	
III	Experimental Procedure and Results . . . . .	182
A.	General Experimental Procedure . . . . .	182

1.	Instrument Power-Up Sequence and Signal Optimization . . . . .	182
2.	Model Compounds Studied . . . . .	185
B.	Characterization of the Instrumentation and Analytes . . . . .	186
1.	Preliminary Studies . . . . .	189
2.	Pulsed Valve Characteristics . . . . .	196
3.	Influence of Diluent Gas on Spectra . . . . .	199
4.	Comparison of Fluorene and 1-Methylfluorene Excitation Spectra . . . . .	204
5.	Axial Expansion Characteristics . . . . .	208
6.	Miscellaneous Characterization Experiments . . . . .	213
a.	Influence of Stagnation Pressure on Spectra . . . . .	213
b.	Influence of Vacuum Cell Pressure on Spectra . . . . .	216
C.	Combined High Spectral-Resolution Laser-Excited Fluorescence Spectroscopy and Gas Chromatography . . . . .	216
1.	Description of the GC-Pulsed Nozzle Interface . . . . .	218
a.	Flow Through a Packed GC Column . . . . .	218
b.	Supersonic Nozzle Flow . . . . .	222
c.	Flow Through the GC-Nozzle Interface Volume . . . . .	223
2.	Additional Experimental Details . . . . .	236
a.	General Chromatography Conditions . . . . .	236
b.	Pulsed Valve Dead Volume . . . . .	238
c.	Additional Gas Chromatograph Details . . . . .	239
d.	Preparation and Storage of Standard Solutions . . . . .	239
e.	Chromatographic Experimental Procedure . . . . .	240

3.	Preliminary Discussion of . . . . .	243
	Chromatographic Results	
4.	Detector Figures-of-Merit . . . . .	245
5.	Detector Selectivity . . . . .	249
6.	Programmed-Wavelength Fluorescence . . . . .	256
	Excitation Chromatograms	
IV.	Conclusion . . . . .	262
A.	Suggested Instrumental Improvements . . . . .	264
B.	Suggested Future Studies . . . . .	265
V.	References . . . . .	267
VI	Appendices . . . . .	274
A.	Supersonic Expansion Calculations . . . . .	274
B.	Compiling and Assembling Research Programs and Subroutines	278
C.	Program and Subroutine Listings . . . . .	284

## LIST OF FIGURES

### Chapter I

<u>Figure</u>		<u>Page</u>
I.1	Liquid solution phase absorbance spectra of 5 $\mu\text{g/ml}$ of fluorene and 1-methylfluorene in cyclohexane. Taken on a Cary 118C spectrophotometer with a spectral bandpass of 0.33 nm.	5
I.2	Representative polynuclear aromatic hydrocarbons (PNAs).	11
I.3	Breakdown of the results of testing 355 PNAs for carcinogenic activity. The numbers in parenthesis are the total number of PNAs comprising each group. Data were compiled from reference 31.	13
I.4	Historical record of PNA concentrations from a Pettaquamscutt River sediment core. Recompiled from reference 36.	16
I.5	Molecular energy level diagram illustrating the various radiative and non-radiative pathways by which an excited molecule can return to the ground state.	21
I.6	Schematic diagram of the vibronic transitions leading to band progressions and band sequences.	26
I.7	Schematic diagram of a supersonic expansion.	33
I.8	Theoretical properties of a supersonic expansion as a function of distance from the nozzle. These curves are calculated for a nozzle diameter, $D$ , of 300 $\mu\text{m}$ , a stagnation pressure, $P_0$ of 1.5 atm of helium, and a reservoir temperature, $T_0$ , of 140°C.	37

### Chapter II

II.1	Block diagram of the laser-excited fluorescence-supersonic expansion experimental system.	57
------	---	----

II.2	Diagram of (A) the birefringent filter micrometer and vernier scale, and (B) the etalon dial and turns marker.	68
II.3	Schematic wiring diagram of the stepper motor translator chassis.	71
II.4	Diagram of the gears and gear ratios used in interfacing a stepper motor to the ultraviolet doubling crystal micrometer knob.	74
II.5	Side view of the ultraviolet doubling crystal stepper motor and the micrometer knob pulley and clamp.	76
II.6	UV doubling crystal stepper motor mounting bracket.	77
II.7	Diagram of the ultraviolet doubling crystal micrometer counter and stepper motor dial configured for a position of 482.3 units.	79
II.8	Experimental optical table configuration.	82
II.9	Front view (looking down the expansion axis) of the supersonic jet measurement cell. The supersonic nozzle and front flange are not shown.	85
II.10	Side view (looking down the detection axis) of the supersonic jet measurement cell. The supersonic nozzle, detector arm, and front flange are not shown.	86
II.11	Diagram of the detection optics.	88
II.12	Schematic diagram of the front flange of the measurement cell. The supersonic nozzle screws into the center of the flange which can be heated by a cartridge heater.	91
II.13	Schematic wiring diagram of the temperature controller chassis.	93
II.14	Diagram of the mounting bracket that allows the measurement cell to be firmly attached to the optical table.	96
II.15	Diagram of the modified Bosch fuel injector used as a supersonic nozzle in this research.	98

II.16	Relationship between the supersonic nozzle, excitation axis, and detector components.	99
II.17	Schematic diagram of the pulsed valve driver circuitry. Component values are listed in Table II.6.	101
II.18	Oscilloscope trace of the signal measured at the pulsed valve driver test point for a 2-ms input pulse.	103
II.19	Schematic diagram of the two methods of sample introduction used in this research; (A) continuously via a heated cell and (B) quantitatively via a gas chromatograph.	105
II.20	Diagram of the heater block used to vaporize solid PNA samples for continuous introduction to the supersonic expansion.	106
II.21	Relationship between the bits of the parallel port and the external lines available through the DB25 connector at the rear of the computer.	112
II.22	Schematic diagram of the IBM PC's 8253 programmable interval timer (PIT), and its relationship to the 8255 Programmable Peripheral Interface (PPI).	114
II.23	Schematic diagram of the parts of the DASH-8 data acquisition and control board that are used in this research. The function of the various I/O lines is also identified.	119
II.24	Representation of the way in which the low and high data bytes, which are returned by the analog to digital converter, are correctly combined to form a datum of the correct magnitude.	121
II.25	A diagram of a typical oscilloscope trace illustrating the relationship between the DELAY 4A gate pulse, the gated integrator output, and the analytical signal present at the gated integrator input.	126
II.26	Schematic diagram of the parts of the original synchronization circuitry that are used in the current research.	127

II.27	Calibration plot of the DELAY 2B potentiometer with two different delay capacitors: 0.1 $\mu$ F ( $\Delta$ ) and 0.22 $\mu$ F ( $\circ$ ). Delays were measured by viewing the time difference between the delay 2B trigger pulse and the laser pulse on an oscilloscope.	130
II.28	Schematic circuit diagram of the synchronization interface board.	132
II.29	Diagram of the back panel connections to the synchronization and data acquisition circuitry.	134
II.30	Timing diagram illustrating the relationship between the various synchronization and data acquisition signals.	136
II.31	Flow Chart of the laser synchronization and triggering loop.	142
II.32	Flow Chart of the combined synchronization and data acquisition loop used by most of the control programs in this research.	143
II.33	Flow chart of the master control menu program GPMENU.BAS illustrating the relationship between the various control and acquisition programs. Dotted lines link programs that share common data files.	149
II.34	A printer screen dump of the GPMENU.BAS menu screen.	150
II.35	Graphics screen dump of the program PEAK showing the various menu options and a partially filled bar graph window.	152
II.36	Flow chart of the laser wavelength calibration program CMX4CAL.	154
II.37	Sample wavelength calibration report for a CMX-4 etalon scan of the 5881.895 Å neon transition.	159
II.38	Example of a birefringent filter calibration report generated by the polynomial fitting program, BIFIT. All wavelengths listed are neon transitions.	161

II.39	Calibration plot of the results listed in Figure II.38. The calibration parameters B0, B1, and B2 are used to predict the birefringent filter micrometer position for a desired wavelength.	162
II.40	Example of an etalon calibration report generated by the simplex optimization program, SIMPLEX.	165
II.41	Example of a scan information file (.OUT extension) generated by the program SPECTRUM for a high-resolution fluorescence excitation spectral scan of fluorene.	170
II.42	Graphics screen dump of the SPECTRUM data acquisition screen showing the laser power peaking window viewed when optimizing the laser power prior to a scan.	171
II.43	Graphics screen dumps of the CHROM data acquisition screen showing (A) the ten blocks displayed on the screen prior to the 20 second injection countdown and (B) the one block that remains after 18 seconds, signaling that the injection should be made.	175
II.44	Example of a REPLOT graphics display showing a programmed wavelength fluorescence excitation chromatogram of fluorene and 1-methylfluorene. Peak areas are calculated and listed in the report below the chromatogram.	180

### Chapter III

III.1	Plot of log vapor pressure versus $1/T$ used to obtain the Clausius-Clapeyron A and B parameters for fluorene.	191
III.2	Comparison of the conventional liquid-solution absorbance spectrum of fluorene (top), and the fluorescence excitation spectrum of fluorene in an argon supersonic expansion on the same wavelength scale (middle), and an expanded scale (bottom).	192



III.3	A high-resolution fluorescence excitation spectrum of the 2960-Å fluorene transition in an argon supersonic expansion. The etalon was rotated into the laser cavity and stepped in 0.025-Å increments synchronously with the birefringent filter to produce the spectrum.	195
III.4	Pulse characteristics of the Bosch valve measured by monitoring the 2960-Å fluorene fluorescence signal as a function of Delay 2B, the laser firing delay. Each data point is the average of 30 consecutive laser shots and the error bars represent the 99% confidence interval.	198
III.5	Fluorescence excitation spectra of fluorene in a helium supersonic expansion measured at delays of 0.6 ms and 1.1 ms relative to the pulsed valve trigger pulse.	200
III.6	Comparison of the fluorescence excitation spectra of fluorene produced in argon and helium supersonic expansions.	202
III.7	The fluorescence excitation spectra of (A) fluorene in helium, (B) IMF and residual fluorene immediately after replacing the fluorene in the sample thimble with IMF, (C) IMF and residual fluorene after approximately 24 min. IMF and residual fluorene after approximately (D) 36 min., (E) 48 min, and (F) 60 min.	206
III.8	Fluorescence excitation spectra of IMF in helium (top) with the laser beam focused approximately 1 mm from the nozzle tip at X=0, and (bottom) with the beam focused 1.9 mm downstream from X=0. Spectra produced with the laser focused (top) 3.5 mm downstream from X=0, and (bottom) 6.4 mm downstream from X=0.	210
III.9	Fluorescence excitation spectra of IMF in argon with the laser focused approximately (A) 1 mm, (B) 1.9 mm, and (C) 3.5 mm downstream from the nozzle tip.	214
III.10	Fluorescence excitation spectra of IMF in helium obtained with stagnation pressures of (top) 7 psi and (bottom) 20 psi as read from the second stage of the high-pressure regulator.	215

III.11	Fluorescence excitation spectra of IMF in helium obtained with delays of (A) 0 s, (B) 1 s, and (C) 5 s between each wavelength step. This delay gives the vacuum pump additional time to evacuate the detector cell and thus reduces the cell pressure, $P_v$ .	217
III.12	Diagram of the configuration used when a packed-column gas chromatograph is used for sample introduction.	219
III.13	Diagram of the GC-nozzle flow interface volume. $F_0$ represents the mass flow of the carrier gas through the GC column outlet and into the interface volume, and $F_v$ is the mass flow from the interface volume and through the supersonic nozzle. $T_0$ , $V_0$ , and $P_0$ are the temperature, volume, and pressure of the interface volume, respectively.	224
III.14	Theoretical flow characteristics of the GC-nozzle interface illustrating the change in $P_0$ , the interface pressure (top), and $F_v$ , the average mass flow of helium through the nozzle (bottom), as a function of the time elapsed after starting the valve pulsing. Data for valve pulse widths of (—) 1 ms, (----) 2 ms, (.....) 3 ms, and (-.-.-) 4 ms, at a 5 Hz repetition rate are shown.	229
III.15	Theoretical flow characteristics of the GC-nozzle interface illustrating the change in $u$ , the average linear velocity of the carrier gas in the column (top), and $u_0$ , the velocity of the carrier gas at the column outlet (bottom), as a function of the time elapsed after starting the valve pulsing. Data for valve pulse widths of (—) 1 ms, (----) 2 ms, (.....) 3 ms, and (-.-.-) 4 ms at a 5 Hz repetition rate are shown.	230
III.16	Theoretical flow characteristics of the GC column and interface volume using the true mass flow of He through the nozzle, $F_{noz}$ , with a 2-ms pulse width, and a 5 Hz rep. rate. The A) interface pressure, B) carrier gas velocity at the column outlet, and C) average carrier gas velocity in the column are presented.	233

III.17	Theoretical flow characteristics of the GC column and interface volume using the true mass flow of He through the nozzle, $F_{noz}$ , with a 3-ms pulse width and a 5 Hz rep. rate. The A) interface pressure, B) carrier gas velocity at the column outlet, and C) average carrier gas velocity in the column are presented.	234
III.18	Fluorescence excitation chromatograms produced by 0.4- $\mu$ L injections of 1000 $\mu$ g/mL solutions of fluorene and 1-methylfluorene. The temperature program used was, 100°C to 250°C at 32°C/min.	244
III.19	Representative fluorescence excitation chromatograms used in the preparation of the 1-methylfluorene calibration plot. These chromatograms were produced by injections of 20, 40, 60, 80, 100, and 200 ng IMF, using a temperature program of 100°C/0 min-250°C/16 min @16°C/min.	247
III.20	Calibration plot of 1-methylfluorene. Error bars represent the 99% confidence interval arising from the average of 9 area measurements for each of the masses injected.	248
III.21	Fluorescence excitation chromatograms of a mixture of 200 ng each of fluorene and 1-methylfluorene using two different excitation wavelengths.	250
III.22	Fluorescence excitation chromatograms of 2- $\mu$ L injections of a Columbia River sediment extract at the excitation wavelengths of FL and IMF. The bottom chromatogram includes a co-injection of 40 ng of a IMF standard.	252
III.23	Fluorescence excitation chromatograms resulting from 2- $\mu$ L injections of a hydrothermal oil sample taken from the Guaymas Basin seabed in the Gulf of California.	254
III.24	Fluorescence excitation chromatograms (top and middle) of a mixture of 100 ng each of FL and IMF, and (bottom) the chromatogram of the same mixture produced by a programmed excitation wavelength scan.	259

## LIST OF TABLES

### Chapter I

<u>Table</u>		<u>Page</u>
I.1	Representative concentration of PNAs in both pristine (non-polluted) and polluted samples.	18
I.2	Representative wavelengths, wavenumbers, frequencies and energies of molecular spectroscopic transitions.	20
I.3	Molar absorptivities and fluorescence quantum yields for PNAs in cyclohexane solution.	24
I.4	Comparison of excited state populations as a function of transition energies and sample temperatures.	30
I.5	Comparison of the PNA critical temperatures which produce totally diffuse spectra and a vapor pressure of 1 mm Hg.	31
I.6	Sample supersonic expansion parameters as a function of distance from the nozzle tip.	38
I.7	Detection limits reported for laser-excited fluorescence determinations of PNAs in supersonic expansions.	49
I.8	Survey of high-resolution fluorescence spectra obtained on PNAs in supersonic expansions.	51

### Chapter II

II.1	CMX-4 laser specifications.	58
II.2	CMX-4 wavelength control stepper motor and micrometer characteristics.	67
II.3	D3001 translator: connector C1 terminal identities for the stepper motor driver lines.	72
II.4	D3001 Translator: connector C2 terminal identities for the stepper motor control lines.	72
II.5	Supersonic jet vacuum cell O-ring identification.	87

II.6	List of electronic components used in the construction of the pulsed valve driver.	102
II.7	Summary of the computer and peripherals utilized in this research.	110
II.8	Parallel port 2 bit assignments: control of the CMX-4 wavelength stepper motors.	113
II.9	MetraByte DASH-8 data acquisition and control interface board control and status registers.	118
II.10	Offset binary analog-to-digital conversion results for the DASH-8 ADC.	122
II.11	DASH-8 control and status register assignments and important bit combinations.	123
II.12	Corona PC-synchronization circuitry interface circuit board I/O pin assignments.	133
II.13	Custom data acquisition and control programs used in this research: BASIC programs.	139
II.14	Custom data acquisition and control programs used in this research: assembly language subroutines.	140
II.15	Format of data files required by the calibration program CMX4CAL.	156
II.16	Format of the data file CMX4CAL.DAT.	163
II.17	Format of the default parameters file SPECTRUM.DEF.	169
II.18	Format of the default parameters file CHROM.DEF.	174
II.19	Format of the data files required by CHROM.	177

### Chapter III

III.1	Properties of the model compounds used in this research.	187
III.2	Vapor pressure of fluorene at several temperatures for calculation of the A and B constants of the Clausius-Clapeyron equation.	190

III.3	Vapor pressure of fluorene calculated at several different temperatures using the Clausius-Clapeyron equation.	190
III.4	Typical experimental conditions for the acquisition of high-resolution fluorescence excitation spectra of fluorene and 1-methylfluorene.	194
III.5	2947 Å 1-methylfluorene fluorescence as a function of the axial distance of the laser beam from the nozzle tip.	212
III.6	Experimental GC and pulsed valve parameters used in the GC-nozzle interface calculations.	227
III.7	Theoretical flow characteristics of the GC-supersonic nozzle flow interface.	231
III.8	Theoretical flow characteristics of the GC-nozzle interface: oscillations of $P_0$ , $u_0$ , and $\bar{u}$ during nozzle pulses.	235
III.9	Representative experimental conditions used in the acquisition of chromatographic data.	237
III.10	Quantitative analysis of Guyamas Basin hydrothermal oil sample.	255
III.11	Response factor data from programmed-wavelength fluorescence excitation chromatograms of a mixture of fluorene and 1-methylfluorene.	260

The Development of a High Spectral-Resolution  
Laser-Excited Molecular Fluorescence System  
and its Application to Gas Chromatography and the  
Determination of Polynuclear Aromatic Hydrocarbons

I. Introduction

Over the past three decades, since its development in the early 1960's, the laser has evolved into one of the more powerful tools available to the spectroscopist. Examples of techniques which were not possible before the development of the laser include coherent anti-stokes Raman spectroscopy [1], laser-enhanced ionization spectroscopy [2] and intracavity-enhanced absorption spectroscopy [3]. In addition to providing the means to effect the phenomena which are observed by these powerful new techniques, lasers can also be used to enhance such conventional methods as atomic and molecular fluorescence spectroscopy. Fluorescence spectroscopy, in particular, benefits both from the added selectivity provided by the narrow bandwidth of the laser, and the added sensitivity supplied by the high irradiance. The potential of lasers to benefit chemical analysis was recognized very early with their application to micro analysis using the laser microprobe [4,5]. Following this early application, the use of lasers in analytical chemistry has expanded greatly as detailed in several excellent compendia [3,6,7].

Lasers, however, are certainly not without their drawbacks. They are often expensive to procure, expensive to maintain, and frequently temperamental. Developing new applications using laser optical sources inevitably adds extra complexity to the system. In many situations, nonetheless, the benefits of lasers far outweigh the added complexity and cost. In the future, as more reliable and inexpensive tunable lasers are developed [8], their use in routine analyses will become more prevalent and laser-based techniques that

were previously thought too complicated to be used routinely may become commonplace.

One area that could benefit from the added sensitivity and spectral selectivity furnished by the laser is the analysis of very complex mixtures such as those found in environmental and industrial samples. These mixtures frequently contain hundreds of components and consequently often demand time-consuming pretreatment and preseparation prior to analysis by high resolution gas or liquid chromatography, often combined with mass spectrometry (GC-MS or LC-MS). For mixtures that can be completely resolved by chromatography, mass spectrometry provides a sensitive method of determination and is widely recognized as the current method of choice for environmental analyses of complex samples [9]. Unfortunately, even with optimized chromatography systems, it is not unusual to observe coeluting isomers that can not be distinguished by their conventional mass spectra. Even worse, when analyzing samples originating from exceedingly complex environmental matrices such as ocean and lake sediment, or animal tissue, insufficient chromatographic resolution can prevent separation of all eluates and an unresolved complex mixture (UCM) may be observed. This mixture consists of hundreds of components and appears as a broad hump in the chromatogram, usually occurring toward the end of the temperature program in gas chromatography. Except under unusual circumstances, it is impossible via conventional mass spectrometry to identify unambiguously the components of this mixture since the mass spectrum will consist of ions originating from many concurrently eluting species.

Consequently, although GC- and LC-MS are excellent methods for the routine analysis of complex mixtures, there are situations where the chromatographic separation requires additional selectivity. This is particularly true in analyses for trace environmental contaminants which are of concern due to their highly toxic or carcinogenic nature: polynuclear aromatic hydrocarbons (PNAs), also known as polycyclic aromatic hydrocarbons (PAHs), for example. These multi-ring aromatic compounds will be discussed in more detail in



later sections, but suffice it to say that they are primarily products of the combustion of fossil fuel, and consequently are widely distributed in the environment [10,11]. In addition, some PNAs exhibit potent, structure-specific carcinogenic activity. This dependence of harmful biological activity on molecular structure means that closely related PNA isomers, which may be difficult to separate via chromatography, can show widely varying biological activity. Furthermore, since the conventional mass spectra of such isomers may be indistinguishable, other methods of analysis may be required to unambiguously determine each analyte.

Such a method must satisfy several requirements. First, it must be sensitive enough to detect PNAs at the sub-nanogram levels frequently found in environmental samples. Next, it must be selective for PNAs, preferably not responding to concomitants present in the sample and not subject to interferences caused by the concomitants. In addition, this selectivity should extend to individual PNAs; the method must be able to distinguish closely related PNA isomers. Finally, the instrumentation should be amenable to interfacing with various types of chromatographic systems, although this would not be necessary if the selectivity of the measurement method were great enough.

Molecular absorbance and, in particular, fluorescence spectroscopy in the ultraviolet (UV) wavelength range are methods that satisfy some of these requirements. Due to the high molar absorptivity and often large fluorescence quantum efficiency of PNAs, these methods are often very sensitive. In addition, their application to both gas chromatography [12-15] and liquid chromatography [16,17] has been demonstrated. Finally, these methods provide two levels of selectivity for PNAs. Intermediate selectivity is obtained through absorbance spectroscopy since, in general, significant UV absorption (near UV,  $> 220$  nm) is limited to those compounds which have delocalized  $\pi$  or  $n$  electrons which can be easily excited to a  $\pi^*$  anti-bonding orbital. Thus, significant absorbance in the UV is associated with unsaturated compounds, including the PNAs, which exhibit various degrees of conjugated multiple bonding.

High selectivity can be obtained via fluorescence spectroscopy since significant molecular fluorescence upon UV excitation, particularly in the gas-phase, is practically limited to multi-ring aromatic compounds.

Unfortunately, the conventional liquid-solution and gas phase fluorescence and absorbance spectra of PNAs tend to be fairly broad with little structure as illustrated by the spectra in Figure I.1. This figure also illustrates the similarity of the spectra arising from closely related PNAs, in this case fluorene and 1-methylfluorene. The liquid-solution absorbance spectra of these two species appear almost identical, which means that if they were present together in a mixture it would be difficult to determine them individually. Fortunately, the bandwidth of these spectra can be greatly reduced from the 10 nm or more widths observed in gas and liquid-solution phase fluorescence spectroscopy to bandwidths of a few angstroms or less by using one of the various "Cryogenic" fluorescence techniques [18].

These techniques can be subdivided into two basic types. The solid-state methods, which include matrix isolation and Shpol'skii spectroscopy, freeze the analyte in a suitable matrix at temperatures of 77 K or less. With careful choice of the matrix and careful control of the cooling procedure, the fluorescence spectra of the solid-state analyte are greatly simplified. The second type of cryogenic technique uses a supersonic expansion to substantially decrease the rotational and, to a lesser extent, vibrational temperature of an analyte molecule. This is accomplished by expanding the analyte, diluted in a monatomic gas, from a high temperature and pressure reservoir, through a small orifice (nozzle) into a vacuum chamber. This process also results in a dramatic simplification of the fluorescence spectra. Not only are the spectra simplified by this process, but small changes in molecular structure can produce relatively large shifts in the position of the observed transitions, allowing spectra to be obtained which uniquely describe individual PNAs [19].

## Liquid-Solution Phase Absorbance Spectra

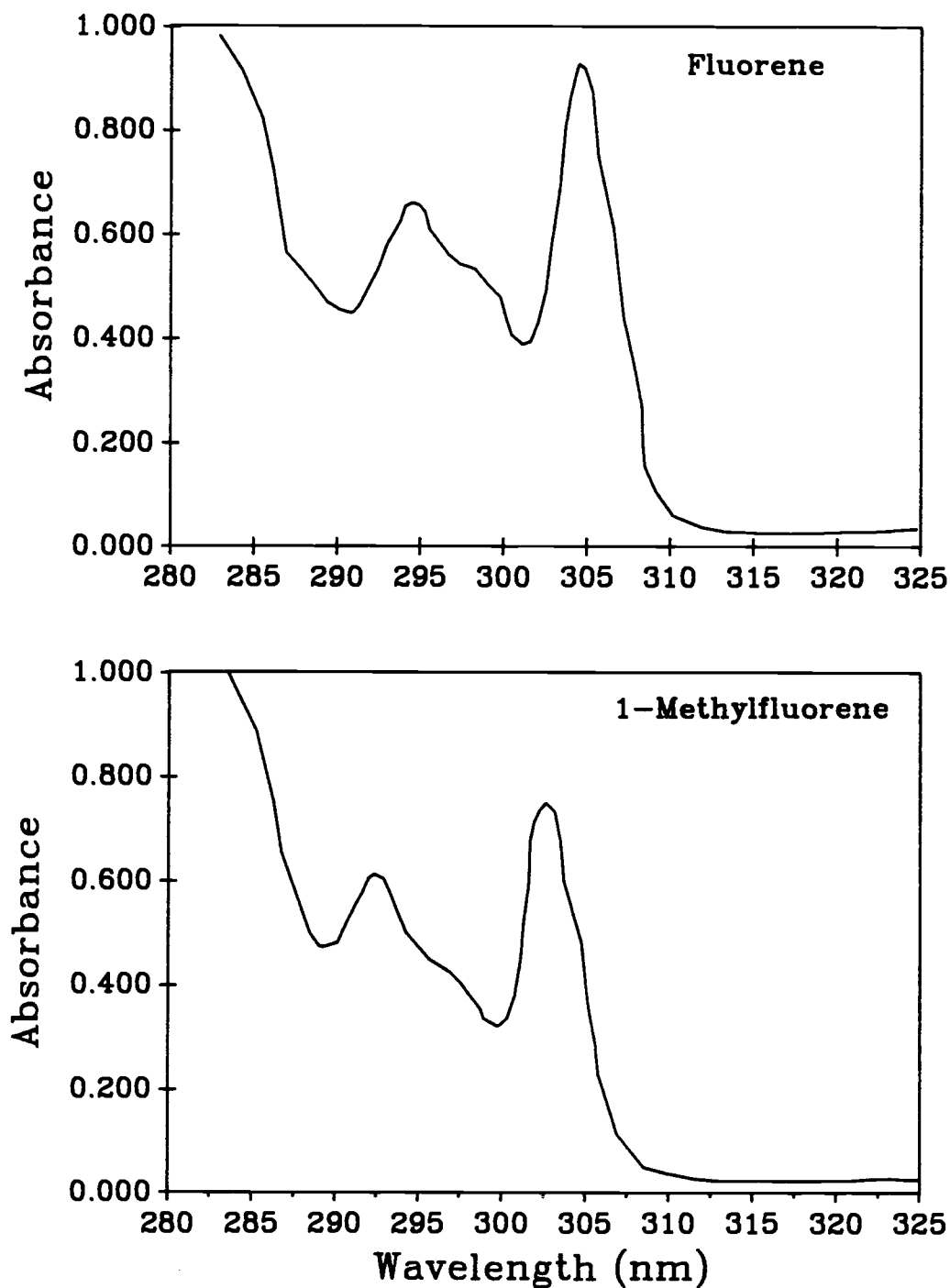


Figure I.1 Liquid solution phase absorbance spectra of 5  $\mu\text{g/ml}$  of fluorene and 1-methylfluorene in cyclohexane. Taken on a Cary 118C spectrophotometer with a spectral bandpass of 0.33 nm.

These different cryogenic methods have several things in common. First, they allow very narrow bandwidth spectra of individual PNAs to be obtained. This can only be accomplished, however, if the bandwidth of the optical source used to excite the molecules is sufficiently narrow to resolve adjacent features present in the spectrum. In addition, since the analyte molecules are dilute, isolated in either a frozen matrix or expanding in an excess of diluent gas, the optical source must also be sufficiently powerful to excite enough of the dilute molecules to allow measurement of their resultant emission.

Lasers can provide high spectral irradiance ( $10^4$ - $10^9$   $\text{W}\cdot\text{cm}^{-2}\cdot\text{nm}^{-1}$  in pulsed systems [20]), concentrated in the desired narrow bandwidth; less than an Angstrom in most instances. Thus the bandwidth of the source can be correctly matched to the bandwidth of the narrow spectral transitions. In addition, the directionality of the laser and its ability to be focused to a diffraction limited spot size are an advantage, particularly in the fluorescence analysis of supersonic jets. The coldest part of the expansion, where the narrowest linewidth spectra will be observed, occurs directly along the axis of the expansion. With careful alignment and a tightly focused beam, it is possible to excite only the coldest molecules which are present at the center of the expansion. Thus, their high irradiance, narrow bandwidth and ability to focus the beam into a small volume, make lasers the optical sources of choice for these spectroscopic techniques.

By combining these high spectral-resolution methods of sample presentation with the narrow bandwidth and high intensity of the laser, very selective and sensitive determinations of PNAs may be effected. With the highest spectral selectivity, it might be feasible to determine PNAs directly in complex mixtures with little or no sample preparation and no preseparation. The most intriguing possibility for such an analysis would be to directly monitor the formation of target PNAs sampled from the environment in which they are created: the smoke stack of a coal-fired power plant or an incinerator for example. A better understanding of the reaction

pathways and intermediates in the formation of these compounds in complex combustion environments might then lead to effective methods to prevent their formation directly at the source.

The supersonic jet lends itself well to such a high-temperature application. It is designed to be used with gas-phase samples and is less subject to the matrix constraints which are imposed when analyzing complex mixtures by the solid-state techniques. For similar reasons the supersonic jet can be interfaced fairly easily to a gas chromatograph (GC); both involve gaseous high-temperature samples and the GC carrier gas, helium or argon, can be used directly as the diluent gas for the supersonic expansion. Indeed, one of the first analytical applications of the supersonic jet involved using a very crude GC as a sample introduction device for the quantitative analysis of methyl-naphthalenes in crude oil [21].

As mentioned earlier, the analyte molecules probed in a supersonic jet are diluted in an excess of an inert gas such as helium. This implies a loss in sensitivity is required to obtain high selectivity. This is indeed one of the trade-offs which must be considered in such an analysis. One of the properties of a supersonic jet, which will be discussed in more detail later, is that gas density decreases as the expansion proceeds away from the nozzle into the vacuum. The rotational and vibrational temperatures, however, also decrease along the expansion axis. Thus, the lowest temperature, highest resolution spectra will be obtained in the region of lowest density. Two factors help to ease the restrictions imposed by this trade-off. First, as the molecules cool, their energy, which was spread over a wide range of energy levels, is concentrated into a few narrow states. This somewhat offsets the loss in sensitivity due to decreasing density. Secondly, the very highest selectivity may not be needed for most analyses, and therefore some selectivity may be sacrificed to enhance sensitivity. This is particularly true if chromatographic pre-separation is utilized. Even low-resolution packed column GC may provide enough chromatographic resolution to ease the requirements for spectral resolution in most analyses. One of the interesting implications of

the properties of the jet is that the spectral resolution can be changed by simply adjusting the point at which the laser intersects the expanding jet. This means that it is possible to fit the spectral resolution to the requirements of an analysis without any dramatic instrumental modifications. Thus, the trade-off between sensitivity and selectivity can be adapted to a particular set of circumstances.

Due to their unique ability to present analyte molecules at cryogenic temperatures while still isolated in the dilute gas phase, supersonic jets have been utilized in fundamental studies of molecular structure and interaction since they were first proposed by Kantrowitz and Grey in 1951 [22]. However, the analytical applications have only begun to appear, beginning with Small's contribution in early 1982 [19]. Since then several additional research groups have investigated various aspects of the application of supersonic jets to analytical chemistry. Definite advances have been made, particularly with respect to capillary GC interfaces and the analysis of liquids and supercritical fluids [23-25]. However, as is to be expected with a technique still in its infancy, a great deal of work needs to be done and many questions remain to be answered.

The database of high resolution PNA spectra is still quite small and must be expanded to make this a viable fingerprinting technique. Also, chromatographic applications, until now, have been limited to monitoring a single wavelength for the duration of the elution, restricting detection to usually a single analyte per run. This limitation precludes the use of internal standard methods of quantitation which will be required if quantitative precision is to be obtained. Alternatively, if the excitation wavelength could be swept rapidly in real time, the system could be programmed to scan to the transition wavelengths characteristic of several different PNAs and internal standards throughout the elution. By scanning between the analyte excitation wavelengths repeatedly, or perhaps based on known retention times, several analytes could be detected in a single elution and internal standards could be used for quantitation.

Finally, in order to make this a commercially viable technique, instrumentation must be developed which is simple to use, reliable, and relatively inexpensive. Unfortunately, current laser technology cannot meet such restrictions and thus ultimately limits the commercial application of laser-based techniques such as this.

The main goal of the research documented in this thesis has been to develop a laser-excited molecular fluorescence system which utilizes a pulsed supersonic expansion to provide high-spectral resolution for the selective determination of PNAs. The instrumentation was designed to maximize sensitivity, thus some spectral selectivity was sacrificed to improve the ability to detect PNAs in the trace amounts characteristic of samples found in the environment. To offset the small losses in spectral selectivity, the system was designed to be interfaced to a packed-column gas chromatograph. In addition to providing added selectivity in the form of chromatographic preseparation, the GC also improves the ability to perform quantitative analyses. Moreover, the entire instrumental system was devised to be controlled by a microcomputer, providing a means by which accurate, reasonably rapid fluorescence excitation scans can be performed. Consequently, versatile excitation wavelength programming during the chromatographic separation is possible. As discussed above, this feature also means that internal standard methods of quantitation can be utilized to improve precision. This thesis describes the development of this instrumentation as well as its characterization using two closely related model PNAs, fluorene and 1-methylfluorene.

#### A. Polynuclear Aromatic Hydrocarbons

The instrumental system that was developed in this research was designed to be very selective, responding mainly to a single class of compounds, the PNAs. In order to understand and justify the

reasons for this concentrated effort, the physical properties of these compounds should be examined.

## 1. Molecular Structure

PNA's are multi-ring aromatic compounds consisting of various combinations of fused benzene or heterocyclic aromatic rings. The simplest PNA is naphthalene which consists of 2 fused rings as illustrated in the upper left-hand corner of Figure I.2. By adding an additional ring onto the basic naphthalene subunit, two isomers, anthracene and phenanthrene, are formed. These two compounds are considered isomers due to the fact that they differ only by the geometric orientation of their rings. This is also the case with benzo[a]pyrene and benzo[e]pyrene which are also of interest due to their dramatically different carcinogenic activity despite being very similar in structure. This emphasizes the point that small changes in structure, in this case the position of a single ring, can have profound implications on physical, chemical, and toxicologic properties. The PNA's discussed thus far, naphthalene, phenanthrene, anthracene, and the benzopyrenes, are all polycyclic aromatic hydrocarbons (PAHs) consisting of only carbon and hydrogen. A related class of compounds, the polycyclic aromatic compounds (PACs), also includes aromatic heterocyclic compounds such as the nitrogen heterocycle, carbazole (Figure I.2), as well as substituted PAHs.

When discussing the structure of PNA's, one physical characteristic stands out that dominates their properties. If the structure of any of the PNA's present in Figure I.2 is examined, it is easily seen that they consist of highly conjugated aromatic rings. These conjugated ring systems are highly resonance stabilized and provide many delocalized  $\pi$  electrons. This resonance stabilization in part explains one of their important properties: PNA's are unusually stable. Another result of these structural characteristics is that these delocalized  $\pi$  electrons are held much more loosely than



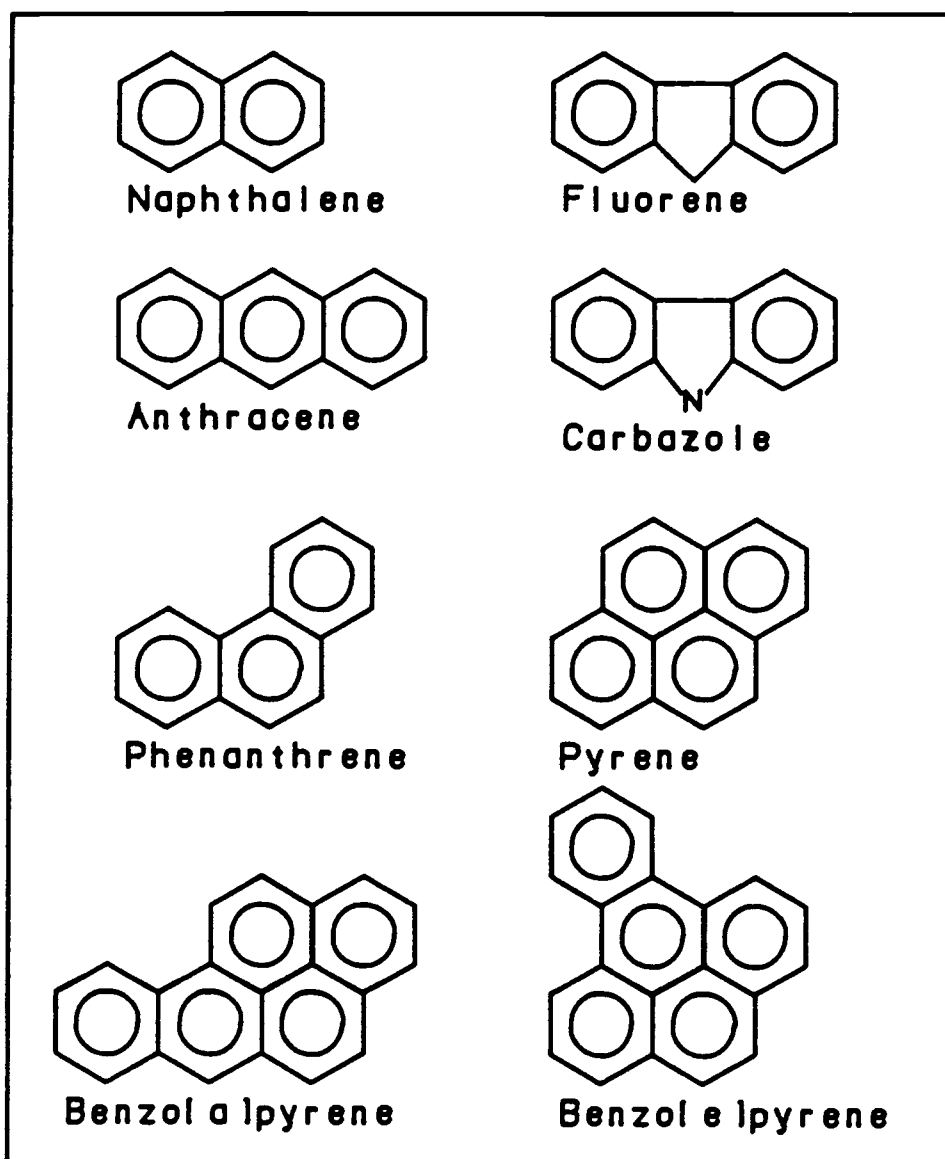


Figure I.2 Representative polynuclear aromatic hydrocarbons (PNAs).

the  $\sigma$  electrons associated with strong covalent bonds between the atoms in the molecule. This factor, combined with the structural rigidity associated with very restricted vibrational and rotational degrees of freedom, provides PNAs with high absorptivities and fluorescence quantum efficiencies. Finally, not only does the unique structure of PNAs contribute to their stability and special spectroscopic characteristics, there is a great deal of evidence linking the structure of PNAs to their notorious biological activity.

## 2. Biological Activity

PNAs have been recognized as potent carcinogens ever since it was reported in 1775 that chimney soot was responsible for the scrotal cancer observed among chimney sweeps [26]. During the following two centuries many additional studies have been performed to determine the biological activity of individual PNAs as well as the metabolic pathways leading to carcinogenesis in a variety of organisms [27-30]. The results of a 1981 literature survey of PNAs tested for biological activity revealed that of 355 compounds compiled, 197 showed at least some carcinogenic activity [31]. A breakdown of these results is shown graphically in Figure I.3. Two points should be revealed concerning these results. First, the original references used in compiling the data only covered studies up to 1976. Certainly a number of additional PNAs have been shown to exhibit carcinogenic activity in the ensuing 12 years. Secondly, only parent and alkyl substituted PNAs were included in the list. Thus, potent carcinogens such as the nitro-substituted PACs [32] were excluded from the list. This helps to stress the fact that a great number of PNAs exhibit some form of biological activity, thus explaining, in part, the great emphasis which has been given to the development of new analytical methodology for their determination.

The development of such methods is complicated by a fact revealed above: small changes in the structure of a PNA can have a

## Carcinogenic Activity of 355 PNAs:

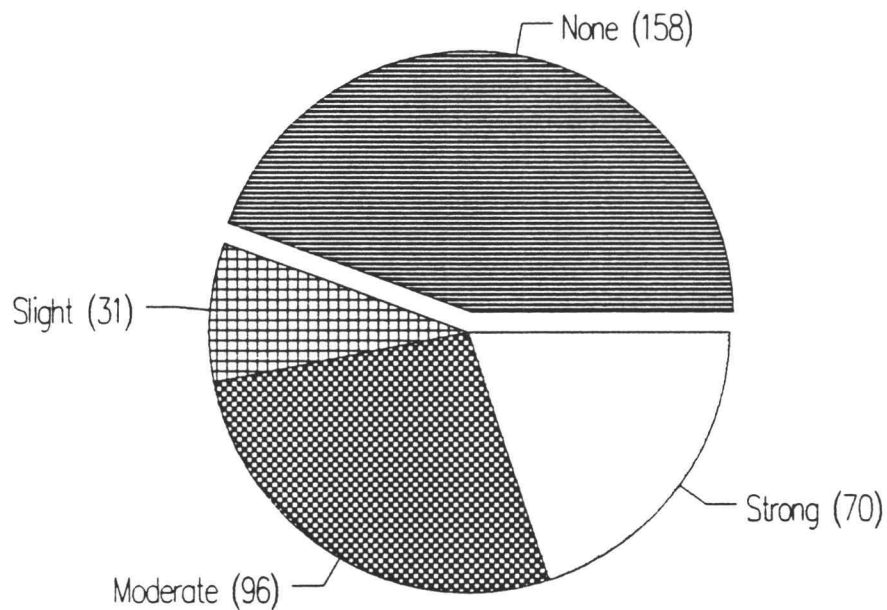


Figure I.3 Breakdown of the results of testing 355 PNAs for carcinogenic activity. The numbers in parenthesis are the total number of PNAs comprising each group. Data were compiled from reference 31.

large effect on its biological activity. For example, chrysene exhibits only slight carcinogenic activity whereas 5-methylchrysene is a potent carcinogen. Furthermore, other methylchrysenes exhibit varying levels of activity [27]. Similarly, as discussed above, two structural isomers, benzo[a]pyrene and benzo[e]pyrene, which differ only in the placement of a single ring, also differ dramatically in their activity. Benzo[a]pyrene is a notorious carcinogen which has been used as an indicator of the overall carcinogenic potential of a variety of samples, while benzo[e]pyrene shows only slight activity. Thus, any analytical method being developed for the analysis of PNAs must be able to differentiate unambiguously very similar species such as isomers differing only in the position of a single ring or alkyl group.

What are the implications of this biological activity? If human exposure to these compounds were limited to isolated cases then there would be considerably less interest in their determination than the current emphasis indicates. This is due to the fact that PNAs, which are often carcinogenic, are also widely distributed in the environment in concentrations ranging from less than 100  $\mu\text{g/kg}$  in deep ocean sediments to greater than 100,000  $\mu\text{g/kg}$  in samples from urban areas [33]. Thus, in order to assess the impact of these compounds on humans and our environment, their sources and distribution should be examined.

### 3. Sources and Distribution

PNAs are almost exclusively formed by the incomplete combustion of organic material. Natural sources of PNAs include forest and prairie fires, volcanic emission, and there has been some evidence for the in-situ synthesis of certain PNAs from the degradation of biological material [11]. Anthropogenic sources of PNAs include combustion of fossil fuels such as coal, gasoline, and diesel fuel. Other anthropogenic sources include agricultural and refuse burning.

In addition, as of 1981, more than 250 PNAs had been identified in tobacco smoke including approximately 30 ng/cigarette of benzo[a]pyrene [34].

The distinction between natural and anthropogenic sources of PNAs is an important one for the following reason [35]. If the major sources of PNAs throughout history are naturally derived, environmental emission would be expected to remain at a fairly constant level with occasional local deviations due to large forest fires or volcanic eruptions. If so, people would have been exposed throughout history to significant but constant levels of PNAs, perhaps allowing a tolerance to be developed to counteract their toxic effects. On the other hand, if major sources are anthropogenic, the environmental emissions would be expected to increase as various activities associated with their production, such as coal combustion, increase. In this case it might be much more difficult for a tolerance to be developed in humans and other living organisms, since environmental emissions would be continuously increasing.

This dilemma has been addressed in many studies. For example, one investigation examined the historical record of PNA emissions by examining sediment cores from the Pettaquamscutt River in Rhode Island [36]. The cores were sectioned into small subcores. Each of these subcores was then dated using  $^{210}\text{Pb}$  dating techniques [37,38] and was analyzed for total PAH concentration. The results of this analysis have been reproduced graphically in Figure I.4. During the years 1820 to 1900 the total level of PNAs remains at a relatively low background level. Around 1900 there is a dramatic increase in environmental levels attributed possibly to the onset of the industrial revolution in the United States. An interesting plateau occurs around 1920 which is thought to correspond to decreases in industrial activity due to the depression. Levels then increase steadily to a peak around 1950, which corresponds to the switch-over from "dirty" sources of power such as coal to "cleaner" sources such as natural gas and hydroelectric. Regardless of the interpretation of these fluctuations in PNA concentrations it is clear that the

## Total Historical PNA Abundance From a River Sediment Core Sample

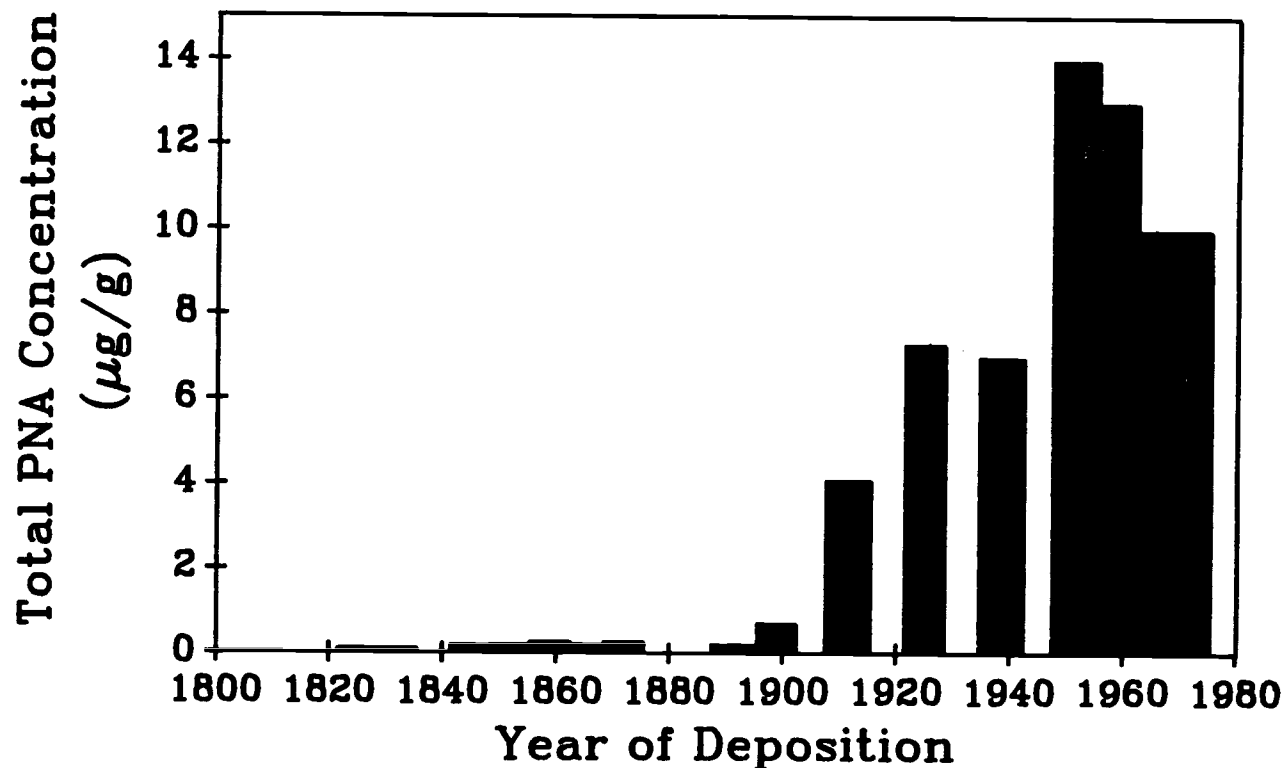


Figure I.4 Historical record of PNA concentrations from a Pettaquamscutt River sediment core. Recompiled from reference 36.

environmental levels measured correlate well with increases in industrial activity in the Eastern United States.

Unfortunately, this isn't a problem associated with only industrialized areas of the United States. This is a worldwide problem because PNAs are an environmentally ubiquitous class of compounds. For example, in a single study [11] significant levels of PNAs were detected in soil and sediment from several areas of the United States including the east coast (Maine), the Midwest (Nebraska), the west coast (Mono Lake and Yosemite National Park in California), as well as isolated areas of Alaska and Wyoming. In addition, significant levels were detected in several areas of Africa and South America including 8 sites along the Amazon River, as well as on 6 different islands in the South Pacific. It should be stressed that these results come from a single series of studies and that it would be possible to find literature citations detailing the detection of PNAs from almost any area of the world which has been sampled [10]. Examples of representative environmental concentrations in a variety of both pristine and polluted samples are listed in Table I.1.

Thus, PNAs are an important class of compounds due to their biological activity, their anthropogenic derivation, and their ubiquity. Consequently, there is a need for very sensitive and selective methods by which to study them in complex environmental matrices. In this research, spectroscopic methods have been chosen to supplement gas-chromatographic separations and accomplish this goal. It is thus worthwhile examining the spectroscopic properties of PNAs.

#### 4. Spectroscopic Properties

The total energy of polyatomic molecules such as PNAs can be considered, to a first approximation, to be divided between the separate energies associated with the following molecular motions.

Table I.1  
Representative Concentration<sup>1</sup> of PNAs in Both  
Pristine (non-polluted) and Polluted Samples

Sample	Pristine	Polluted
Air <sup>2</sup>	0.1-0.5 ng/m <sup>3</sup>	74 ng/m <sup>3</sup>
Water	0.001-0.025 µg/L	0.05-1 µg/L
Sediment	5.5 µg/kg	15 mg/kg
Contaminated Food	n/a	50 µg/kg
Tobacco Smoke	n/a	30 ng/cigarette

<sup>1</sup>Data taken from reference 31, chapter 2.

<sup>2</sup>Benzo[a]pyrene concentration only.



$$E_{\text{tot}} = E_{\text{trans}} + \underbrace{E_{\text{rot}} + E_{\text{vib}} + E_{\text{elec}}}_{\text{Internal Energy}} \quad (\text{I.1})$$

where  $E_{\text{trans}}$  is the translational energy of the molecule associated with its movement through space. The remaining three types of energy comprise the internal energy of the molecule.  $E_{\text{rot}}$  is the rotational energy which relates to the quantized rotation of the entire molecule around its center-of-mass,  $E_{\text{vib}}$  is the vibrational energy which is associated with the movement of individual atoms of the molecule with respect to each other, and  $E_{\text{elec}}$  is the electronic energy of the molecule which is defined by the motion of electrons within the molecule. The relative magnitudes of the separation of these various internal energy levels,  $\Delta E$ , is summarized in Table I.2.

To better understand the nature of these processes, a schematic molecular energy level diagram can be examined. Such a diagram is illustrated in Figure I.5.  $S_0$ ,  $S_1$  and  $S_2$  are the ground, first and second excited singlet electronic states, respectively.  $T_1$  is the first excited triplet electronic state. Associated with each electronic state are several vibrational energy levels which are shown here as horizontal lines of decreasing length. Further, each vibrational level will also have several rotational energy levels associated with it, which are represented here as the small lines of increasing separation at the end of each vibrational level. Radiative transitions such as excitation and absorption (E/A), fluorescence (F), and phosphorescence (P) are illustrated as solid, straight lines. Non-radiative transitions such as intersystem crossing (IS), and internal conversion (IC) are shown as wavy lines.

When a molecule such as a PNA absorbs a photon ( $h\nu$ ) it is generally excited to a vibrationally excited state of one of the excited singlet states ( $S_1, S_2, \dots$ ). Vibrational relaxation (VR) and internal conversion to the lowest vibrational state of  $S_1$  usually occur before any other processes, such as fluorescence, can

Table I.2  
Representative Wavelengths, Wavenumbers, Frequencies  
and Energies of Molecular Spectroscopic Transitions

Transition	Energy (kJ/mol)	$\Delta E$ Wavelength	Wavenumbers (cm <sup>-1</sup> )	Frequency (sec <sup>-1</sup> )
Rotational	0.12	1 mm	10	$3 \times 10^{11}$
Vibrational	24	5 $\mu\text{m}$	2000	$6 \times 10^{13}$
Electronic	400	300 nm	33,000	$1 \times 10^{15}$

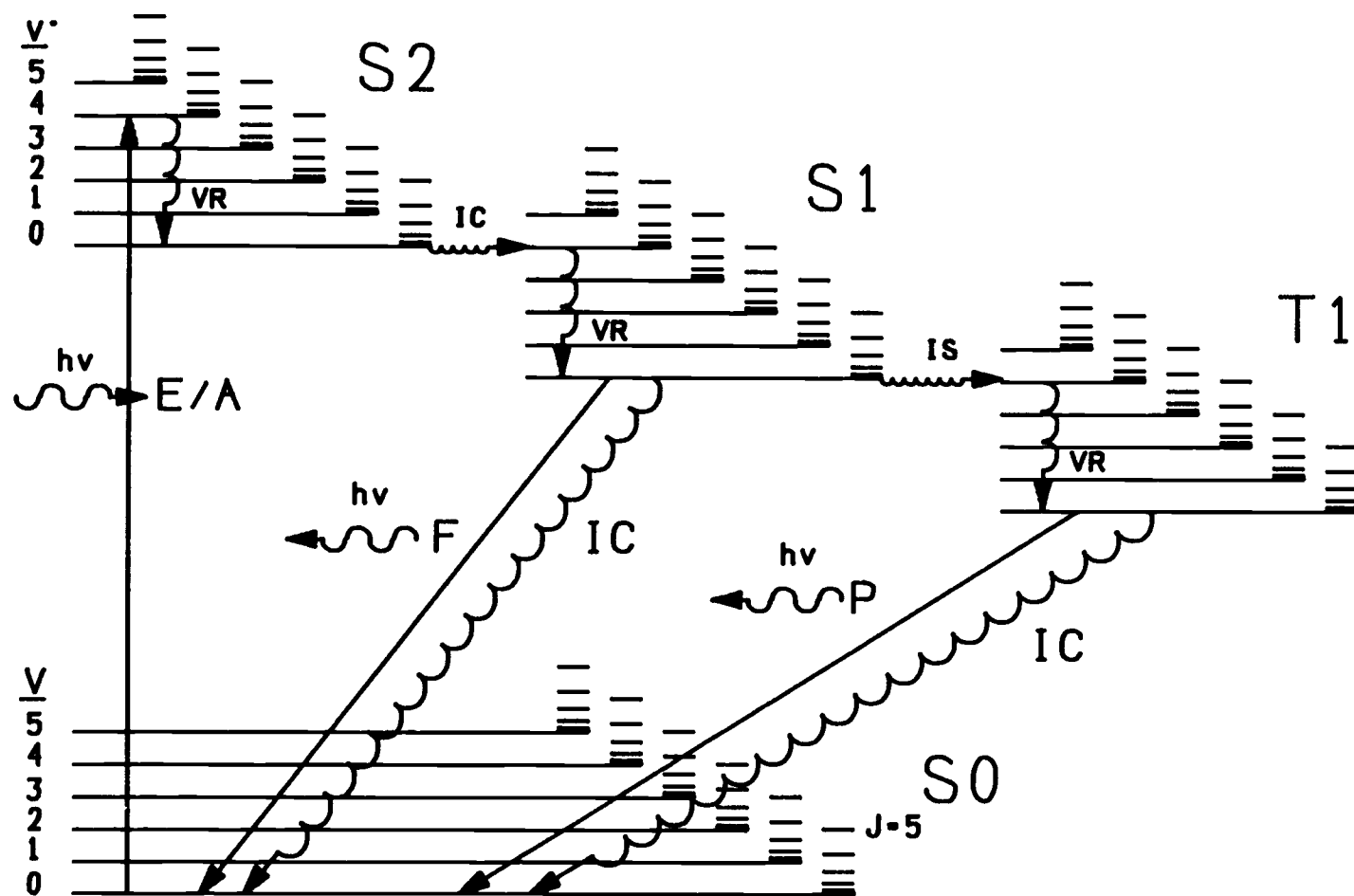


Figure I.5 Molecular energy level diagram illustrating the various radiative and non-radiative pathways by which an excited molecule can return to the ground state.

occur. The molecules in the excited state can then return to the ground state by several routes. If the upper vibrational levels of the  $S_0$  state overlap the lower vibrational levels of  $S_1$  then significant internal conversion can occur causing a non-radiative transition to the ground state. Another non-radiative path involves a change of electron spin accompanied by intersystem crossing to the first excited triplet state,  $T_1$ . This "forbidden" transition eventually results in either phosphorescence or internal conversion back to  $S_0$ . Finally, if neither of the non-radiative pathways from  $S_1$  are favored, fluorescence from  $S_1$  to one of the vibrational levels of  $S_0$  can occur.

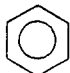
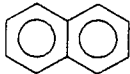
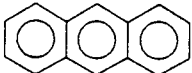
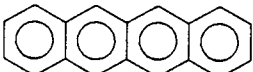
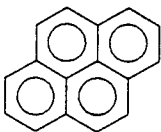
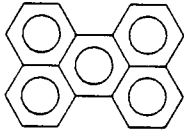
As stated earlier, PNAs exhibit high fluorescence quantum yields. This indicates that fluorescence must be the main pathway for the molecule to return to  $S_0$ . If the structure of any of the PNAs in Figure I.2 is examined it is easily seen that they consist of highly conjugated aromatic rings. These conjugated ring systems are highly resonance stabilized and provide many delocalized  $\pi$  electrons. These  $\pi$  electrons are held much more loosely than the  $\sigma$  electrons which are associated with strong covalent bonds between atoms in the molecule. Consequently, the  $\pi$  electrons can be excited to  $\pi^*$  antibonding orbitals relatively easily (in the near ultraviolet in contrast to the vacuum ultraviolet for  $\sigma \rightarrow \pi^*$  transitions). In addition, because the large PNAs can offer many of these  $\pi$  electrons, molar absorptivities are often high.

Since the rate of fluorescence is proportional to the rate of absorption, molecules that exhibit high absorptivities would be more likely to exhibit strong fluorescence. However, for this to be true, fluorescence must be the favored method of depopulating the excited state. PNAs are very rigid molecules which helps to minimize the number of vibrational modes the molecule exhibits, which in turn helps to minimize non-radiative processes such as  $S_1$  to  $T_1$  intersystem crossing, and  $S_1$  to  $S_0$  internal conversion. In fact, PNAs are an almost ideal class of fluorophore with fluorescence quantum yields approaching 1.0 in some cases (e.g., perylene).

These assertions can be illustrated more quantitatively if Table I.3 is examined. This table consists of the molar absorptivities and fluorescence quantum yields for a series of PNAs in cyclohexane solution. Data was extracted from the compilation of liquid-solution phase PNA spectra by Berlman [39]. Note that as the PNAs increases in size from benzene (1 ring) to tetracene (4 rings in a linear configuration), the molar absorptivities increase from 210 to 12,000. This is due to the fact that as the size of the PNAs increase, additional  $\pi$  electrons become available for excitation. Note also the increase in fluorescence quantum yield from benzene to anthracene. This can be explained by a decrease in nonradiative deactivation pathways such as intersystem crossing. The decrease in quantum yield from anthracene to tetracene is probably due to the fact that the large linear configuration of tetracene may allow additional vibrational modes which lead to non-radiative intersystem crossing or internal conversion.

It is evident from this discussion that PNAs are amenable to study via fluorescence. Moreover, this method offers several advantages including enhanced sensitivity. Since PNAs exhibit high absorptivities along with high fluorescence quantum yields, the probability that a photon will be absorbed and reemitted as fluorescence is relatively high. Thus fluorescence is a very sensitive method by which to study the PNAs. The second advantage is selectivity. Only compounds that absorb will be able to fluoresce upon exposure to ultraviolet radiation (absorption is necessary but not sufficient for fluorescence). In addition, only those compounds for which intersystem crossing and internal conversion are minimized will show appreciable fluorescence. PNAs, particularly in the gas phase, are among the few compounds which exhibit both high absorptivities and high fluorescence quantum efficiencies upon ultraviolet excitation. Consequently, fluorescence spectroscopy is a very selective method by which they can be studied.

Table I.3  
Molar Absorptivities and Fluorescence  
Quantum Yields for PNAs in Cyclohexane Solution<sup>1</sup>

Compound	Structure	Absorptivity	Quantum Yield
Benzene		210	0.07
Naphthalene		6000	0.23
Anthracene		10,000	0.36
Tetracene		12,000	0.21
Pyrene		55,000	0.32
Perylene		44,000	0.94

<sup>1</sup>Data compiled from reference 38.

### a. Liquid-Solution Phase Spectra

One of the goals of this research is to obtain narrow bandwidth fluorescence excitation spectra of PNAs. Since fluorescence is often measured on samples in a room-temperature liquid solution, it is important to determine if fingerprint spectra can be obtained from such samples. Consequently, the characteristics of the condensed phase fluorescence excitation spectra of PNAs must be examined.

Structure in the observed spectrum will be a function largely of the electronic and vibrational transitions since rotations will be greatly perturbed by solvent associations and collisions. Due to solvent-solute interactions, changes in refractive index and dielectric constant, the frequency of liquid-solution phase spectra are often shifted in frequency toward the red relative to the gas phase spectra. Furthermore, the condensed phase spectra of PNAs are often broad and diffuse, exhibiting only a few features. This is thought to be due to several factors including vibrational sequence congestion. Vibrational sequence congestion arises from the fact that at normal experimental temperatures (*i.e.*, room temperature), many of the vibrational levels of the ground electronic state are significantly populated [40]. When the molecule is excited from  $S_0$  to  $S_1$ , the excitation can occur from any of these ground state vibrational levels to the corresponding vibrational level in the excited electronic state as illustrated by the band sequence depicted in Figure I.6. Because there are so many transitions differing by only the small differences between ground and excited state vibrational frequencies, the individual transitions cannot be instrumentally resolved and the spectrum appears broad and featureless.

Other sources of broadening include homogeneous and inhomogeneous broadening arising from solvent or nearest neighbor interactions. For example, a solute which is isolated in solution by the solvent will have a cage of solvent molecules form around it.

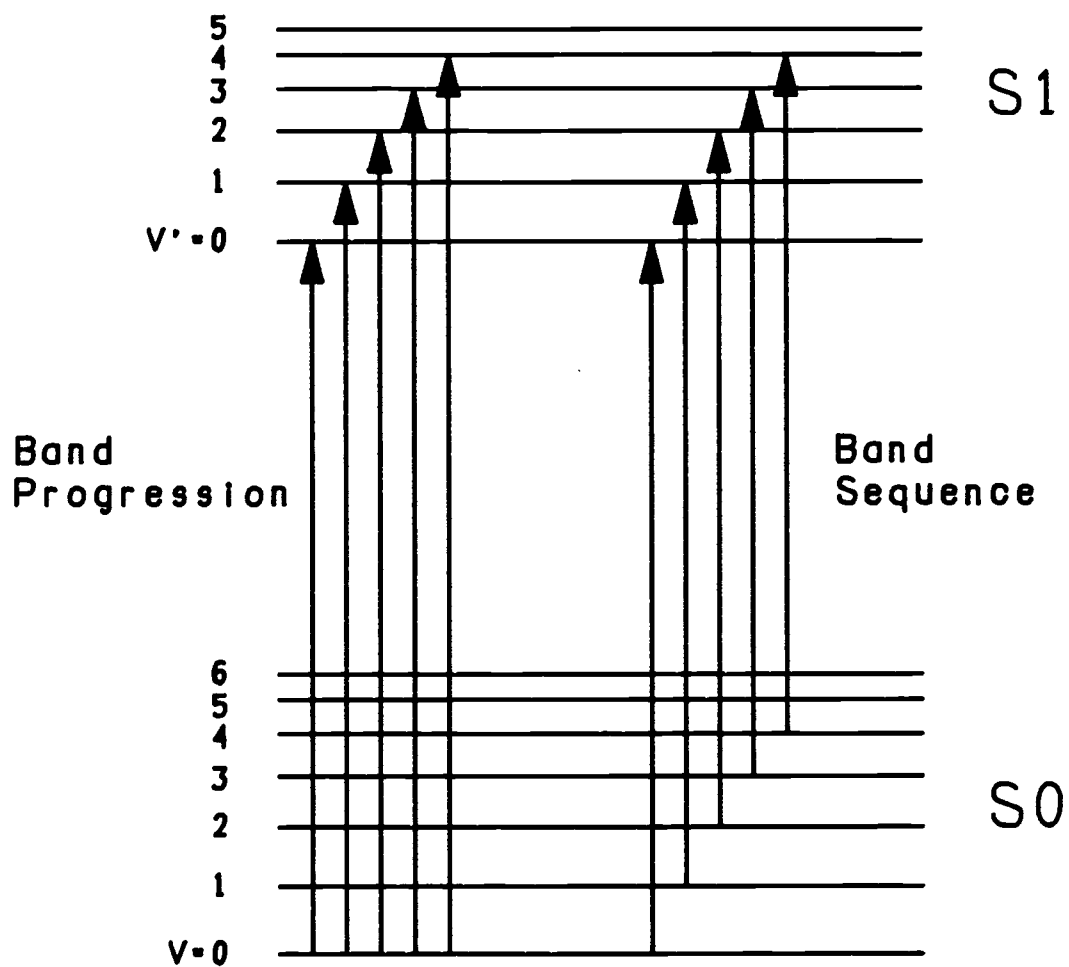


Figure I.6 Schematic diagram of the vibronic transitions leading to band progressions and band sequences.



This solvent cage can exert a force on the solute through dipole-dipole interactions or hydrogen bonding [41,42]. These forces, in turn, affect the energy of the excited state. Consequently, local variations in the orientation of molecules comprising the solvent cage can cause shifts in the solute's excited state energy levels, causing the spectrum to become broadened.

Figure I.1 contains the liquid solution phase spectra of fluorene and 1-methylfluorene in dilute cyclohexane solution. These spectra are broad with only a few strong features, and appear almost identical in terms of wavelength, intensity, and bandwidth. Thus, it would be difficult to fingerprint these molecules and identify them individually in a mixture without resorting to special deconvolution techniques. Consequently, the use of room-temperature liquid-solution phase spectra of PNAs is inconsistent with our goal of acquiring unique, high-resolution spectra of the components of complex mixtures.

The resolution of liquid-phase spectra can be improved by choosing a solvent that minimizes solvent related broadening. For instance, cyclohexane has been shown to provide sharper spectra of certain PNAs than solvents such as benzene or ethanol [39]. Another possibility would be to cool the sample to reduce thermal sequence congestion. Examples of low-temperature ( $\leq 77$  K) methods by which high resolution spectra can be obtained are matrix isolation, Shpol'skii, and site selection or fluorescence line narrowing spectroscopy. These methods do allow high resolution spectra to be obtained, but interfacing them to a gas chromatograph is cumbersome, and the matrix can still influence the frequency characteristics of the spectra. A final possibility is to eliminate the effects of condensed phase broadening entirely by making measurements in the gas phase.

## b. Gas-Phase Spectra

Once again it must be determined if gas-phase fluorescence excitation spectra are consistent with the goals of this research. Therefore, the characteristics of gas-phase spectra will be examined. The observed gas-phase fluorescence excitation spectrum will be a function of combined rotational, vibrational and electronic transitions (rovibronic transitions). Vibrational sequence congestion is once again a major cause of diffuseness (broadening) in these spectra. In addition, each vibrational transition will have a series of rotational transitions associated with it. Rotational constants,  $B$ , are proportional to the inverse of the moment of inertia of the rotating molecule. The moment of inertia,  $I$ , is the sum over all atoms,  $i$ , of the product of the mass of an individual atom,  $m_i$ , times the square of its distance from the molecular center-of-mass,  $r_i$ .

$$I = \sum m_i r_i^2 \quad (I.2)$$

PNAs are large molecules, consequently the  $r_i$  will be large, causing the moment of inertia to be large. This causes the rotational constants to be very small, which in turn indicates that the rotational energy levels will be very closely spaced. This means that at experimental temperatures, many of the rotational levels will be populated causing a pseudo-continuum envelope of rotational transitions to be associated with each vibrational transition. These thermal effects can be examined by observing the influence of temperature and transition energy on the fraction of the molecular population which reside in excited states as described by the Boltzmann distribution.

$$N_i/N_0 = \exp[- i \Delta E_{0 \rightarrow i} / kT ] \quad (I.3)$$

where  $N_i$  is the number of molecules in the excited state,  $i$ ,  $N_0$  is the number of molecules in the ground state,  $\Delta E_{0 \rightarrow i}$  is the difference in energy between the ground state ( $E_0$ ) and the  $i^{\text{th}}$  excited state ( $E_i$ ),  $k$  is the Boltzmann constant, and  $T$  is the temperature. Values of the Boltzmann factor ( $\exp[-\Delta E/kT]$ ) as a function of  $T$  and  $\Delta E$  are compared in Table I.4. From this table it is clear that even at room temperature, a majority of the molecules will reside in a variety of rotationally excited states. In addition, several low energy vibrational modes will also be significantly populated.

The implications of these sources of broadening are as follows. As the temperature of the sample increases, more vibrational and rotational levels will become thermally populated causing an increase in sequence congestion. In addition, as the size of the absorbing molecule increases, additional vibrational modes will be added and rotational energy level spacings will decrease, also causing increases in sequence congestion.

These factors can be brought into perspective by examining Table I.5, compiled from data presented by Byrne and Ross at the University of Sydney [40,43].  $T_{\text{diff}}$  is the temperature at which they calculate that the gas-phase spectrum of the indicated molecule will become totally diffuse.  $T_{\text{min}}$  is the temperature required to give a vapor pressure of 1 mm: the minimum vapor pressure necessary to make the absorbance measurement. As PNAs increase in size from benzene (1 ring) to anthracene (3 rings),  $T_{\text{diff}}$  decreases below  $T_{\text{min}}$ . Thus, even a relatively small PNA such as anthracene would be expected to exhibit a totally diffuse spectrum at experimentally useful temperatures. Indeed, the observed gas-phase spectra of PNAs are broad with few resolvable features [44] which leads to the paradox: how can the sample be heated to a temperature which allows enough PNA molecules to be present in the gas phase for detection, without destroying fine structure by thermal broadening or matrix interactions? One answer involves using a supersonic expansion to cool the internal energies of the PNAs while allowing them to remain in an isolated state, free from intermolecular interactions.

Table I.4

Comparison of Excited State Populations as a Function  
of Transition Energies and Sample Temperatures

Transition	$\Delta E(\text{cm}^{-1})$	T(K)	$kT(\text{cm}^{-1})$	$\exp(-\Delta E/kT)$
Rotational	10	10	7	0.2
	10	100	70	0.9
	10	298	200	0.95
	10	420	290	0.97
Vibrational	100	10	7	$6 \times 10^{-7}$
	100	100	70	0.2
	100	298	200	0.6
	100	420	290	0.7
	300	10	7	$2 \times 10^{-19}$
	300	100	70	0.01
	300	298	200	0.2
	300	420	290	0.4
	1000	10	7	$1 \times 10^{-62}$
	1000	100	70	$6 \times 10^{-7}$
	1000	298	200	0.007
	1000	420	290	0.3
Electronic	30,000	10	7	$< 10^{-99}$
	30,000	100	70	$< 10^{-99}$
	30,000	298	200	$7 \times 10^{-66}$
	30,000	420	290	$1 \times 10^{-45}$

Table I.5

Comparison of the PNA Critical Temperatures Which Produce  
Totally Diffuse Spectra and a Vapor Pressure of 1 mm Hg

Compound	$T_{\text{diff}} (^{\circ}\text{C})^1$	$T_{\text{min}} (^{\circ}\text{C})^2$
Benzene	347	-33
Naphthalene	157	57
Anthracene	77	150

<sup>1</sup> $T_{\text{diff}}$  is the temperature at which the spectra are calculated to become totally diffuse [40].

<sup>2</sup> $T_{\text{min}}$  is the temperature required to give a vapor pressure of 1 mm Hg [43].

## B. Supersonic Expansions

A supersonic expansion consists of a high temperature ( $-77^{\circ}\text{C} \leq T_0 \leq 400^{\circ}\text{C}$ ), high pressure ( $P_0 > 1 \text{ atm}$ ) reservoir, or nozzle, in contact with a vacuum through a small orifice (Diameter,  $D, \geq .02 \text{ mm}$ ) as illustrated in Figure I.7. The orifice is designed to have a diameter that is greater than the mean free path of the gas in the reservoir. This means that as the gas particles rush towards the vacuum via the orifice, there will be many two-body collisions. Since collisions which impart an axial component to the velocity are most effective at driving a gas particle from the reservoir, the perpendicular components of the gas velocity will be greatly reduced. In addition, as fast particles collide with slower moving particles in and downstream from the nozzle, translational energy is transferred from the faster to the slower particles and their velocities will become closer in magnitude.

The result of these processes is a narrowing of the velocity distribution of the expanding gas as well as a shift towards higher net velocities. In a static gas at room temperature, gas particles will have random velocities distributed around a mean velocity as described by the Maxwell-Boltzmann distribution. The standard deviation of the velocity distribution is defined by the relation  $(0.47kT/m)^{1/2}$  [45]. As the temperature of the gas decreases, the standard deviation, or width, of the velocity distribution also decreases. Thus, the width of the velocity distribution can be considered to be a measure of the translational temperature of the gas. This is also true in a supersonic expansion; the net result of the expansion is a cooling of the translational energy to very low temperatures.

Another way to view the cooling process is as follows. The energy of the gas molecules moving randomly about their high temperature reservoir can be considered to be heat energy. The

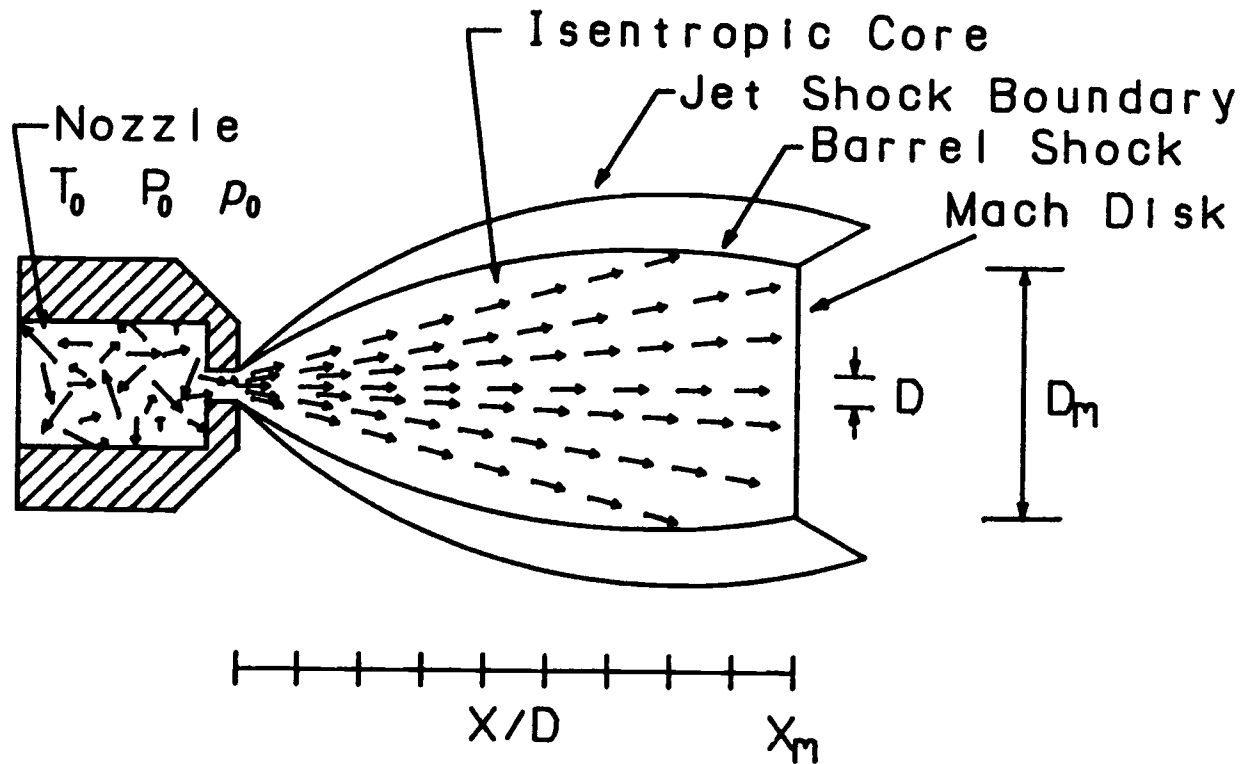


Figure I.7 Schematic diagram of a supersonic expansion.

expansion simply converts this heat into mechanical work in the form of directed mass flow. Since heat energy is consumed in this process, the temperature must fall [46].

That the translational temperature is so low is of little interest in itself except in the case of expansions of purely monatomic gases. However, when a large molecule with significant internal energy is diluted into an expansion of a monatomic gas, collisions with inert gas atoms quickly accelerate the larger molecules to comparable velocities. These collisions also allow the vibrational and rotational energy of the larger molecule to be converted into translational energy of the diluent gas. Since monatomic gases have no vibrational or rotational degrees of freedom, this conversion can be fairly efficient and the effective vibrational and rotational temperature of the larger molecules decreases. The rotational energy of the molecules comes to equilibrium with the translational energy of the inert-gas bath relatively quickly during these collisions. Consequently, the rotational temperatures observed downstream in the expansion are close to the translational temperatures ( $< 1-2$  K). Vibrational energy does not equilibrate as quickly with the translational bath since vibrational relaxation times are longer than rotational relaxation times [47]. Consequently, vibrational temperatures observed in a jet ( $> 10-100$  K) are typically higher than the translational or rotational temperatures but are still low enough to reduce vibrational congestion. Since most molecules already reside in the lowest electronic state even at room temperature, no change in electronic energy is observed.

Downstream from the nozzle collisions cease and the molecules become frozen at their particular internal temperature since it is the collisions which allow internal energy to equilibrate with translational energy. At this point the molecules are in an ideal spectroscopic state. They are internally cold and are free from intermolecular effects in a dilute, isolated state. Consequently, the molecular spectrum measured on these molecules is simple with only electronic and a few vibrational transitions evident. It should



be noted that even though the rotational temperature is quite low, there are still low energy rotational levels which are occupied. This means that each vibronic transition observed in the cooled spectrum will often have a rotational envelope associated with it which defines the width of the observed vibronic transition.

Condensation of the expanding gas ultimately limits the cooling capacity of the jet. Consequently, large molecules such as PNAs, which have a great deal of internal energy and which are normally solids at room temperature, would be expected to be cooled relatively inefficiently in the jet. Small, monatomic gases with no internal energy, such as helium, on the other hand, would be expected to achieve the lowest temperatures: this is indeed true, with temperatures of 0.03 K having been recorded for a free jet of pure helium [48]. Because the expansion of a pure molecule the size of a PNA would result in little cooling, they are instead seeded into an excess of a monatomic gas as discussed earlier. Because the monatomic diluent gas is in excess, most of the collisions will be between diluent gas particles or diluent gas particles and the larger molecules. Although, the expansion is not pure, rather a mixture of the analyte molecule and the diluent gas, the overall properties of the expansion will be characterized by the diluent gas since it is present in such an excess. The theoretical properties of continuous supersonic expansions of such small ideal gases have been described in several communications [45,49-52] and it is worthwhile examining these properties to gain a further understanding of the supersonic jet.

A final remark concerning the nomenclature used in describing these expansions is necessary. The term free-jet expansion refers to an expansion in which no collimating elements or skimmers invade the central axis of the expansion, which is termed the isentropic core. Often, however, it is desirable to select only the coldest, most collimated particles located along the axial portion of the expansion. In this case, a skimmer cone is placed in the isentropic core and the expansion is termed a "molecular beam".

## 1. Theoretical Description of a Supersonic Expansion

An isentropic expansion of an ideal gas will obey the following thermodynamic relationship [51].

$$T/T_0 = (P/P_0)^{(1-\gamma)/\gamma} = (\rho/\rho_0)^{\gamma-1} = [1 + [(\gamma-1)/2] M^2]^{-1} \quad (I.4)$$

Where  $T$  and  $T_0$  are the temperature of the gas in the expansion and the reservoir, respectively;  $P$  and  $P_0$  are the pressure of gas in the expansion and the stagnation pressure of the gas in the reservoir;  $\rho$  and  $\rho_0$  are the densities of the gas in the expansion and the reservoir;  $\gamma$  is a constant which equals  $C_p/C_v$ , the ratio of the constant pressure and constant volume thermodynamic heat capacity constants, and is equal to 1.67 for a monatomic gas; and  $M$ , the Mach number, is equal to the velocity of the expanding molecule,  $u$ , divided by the local speed of sound,  $a$ . Ashkenas has shown that the Mach number can be estimated from the following expression [50].

$$M_a = A (X/D)^{\gamma-1} - B (X/D)^{\gamma-1} \quad (I.5)$$

Where  $X$  is the distance downstream from the nozzle,  $D$  is the nozzle diameter, and  $A$  and  $B$  are constants which depend on  $\gamma$ . This expression is derived for an ideal gas expanding continuously through a nozzle and is valid beginning a few nozzle diameters downstream from  $X = 0$ .

These expressions were programmed into an electronic spreadsheet program (QUATTRO, Borland International, Scotts Valley, CA) using a modified version of a spreadsheet developed by Dr. Mark Maroncelli, previously of Dr. Joe Nibler's research group. The various expressions and spreadsheet format used are outlined in Appendix A. The results are plotted graphically in Figure I.8 and condensed into Table I.6. Note that equation I.5 is only valid downstream from  $X/D = 1$ . In order to estimate the Mach number prior to this point an exponential fit of the expansion parameters was

## Supersonic Expansion Theoretical Axial Properties

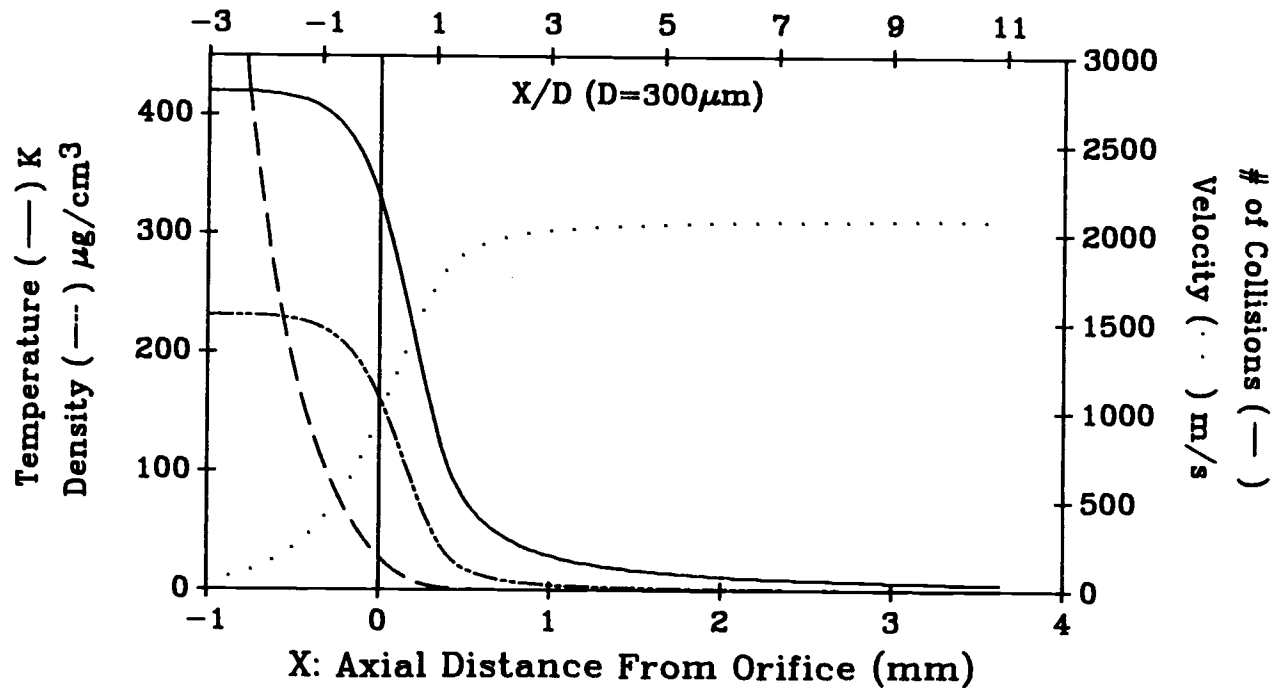


Figure I.8 Theoretical properties of a supersonic expansion as a function of distance from the nozzle. These curves are calculated for a nozzle diameter,  $D$ , of  $300 \mu\text{m}$ , a stagnation pressure,  $P_0$  of 1.5 atm of helium, and a reservoir temperature,  $T_0$ , of  $140^\circ\text{C}$ .

Table I.6

Sample Supersonic Expansion Parameters as a Function of  
Distance From the Nozzle Tip<sup>1</sup>

X/D	X(mm)	M(X)	T(K)	$\rho$	a(m/s)	u(m/s)	$\nu(\text{sec}^{-1})$	Collisions
-3	-0.9	0.04	420	43.35	1207	54	1.15E+10	
-2	-0.6	0.12	418	43.08	1205	147	1.14E+10	23384
-1	-0.3	0.33	405	41.12	1186	393	1.07E+10	8201
0	0	0.90	331	30.30	1071	965	7.14E+09	2220
1	0.3	2.45	140	8.36	697	1707	1.28E+09	225
2	0.6	4.65	51	1.85	421	1959	1.71E+08	26
3	0.9	6.37	29	0.78	317	2017	5.47E+07	8
4	1.2	7.87	19	0.43	260	2042	2.47E+07	4
5	1.5	9.23	14	0.27	223	2055	1.34E+07	2
10	3	14.93	6	0.07	139	2077	2.04E+06	1
20	6	23.90	2	0.02	87	2085	3.16E+05	0
50	15	44.21	1	0.00	47	2089	2.72E+04	0
100	30	70.28	0	0.00	30	2090	4.27E+03	0

<sup>1</sup>Calculations assume a nozzle diameter (D) of 300 $\mu\text{m}$ , a stagnation pressure of 1.5 atm helium, and a reservoir temperature of 420 K. M(X) refers to the Mach number,  $\rho$  is the density of particles in the expansion in moles/m<sup>3</sup>, a is the local speed of sound, u is the velocity of the particles in the expansion,  $\nu$  is the collision frequency, and the collision values refer to the number of collisions which have occurred since the last X.

used. This allowed the Mach number to exhibit a smooth transition from within the reservoir,  $X/D < 0$ , to the point at which equation I.5 takes over at  $X/D = 1$ . Since the region close to the nozzle is very complex and difficult to model, it should be realized that there is not necessarily any physical validity to the data in the region prior to  $X/D = 1$ .

The data presented in Figure I.8 and Table I.6 are for typical experimental parameters used in this research; a nozzle diameter of  $300\text{ }\mu\text{m}$ , a stagnation pressure of 1.5 atm of helium, and a nozzle temperature of 420 K. The important points to note about these data are that first, the velocities that are achieved in the expansion are not as high as might be inferred from the term "supersonic jet". The fact that the Mach numbers do increase to values much greater than 1 does indicate that the expansion is indeed supersonic. This is not, however, due to the fact that the gas velocities are exceedingly high, but to the fact that the local speed of sound is so low. The speed of sound is defined by

$$a = [\gamma R T_{tr} / M]^{\frac{1}{2}} \quad (I.6)$$

Thus as the translational temperature drops, the local speed of sound also drops well below the velocity of the expanding gas, rendering the expansion supersonic. Note also that the density of the gas also drops rather quickly as it expands away into the vacuum. As alluded to earlier, this property impacts significantly on the sensitivity of any spectroscopic method used to probe the expansion. Finally, collisions are observed to fall off very rapidly and relatively few collisions occur very far downstream from the nozzle.

It is clear from this discussion that binary collisions between gas particles are responsible for the observed cooling effect. Thus, by maximizing the number of collisions that occur in the expansion, the lowest temperatures can be obtained. As the expansion proceeds downstream, however, collisions eventually cease and a limiting, or terminal Mach number,  $M_T$ , is reached. Anderson and Fenn have shown

that for an Argon expansion the terminal Mach number is dependent only on the stagnation pressure and the nozzle diameter [53]:

$$M_T(\text{Ar}) = 133 (P_0 D)^{0.4} \quad (\text{I.7})$$

Thus, in the absence of condensation, increasing either the stagnation pressure or the nozzle diameter should increase the number of binary collisions, and thus, increase the terminal Mach number and the degree of cooling provided by the jet. There are two major limitations to the indiscriminate increase of  $P_0 \cdot D$  in an attempt to increase cooling. First, it has been shown that the formation of diluent gas clusters and van der Waals complexes of the analyte with the diluent gas also depends on the stagnation pressure and nozzle diameter, scaling with  $P_0 \cdot D^q$  [54], where  $q$  is a constant which is dependent on the diluent gas. The formation of clusters signal the onset of condensation, which will result in a warming of the expansion. Secondly, increasing  $P_0 D$  also places increasingly excessive demands on the pumping system to maintain the vacuum. Fortunately, there are solutions to the pumping capacity problem.

Instead of relying on powerful and expensive pumping systems to maintain expansions in a "perfect" vacuum, Campargue realized that a vacuum of moderate pressure ( $\leq 1$  Torr) would produce a free-jet shock-wave structure [55,56] as illustrated by Figure I.7. The most interesting property of such a structure is the formation of the shock wave that occurs when the expanding gas particles with the greatest kinetic energy collide with and repel the warm background gases of the vacuum chamber. This is illustrated by the boundary shock wave of Figure I.7. Within the region defined by the barrel shock and the Mach disk, the expansion behaves as if it were in an infinite vacuum. This area has been referred to as the "zone of silence" or the isentropic core of the expansion. Expanding particles within this region will exhibit the temperature, pressure and density relationships described previously (equations I.4-5). This technique has the added advantage that much higher mass flow rates can be utilized since a perfect vacuum is not needed. Thus,

increases in the sensitivity of spectroscopic measurements are also attained.

Two additional theoretical parameters can be calculated for these types of expansions [50]. The location of the Mach disk downstream from the nozzle opening can be estimated by:

$$X_m = 0.667 D (P_0/P_{cell})^{\frac{1}{2}} \quad (I.8)$$

A nozzle diameter of 300  $\mu\text{m}$ , a stagnation pressure of 1.5 atmospheres, and a vacuum cell pressure of 20 mTorr results in a Mach disk location 48 mm from the nozzle opening. The diameter of the Mach disk can then be calculated:

$$D_m = 0.45 X_m \quad (I.10)$$

which gives 22 mm for the Mach disk described above. Obviously these numbers are rough estimates, but they do give an idea of the relative size of the shock wave.

The second means of reducing the demands on the pumping system is to use one of the various pulsed valve designs as described in the following section. Since the gas only flows into the vacuum while the valve is open, it is only necessary for the pump to be able to evacuate the system before the next pulse.

## 2. Nozzles

It is evident from these previous discussions that the formation and characteristics of a supersonic expansion are highly dependent on the nature of the nozzle that is used as the interface between the sample reservoir and the vacuum cell. This is reflected in the fact that nozzle design is an area of continuous, active research. In addition, no one nozzle design meets the requirements of all the varied studies that utilize supersonic expansions. For

instance, a nozzle designed to maximize the production of van der Waals clusters would be a poor choice for the analysis of a pure substance. Thus, a variety of different nozzles have been developed and described in the literature, each of which meets the needs of the particular investigation. Nozzles can be subdivided into two basic groups, continuous and pulsed. In addition, these nozzles can be either axis-symmetric (circular) or slit shaped, depending on the application.

Slit-shaped, planar nozzles have certain advantages over conventional circular nozzles. Theoretical and experimental investigations indicate that the density in a planar expansion,  $\rho/\rho_0$ , decreases more slowly than for a circular nozzle [57]. This means that a molecule traveling the same distance in each type of nozzle will undergo more collisions in the planar nozzle. This allows  $T_{\text{vib}}$  and  $T_{\text{rot}}$  to relax farther toward equilibrium with  $T_{\text{trans}}$ . Unfortunately,  $T_{\text{trans}}$  also relaxes more slowly in the planar expansion. This means that in a planar expansion  $T_{\text{rot}}$ ,  $T_{\text{vib}}$ , and  $T_{\text{trans}}$  are closer in magnitude but reach a higher ultimate temperature. A more obvious advantage is the improvement in sensitivity which is available due to the increased downstream density. In addition, the longer pathlength available from the planar expansion allows absorbance measurements to be made [58].

#### a. Continuous-Flow Nozzles

The pioneering studies by Kantrowitz and Grey [22] and Campargue [56] utilized axis-symmetric continuous-flow nozzles to produce supersonic expansions and they have continued to be widely used since then. Continuous expansions have the advantage that they are relatively easy and inexpensive to construct and can be heated to very high temperatures or cooled to very low temperatures with little complication. Their disadvantages include the considerable pumping requirements stressed earlier, and the poor duty factor exhibited



when they are used with pulsed laser systems; only a small fraction of the gas flowing continuously through the nozzle will be sampled by the laser.

Small's early analytical studies of supersonic expansions were carried out using a continuous expansion created simply by heating a piece of pyrex glass tubing until a pinhole was formed [19]. More recently, Johnston described a circular, continuous nozzle which utilized an outer sheath gas to focus the expanding analyte back toward the expansion axis, thereby increasing the downstream density and thus improving detection limits [24,25]. The nozzle was ultimately designed for use as a gas chromatographic inlet, and for the analysis of liquids and supercritical fluids. Finally, Rice experimentally characterized the expansions resulting from slit-shaped nozzles using a continuous, planar nozzle [57].

#### b. Pulsed-Flow Nozzles

Pulsed-Flow nozzles have the advantages outlined earlier of reducing vacuum pumping requirements and exhibiting a better duty factor when matched with pulsed lasers. The most common pulsed valve design is the modified automobile fuel injector [59-60]. A stock fuel injector is typically modified by drilling a hole of the desired diameter in a metal shim, which is then attached to the face of the fuel injector valve. A current pulse is applied to the solenoid windings of the valve, causing an internal stainless steel plunger to slide back, breaking the vacuum seal. When the current is turned off the plunger is forced back against the sealing face by a spring, thereby reestablishing the vacuum seal. This type of valve has several advantages including the fact that it is reasonably inexpensive (approximately \$40.00 from an auto parts supplier). In addition, the valve duty cycle can be easily adjusted by the external triggering circuitry. Finally, since the valves are designed to be used continuously in automobiles they can be reliably used over

several hundred thousand pulses (unless a caustic sample is used which etches the sealing surface), and they can be operated at reasonably high temperatures ( $\leq 150^{\circ}\text{C}$ ).

The main disadvantage is that these valves have a minimum pulse width of approximately 0.5 ms which may be too long for many studies. In addition, the interior of the valve is constructed of stainless steel which might act as a catalyst, aiding in decomposition or reaction of the analyte. Finally, exceedingly high temperatures are not possible since the solenoid windings are held in place by a plastic spacer and silicone O-rings which will deform at temperatures above  $150^{\circ}\text{C}$ . Ishibashi has addressed this last problem by disassembling a stock valve and replacing the plastic parts with Teflon [61]. The modified valve could then be operated at temperatures up to  $300^{\circ}\text{C}$ .

Pulsed valves with narrower minimum pulse widths are commercially available but have limited maximum operating temperatures as discussed by Ishibashi [61]. An example of a narrow pulse-width valve is the 10- $\mu\text{s}$  valve developed by Gentry and Giese [62]. In this design, a flexible metal bar seals against an O-ring encircling the nozzle opening. When a current pulse flows through the bar, it flexes and breaks the seal, allowing a 10- $\mu\text{s}$  burst of gas to flow into the vacuum.

More recently, Callis described a pseudo-pulsed valve system that was used as a capillary GC interface [23,63]. Because capillary GC flow rates are too low to provide the stagnation pressure necessary to achieve significant cooling, a novel pulsed/continuous nozzle was designed. The capillary column effluent flows into an antechamber containing a 416- $\mu\text{m}$  orifice leading directly into a vacuum cell. The antechamber is also backed by a commercial pulsed valve with a 760- $\mu\text{m}$  orifice. The pulsed valve, backed by 1.65 atm of Argon, pulses open for 600  $\mu\text{s}$  at 5 Hz. As the pressure in the antechamber rises during the period the pulsed valve is open, the temperature of the expansion, flowing continuously out of the narrower antechamber orifice, drops. An advantage of this design is that the antechamber can be heated to high temperatures ( $220^{\circ}\text{C}$ ) to

prevent condensation of the analyte, while the commercial valve can be kept relatively cool, below its maximum operating temperature.

Amirav reported the first pulsed planar nozzle which consisted of two concentric tubes with 0.2 mm by 35 mm slits cut in them [58]. The space between the tubes was lubricated with MoS<sub>2</sub> powder and the inside tube was rotated to produce 150  $\mu$ s pulses at 12 Hz during the period of time the two slits lined up. Another pulsed, slit-shaped nozzle design is based on the fuel injector valve described earlier [64]. In this case, a small hole is drilled directly in the center of the shim attached to the face of the valve. The nozzle tip, including the shim, is then placed on a translation stage in the path of a tightly focused Nd:YAG laser. The laser beam is first centered on the shim by monitoring the beam power through the rear of the starter hole while translating the nozzle back and forth across the beam. Once centered, the laser is brought to full power and the nozzle is slowly translated linearly across the beam, thus cutting a narrow slit in the shim. The resulting slit has dimensions of 200  $\mu$ m by 600  $\mu$ m, typically, and is often more oval shaped than planar. Since the aspect ratio (length divided by width) of such a nozzle is fairly low, planar characteristics will probably only be observed very close to the nozzle, with circular characteristics prevailing further downstream [57]. However, gains in pathlength are certainly realized by such an expansion.

It is evident from the previous discussions that the type of nozzle used in an experiment is dependent on the type of measurements being made, with no single design applicable to all experiments. Consequently, the selection or design of the nozzle is an important consideration when developing a new method utilizing supersonic expansions. In the case of this research, the nozzle design and other jet parameters, such as the type of diluent gas and the stagnation pressure, must be considered in terms of their effect on chromatographic separations.

### C. Chromatographic Interfacing Considerations

#### 1. Carrier / Diluent Gas

Perhaps the most interesting component of both GC separations and supersonic cooling is the carrier/diluent gas. Fortunately for this work, both systems operate well when a monatomic gas such as helium or argon is chosen as the carrier gas. Under first consideration, a heavy carrier gas such as argon might be considered ideal for achieving both high chromatographic and spectroscopic resolution.

This can be explained as follows. Since longitudinal diffusion of the analyte in a gas chromatography column is inversely proportional to the density of the carrier gas, the use of denser gases, such as argon, would be expected to result in less longitudinal diffusion, and thus produce narrower peaks and higher resolution. This is indeed true as long as the linear flow rate is maintained at its optimum value. However, if the carrier gas velocity is increased to decrease analysis times, the separation efficiency and thus the resolution decreases rather quickly. On the other hand, helium, which is less efficient at its optimum flow rate than argon, exhibits a slower decrease in separation efficiency with increasing flow velocity (*i.e.*, a flatter van Deemter curve). Thus, if helium is chosen as the carrier gas, higher flow rates can be used to decrease analysis times with only a relatively small sacrifice in separation efficiency. Thus, even though helium does not provide the highest ultimate separation efficiency, it is a widely used carrier gas due to other factors such as the potential decrease in analysis time.

The situation is similar for the choice of diluent gas in a supersonic expansion. Higher molecular weight gases such as argon or xenon can accelerate the large PNA molecules via collisions much more quickly than can the very light helium. In addition, the collisions

of the heavier gases are more efficient at transferring internal energy. Thus, cooling occurs more rapidly for the heavier gases than for helium and thus a greater degree of cooling can be reached before collisions cease [65]. As a result, argon, which is also relatively inexpensive, is often used as a diluent gas with excellent results. Unfortunately, these larger gases are also much more polarizable than helium, and thus are more likely to form van der Waals complexes, resulting in a shift in the observed transitions, and a warming of the expansion [66]. If condensation and the formation of clusters is a problem under a desired set of experimental conditions, then helium or neon would be a better choice for a diluent gas.

## 2. Nozzle Interface

Likewise, since the nozzle is the interface between the chromatographic system and the spectroscopic system, consideration must be given to the optimum configuration for both the chromatography and spectroscopy. The nozzle orifice diameter, the magnitude of the vacuum, the valve pulse width and rate, if applicable, and the column inlet pressure, will all affect the chromatographic column flow rate as well as the properties of the supersonic expansion. If the nozzle flow rate is too small as a result of a small diameter orifice, or a low pulse width or rate, the average linear velocity of the GC carrier gas might be reduced, allowing significant longitudinal diffusion to occur, decreasing the chromatographic resolution. Conversely, if the orifice diameter is too large, the column outlet pressure would be essentially that of the vacuum, which might result in excessive flow rates which would also adversely affect the chromatographic resolution.

On the other hand, the effective back pressure at the column outlet, which is also a function of the variables cited above, will affect the characteristics of the expansion and thus the spectral resolution.

Other nozzle-related factors that can degrade chromatographic performance include cold trapping of high molecular weight vapor phase analyte molecules on unheated nozzle surfaces. Such cold-trapping results in tailing of the chromatographic peak or, even worse, clogging of the nozzle orifice. Thus, it is desirable to heat the nozzle to high temperatures, preferably near or above the boiling point of the analyte molecules, 250-300 °C if possible. Also, the dead volume of the nozzle and any transfer lines leading from the column to the nozzle can contribute to broadening of the chromatographic peak. Thus, transfer line volumes should be minimized, as should the dead volume of the nozzle. Finally, if it is anticipated that labile species will be determined, the nozzle should be constructed of materials which will minimize decomposition or reaction.

With these considerations in mind, it is worthwhile to examine the applications of supersonic expansions to the analysis of PNAs, particularly with respect to supersonic expansion / chromatography interfaces. In addition, the "library" of high resolution spectra, extracted from the chemical literature will also be examined.

#### D. Applications of Supersonic Expansions to the Fluorescence Determination of PNAs

Analytical applications of supersonic expansions have been reviewed by several authors [67-69]. In addition, there have been major advances in the field since the publishing of these reviews, including improvements in detection limits and chromatographic interfaces. Table I.7 is a summary of detection limits reported for the laser excited fluorescence analysis of PNAs measured in supersonic expansions. It can be seen that many of these detection limits are at least close to the desired sub-nanogram level, and one system has achieved a detection limit (50 pg) which rivals even the flame ionization detector. Thus, detection limits are approaching

Table I.7

Detection Limits Reported for Laser-Excited Fluorescence  
Determinations of PNAs in Supersonic Expansions

PNA	Sample Introduction	Detection Limit	Ref.
Perylene	Heated Cell	100 ng	70
Naphthalene	Crude GC	60 ng	21
Naphthalene	Capillary GC	0.05 ng	24
1-Methylnaphthalene	Crude GC	14 ng	21
2-Methylnaphthalene	Crude GC	40 ng	21
1-Methylanthracene	Capillary GC	3 ng	23
2-Methylanthracene	Capillary GC	6 ng	23
9-Methylanthracene	Capillary GC	2 ng	23

the levels required to make it a competitive method. One area, however, which is still sorely lacking in scope is the "library" of published high resolution spectra.

## 1. Survey of Published Spectra.

The characteristics of available high-resolution fluorescence spectra of a variety of PNAs in supersonic expansions are summarized in Table I.8. This information was gleaned from the chemical literature and originates from both fundamental studies and analytical applications. Note that there are only 14 unique PNAs represented here and these 14 derive from only 7 parent PNAs. Thus, it is obvious that there is a dearth of published spectra, thereby placing severe limitations on the use of this method for fingerprinting the components of complex mixtures. Consequently, the spectra of a wide variety of parent PNAs and their substituted analogs need to be obtained and published for use by those considering the use of this method for qualitative and quantitative analysis.

Of particular interest is the location of the origin band representing excitation from the lowest vibrational level of the ground electronic state to the lowest vibrational level of the first excited singlet state. In sufficiently cooled molecules this transition, often called the 0-0 transition, will be the lowest energy, longest wavelength transition in the spectrum. This transition and those at shorter wavelengths, representing excitation to excited vibrational levels of the excited electronic state, are often intense and unique to a particular PNA and thus can be useful in fingerprinting PNAs. Since the origin wavelength is only known accurately for a few compounds (see Table I.8), alternate methods must be used to locate the origin in previously uncharacterized compounds.



Table I.8

Survey of High-Resolution Fluorescence Spectra Obtained on PNAs in Supersonic Expansions

PNA	Formula	Type <sup>1</sup>	Scan Range (Å)	Origin (Å) <sup>2</sup>	Refs.
Naphthalene <sup>3</sup>	C <sub>10</sub> H <sub>8</sub>	Ex	3080-3085	---	24
Naphthalene <sup>3</sup>	C <sub>10</sub> H <sub>8</sub>	Ex	3070-3160	3123.0	19
1-Methylnaphthalene <sup>3</sup>	C <sub>11</sub> H <sub>11</sub>	Ex	3070-3160	3147.4	19
2-Methylnaphthalene <sup>3</sup>	C <sub>11</sub> H <sub>11</sub>	Ex	3070-3160	3154.4	19
Fluorene <sup>3</sup>	C <sub>13</sub> H <sub>10</sub>	Ex	2890-2990	2960.2	67
Anthracene <sup>3</sup>	C <sub>14</sub> H <sub>10</sub>	Em	3600-4200	---	61
Anthracene <sup>3</sup>	C <sub>14</sub> H <sub>10</sub>	Ex	3610-3840	---	67
9,10-Dichloroanthracene	C <sub>14</sub> H <sub>10</sub> Cl <sub>2</sub>	Ex	3850-3865	3854.1	58
9,10-Dichloroanthracene	C <sub>14</sub> H <sub>10</sub> Cl <sub>2</sub>	Ex	3852-3856 + 3805-3810	3854.25	67
1-Methylantracene <sup>3</sup>	C <sub>15</sub> H <sub>13</sub>	Ex	3620-3740	---	23
2-Methylantracene <sup>3</sup>	C <sub>15</sub> H <sub>13</sub>	Ex	3620-3740	---	23
9-Methylantracene <sup>3</sup>	C <sub>15</sub> H <sub>13</sub>	Em	3600-4200	---	61
9-Methylantracene <sup>3</sup>	C <sub>15</sub> H <sub>13</sub>	Ex	3620-3740	---	23
9-Methylantracene <sup>3</sup>	C <sub>15</sub> H <sub>13</sub>	Ex	3610-3840	---	67
9,10-Dimethylantracene <sup>3</sup>	C <sub>16</sub> H <sub>16</sub>	Em	3600-4200	---	61
9,10-Dimethylantracene <sup>3</sup>	C <sub>16</sub> H <sub>16</sub>	Ex	3610-3840	---	67
Fluoranthene	C <sub>16</sub> H <sub>10</sub>	Ex	3600-4000	3965.6	60
Tetracene	C <sub>18</sub> H <sub>12</sub>	Ex	4400-4500	---	67
Perylene	C <sub>20</sub> H <sub>12</sub>	Em	4200-5000	---	70
Perylene	C <sub>20</sub> H <sub>12</sub>	Ex	4140-4170	4154.2	70
Benzo[a]pyrene	C <sub>20</sub> H <sub>12</sub>	Em	3900-4700	---	70

<sup>1</sup>Ex = excitation spectrum, Em = emission spectrum<sup>2</sup>The wavelength of the 0-0 transition if it is identified explicitly.<sup>3</sup>Spectrum is part of the spectrum of a mixture of PNAs, not a pure spectrum.

One possibility would be to use the origin wavelength as determined by one of the solid-state cryogenic techniques as the starting point for a search. The origin of the PNA frozen in a solid matrix will be shifted in wavelength relative to the isolated PNA due to matrix interactions and thus can only be used as a starting point to find the origin of the isolated PNA. For instance, the origin of naphthalene as measured in 3-methylpentane glass at 10 K is 3153.5 Å [71], while in the supersonic expansion it is located at 3123.0 Å [19]; a difference of 30 Å. Similarly, the origin of fluorene frozen in the same glass is 3006.9 Å [71], while it is located at 2960.2 Å in the supersonic expansion [67]; a difference of 47 Å. Unfortunately, the library of the spectra of solid state PNAs is not much more extensive than that for PNAs in supersonic expansions.

The most realistic solution to this problem has been discussed by Lubman [72] and involves simply using the gas-phase absorbance spectrum as a guide to the location of the origin. The origin band will be located close to the long wavelength onset of absorbance. Thus, by examining the gas-phase absorbance spectrum, the origin location can be estimated, often to within several nanometers [72]. This method has the additional advantage that the instrumentation required to obtain the absorbance spectra is available to most any analytical laboratory.

## 2. Survey of Analytical Applications

As discussed previously, the first true analytically oriented application of supersonic expansions was described by Warren, Hayes and Small [19] in 1982. In this study, the high resolution fluorescence excitation spectrum of a mixture of naphthalene, 1-methylnaphthalene and 2-methylnaphthalene was presented to illustrate the great selectivity of the method. The selectivity was emphasized by the fact that many of the peaks in the spectrum were baseline resolved. No detection limits, or real samples were

examined. However, later that same year Hayes and Small published the results of a quantitative analysis of the same three substances [21]. In this study samples were introduced to the expansion via a very crude GC consisting of an 8-inch length of pyrex tubing packed with 3% OV-101 on 80/100 mesh packing support. The "GC" was simply used as a means to quantitatively transfer the samples in the gas phase to the nozzle, which consisted of a 150- $\mu$ m pin hole in the end of a sealed capillary tube. Detection limits of 14-60 ng were reported and the method was applied to the quantitative analysis of crude oil. The results obtained by the fluorescence analysis agreed well with those obtained via GC-MS. During this same period, Amirav also discussed potential analytical applications, illustrated by the qualitative identification of a fluorene impurity in "pure" biphenyl [67].

It was clear from these early investigations that this was potentially a very powerful analytical technique due to the excellent selectivity and reasonable sensitivity. Since the fluorescence spectroscopy and spectroscopic instrumentation had been reasonably well characterized in many previous fundamental studies, it was also realized that the most substantial improvements could be made with regards to the chromatography and the ability to perform quantitative analyses. Consequently, much of the effort since that time has been directed toward optimization of the chromatography and the development of nozzles and interfaces which are compatible with various chromatographic systems.

During the past decade, capillary gas chromatography has become one of the most powerful tools available to the analyst attempting the determination of the components of complex organic mixtures. It is no surprise then that the development of capillary GC interfaces to supersonic expansions has been stressed by many of the most recent studies in this field. Such an interface is non-trivial due to the disparate flow rates associated with capillary chromatography and a supersonic expansion. A capillary GC-supersonic expansion interface must allow the GC to operate at low flow rates, 2 mL/min typically, while providing much higher flow through the nozzle, 300-400 mL/min.

Two different interfaces have been designed which address this problem.

The nozzle interface designed by Callis, which was described earlier, utilizes a heated antechamber into which the capillary column effluent flows continuously [23,63]. A commercial valve then pulses argon backing gas into the chamber, increasing the back pressure and thus the flow rate through the antechamber orifice into the expansion. This design allows the capillary column to be operated at the desired low flow rate of 1-2 mL/min, while flow through the antechamber nozzle is substantially higher, determined by the gas introduced through the pulsed valve. Detection limits of 2-6 ng were reported for isomeric methylanthracenes and the system was applied to the analysis of an air particulate filter extract from a tire fire in Everett Washington.

The second capillary GC interface is described by Johnston and, as described earlier, utilizes a sheath gas to focus the column effluent to the center of the expansion, thereby increasing the on-axis density [24,73]. In this design the inner nozzle, which is connected to the outlet of the capillary column, is operated at the desired low flow rate, while the concentric outer nozzle bearing the sheath gas is operated at the higher flow rates characteristic of the supersonic expansion. The on-axis density is reported to be increased by a factor of 20 and detection limits are correspondingly lower. The detection limit for naphthalene was reported to be 50 pg which is a factor of 20-40 times lower than the unfocused results reported by Callis. The method was applied qualitatively to the analysis of unleaded gasoline. In addition, this same nozzle has been used for the analysis of PNAs in liquids and supercritical fluids, although the focusing enhancement appears only to apply to gas-phase samples [25]. The ability to obtain high resolution spectra of liquid samples is particularly important since the resolution of liquid chromatography (LC) systems is substantially lower than that of capillary GC. Thus, there is an even greater need for selective detection methods in LC than in GC [74].

In conclusion, it is entirely likely that one might question the utility of interfacing a laser, which is very expensive, complicated, and frequently unreliable, to a chromatographic system costing many times less and for which many sensitive detectors are already available. Hopefully, however, the previous discussions have helped to explain the motivation behind this effort and the great benefits which might be attained with any successes. Additional insight may be obtained by considering the situation from the opposite point of view as is done by Yeung [74].

". . .laser spectroscopy in its various forms . . . does indeed provide valuable information to the analytical chemist, and such measurements are generally greatly enhanced if one incorporates some form of chromatographic separation prior to the spectroscopic measurement, with almost no increase in cost or inconvenience."

In addition, it is hoped that the results of the research presented in the following pages will help to emphasize the great benefits to be gained by the application of lasers and supersonic expansions to analytical chemistry, and in particular their union with chromatographic separations.

## II. Instrumentation

The instrumentation employed in this research originates from a variety of sources including commercial manufacturers and previous research projects. Much of the required equipment, however, was not available commercially or in our department. Consequently, a great deal of custom design work was also necessary. In addition, much of the instrumentation which was adopted from other applications had to be modified to allow proper interfacing to the desired experimental system. The overall instrument configuration is outlined by the block diagram shown in Figure II.1. In the following sections, each component of the instrumentation is described, with an emphasis placed on the custom designed components and interfacing the system to a microcomputer.

### A. Laser System

#### 1. Chromatix CMX-4 Dye Laser

The laser used for all experiments was a Chromatix CMX-4 flashlamp-pumped tunable dye laser (Chromatix Inc., Sunnyvale, CA). The important characteristics of this laser have been described elsewhere [75] and are summarized in Table II.1. Briefly, the CMX-4 utilizes a linear flashlamp to pump the laser dye which is flowing rapidly through a quartz flow tube. The flashlamp and dye flow tube are placed at each foci of an elliptical reflector cavity to ensure efficient use of the energy provided by each pulse of the flashlamp. The laser dye used for all experiments was rhodamine 590 chloride (Exciton Chemical Co., Dayton, OH) prepared at a concentration of  $1.1 \times 10^{-4}$  M in four liters of 50% methanol- 50% deionized water.

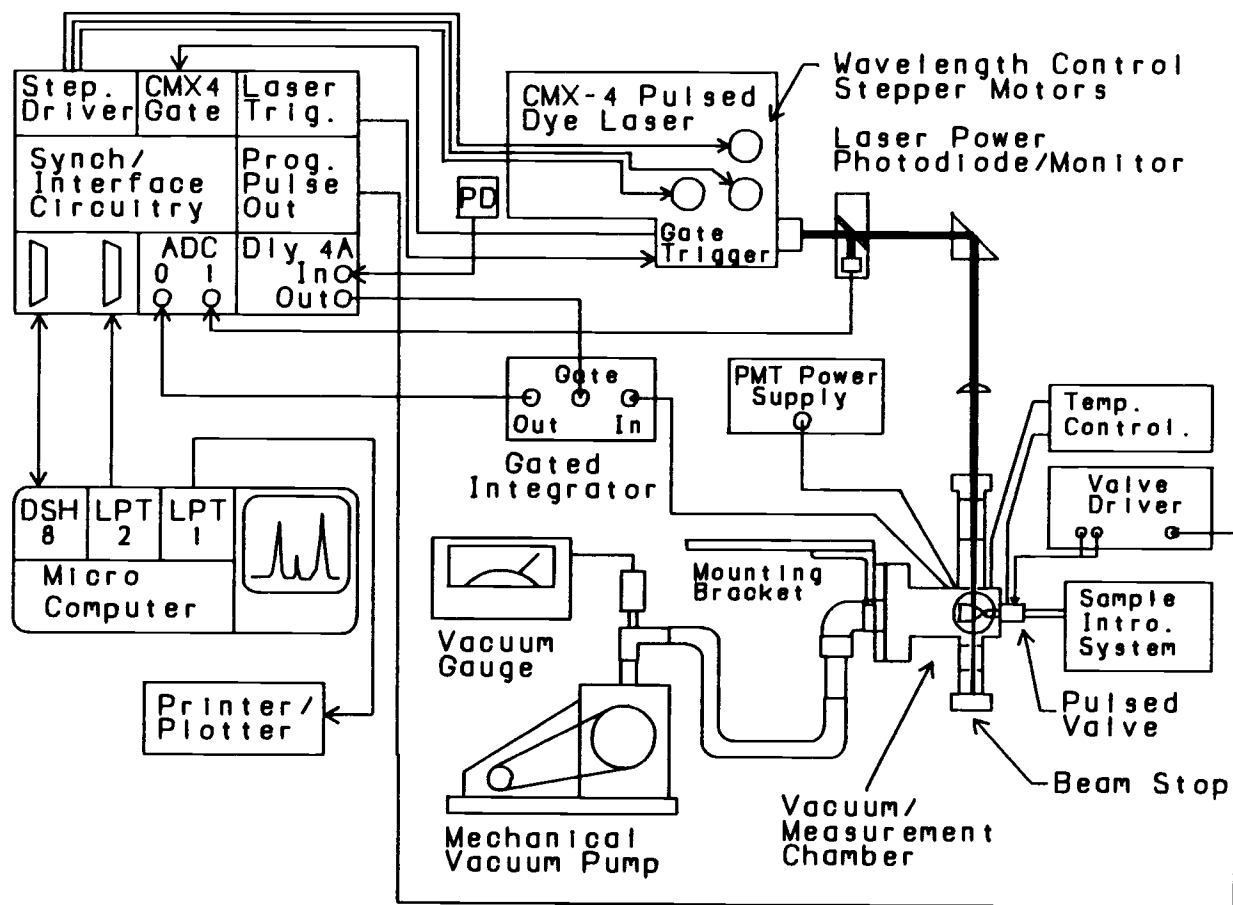


Figure II.1 Block diagram of the laser-excited fluorescence-supersonic expansion experimental system.

Table II.1  
CMX-4 Laser Specifications

Parameter	Nominal Value
Tuning Range	
Visible	435 to 730 nm
Ultraviolet	265 to 365 nm
Bandwidth	
Birefringent Filter Only	3 cm <sup>-1</sup>
With Intracavity Etalon	0.1-0.15 cm <sup>-1</sup>
Output Power (nominal)	
Visible	46 mw
Lamp Voltage @ 6 KV, R6G Dye @ 5985 Å, 5 pps	
Ultraviolet	15 mw
Lamp Voltage 7kV R6G Dye @ 6000 Å, 10 pps	
Pulse Duration	1 μs
Repetition Rate	30 pps (Max)
Front Panel selectable	5,10,15,20,30 pps
By External Triggering	0 to 30 pps
Pump Source	Linear Flashlamp (Model L-1832, ILC Technology, Sunnyvale, CA)
Wavelength Calibration	Via laser-induced impedance changes in a pulsed, hollow cathode lamp:
Calibration Accuracy:	
Birefringent Filter	±0.25 Å
Etalon and B.F.	±0.05 Å
Ultraviolet Wavelength Generation	Via second harmonic generation in an angle-tuned ADP crystal



### a. Triggering Requirements

The laser can be triggered to fire only while the 60-Hz line supply power is in the positive portion of its cycle. This places an upper limit of 30 Hz on the available repetition rates. In the current research, the laser is triggered by external circuitry to ensure synchronization with the control and detection systems. The CMX-4 provides a square wave synchronization signal at its GATE OUT terminal which is held high (+10 V) during the period of time that the laser is able to be triggered. The synchronization circuitry described in later sections, monitors this signal to determine when to externally trigger the laser. The external trigger is a 12-V, 0.8- $\mu$ s pulse which is sent to the trigger input terminal on the CMX-4. In order to prolong flashlamp life, a repetition rate of 5 pulses per second (pps) was used for most experiments. Flashlamps typically last for 600,000 shots before they shatter, which usually necessitates complete disassembly of the optical cavity to remove all glass splinters.

### b. Laser Wavelength Selection

Two intracavity tuning elements are used to select the lasing wavelength and bandwidth. Coarse control of the wavelength is maintained by a five-plate quartz birefringent filter. The birefringent filter allows a  $3\text{-cm}^{-1}$  ( $\approx 0.25 \text{ \AA}$  at  $3000 \text{ \AA}$ ) bandwidth of laser radiation to pass through with its polarization unaffected as determined by the angle of the optical axis of the crystal with respect to the beam axis. Those wavelengths within the birefringent filter's bandwidth pass unattenuated through the various Brewster angle surfaces in the optical cavity. Wavelengths outside the

bandwidth of the birefringent filter exit with their polarizations rotated to some extent and thus are partially reflected out of the optical path by the Brewster windows. Since laser action requires photons to make multiple passes through the optical cavity, only those wavelengths which experience minimal losses will be able to exceed the lasing threshold. Rotation of the birefringent filter by a stepper-motor-controlled micrometer determines the effective refractive index of the filter and thus the coarse lasing wavelength.

If a narrower laser bandwidth is required, a high-finesse Fabry-Perot etalon is rotated into the optical cavity. This intracavity etalon reduces the laser bandwidth to approximately  $0.15 \text{ cm}^{-1}$  ( $0.015 \text{ \AA}$  at  $3000 \text{ \AA}$ ) with a corresponding loss of approximately 50% of the laser power. The etalon is characterized by two closely spaced, reflective surfaces separated by a distance,  $d$ , and possessing a refractive index,  $\eta$ . The wavelengths which will constructively interfere when passing through the etalon, and thus experience the least attenuation, are defined by

$$m\lambda = 2d\eta \quad (\text{II.1})$$

Thus, by changing the etalon thickness, the wavelengths passed by the etalon are also changed. In the CMX-4 the effective etalon thickness, and thus the lasing wavelength, is altered by changing the etalon's angle with respect to the axis of the laser beam [76]. The etalon angle is also adjusted by a stepper-motor-controlled micrometer.

### c. Ultraviolet Wavelength Generation

The CMX-4 is also outfitted with an ultraviolet wavelength generation option consisting of three ammonium dihydrogen phosphate (ADP) non-linear frequency doubling crystals. These intracavity crystals provide a means by which the fundamental lasing wavelength,

located in the visible wavelength range, can be doubled in frequency. Thus, the CMX-4 is also capable of delivering a tunable source of laser radiation in the ultraviolet wavelength range.

These nonlinear crystals operate in the following manner. When an electric field is incident on one of these crystals, a polarization of the electric charges within the crystal occurs, which can be described approximately by the following power series:

$$P = \chi^{(1)}E + \chi^{(2)}E^2 + \chi^{(3)}E^3 + \dots \quad (\text{II.2})$$

where  $P$  is the induced polarization,  $E$  the electric field arising from, in this case, the laser radiation, and the  $\chi$  terms are the susceptibilities. With conventional sources the incident electric field is small enough that only the first term in equation II.2 is significant and the induced polarization is proportional to the electric field. However, if the applied electric field is very intense, such as that produced by a laser, the situation becomes more complex since the higher order terms become significant and the induced polarization is no longer "linear" with respect to the applied electric field.

The second harmonic generation (SHG) or frequency doubling phenomena used to generate ultraviolet radiation from visible fundamental radiation is related to the second order susceptibility,  $\chi^{(2)}$ . To illustrate how the frequency is doubled, the expression for a simple electromagnetic wave with  $E = E_0 \sin \omega t$ , can be substituted into the second term of equation II.2, resulting in the following expression, after the appropriate trigonometric identity is used:

$$\frac{1}{2}\chi^{(2)} \cdot E_0^2 \cdot (1 - \cos 2\omega t) \quad (\text{II.3})$$

Thus, the laser radiation induces an oscillation in the crystal at twice the frequency ( $\cos 2\omega t$ ) of the fundamental laser frequency. In order to ensure that the fundamental and second harmonic waves remain in phase throughout the crystal, they must be "phase matched". This

is accomplished by rotating the crystal, which is birefringent, so that the refractive index for the extraordinary, frequency-doubled wave is the same as that of the ordinary, fundamental wave.

The three different crystals in the CMX-4 have their optical axes oriented at successively larger angles with respect to the beam axis. As the fundamental wavelength increases, requiring larger crystal rotation angles, the next crystal is inserted into the cavity. This minimizes the reflective losses which would occur if a single crystal had to be rotated to very large angles with respect to the laser beam. The crystal rotation angle is adjusted by a micrometer which was interfaced to a stepper motor in this project to provide computer control of the phase-matching angle. The stepper motor system and computer interface will be described in later sections.

Stepper motor control of the etalon, birefringent filter and doubling crystal is required to provide a means by which computer-controlled fluorescence excitation wavelength scans can be obtained. In addition, accurate wavelength calibration of the laser is greatly simplified if it can be performed under computer control.

#### d. Wavelength Calibration of the CMX-4 Laser

##### (1) Etalon and Birefringent Filter

The method used to wavelength calibrate the CMX-4 etalon and birefringent filter has been described in detail by Beenen and Piepmeier [75,76]. Briefly, the CMX-4 laser beam is directed into the cathode of a commercial, pulsed hollow cathode lamp. When the laser is tuned to a spectral transition of one of the atomic species present in the lamp discharge, these atoms can be ionized. This causes the impedance of the discharge to change due to the presence of an increased number of charged species. The laser-induced

impedance change (LIIC), or optogalvanic effect (OGE), is observed by monitoring the change in the lamp voltage at the output of signal processing circuitry described elsewhere [75,77]. By scanning the laser wavelength across the atomic transition, which is narrower in bandwidth than the laser, a convoluted spectral profile of the laser beam centered around the transition wavelength, is obtained. Since the wavelengths of these atomic transitions are precisely known, the wavelength of the laser at the center of the spectral profile can be determined. The etalon and birefringent filter micrometer positions at the center of the spectral profile are recorded for several known transitions and can be fit to suitable equations.

The wavelength-micrometer position relationship for the birefringent filter is fairly simple and can be described accurately by a quadratic polynomial [76]. Consequently, the birefringent filter calibration data are fit to a second order polynomial and the three regression coefficients, B0, B1, and B2 can be used to predict the wavelength of a particular micrometer setting to within  $\pm 0.25$  Å.

Unfortunately, the situation for the etalon is not quite so simple. One of the disadvantages of using an etalon for tuning a dye laser is the fact the relationship between etalon position and wavelength is rather complicated and multivalued. During previous work in this lab it was determined that the position of the etalon dial setting is related to the wavelength by the following equations [76]:

$$m\lambda_{\text{air}} = \frac{2t}{\eta_1} [\eta_2^2 - \eta_1^2 [1 - (\text{Eighty}^2 \cos^2 \Phi) / (x^2 + \text{Eighty}^2)]]^{\frac{1}{2}} \quad (\text{II.4a})$$

or, rearranging,

$$x = \text{Eighty} \left[ \frac{\cos^2 \Phi}{(m\lambda_{\text{air}}/2t)^2 - (\eta_2/\eta_1)^2 + 1} - 1 \right]^{\frac{1}{2}} \quad (\text{II.4b})$$

where  $x$  is the etalon turns number;  $\text{Eighty}$  is the product of the pitch of the screw used to change the etalon tilt angle and the 2.00-inch lever arm which connects the screw with the etalon mount;  $\Phi$  is the slight angle the etalon is tilted to prevent feedback of the laser into the active medium;  $m$  is the etalon order;  $t$  is the thickness of the etalon;  $\lambda_{\text{air}}$  is the wavelength in air; and  $\eta_1$  and  $\eta_2$  are the refractive indices of air and quartz, respectively, at  $\lambda_{\text{air}}$ .

A simplex optimization of the calibration parameters  $\text{Eighty}$ ,  $\cos^2 \Phi$ ,  $t$ , and a fourth term,  $\Delta x$ , is then implemented to obtain the best values for these parameters; the best values being those which most accurately describe the relationship between  $x$  and  $\lambda_{\text{air}}$ . The fourth etalon calibration parameter,  $\Delta x$ , is the difference between the true etalon zero and the etalon dial reading of 0.000. The true etalon zero is measured by tilting the etalon until the reflection of the laser beam off the etalon surface is visibly observed to be in the same horizontal plane as the laser beam as viewed on an index card outside of the cavity. The etalon turns number,  $x$ , in equations II.4a and II.4b is thus the dial reading +  $\Delta x$ . The response used in the simplex optimization is the inverse of the sum of the square of the differences between the wavelengths calculated using the adjustable calibration parameters in equation II.4a and the true wavelengths, for a number of position-wavelength pairs:

$$\text{Simplex Response} = 1 / [ \sum ( \lambda_{\text{true}} - \lambda_{\text{calc}} )^2 ] \quad (\text{II.5})$$

Thus, the simplex response increases as the calculated wavelengths approach the true wavelengths summed over all transitions (as the sum of the squared residuals decreases). This method has been used to obtain calibration parameters which allow the wavelength to be set within  $\pm 0.05 \text{ \AA}$  for all wavelengths used in the calibration. The software used to perform these calibrations will be discussed in subsequent sections.

## (2) UV Doubling Crystal

The relationship between the UV doubling crystal phase matching angle and the fundamental laser wavelength can also be described by a quadratic polynomial. The phase matching angle for a particular fundamental wavelength is determined by first scanning the laser to the desired wavelength using the calibration parameters determined above. The doubling crystal is then rotated to optimize the power of the second harmonic beam. The UV counter value at the optimum position is then recorded and a second order polynomial fit is performed on a number of these wavelength-counter value pairs over the wavelength range of interest. The three regression coefficients,  $U_0$ ,  $U_1$  and  $U_2$  can then be used to accurately predict the UV counter value for a desired wavelength.

## 2. Stepper Motor Control of the CMX-4 Laser

As indicated above, all three of the laser tuning elements are interfaced to stepper motors to provide computer control of their position. Both the etalon and birefringent filter interfaces were developed in a previous project and have been described elsewhere [78]. In addition, as part of the current research, the doubling crystal micrometer was also interfaced to a stepper motor. All three stepper motors have a resolution of 200 steps/revolution with  $1.8^\circ$  step angles and maximum step rates of greater than 1000 steps/sec.

The computer interface to these motors is described in a subsequent section. However, it is worth noting that each stepper motor is controlled by a commercial translator which converts a single pulse from the computer into a single motor step. The important factor then becomes the relationship between a stepper

motor step and the relative movement of the particular micrometer (the resolution of one step). All three of the CMX-4 micrometers are read in a different manner, have different micrometer scales and different stepper motor interfaces. This means that the micrometer-stepper motor step resolution is different for each of these tuning elements. Some of the characteristics of these micrometers and the resultant relationship to the stepper motors are summarized in Table II.2. It should be noted that in all three cases the calibrated resolution provided by the stepper motor interfaced micrometer (see Units/Step column of Table II.2) is greater than that provided by the micrometer scale alone (see Units Between Scale Markings column). This is because the stepper motor can accurately position the micrometer between division markings, whereas when positioning the micrometer by hand, the micrometer must be aligned directly on a division marker to be in an accurately known position.

#### a. Birefringent Filter and Etalon

The birefringent filter micrometer position is read from a vernier scale located beneath the micrometer knob as illustrated by Figure II.2A. An angled mirror is used to view the scale more easily. In the discussions that follow, movement of the various micrometers and dials is reported in terms of a micrometer "unit". This unit is simply a change of 1.00 on the scale of the particular micrometer. Thus, for instance, the birefringent filter micrometer requires four complete rotations to change its scale reading by 1.00. This means that one rotation of the birefringent filter micrometer will change its scale reading by 0.25 units. The scale of the micrometer was marked at spacings of 0.01 units. This represents the smallest calibrated change that can be set by hand. The stepper motor is not connected directly to the micrometer knob, but rather drives several gears which ultimately provide a step resolution of



Table II.2  
CMX-4 Wavelength Control Stepper Motor  
and Micrometer Characteristics

	Characteristics			
	Micrometer		Stepper Motor	
Tuning Element	Micrometer Units/Rev.	Units Between Scale Markings	Steps/Micr. Div.	Units/Step
B.F.	0.25	0.01 Units	11.12	0.0009
Etalon	1.00	0.01 Units	2.0	0.005
UV	26.7	0.2 Units	10	0.1

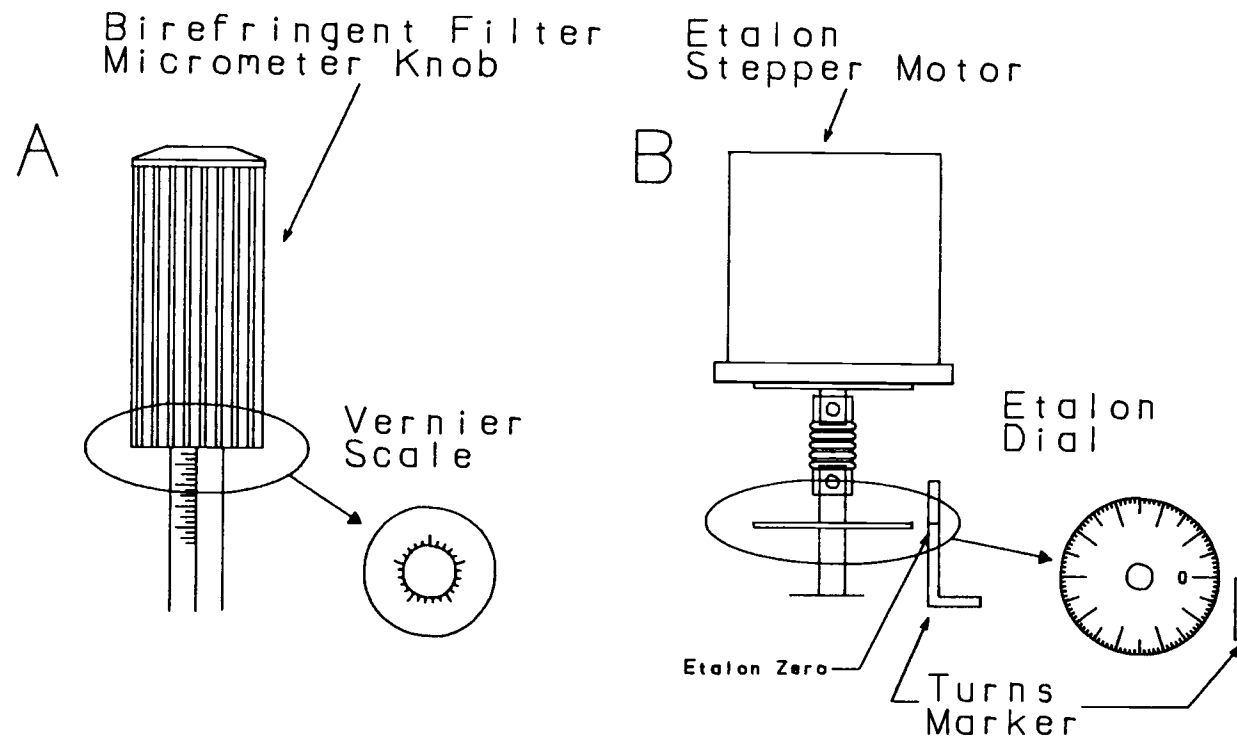


Figure II.2. Diagram of (A) the birefringent filter micrometer and vernier scale, and (B) the etalon dial and turns marker.

11.12 steps per micrometer division (1111.65 steps per 1 micrometer unit). Finally, at a wavelength of 5900 Å one step of the birefringent filter stepper motor corresponds to a wavelength change of 0.07 Å.

The etalon position is read from a dial located below the stepper motor as illustrated in Figure II.2B. One complete turn of the dial, arising from one revolution of the stepper motor (200 steps), represents one etalon unit or "turn". The individual divisions on the dial indicate fractions of a turn. Since the stepper motor is coupled directly to the micrometer, one step of the motor results in  $1/200$  of a turn which is 0.005 units. It should be noted that only fractions of turns can be read directly off the dial (at the edge of the turns marker as illustrated in Figure II.2B). The only full turn graduation that has been marked is the zero position found by stepping the etalon until the top edge of dial lines up with the small line scratched across the edge of the turns marker. Thus, the dial in Figure II.2B is set to 0.000 turns. As the etalon turns are increased, the dial moves up and away from the zero marker and the user must keep track of the current number of full-turns from zero, while the turn fraction is read directly off the dial. Finally, one step of the etalon at 5900 Å represents a wavelength change of 0.006 Å.

#### b. Ultraviolet Doubling Crystal

In order to automate ultraviolet wavelength scans a stepper motor was interfaced to the CMX-4 doubling crystal phase-matching micrometer knob. This provides a means by which a microcomputer can control the phase matching angle.

### (1) Stepper Motor and Translator

An Aerotech Model D3001 Stepping Translator and Model 45SM, 45 oz-in, 200 step per revolution stepper motor (Aerotech, Inc., Pittsburgh, PA) were used to control the doubling crystal. The D3001 is a single circuit board translator that contains all the hardware and functions required to drive a stepper motor. The only additional components needed to use the translator are a 115 VAC input power line and the various digital I/O lines required to provide external control. These connections were made by placing the translator board in a chassis and interfacing the board with the various external connectors illustrated in the schematic diagram in Figure II.3. In this figure connectors J1 and J3 are the edge connectors on the translator board itself, and C1 and C2 are Amphenol bulkhead connectors located at the rear of the chassis. Connector C1 provides access to the six stepper motor driver lines identified in Table II.3. Connector C2 is used to bring the control lines in from the computer circuitry. The control lines are identified in Table II.4. Note that control of the stepper motor is made through the computer's parallel printer port (LPT). The details of this control are discussed in a subsequent section.

An important characteristic of the design of the translator is that the direction line must be set at least  $0.5 \mu\text{s}$  before sending a clock pulse to step the motor. Also, in the current configuration, holding the remote direction line high (+5 V) results in the crystal being stepped in the positive direction (as read on the counter), while holding the remote direction line logic low (0 V) will result in the crystal being stepped in the negative direction.

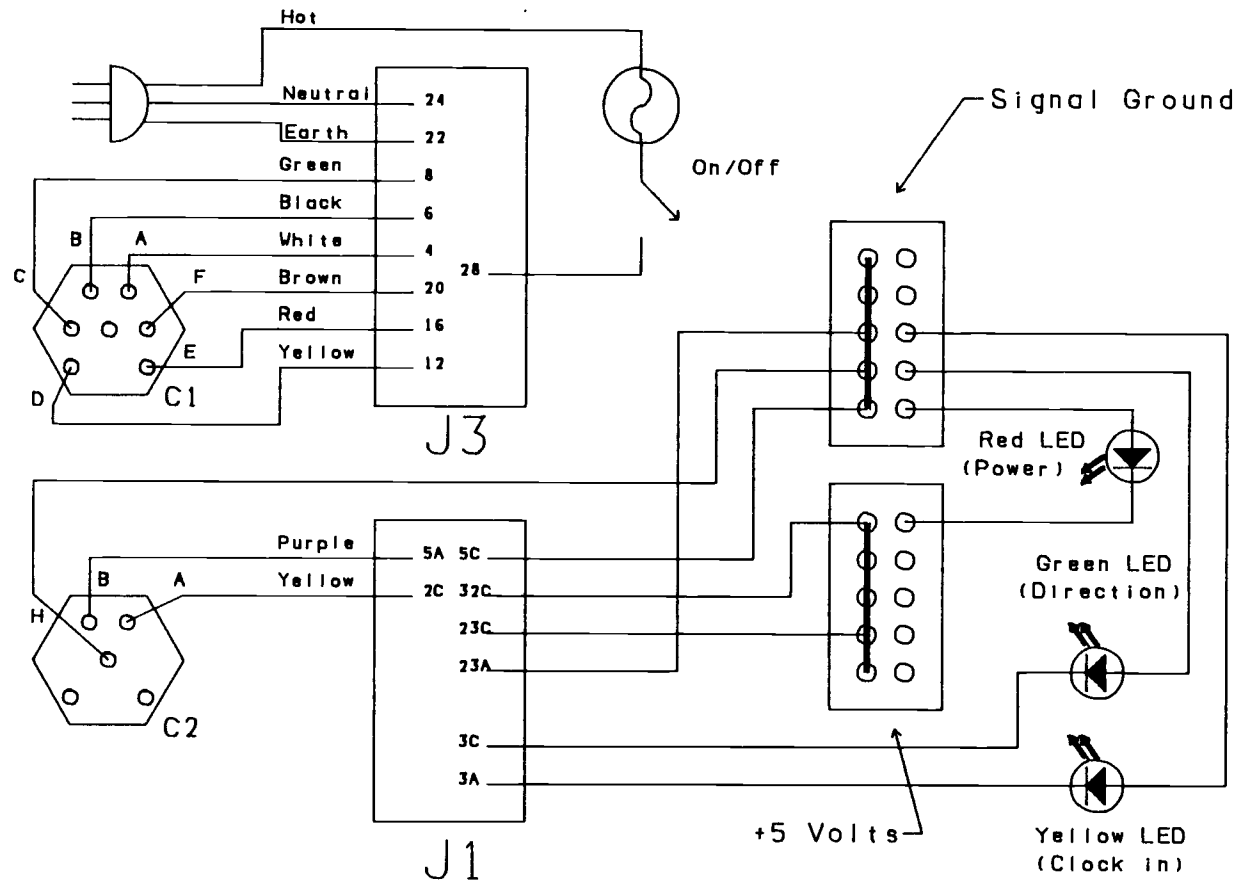


Figure II.3 Schematic wiring diagram of the stepper motor translator chassis.

Table II.3

D3001 Translator: Connector C1 Terminal Identities  
for the Stepper Motor Driver Lines

Stepper Motor Wire Color	Connector C1 Pin Number	Edge Connector J1 Lead Number
White	A	4
Black	B	6
Green	C	8
White/Green	D	12
Red	E	16
White/Red	F	20

Table II.4

D3001 Translator: Connector C2 Terminal Identities  
for the Stepper Motor Control Lines

Connector C2 Pin Number		Translator Function	Connections	
			Internal	External
A	Remote Direction: Logic High = Step Crystal +		J1 terminal 2C	Computer LPT pin 6
B	Remote Clock: +5 V pulse Steps Motor 1 step		J1 terminal 5A	Computer LPT pin 7
H	Signal Ground		Signal Ground Terminal Strip	Computer LPT pin 19

## (2) Stepper Motor Gearing

The main consideration in interfacing the stepper motor to the doubling crystal micrometer knob was using a gear ratio which provided a reasonable number of integer steps per each unit change on the UV counter. In addition, the step resolution, also determined by the gear ratio, had to be high enough to allow the phase matching angle to be precisely set, but not so high that an excessive number of steps would be required when changing wavelengths. The gears used in this research, and their configuration are outlined in Figure II.4. The UV counter, gear G1 and the belt connecting G1 to the micrometer knob (the micrometer knob itself acts as a 48-groove gear) are part of the stock CMX-4 UV doubling crystal system. These components are set up as follows. One complete revolution of G1 produces a ten-unit change on the UV counter. In addition, the gear ratio of G2 to G1 is 2.67 (48 grooves/18 Grooves). This means that one rotation of the micrometer knob results in 2.67 rotations of G1 and 26.7 units change on the counter.

In the process of evaluating the stepper motor interface, it was determined that a resolution of 0.1 counter unit per step of the stepper motor would provide sufficient resolution for this application. This was accomplished by attaching a 36-groove gear (G3) to the spindle of the stepper motor, providing a G3/G2 gear ratio of 0.75. Thus, a complete rotation of the stepper motor (200 steps) rotates the micrometer knob 0.75 turns. This in turn results in 2 full rotations of G1 and a change of 20.0 counter units. One step of the stepper motor thus results in a 0.1-unit change on the counter (20 counter units/rev. \* 1/200 rev./step).

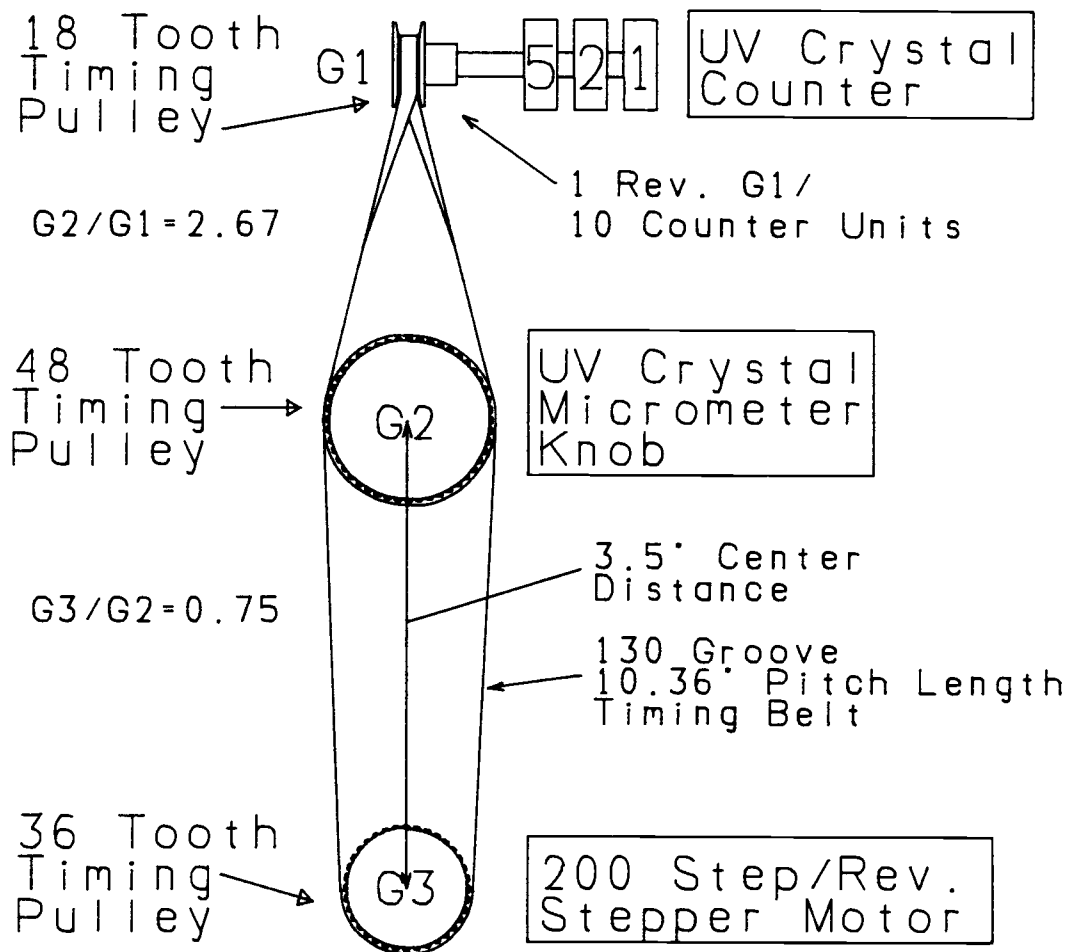


Figure II.4 Diagram of the gears and gear ratios used in interfacing a stepper motor to the ultraviolet doubling crystal micrometer knob.



### (3) Stepper Motor Mount

Two pieces of hardware had to be designed and constructed to allow the stepper motor and its gear to be physically mounted to the laser. First, a clamp was designed to attach a 48-groove timing pulley to the top of the micrometer knob. This was necessary because the pitch of the integral gearing of the micrometer knob is non-standard. Consequently, no matching belt or gear could be purchased which had the same pitch as the knob. By anchoring a standard size pulley to the top of the micrometer this problem was solved. The pulley clamp is shown in Figure II.5, which also illustrates the general configuration of the stepper motor mounting system. The stepper motor was mounted to an existing platform on the CMX-4 laser which also holds the etalon and birefringent filter stepper motors. The mounting bracket, diagrammed in Figure II.6, allows the stepper motor to be anchored firmly to the laser with its gear positioned in the same horizontal plane as the gear clamped to the top of the doubling crystal knob. The slots milled in the base of the mount allow it to slide and thus adjust the pressure on the belt connecting the two gears. The optimum mount position is when the back edge of the motor mount aligns evenly with the back edge of the mounting platform. In this position the belt is tight enough that there is no significant "play" when changing directions, but not so tight that the micrometer binds. The mount must be slid towards the micrometer to install or remove the timing belt. Removal of the belt and the micrometer clamp is necessary if access to the interior of the laser is required (*i.e.*, to clean the spark gap) since the clamp interferes with the removal of the outer laser chassis.

### (4) Reading the Stepper Motor Position

A 100-division dial is mounted on the stepper motor spindle to

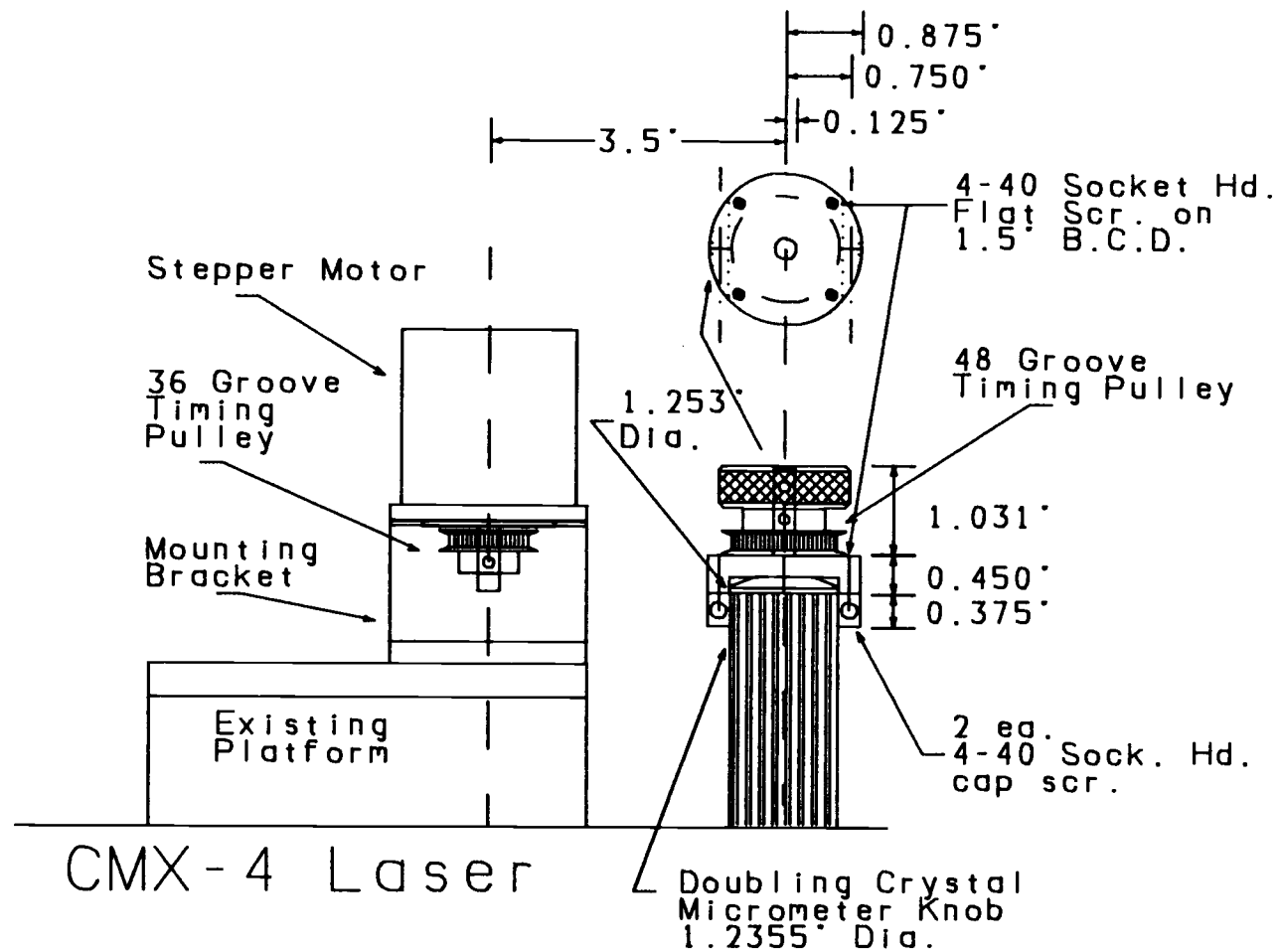


Figure II.5 Side view of the ultraviolet doubling crystal stepper motor and the micrometer knob pulley and clamp.

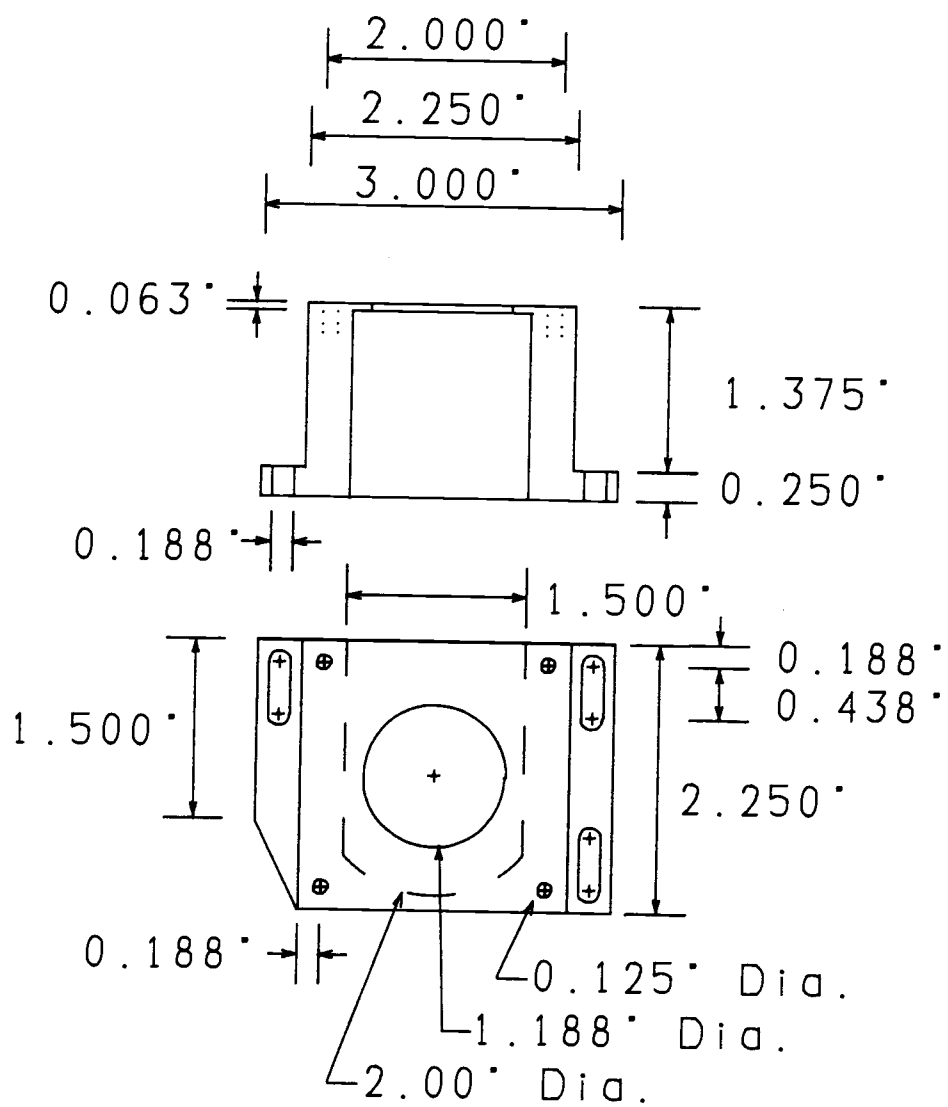


Figure II.6 UV doubling crystal stepper motor mounting bracket.

provide a means by which fractions of a UV counter unit can be read precisely. Position is read relative to a marker scratched on the top of the stepper motor. Since the stepper motor provides 200 steps per revolution, one step of the motor moves the dial 0.5 divisions. In addition, as discussed previously, one step of the motor also moves the UV counter by 0.1 unit. Thus, each division on the dial represents 0.2 counter units. It should be noted that as a result of the relationship between the total number of divisions on the dial (100), and the number of dial divisions which correspond to a 1 unit change on the counter (5), there is no particular correlation between the numeric units value printed on the dial (10,20,...) and the counter's position. Thus, the doubling crystal position cannot be read by adding the counter reading directly to the dial reading. Rather, the actual position is calculated first by reading the UV counter and then counting the number of stepper motor steps the marker is located past a major division on the dial (5,10,15,...). This is illustrated by the example in Figure II.7. In this example the counter is located between 482 and 483 and the dial marker is located 3 steps past a major division (in this case 60). Thus, the UV micrometer position in this example is 482.3.

### 3. CMX-4 Cooling Water and Laser Dye Pumping System

FitzPatrick and Piepmeier have shown that the spatial mode structure of a laser beam is dependent on the difference in temperature between the laser dye and the laser cooling water [79]. In spectroscopic experiments it is often desirable to ratio the analytical signal with the signal from a photodetector monitoring the source power, thereby correcting the analytical signal for fluctuations in the source energy. If the spatial mode structure of the laser beam changes from pulse to pulse, different portions of the photodetector are illuminated which can lead to irreproducible source energy measurements. To minimize this source of noise, the CMX-4

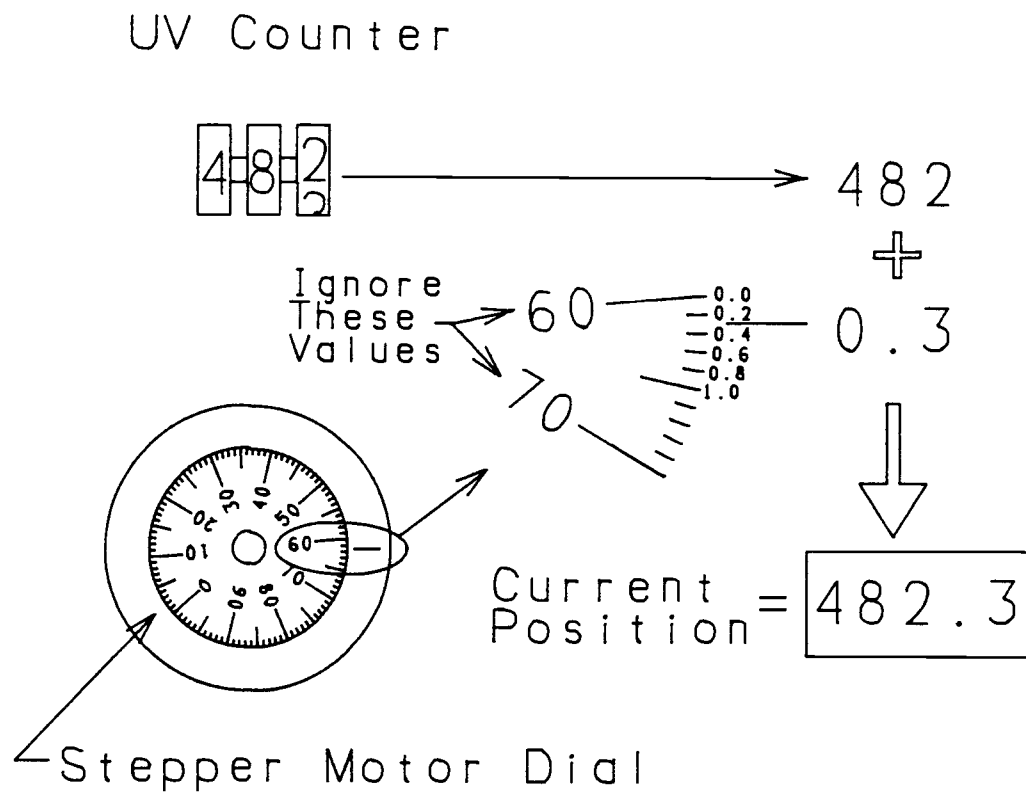


Figure II.7 Diagram of the ultraviolet doubling crystal micrometer counter and stepper motor dial configured for a position of 482.3 units.

laser dye was maintained at a temperature approximately 2 °C greater than the temperature of the cooling water that circulates through the laser cavity using a refrigerated constant-temperature bath. In the early stages of this research difficulties in maintaining the cooling water temperature were experienced. This problem was eventually traced to the coils of the refrigerated bath which had become coated with algae preventing efficient heat transfer. After cleaning the coils the problem disappeared.

The laser dye, which is made up in four liter batches, is placed in a stainless steel container insulated by a styrofoam jacket and is cooled by water flowing through stainless steel tubing coils immersed in the dye. A small pump (Model 120-405, Micropump Corp., Concord, CA) is used to circulate the laser dye rapidly (approximately 5 LPM) through the dye flow tube in the laser cavity.

#### 4. Laser Power and Synchronization Photodiodes

Two photodiodes are used in this research; one to synchronize the detection system and the other to measure the energy of each laser pulse for correction of the analytical signal as discussed above. Both of these photodiodes and their associated circuitry have been described in detail elsewhere [75,80]. The synchronization photodiode is located at the rear of the laser, behind the rear cavity reflector. When the laser fires, enough of the beam passes through the rear reflector and onto the photodiode that an electrical pulse is generated. This pulse is then used by the detector synchronization circuitry as a signal that the laser has fired.

As the laser beam exits the CMX-4, it passes through a beam splitter which directs a fraction of the beam onto a second photodiode. The current produced when the beam strikes the photodiode is integrated by support circuitry and is held at its final value by a storage capacitor and is sampled by an analog-to-digital converter discussed in a subsequent section. The

module in which this laser power photodiode is located also has a small slot which allows one of several neutral density filters to be inserted into the beam path to prevent saturation of the photodiode. When operating in the visible wavelength range, a 1.5 absorbance unit filter is normally used, while in the ultraviolet range no filter is required.

## 5. Beam Blocker/Filter Holder

The final component of the laser system is a beam blocker module. This module serves two functions. First, it contains a solenoid actuated shutter which can be opened and closed under computer control. This provides a means by which the detector dark current signal can be obtained under normal operating conditions with the laser pulsing. This module also contains a slot into which a color glass filter can be inserted to filter the fundamental radiation from the frequency doubled beam during experiments requiring only ultraviolet excitation radiation.

## B. Optical Table Configuration

The CMX-4 laser, vacuum/measurement chamber and assorted optics are mounted on a 4 x 10 foot optical table (Newport Research Corporation, Fountain Valley, CA) tapped with  $\frac{1}{4}$ -20 screw holes on 1 inch centers. The configuration of the components mounted on the table is shown in Figure II.8. The laser beam exits the CMX-4 and passes through the beam blocker and the laser power monitor before being reflected 90° by a corner mirror. The beam travels past the edge of the optical table and is reflected 90° down toward the floor by a second mirror. It then passes through a plano-convex

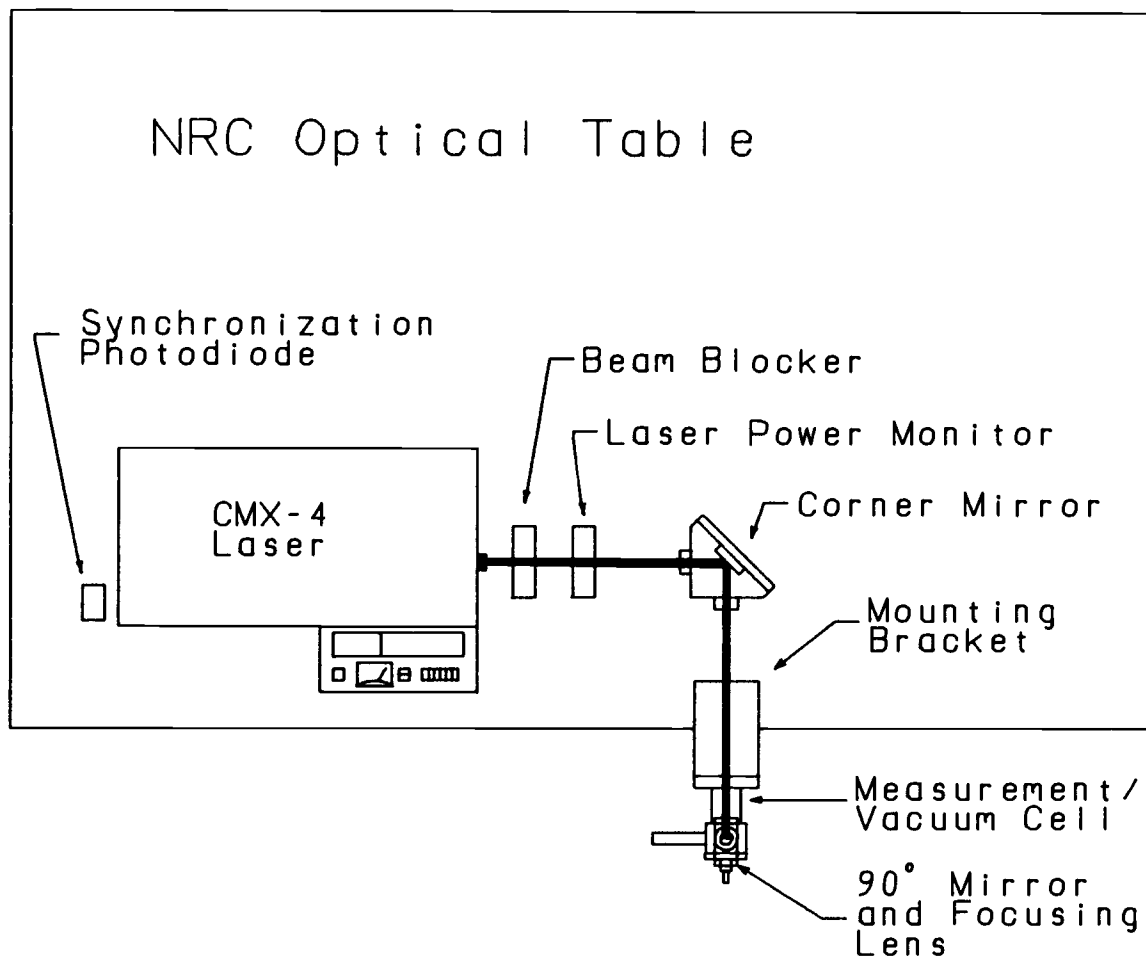


Figure II.8 Experimental optical table configuration.



fused-silica lens with a 12-inch focal length (Esco Products Inc., Oakridge, NJ) before entering the measurement chamber which is also anchored to the optical table.

### C. Measurement/Vacuum Cell

The measurement cell is an important, but sometimes overlooked part of most spectroscopic systems. Whether a simple cuvette or a more complex system such as the cell used in this work, it acts as the interface between the radiation source, the sample, and the detection system and thus is of particular importance in ensuring reproducible results. The design of the cell can often mean the difference between success and failure in the development of a new spectroscopic system. The design of the measurement cell was of particular importance in this research due to the conditions under which it had to be operated. The interior of the cell had to be held under a vacuum while still providing access to the excitation laser beam, the supersonic nozzle, and the detection system. In addition, to prevent condensation of the analyte and other sample components on the interior walls, the collection optics, and in particular the nozzle tip, the cell had to be heated to high temperatures. On the other hand, the photomultiplier tube detector had to be kept reasonably cool to minimize thermally induced noise and excess dark current.

Other spectroscopic requirements included the ability to focus the laser very close to the nozzle tip to be able to sample the highest density portion of the expansion. In addition, it was desired to place the detector and collection optics as close to the laser beam-expansion intersection as possible to maximize the collection of analyte fluorescence emission. Some control over the laser beam-expansion intersection point was also desired for both alignment purposes and to allow studies of the axial characteristics of the expansion. Finally, as is the case with any fluorescence

measurement, stray light and scattered laser radiation had to be minimized. This point was of particular importance since it was hoped that the detector could be operated with no emission wavelength selection (*i.e.*, no emission filter or monochromator) to maximize throughput of the analyte fluorescence emission.

The main body of the cell that was designed for this research is illustrated in Figures II.9 and II.10. All components are constructed of aluminum and have been anodized black, both to reduce stray and scattered light and to increase the durability of the components. Vacuum seals between the various components of the cell are made with Viton O-rings and the screw holes located in the main cell block are threaded with replaceable heli-coil thread inserts. The various O-rings used by the measurement cell are summarized in Table II.5. The entrance window is a 1-inch diameter by 0.25-inch thick fused silica disc (Esco Products Inc., Oakridge NJ) and three entrance baffles with 0.196-inch diameter apertures are spaced along the 6-inch entrance arm of the cell, again to help reduce stray and scattered light. The detector arm of the cell is located at a 90° angle to the entrance arm and contains a small collection optics bundle, which will be described later, as well as the hardware necessary to mount a head-on photomultiplier tube. Finally, the laser beam exits into a 4-inch beam stop, which is also baffled to prevent back scattering of the laser radiation. Specific details about individual components of the cell are described in the following sections.

## 1. Detection Optics

A schematic diagram of the detector collection optics can be found in Figure II.11. A fused silica disc, which is identical to the disc used as the entrance window, is located at the vacuum end of detection optical group and provides the surface against which the vacuum seal is made. Next, two small Delrin spacer rings hold a one

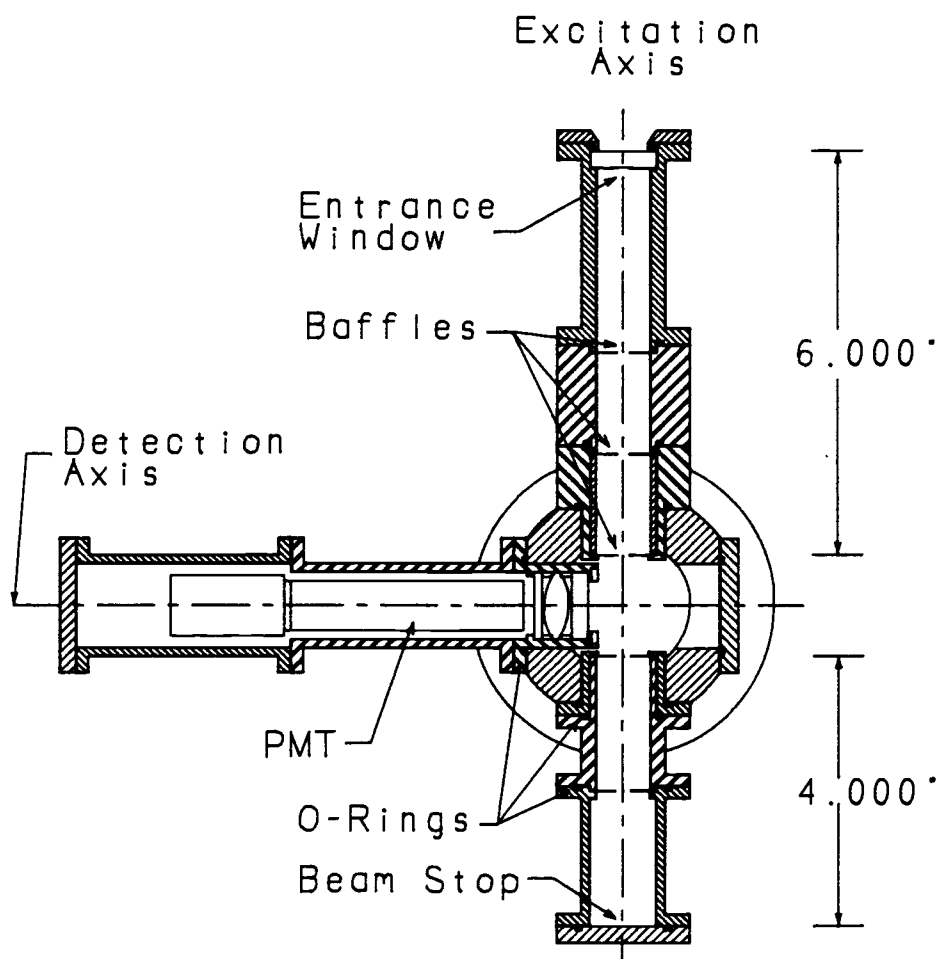


Figure II.9 Front view (looking down the expansion axis) of the supersonic jet measurement cell. The supersonic nozzle and front flange are not shown.

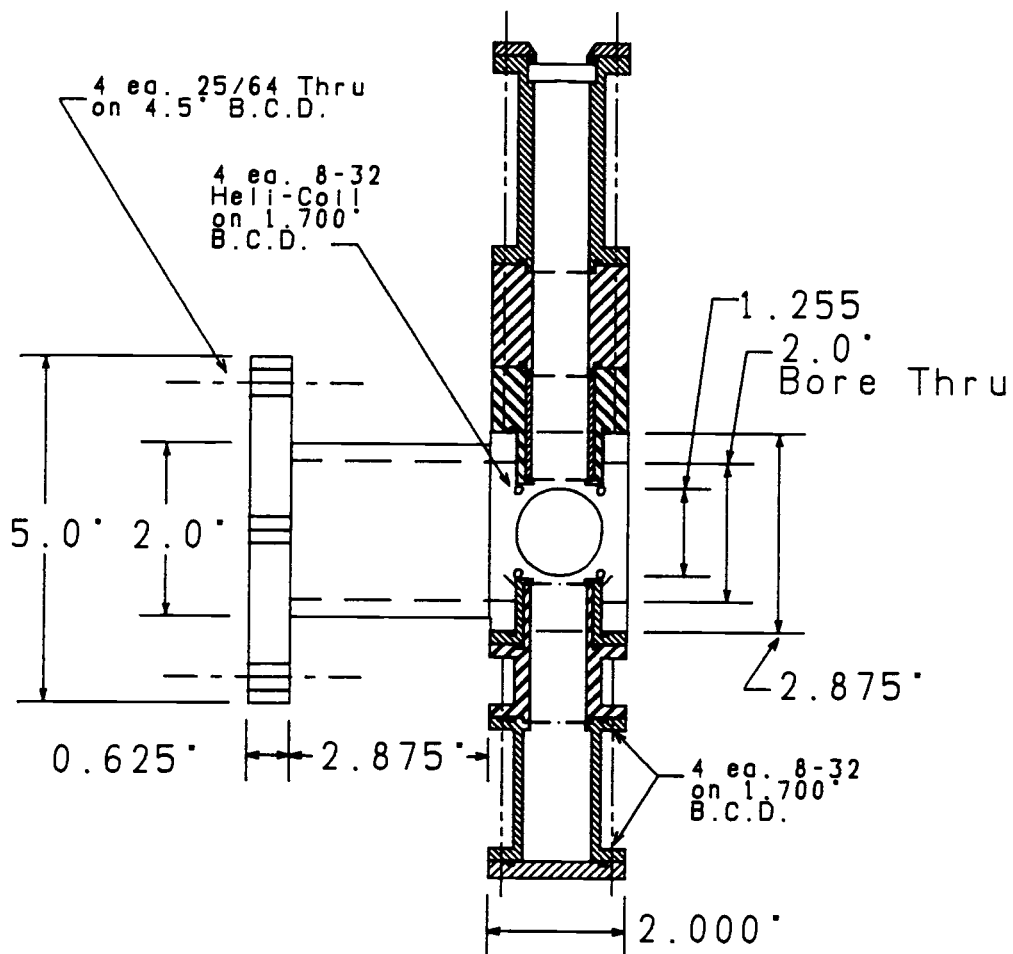


Figure II.10 Side view (looking down the detection axis) of the supersonic jet measurement cell. The supersonic nozzle, detector arm, and front flange are not shown.

Table II.5  
Supersonic Jet Vacuum Cell  
O-Ring Identification

Part	Parker Size	Dimensions (i.d. x W)	Stockroom # <sup>1</sup>
Inner Nozzle	2-010	0.239 x 0.070" (1/4 x 1/16)	FOD 025
Nozzle Tip	2-011	0.301 x 0.070" (5/16 x 1/16)	FOD 030
PMT and Entrance Windows	2-020	0.864 x 0.070" (7/8 x 1/16)	FOD 080
Entrance and Exit Tube Baffles	2-022	0.989 x 0.070" (1 x 1/16)	FOD 085
Flange Covers	2-026	1.239 x 0.070" (1-1/4 x 1/16)	FOD 105
Nozzle Flange	2-033	1.989 x 0.070 (2 x 1/16)	N/A
Diffusion Pump Flange	2-236	3.234 x 0.139 (3-1/4 x 1/8)	N/A

<sup>1</sup>The Oregon State University Chemistry Department stockroom number.

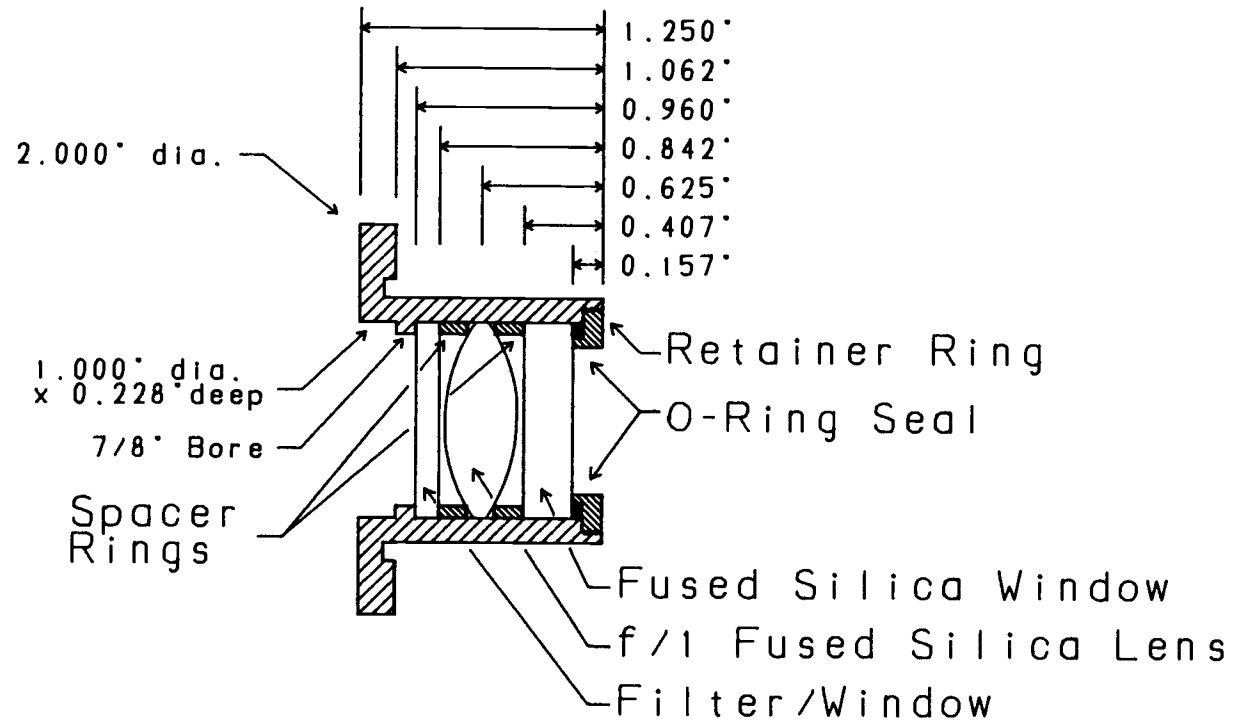


Figure II.11 Diagram of the detection optics.

inch diameter, biconvex, 1 inch focal length, fused-silica lens (Esco Products Inc., Oakridge, NJ) upright between the vacuum window and another 1/8-inch window/filter. When this optics group is mounted in the cell, the lens is located one inch from the intersection point of the excitation (laser beam) axis and the expansion axis of the supersonic nozzle. Either a transparent fused-silica disk or a variety of color glass filters can be inserted into the 1/8-inch window space at the detector end of the optics group. However, a transparent fused silica disk was used as the detector window for all experiments in this research. The components of this optical group are clamped firmly into place by a retainer ring which screws onto the vacuum window. The O-ring on the inside of retainer ring forms a vacuum seal against the window, separating the PMT detector and electronic connections from the vacuum.

## 2. Detector

The photodetector used to detect analyte fluorescence emission is a Hamamatsu R1464 head-on photomultiplier tube (Hamamatsu Corp., Middlesex, N.J.). The PMT is placed in a commercial socket assembly (Model E974-05, Hamamatsu Corp., Middlesex, N.J.) which is installed inside the detector arm of the measurement cell. A commercial encapsulated, modular power supply (Model C1309-02, Hamamatsu Corp., Middlesex, N.J.) was used to supply the high voltage to the PMT. This power supply requires a +15-VDC, 170-mA input voltage and has a resistor-adjustable output voltage range of -170 to -1100 VDC. The output voltage is set by a ten-turn precision potentiometer and is monitored continuously by digital voltmeter.

The PMT slides into the detector arm and can be anchored so that its front surface (the photocathode) is located an adjustable 1 to 2 inches from the collecting lens of the detection optics (Figure II.16, located in a subsequent section, illustrates the relationship between the detector, optics, supersonic nozzle, and the excitation

axis). Power and signal connections to the PMT are made through a flange at the rear of the detector arm.

### 3. Heated Nozzle Flange

The supersonic nozzle is screwed into a flange which is bolted onto the front of the measurement cell. A schematic diagram of the flange can be found in Figure II.12. With the flange attached directly to the face of the cell, the tip of the nozzle is located at the intersection of the excitation axis and the detection axis. In order to provide some means by which the supersonic expansion could be probed farther down stream from the nozzle tip, several spacers were constructed. These spacers can be placed between the nozzle flange and the cell face, allowing the nozzle tip to be moved back from the excitation axis a distance determined by the thickness of the spacer(s) used. The three spacers used in this work have widths of 4.5, 6.4, and 8.0 mm. It should be noted that in order to insert or change a spacer, the vacuum must be broken and the nozzle flange must be removed.

The nozzle flange was also designed to allow the tip of the nozzle to be heated to prevent condensation of the analyte in the nozzle and clogging of the orifice. Two holes are drilled into the aluminum block surrounding the nozzle tip: a 1/4-inch hole for insertion of a cartridge heater, and a 1/8-inch hole for insertion of a thermocouple probe. Finally, the nozzle flange also has a detector aperture plate that can be attached to the end of the flange, between the nozzle tip and the detector. The aperture consists of a small slot centered on the expansion axis and extending 1.5 inches beyond the end of the flange. The aperture plate acts as a spatial filter, preventing light scattered from surfaces within the chamber from reaching the detector. In addition, since the aperture slit is centered along the expansion, only fluorescence emission from the coldest, on-axis, part of the expansion is collected; warmer



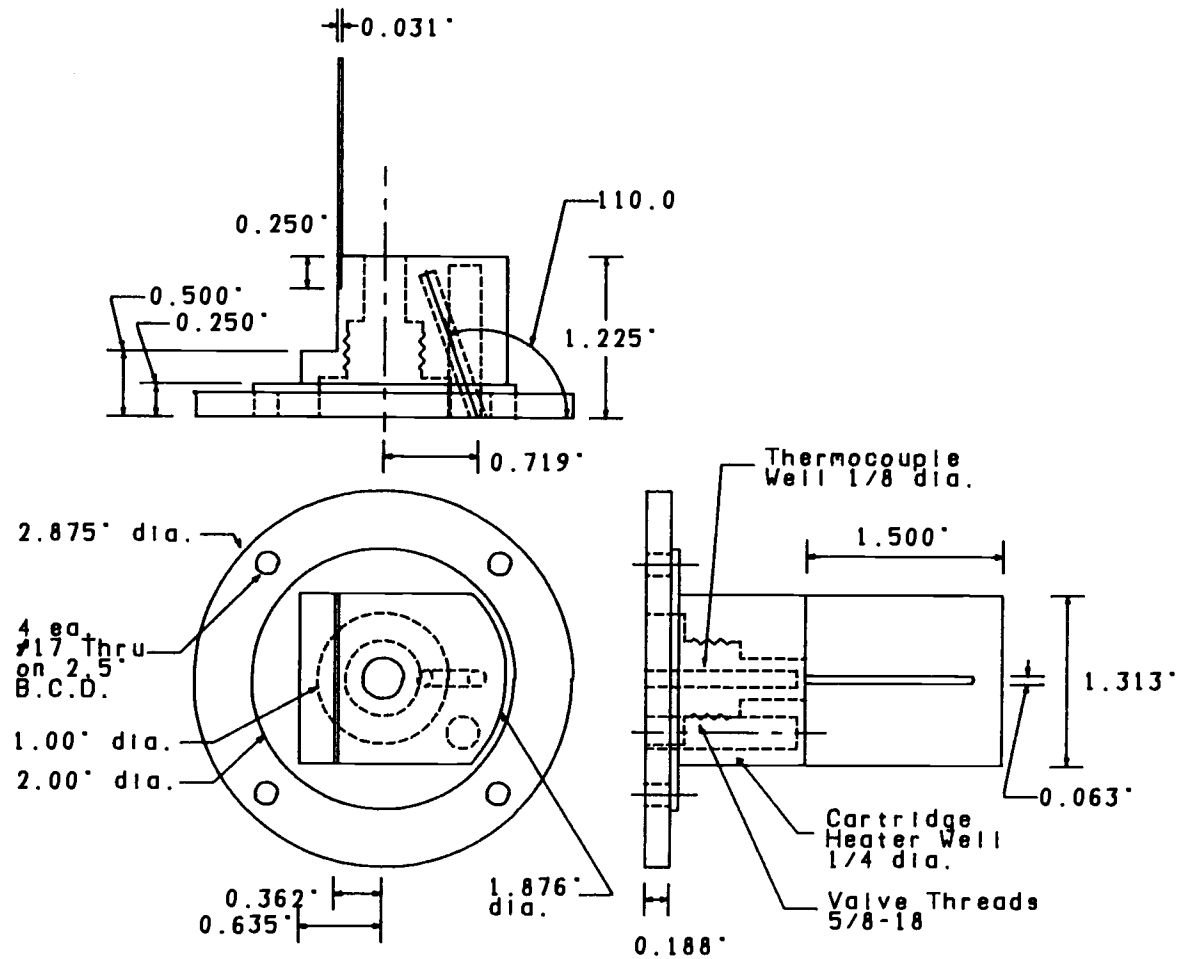


Figure II.12 Schematic diagram of the front flange of the measurement cell. The supersonic nozzle screws into the center of the flange which can be heated by a cartridge heater.

off-axis fluorescence emission is blocked. Three aperture plates with slit widths of 1/32, 1/16, and 3/32 inch were constructed, and can be interchanged depending on the requirements of the experiment.

#### 4. Temperature Control System

##### a. Temperature Controllers and Heaters

As mentioned several times before, the measurement cell and, in particular, the nozzle tip, have to be heated to high temperatures (100-300 °C) to minimize "cold trapping" of the analyte molecules on the various surfaces they might come in contact with. Temperature control of the measurement cell is accomplished using commercial temperature controllers combined with suitable cartridge heaters, thermocouples, and a mica band heater. Two model CN9000 temperature controllers (Omega Engineering, Stamford CT) were used to monitor the temperature of the nozzle flange and the sample heater block used in the continuous sample introduction experiments described later. These temperature controllers are small, self contained, microprocessor controlled units that require only 120 VAC input power and the proper thermocouple and heater for a particular application. For reasons of convenience and safety, the controllers were placed in a chassis. The wiring diagram of the temperature controller circuitry is shown in Figure II.13. Note that each controller has two on/off switches associated with it; one is the master power switch, while the other is placed in series with the heater. This allows the controller to be switched on and to display the temperature without sending current to the heater, which is useful when the system is being cooled down from operating temperatures.

From preliminary investigations it was determined that the mechanical relay included with the CN9000 could not be cycled quickly enough to properly control the temperature of the nozzle flange.

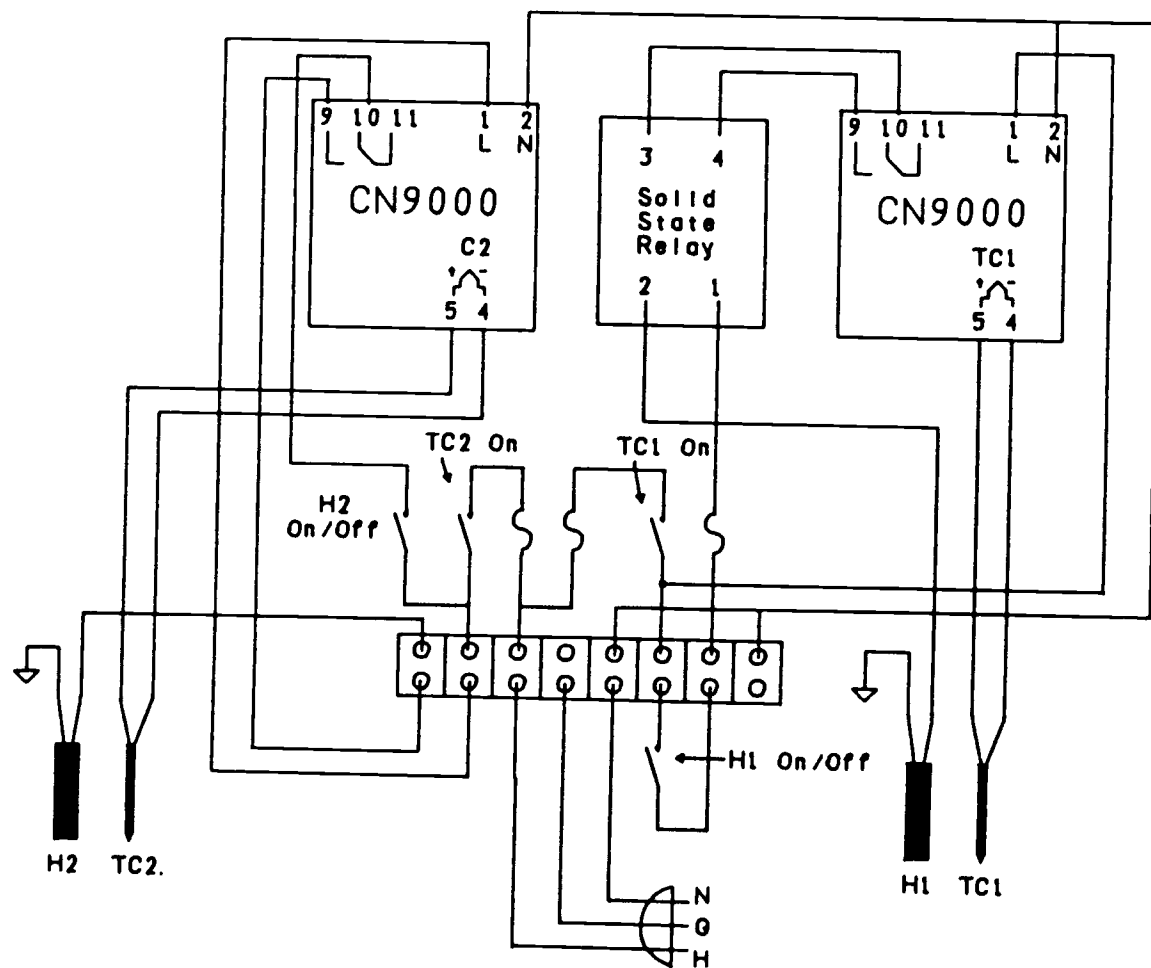


Figure II.13 Schematic wiring diagram of the temperature controller chassis.

Consequently, the mechanical relay in one of the controllers was replaced with a digital switch (BD9022 pulse output board, Omega Engineering, Stamford CT). The digital switch drives an external 10-A. solid state relay (Model SSR, Omega Engineering, Stamford CT) which can be cycled at higher rates and properly controls the flange temperature. Each temperature controller uses an 80-W cartridge heater (Firerod type, Watlow, St. Louis, MO) and a type K thermocouple (AFS type, Watlow, St. Louis, MO) to monitor and control the temperature of the nozzle flange and a sample heater block which will be described later. In addition, a 2.5-inch i.d. by 1.5-inch wide mica band heater (Watlow, St. Louis, MO), powered by a Variac transformer encircles and heats the main body of the measurement cell to ease the heating requirements placed on the smaller nozzle flange cartridge heater.

#### b. Photomultiplier Tube Cooling Coils

Although it is desirable to heat the measurement cell to high temperatures, the PMT, which is also part of the cell, must be kept cool to minimize thermal emission contributions to the dark current signal. This was accomplished by wrapping 1/4-inch o.d. copper refrigeration tubing around the part of the detector arm that contains the PMT. The coils surround and are clamped solidly to the detector arm using hose clamps to ensure good heat transfer between the arm and the coils. 18-°C Cooling water from the refrigerated bath is then circulated through the coils using an auxiliary pump.

#### 5. Mounting Bracket

Originally the measurement cell was designed to mount on the diffusion pump flange of an existing GC-MS system. However,

vibration and alignment problems were observed with this configuration due to the fact that the diffusion pump was mounted on a small, mobile cart which could easily be bumped. To solve this problem, a mounting bracket was designed which allowed the measurement cell to be firmly anchored to the optical table. A schematic diagram of this bracket is shown in Figure II.14. The main characteristics of the mounting bracket are, first, that it is designed to hang the measurement cell off the edge of the optical table at a height that allows easy interface to the gas chromatograph. Also, connection to the vacuum pumping system is made through a right angle pipe fitting protruding from the rear of the mating flange. This configuration is much more stable than the previous configuration and has been an important factor in obtaining reproducible results.

#### D. Vacuum Pumping System

The only vacuum pump used in this research is an Edwards model ED200 200 liter-per-minute, two-stage, mechanical pump (Edwards High Vacuum, Sussex, England). Vacuum chamber pressure is measured by a GT-100 thermocouple vacuum gauge (Consolidated Vacuum Corp., Rochester, NY) which displays pressure down to  $10^{-3}$  Torr on an analog meter. With the vacuum chamber properly sealed, the mechanical pump is able to maintain a vacuum pressure equal to, or less than  $10^{-3}$  Torr (0 Torr on the gauge meter). Problems with pump vibrations coupling to the measurement chamber through the vacuum tubing were eliminated by clamping the vacuum tubing solidly to a heavy weight on the floor next to the pump. Typical chamber pressures with the supersonic nozzle pulsing continuously range from 10 - 100 mTorr depending on the valve pulse width, and the stagnation pressure.

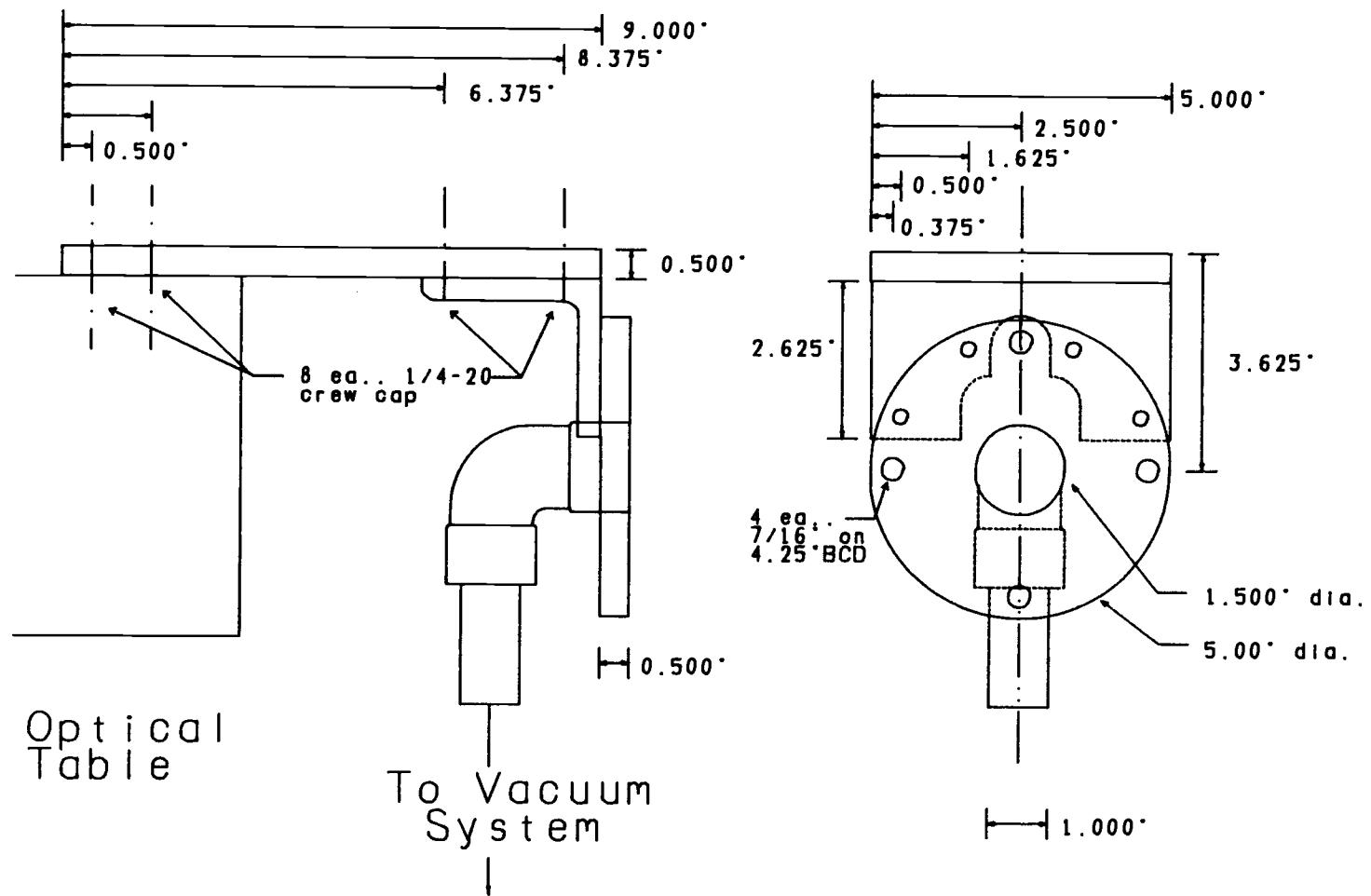


Figure II.14 Diagram of the mounting bracket that allows the measurement cell to be firmly attached to the optical table.

### E. Supersonic Nozzle

The supersonic nozzle used in this research is a modified Bosch fuel injector (Type 0280 150152) from a BMW automobile. A schematic diagram of the valve is shown in Figure II.15. In addition, the spatial relationship between the pulsed valve, excitation axis, detector optics, and PMT is illustrated in Figure II.16.

The stock valve is modified in the following manner. First, the valve tip is removed exposing the internal components: a solenoid plunger, a slotted washer that limits the travel of the plunger, and a spring that seals the plunger against the valve tip when the valve is closed. A brass shim is then soft soldered onto the face of the valve tip and a hole of the desired diameter is drilled through the center of the shim. An orifice diameter of 330  $\mu\text{m}$  was used for all experiments in this research. The region of the valve directly behind the valve tip is then threaded with 5/8-18 threads so that it can be screwed securely into the nozzle flange. Next, the flexible hose is removed from the rear of the valve, and the ribbed tube to which it is sealed turned down to a 5/16-inch o.d. for attachment of a tube fitting. One final modification involves replacing the silicone O-ring that seals the valve tip into the body of the valve with an undersized Viton O-ring (Parker 2-010). This improves the ability of the valve to hold a vacuum at the high-temperatures used in this experiment.

Particularly when the valve is new, there are often problems getting it to seal when first placed in the measurement cell. If the leak is particularly bad, a spare plunger is placed in the chuck of a drill press and a small amount of polishing compound is dabbed on the tip of the plunger. The valve tip is then repeatedly pressed upward against the rotating plunger tip to polish the inside surface of the valve tip. The valve tip must then be scrupulously cleaned to remove any metal flakes or excess polishing compound. This procedure is

## Modified Bosch Fuel Injector

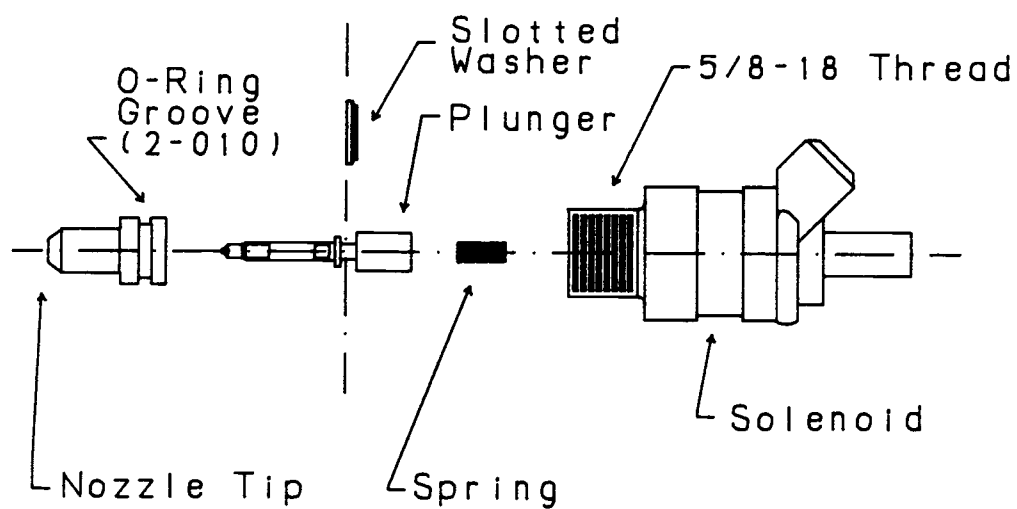


Figure II.15 Diagram of the modified Bosch fuel injector used as a supersonic nozzle in this research.



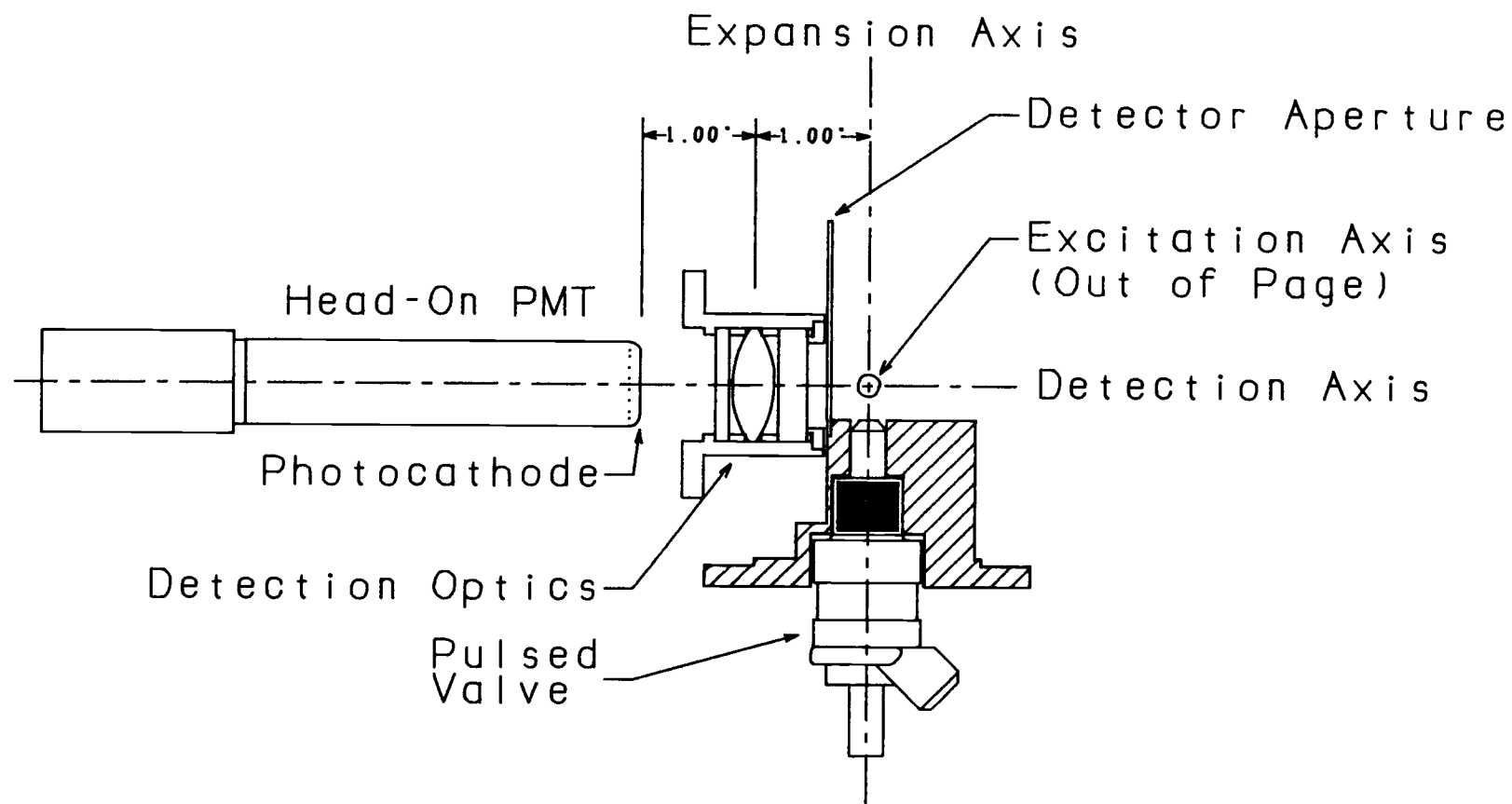


Figure II.16 Relationship between the supersonic nozzle, excitation axis, and detector components.

usually required with a new valve to remove solder residue. Normally, however, simply rotating a solvent-soaked cotton swab against the inside surface of the valve tip, and polishing the mating surface of the plunger tip is sufficient.

## 1. Driver Circuit

The valve is opened by sending a current pulse through the solenoid windings, forcing the plunger away from the valve tip. The duration of this current pulse determines the period of time the valve remains open. The circuitry that supplies the current pulse is illustrated in Figure II.17, while the components are listed in Table II.6. The schematic diagram used to build this circuit was obtained from Dr. Joe Nibler who uses a similar pulsed valve system in his own group's research [81]. When a +5-VDC pulse is brought into the trigger input of the driver, the current that is necessary to open the valve is sent through the valve windings. The valve remains open as long as the trigger input is held high. As soon as the trigger input is brought to ground (0 V), the valve closes. Thus, the pulse width and duty cycle of the valve can be easily set by simply changing the characteristics of the input trigger pulses. It is important that the input trigger pulse be a true +5 VDC since normal TTL voltages (2.4-4.5 VDC for logic 1) are not high enough to trigger the driver to open the valve properly. Using this driver and the Bosch valve described above, valve pulse widths ranging from approximately 0.5 ms to continuous operation are possible.

Finally, a driver test point is provided which allows the voltage supplied across the valve to be monitored on an oscilloscope. An example of an oscilloscope trace of the test point for a 2-ms input trigger pulse is shown in Figure II.18.

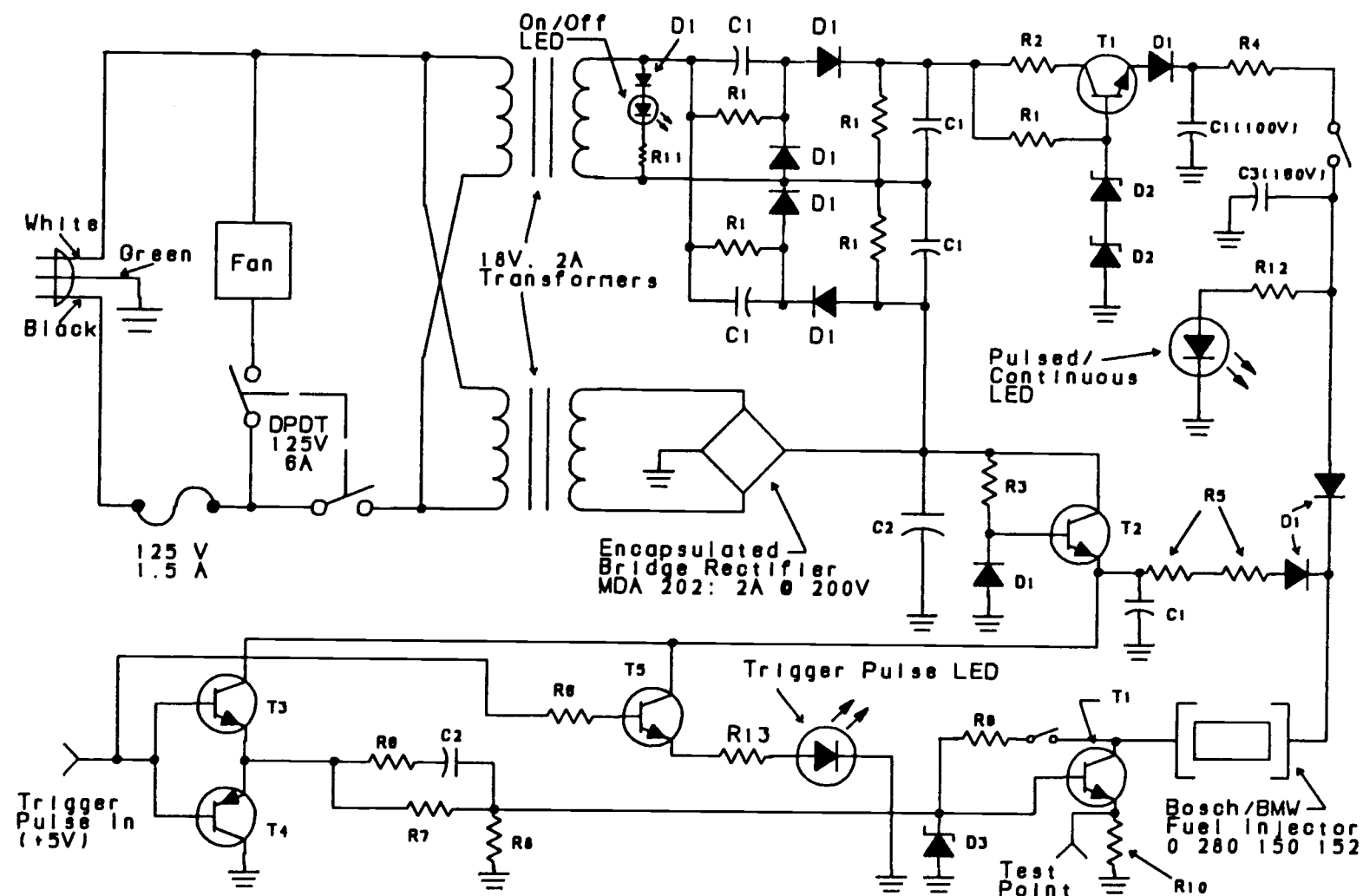


Figure II.17 Schematic diagram of the pulsed valve driver circuitry. Component values are listed in Table II.6.

Table II.6

List of Electronic Components used in the  
Construction of the Pulsed Valve Driver

Designation	Description	Other Comments	# Used
RESISTORS			
R1	4.7 k $\Omega$ , 0.5 W		5
R2	4.7 $\Omega$ , 1 W		1
R3	680 $\Omega$ , 1 W		1
R4	560 $\Omega$ , 5 W		1
R5	5 $\Omega$ , 10 W		2
R6	100 $\Omega$ , 0.25 W		1
R7	1 k $\Omega$ , 0.25 W		1
R8	330 $\Omega$ , 0.25 W		1
R9	22 $\Omega$ , 0.25 W		1
R10	0.33 $\Omega$ , 5 W		1
CAPACITORS			
C1	220 $\mu$ F, 50 V	Electrolytic	6
C2	4.7 $\mu$ F, 50 V	Electrolytic	2
C3	10 $\mu$ F, 50V	Electrolytic	1
DIODES			
D1	Rectifier	Type 1N 4006	8
D2	24 V, 1W Zener	Type 1N 4749	2
D3	15 V, 1W Zener	Type 1N 4744	1
TRANSISTORS			
T1	NPN Power	Type TIP 41B	2
T2	NPN Power	Type TIP 41	1
T3	NPN Small Signal	Type MPS A05	1
T4	PNP High Voltage	Type 2N 5401	1

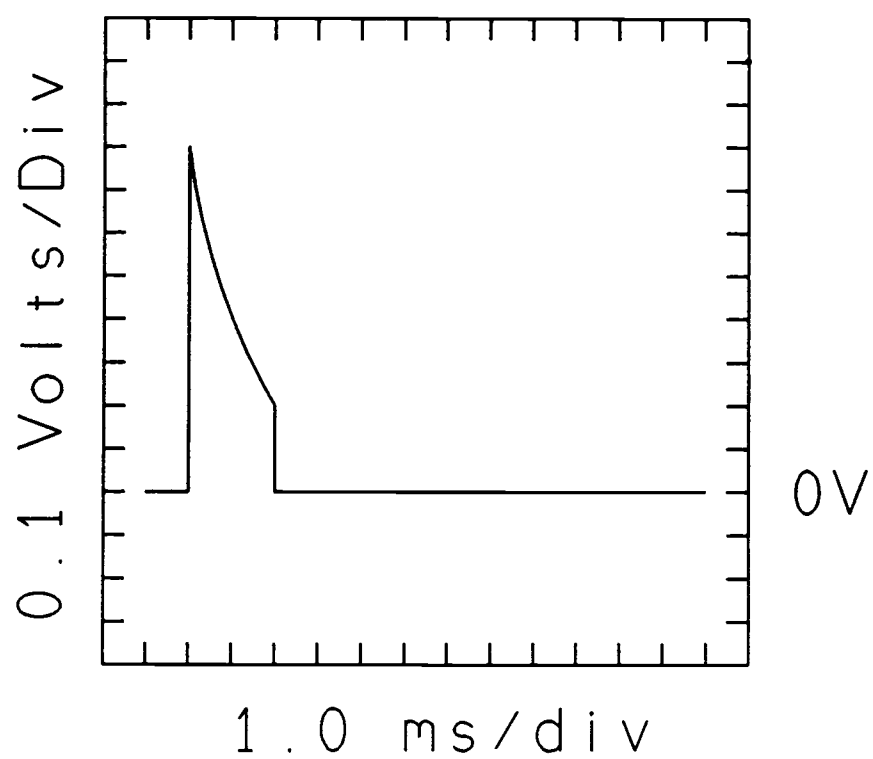


Figure II.18 Oscilloscope trace of the signal measured at the pulsed valve driver test point for a 2-ms input pulse.

## F. Sample Introduction System

The final component of the instrumentation is the sample introduction system. Two different methods were used to present the sample to the supersonic nozzle. Figure II.19 illustrates these two methods of sample introduction, which are also described below.

### 1. Continuous Sample Introduction

Instrumental characterization experiments requiring the acquisition of fluorescence excitation spectra, need a constant, continuous supply of the analyte. In this case, the solid PNA sample is placed in a 0.25-inch o.d. by 1-inch long pyrex glass thimble. The thimble is then sealed in one arm of a 0.25-inch Swagelok "Tee" tube fitting (Crawford Fitting Co., Solon, OH) using a one-piece Viton ferrule (Type SF-400-VG1, Alltech, Deerfield, IL). The diluent gas is brought into the second arm of the tee while the remaining arm is connected directly to the pulsed valve using a 5/16- to 1/4-inch Swagelok reducing union (Crawford Fitting Co.).

A small heater block was constructed to clamp around the sample thimble in the arm of the tee fitting. The heater block, which was constructed of aluminum, is shown in Figure II.20. Two holes are drilled into the block on each side of the thimble for insertion of the cartridge heater and thermocouple described previously. The temperature controller is then used to heat the sample which vaporizes, mixes with the diluent gas and flows through the valve and into the expansion. The effective concentration of the analyte in the valve is determined by the temperature of the heater block and the back pressure of the diluent gas.

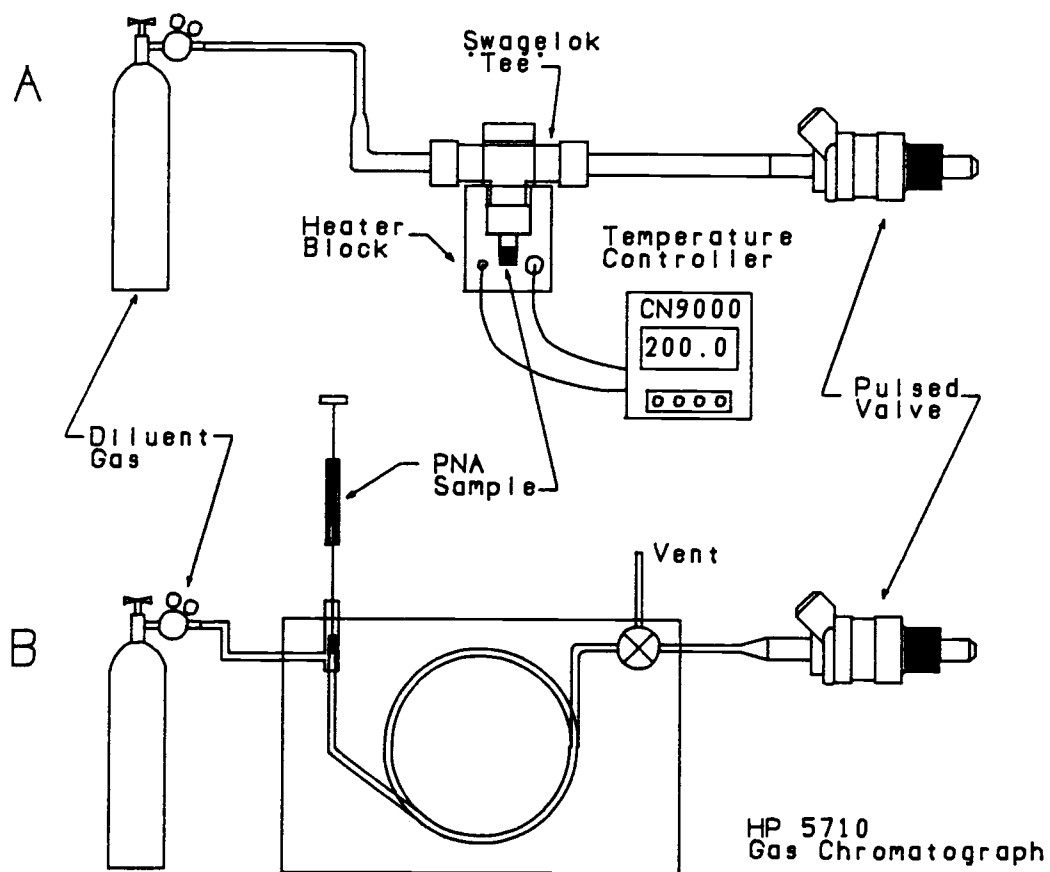


Figure II.19 Schematic diagram of the two methods of sample introduction used in this research; (A) continuously via a heated cell and (B) quantitatively via a gas chromatograph.

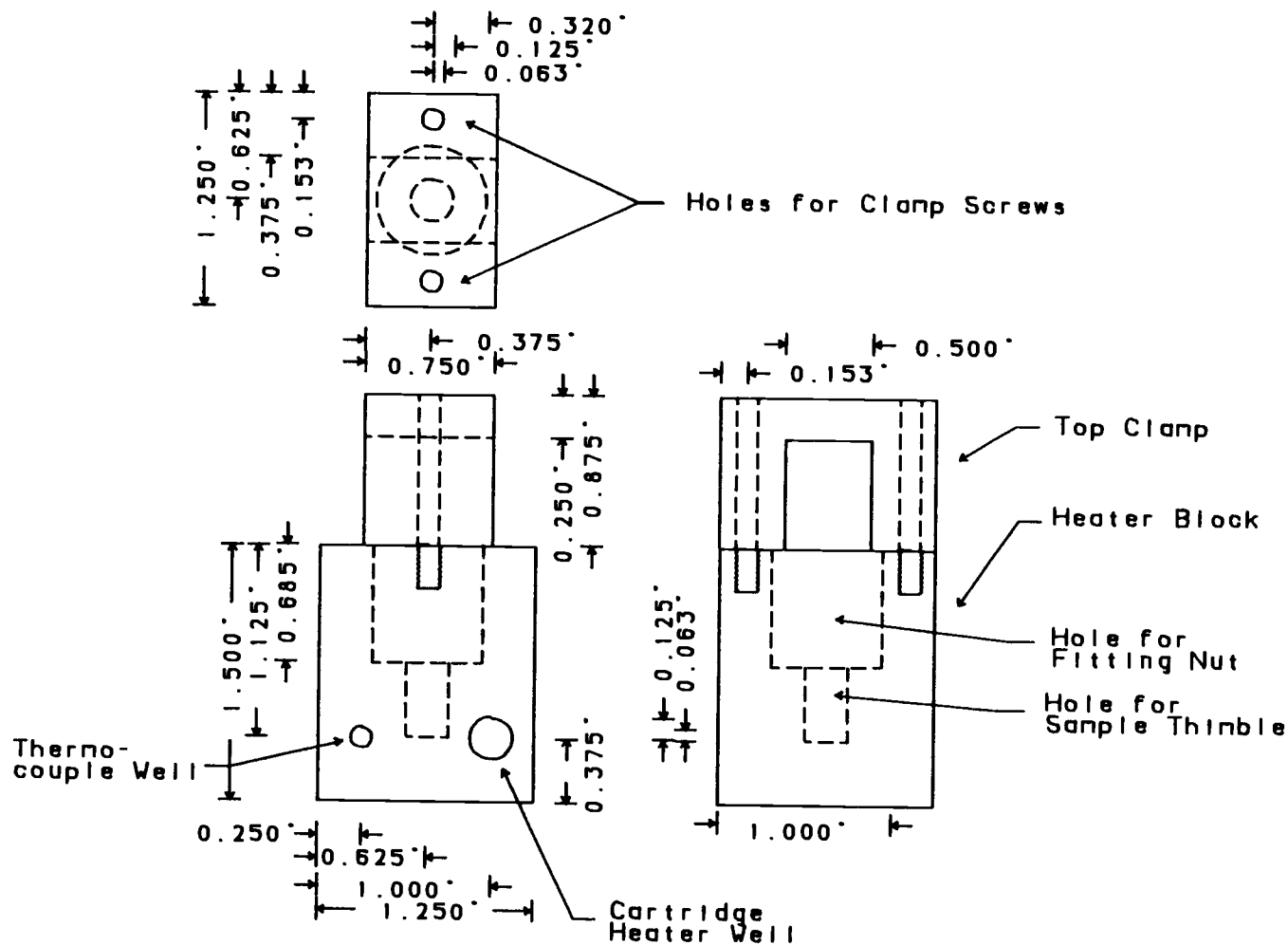


Figure II.20 Diagram of the heater block used to vaporize solid PNA samples for continuous introduction to the supersonic expansion.



## 2. Quantitative Sample Introduction System: Gas Chromatograph

The second sample introduction system that was used in this research is a Hewlett-Packard model 5710A gas chromatograph (GC) (Hewlett-Packard, Avondale, PA). The intended use of the GC in this work is both as a method of preseparation and as a means by which the PNA sample can be introduced quantitatively to the nozzle. The details of the chromatography will be discussed in the experimental section of this thesis, but it is worth noting a few features of the GC. This GC was originally designed for use with a Hewlett-Packard 5780A GC-MS and thus already had the heated transfer lines necessary for interfacing to an external detection system such as the measurement cell used in this work. It is designed for packed column chromatography and provides separate, insulated, temperature-controlled heaters for the injection port, oven, and transfer line. The oven temperature controller allows either isothermal or temperature programmed operation. The heated transfer line is a 6-inch piece of 1/8-inch o.d. copper tubing extending from the column outlet, located within the oven, out through the side of the GC where it is connected to the pulsed valve via a 5/16- to 1/8-inch Swagelok reducing union. A second useful feature derived from its intended use on a GC-MS is the existence of a bypass valve located at the outlet of the column. When the bypass valve is open, the majority of the column effluent flows out through the rear of the GC and is vented to the atmosphere rather than flowing into the detector. This was a particularly useful feature in this work since it provided a means by which flow through the column could be maintained without requiring the supersonic valve to pulse continuously.

## G. Computerized Data Acquisition and Control System

The microcomputer has become an important component of most analytical instrumentation; rarely does one observe a new instrument that does not have an integral microcomputer controlling important functions and providing at least rudimentary data analysis capabilities. As the complexity of an instrument increases, the demands placed on computational capabilities and the management of synchronization, control and acquisition functions also increases, often dramatically. The microcomputer is ideally suited to meeting these demands. In addition, the microcomputer is also a powerful tool for the rapid and efficient analysis and presentation of experimental data.

The instrumentation used in this research, which was described in the previous sections, is an example of a reasonably complex system that requires a microcomputer to execute the various control and acquisition functions. Both the hardware and the software that were developed to accomplish this control are outlined in the following sections. A fair amount of detail is provided both as a guide for those who use the system in the future, and as a tribute to the time and energy spent developing the system.

### 1. Computer

The computer that was used in this research is an IBM PC compatible Corona PPC-1 which operates at the PC standard 4.77 MHz clock speed. This computer has 512 kilobytes (kb) of motherboard memory, one serial communications port (COM1), and one parallel printer port (LPT1). In addition, one 360 kb floppy disk drive, and a Mitsubishi MR522 20 Megabyte (Mb) hard disk have been installed for

program and data storage. The hard disk is controlled by a DTC 5150CX hard disk controller. In order to increase the system memory from 512 kb to the 640 kb required by many applications, a Tall Trees Systems JRAM-3 memory expansion board was installed. This board can hold up to 2 Mb of random access memory (RAM) through the installation of 256 kb dynamic RAM chips. Part of this memory is used to backfill the system memory, bringing it up to the MS-DOS limit of 640 kb of linear addressable system memory. The remainder of the memory can be partitioned between several applications, including virtual RAM disks, a print spooler, or Lotus-Intel-Microsoft (LIM) expanded memory. In addition, this board provides both a second parallel port (LPT2), a second serial port (COM2), as well as a battery backed-up real-time clock. An Intel 8087 math coprocessor was also added to the system to improve the speed at which floating point math operations are executed. Finally, since the Corona supports only its own native 640 x 325 resolution monochrome graphics, a color graphics adaptor (CGA) was added to the system to allow the BASIC language graphics functions to be used in the 640 x 200 resolution CGA mode. The CGA graphics are displayed on an external monochrome composite monitor. The computer system and peripherals used in this research have been summarized in Table II.7.

## 2. Native PC Hardware Used for Instrument Control

### a. Parallel Port

A maximum of three parallel printer ports can be installed in an IBM PC. These three ports are identified by three unique port addresses: 956 (3BC hex), 888 (378 hex), and 632 (278 hex). Normally, these ports are used to send characters to a Centronics compatible parallel printer such as the Gemini-10X used in this research. It is, however, possible to use these ports to control

Table II.7

Summary of the Computer and Peripherals  
Utilized in this Research

Component	Manufacturer
<b>Computer System</b>	
Corona PPC-1 Microcomputer with 512 kb RAM, 1 serial port, 1 parallel port, and 1 360 kb floppy disk drive.	Cordata Thousand Oaks, CA
20 MB Internal Hard Disk Model MR522	Mitsubishi America Torrance, CA
8087 Math Coprocessor	Intel Corporation Hillsboro, OR
<b>Expansion Boards</b>	
Hard Disk Controller Model 5150CX	Data Technology Corp. Santa Clara, CA
Memory Expansion Board Model JRAM-3	Tall Trees Systems Palo Alto, CA
Color Graphics Adaptor Model CGG	Mitsuba Corporation San Dimas, CA
Data Acquisition and Interface Board, Model DASH-8	MetraByte Corp. Stroughton, MA
<b>External Peripherals</b>	
Parallel Dot Matrix Printer Model Gemini 10X	Star Micronics Irvine, CA
Composite Monochrome Monitor Model 300A	Amdek Elk Grove Village, IL

external devices that respond to TTL voltages. If a data byte is written to a port address to which an active parallel port is attached, the 8 parallel lines will assume the voltage levels corresponding to the logic level of each of the individual bits of the data byte. The relationship between each bit of the parallel port and the external lines available through the DB25 connector on the rear of the computer is illustrated by Figure II.21; Bits 0-7 of the port correspond to pins 2-9 of the DB25 connector.

In this research the first parallel port is used as a printer port, sending characters to the Gemini-10X printer. The second installed parallel port, which is located on the JRAM-3 board, is used to control the etalon birefringent filter, and UV doubling crystal stepper motors. This second port is currently configured to respond at address 632 (*i.e.*, LPT3). The control software can cause each of these tuning elements to be moved by one step by initiating a low to high transition on the desired parallel port line. Only the first six bits of the parallel port are currently used and the function of each of these bits in controlling the CMX-4 stepper motors is identified in Table II.8. The actual program code used to accomplish this stepping is discussed in the software section of the thesis.

#### b. 8253 Programmable Interval Timer

Every PC has an 8253A programmable interval timer (PIT) chip which is used by the system to update the time-of-day clock, and synchronize the refresh of the dynamic system memory, as well as to perform several other functions. This chip has three independent timers as outlined in Figure II.22. Each of these timers is clocked at the same base frequency, 1.19318 MHz, which is simply the PC bus clock rate divided by four. The 8253 timers can be set to operate in one of six different modes, ranging from mode 0, which produces an interrupt on the terminal count (when the count register decrements

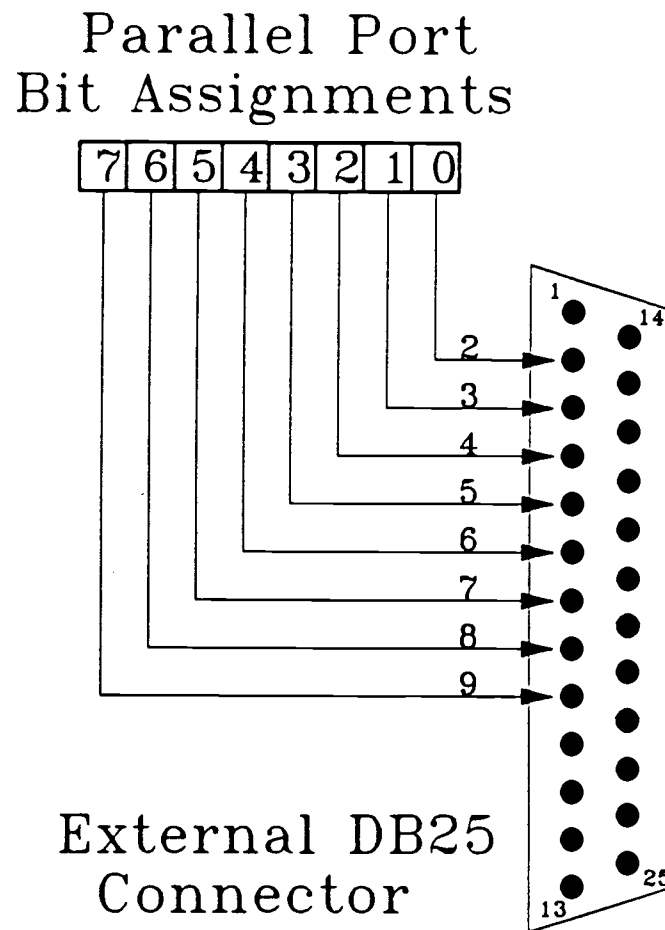


Figure II.21 Relationship between the bits of the parallel port and the external lines available through the DB25 connector at the rear of the computer.

Table II.8

Parallel Port 2 Bit Assignments:  
Control of the CMX-4 Wavelength Stepper Motors

Bit (Dec. Value)	Pin	Function
0 (1)	2	Step Etalon +1 Step
1 (2)	3	Step Etalon -1 Step
2 (4)	4	Step Birefringent Filter +1 step
3 (8)	5	Step Birefringent Filter -1 step
4 (16)	6	UV Crystal Stepper Motor Direction
5 (32)	7	Step UV Crystal $\pm 1$ step.

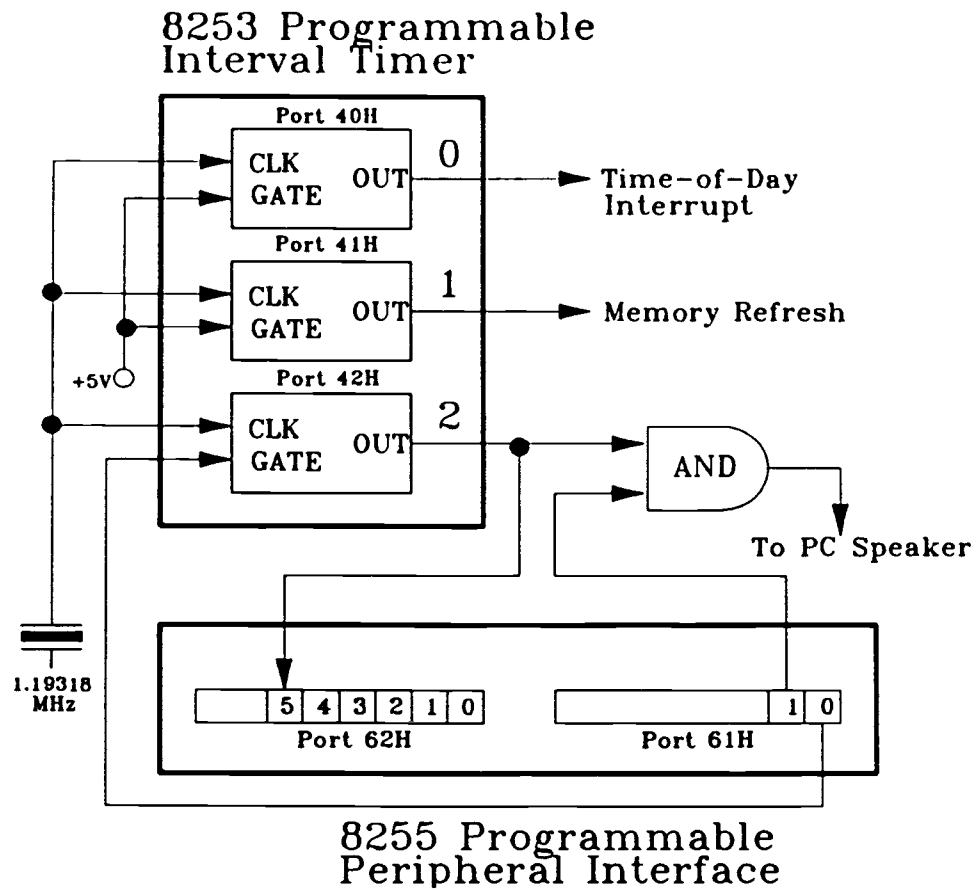


Figure II.22 Schematic diagram of the IBM PC's 8253 programmable interval timer (PIT), and its relationship to the 8255 Programmable Peripheral Interface (PPI).



from 1 to 0), to mode 5, which sets the timer up as a hardware triggered strobe [82]. By loading the correct value into the timer's count register and setting the correct mode, a known output frequency or pulse width can be produced. This provides a means by which short delays of known length can be generated by the PC. Further, since every PC has an 8253 which is clocked at the same base frequency, these delays will be both machine independent, and programming language independent.

There are many cases in this research where pulses of a known, controllable width and rate must be sent to an output port, the prime example being the pulsing of LPT2 to step the CMX-4 stepper motors. In the early control programs the delays used to generate these pulses were created by using FOR/NEXT loops in interpreted BASIC. However, as these programs were rewritten, or upgraded to compiled BASIC, it was discovered that the delay times would change, often drastically. Each time this would happen, the loop counters would have to be reset by trial and error. It was soon decided that a software independent method of generating pulses was needed, and software was written which programmed the 8253, allowing the generation of pulses, pulse trains, and delays of known duration and frequency. These routines are described in detail in the software section of this thesis.

Timer 2 of the 8253 is particularly well suited to this application. Not only will its use not interfere with important system functions (unlike timers 0 and 1), but it is the only timer whose output is connected to a port which can be read by software. As is illustrated by Figure II.22, the PC's 8255 programmable peripheral interface (PPI), which also has several other system I/O functions, is used to control the gate of Timer 2 while also providing access to its output. It is also apparent from this figure that the normal use of Timer 2 is as a programmable sound generator for the PC. Several good articles have been written on the use of the 8253 Timers for generating sounds and timing program execution [83-86]. These references were indispensable in determining how to configure the 8253 for this application.

The desired timer, in this case Timer 2, is selected and placed into the correct mode by writing a control byte to the control register located at port 43H (43 hexadecimal, 67 decimal). The count which will produce the proper output delay is then placed into the count register for the timer. These count registers are located at ports 40H, 41H, and 42H for Timer 0, Timer 1, and Timer 2, respectively. In order for Timer 2 to decrement its count upon the receipt of the input clock pulses, its gate must be enabled by writing a one to bit 0 of the 8255 PPI at port 61H. The output of Timer 2 is sent to both the PC speaker, and bit 5 of Port 62H of the PPI. Thus, by polling bit 5 of Port 62H, the output status of Timer 2 can be monitored. It should be noted that this is only true for an IBM PC or clone, NOT for an IBM AT, or other AT type computer. In addition, it should be noted that the MetraByte DASH-8 board, which will be discussed in the following section, also contains an identical 8253 PIT chip which could just as easily have been used for this application. This, however, would have defeated the goal of having a machine-independent timing source (the PC would require a DASH-8).

### 3. Other Data Acquisition and Control Hardware

#### a. MetraByte DASH-8 Data Acquisition and Control Board

A MetraByte Corporation DASH-8 data acquisition and control board was used as the main interface between the microcomputer and the laser synchronization, control, and detection subsystems. This is an inexpensive half-length board which includes a 12-bit successive-approximation analog-to-digital convertor (ADC) with a 35- $\mu$ s conversion time, an 8253 programmable interval timer clocked at 2.39 MHz, 4 digital output lines, and 3 digital input lines. The various DASH-8 functions are controlled by writing to and reading

from several control and status registers. These registers are all located relative to a base address which is set through DIP switches on the DASH-8 board. The base address used in this research was 816 (330H), and the registers which are offset from this address are summarized in Table II.9

### (1) Analog-to-Digital Converter

The signal that is to be converted by the ADC is selected by an on-board 8-to-1 Channel multiplexer (MPX) whose output channel is sent to a sample and hold (S/H). The S/H holds the signal locked so that the ADC can perform its successive approximation conversion on a constant signal. In the current configuration, two of the MPX input channels are used. Channel 0 is connected to the analog output of an Evans Associates Gated Integrator (G.I.), whose input is connected to either the fluorescence photomultiplier tube, or the optogalvanic circuitry during calibration. Channel 1 is connected to the laser power monitor (LPM) output. A block diagram of the parts of the DASH-8 board that are used in this research, including the MPX-S/H-ADC combination described above, is provided in Figure II.23.

During the conversion, bit 7 of the DASH-8 status register, also called the end-of-conversion (EOC) flag, is held high. When the conversion is finished the EOC flag drops low indicating that data is available at the two ADC registers located at offset 0 (Low byte), and offset 1 (High Byte). As illustrated by Figure II.23, the twelve bit ADC is left-justified. This means that the high byte contains the eight most significant bits, while the high four bits of the low byte contain the four least significant bits of data. The four lowest bits of the low byte, marked by X's in Figure II.23, are not significant and are ignored. In order to correctly interpret the magnitude of the ADC data, the low byte and high byte must be combined into a single 16 bit value (short integer):

Table II.9

MetraByte DASH-8 Data Acquisition  
and Control Interface Board  
Control and Status Registers

Register Name	Read/Write	Port Address	Function
ADC Register 1 "	Read Write	Base Address + 0 "	ADC Data Low Byte Trigger 8 bit ADC
ADC Register 2 "	Read Write	Base Address + 1 "	ADC Data High Byte Trigger 12 bit ADC
DASH-8 Status	Read	Base Address + 2	Bits 0-2: MPX Status Bit 3: IRQ Status Bits 4-6: Dig. Inputs Bit 7: EOC Status
DASH-8 Control	Write	Base Address + 2	Bits 0-2: Set MPX Chan. Bit 3: Set Interrupts Bits 4-7: Dig. Outputs
Counter 0 Data "	Read Write	Base Address + 4 "	Return Current Count Load Counter 0
Counter 1 Data "	Read Write	Base Address + 5 "	Return Current Count Load Counter 1
Counter 2 Data "	Read Write	Base Address + 6 "	Return Current Count Load Counter 2
Counter Control	Write	Base Address + 7	Bit 0: Sets BCD or DEC Bits 1-3: Set Mode Bits 4-5: Set Operation Bits 6-7: Set Counter

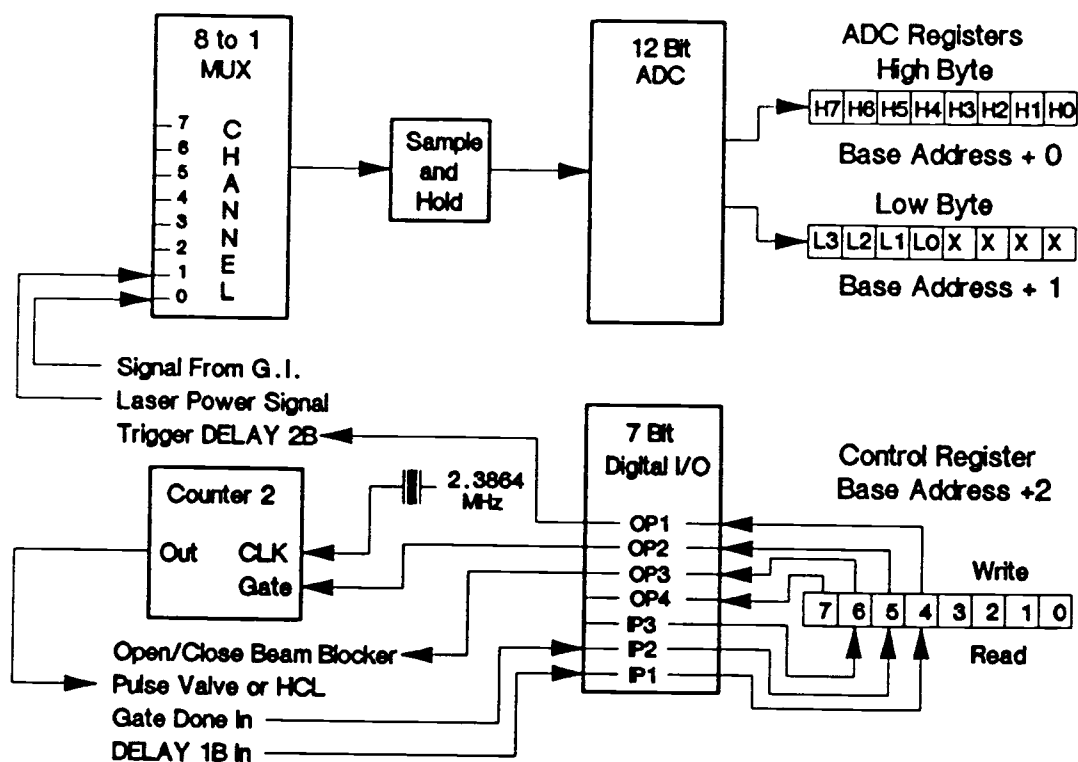


Figure II.23 Schematic diagram of the parts of the DASH-8 data acquisition and control board that are used in this research. The function of the various I/O lines is also identified.

$$\text{Value} = (\text{High Byte} * 16) + (\text{Low Byte} / 16) \quad (\text{II.6})$$

Figure II.24 illustrates the way in which this mathematical operation correctly combines the two data bytes. Finally, the ADC has a fixed input range of  $\pm 5$  V which with 12 bits of resolution gives a voltage resolution of 0.0024 V. The ADC produces an offset binary code as the result of a conversion. Table II.10 lists the offset binary result of several conversions as a function of input voltage.

## (2) Digital Input/Output

The DASH-8 also has three digital input lines, designated IP1-IP3, and four digital output lines, designated OP1-OP4. These lines are used for synchronization and control of the laser system. The input lines, IP1-IP3, are accessed through a read from bits 4-6, respectively, of the status register located at an offset of two from the base address. The two input lines currently employed in this work, IP1 and IP2, are used for synchronization and their individual functions will be described in the timing and synchronization section. Similarly, three of the four digital output lines are utilized, and are accessed by a write to bits 4-7 of the control register. OP1 is used to trigger the circuitry that fires the laser, while OP3 is used to open and close the CMX-4 beam blocker. The third output port, OP2, gates counter 2 of the DASH-8 8253 PIT which outputs the pulse that fires the Bosch valve. Table II.11 lists the status register read and write bit assignments along with a number of the bit values that must be written to the status register to accomplish the indicated control function.

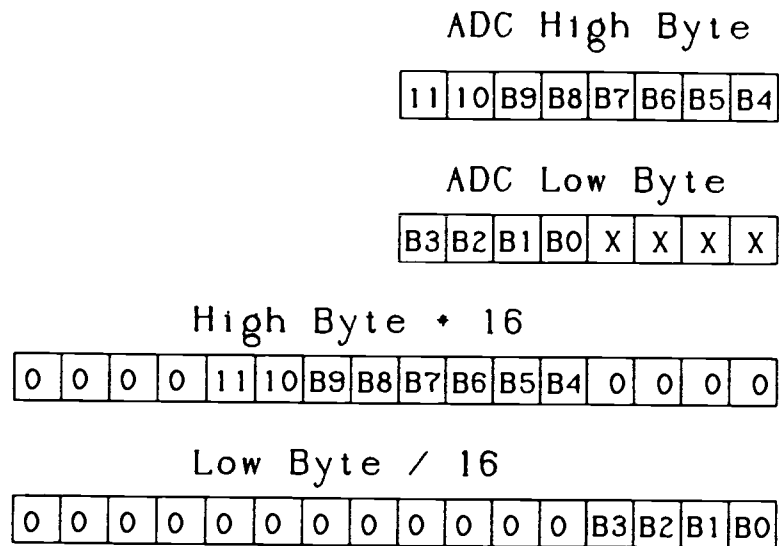


Figure II.24 Representation of the way in which the low and high data bytes, which are returned by the analog to digital converter, are correctly combined to form a datum of the correct magnitude.

Table II.10

Offset Binary Analog-to-Digital  
Conversion Results for the DASH-8 ADC

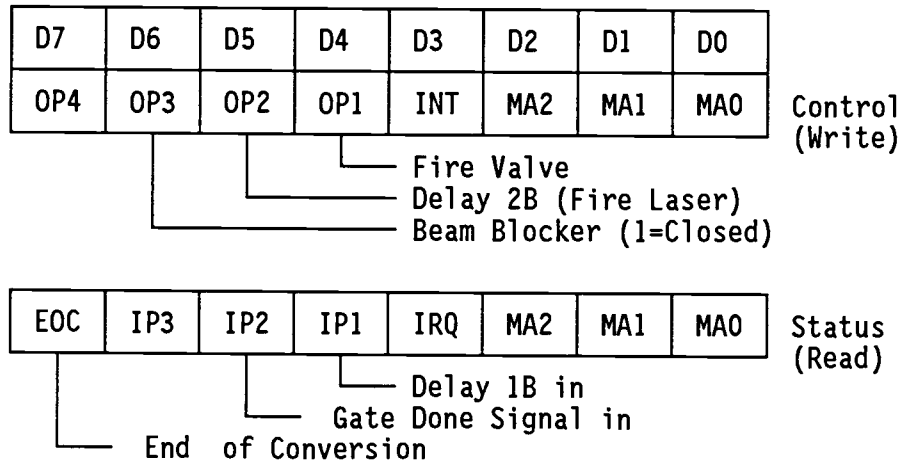
Input Voltage	ADC Result			Hex	Dec.
	Binary				
+4.9976 V	1111	1111	1111	FFF	4095
*		*		*	*
*		*		*	*
+2.5000 V	1100	0000	0000	C00	3072
*		*		*	*
*		*		*	*
+0.0024 V	1000	0000	0001	801	2049
0.0000 V	1000	0000	0000	800	2048
-0.0024 V	0111	1111	1111	7FF	2047
*		*		*	*
*		*		*	*
-2.5000 V	0100	0000	0000	400	1024
*		*		*	*
*		*		*	*
-5.0000 V	0000	0000	0000	000	0



Table II.11

DASH-8 Control and Status  
Register Assignments and Important bit Combinations

Base Address + 2



Description	Binary								Decimal
	D7	D6	D5	D4	D3	D2	D1	D0	
Fire Valve Only	0	0	0	1	0	0	0	0	16
Fire Laser Only	0	0	1	0	0	0	0	0	32
Fire Laser and Valve	0	0	1	1	0	0	0	0	48
Block Beam	0	1	0	0	0	0	0	0	64
Fire Laser with Beam Blocked	0	1	1	0	0	0	0	0	96
Fire Laser, & Valve with Beam Blocked	0	1	1	1	0	0	0	0	112
Set MPX to CH0	0	0	0	0	0	0	0	0	0
Set MPX to CH1	0	0	0	0	0	0	0	1	1
Set MPX to CH1 with Beam Blocked	0	1	0	0	0	0	0	1	65

### (3) Programmable Interval Timer

Both the laser induced fluorescence and laser calibration subsystems require an external pulse to initiate the signal of interest. In the former case, a +5-V pulse is used to open the Bosch valve in the measurement cell, while the latter, operating in the pulsed mode, needs a pulsed signal to trigger the hollow cathode lamp used as a wavelength standard. In order to provide the most versatile interface to these different subsystems, an easily variable source of well-defined pulses was developed using the DASH-8 8253 Programmable Interval Timer (PIT). By placing the 8253 PIT in mode 1, it can be configured as a programmable one-shot. In this mode the counter will make a high to low transition at its output and start counting down when it receives a rising edge on its gate input. When the counter reaches the terminal count (0) the output is brought back to +5 V. A logic low pulse whose width is defined by the count value is thus produced. In the case of the DASH-8 timer, the clock input of Counter 2 is connected to a 2.3854 MHz oscillator as illustrated in Figure II.23. Thus, each "tick" of the counter will take 419 ns. Since the count register is a 16 bit register, the largest value which can be placed into it is 65535. This gives a possible output pulse width range of 419 ns to 27.5 ms, which easily meets the requirements of this research.

#### b. Evans Associates Gated Integrator.

The signal arising from both the optogalvanic (OGE) calibration experiments and the fluorescence experiments is a pulse and closely tracks the laser pulse. Particularly in the case of the OGE measurements, the analytical signal is small compared with other

large voltage fluctuations that occur during the pulse. If the entire signal were integrated and acquired, it would be impossible to differentiate the analytical signal from the large background. Consequently, an Evans Associates Model 4120 gated integrator module (Evans Associates, Berkeley CA) was used to integrate the signal only during the period that the analytical signal is present. This gated integrator subsystem, which has been described in previous work [87], has three inputs: an analog input, an analog output, and a gate input. The analog input is connected directly to the PMT anode by a shielded cable during fluorescence measurements; the photoanodic current charges the gated integrator. During wavelength calibration, the analog input is connected to the OGE circuit "Computer Out" terminal. The analog output is connected to channel 0 of the DASH-8 ADC multiplexer. Finally, the gate input is connected to the output of DELAY 4A, which is described in more detail in a subsequent section. DELAY 4A provides a  $1\text{-}\mu\text{s}$  pulse which can be delayed from the beginning of the laser pulse. This  $1\text{-}\mu\text{s}$  pulse gates the gated integrator; integration of the signal occurs during the period of time the gate pulse is high. The relationship between the analytical signal (in this case an OGE signal), the gate pulse, and the analog output of the gated integrator is illustrated by Figure II.25. It should be noted that in the case of both the fluorescence and OGE signals, a positive change in the signal produces a negative change in the gated integrator output as illustrated in the figure.

#### 4. Laser and Detector Timing and Synchronization Electronics

Control of the CMX-4 laser and the circuitry that aids in the synchronization and processing of the desired detector signal was originally accomplished through an interface to a Digital Equipment Corporation PDP 11-20 minicomputer [75,80]. The parts of the original synchronization circuitry that are used in the current research are illustrated by the block diagram in Figure II.26, and

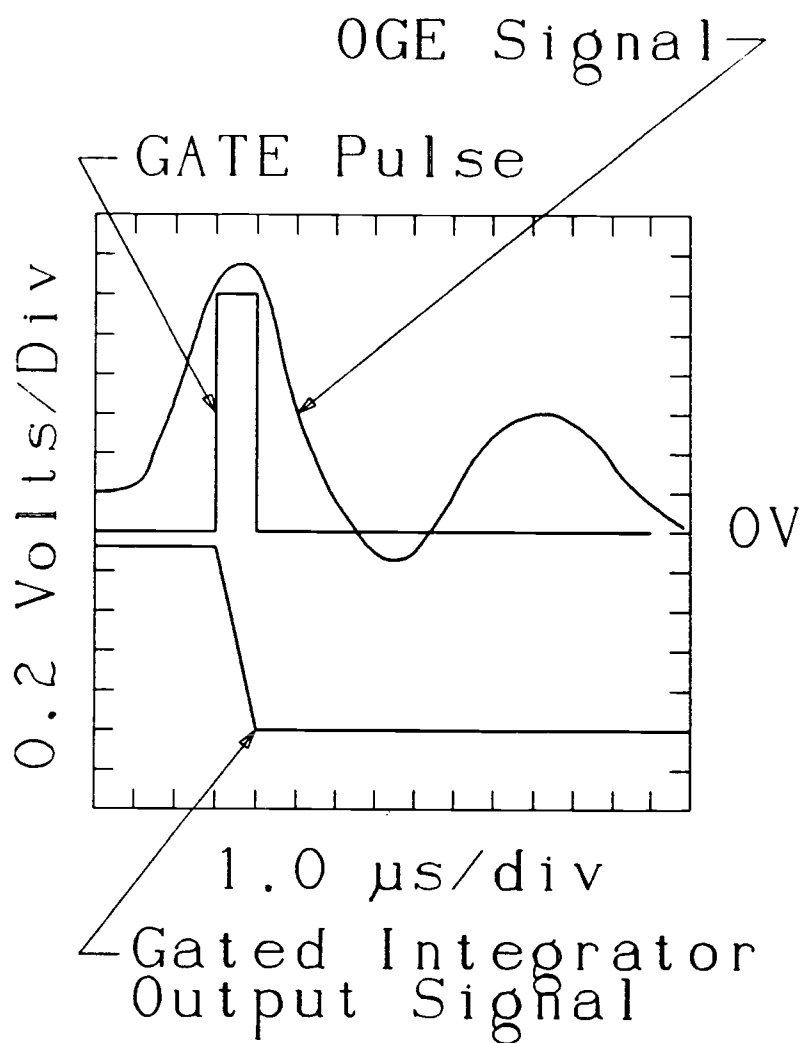


Figure II.25 A diagram of a typical oscilloscope trace illustrating the relationship between the DELAY 4A gate pulse, the gated integrator output, and the analytical signal present at the gated integrator input.

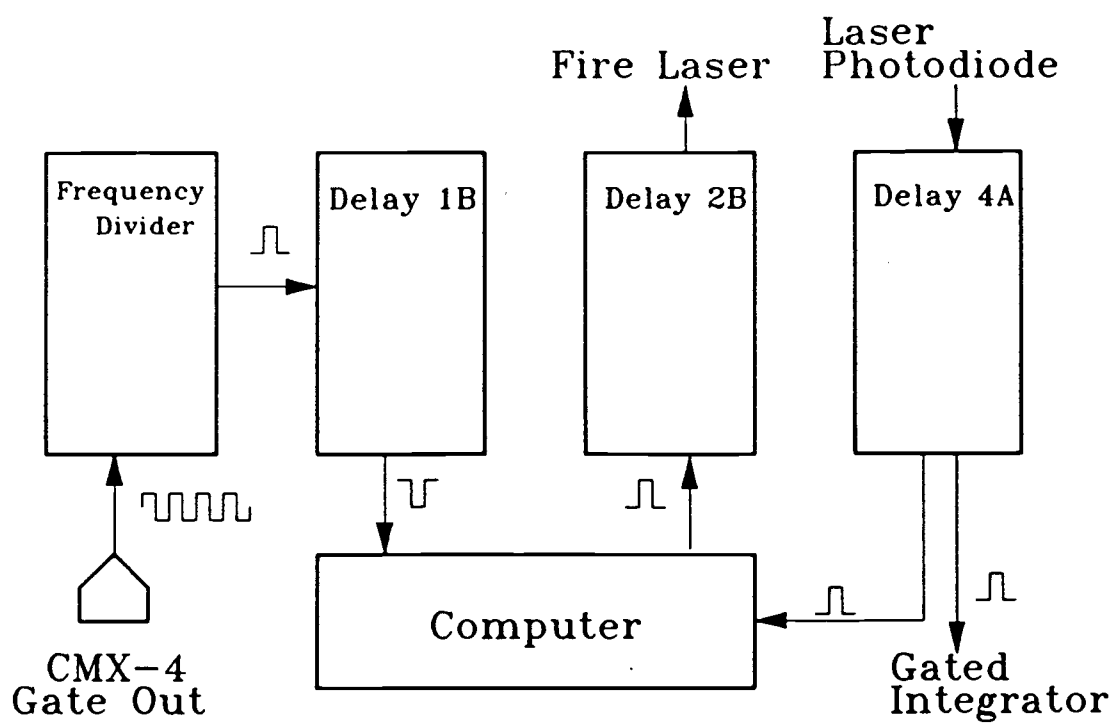


Figure II.26 Schematic diagram of the parts of the original synchronization circuitry that are used in the current research.

will be described in more detail below. In addition, because the original computer had certain hardware limitations, including only a small amount of core memory for program editing and execution, and only a paper tape drive for permanent storage, it was decided that the entire system should be interfaced to an IBM PC compatible microcomputer. Since the PC uses a different hardware configuration, as described in previous sections, additional circuitry had to be designed to allow the PC to interface with the existing system.

#### a. General Overview: Delays

Synchronization of the experimental system occurs on many levels, but begins with the timing requirements of the CMX-4 laser. As discussed earlier, the laser can only be externally triggered and fired while the 60-Hz AC power supplied to it is in the positive portion of its cycle. To aid in determining when the laser can be externally triggered, the CMX-4 provides a GATE OUT signal which is synchronized with the AC line voltage. When the GATE OUT signal is high, the laser can be fired. One consequence of this triggering requirement is that the laser is limited to a maximum repetition rate of 30 Hz.

The CMX-4 GATE OUT signal, which is used as the clock for the entire system, is first fed into a frequency divider circuit which has been described in detail elsewhere [80]. The purpose of the frequency divider is to select the rate at which the laser will be triggered. The divisor is selected through a set of DIP switches located on the front of the synchronization panel. The divided clock signal then triggers a monostable multivibrator circuit, DELAY 1B, which outputs one 23- $\mu$ s, logic low pulse for each input clock pulse. The DELAY 1B pulse is then detected directly by the computer software, signaling that the laser can be fired.

After detecting DELAY 1B, the controlling program sends out a simultaneous pair of pulses on two digital output lines. One of

these output pulses triggers Counter 2 of the DASH-8 to immediately output a pulse whose width has been selected under software control. This programmed pulse is used to fire either the hollow cathode lamp during calibration, or the fuel injector valve during fluorescence experiments. The other software generated pulse triggers a second delay, DELAY 2B. This is a variable delay which can be set by a potentiometer located on the front panel of the synchronization unit. When this delay is finished, a +12-V, 1- $\mu$ s pulse is sent to trigger the laser. Thus, DELAY 2B allows the firing of the laser to be delayed for selected periods after either the pulsed valve, or hollow cathode lamp has been fired. This provides a means by which different periods of the pulsed valve expansion, or hollow cathode pulse can be probed. A calibration plot for DELAY 2B using 0.1- $\mu$ F and 0.22- $\mu$ F ceramic-disk capacitors is given in Figure II.27.

After receiving the trigger pulse, there is an inherent delay of 4.5  $\mu$ s before the CMX-4 fires. Once the laser fires, its output is monitored, for purposes of synchronization, by a photodiode located at the rear of the laser cavity. The output of this photodiode tracks the laser power output and is used to trigger a third delay, DELAY 4A (DELAY 3 is not implemented in this research). DELAY 4A is also a variable delay which can be set by a potentiometer on the front panel of the synchronization unit. At the end of this delay, a 1.7- $\mu$ s pulse is sent to gate the Evans gated integrator. Thus, DELAY 4A determines the part of the detector signal that will be integrated after the laser has fired, allowing the temporal characteristics of the detector signal to be examined.

#### b. Interface Circuitry

Because of the change in the type of controlling computer, additional circuitry had to be designed to allow the PC/DASH-8 combination to communicate with the synchronization electronics. The simplest function this circuitry performs is pulling the PC's TTL

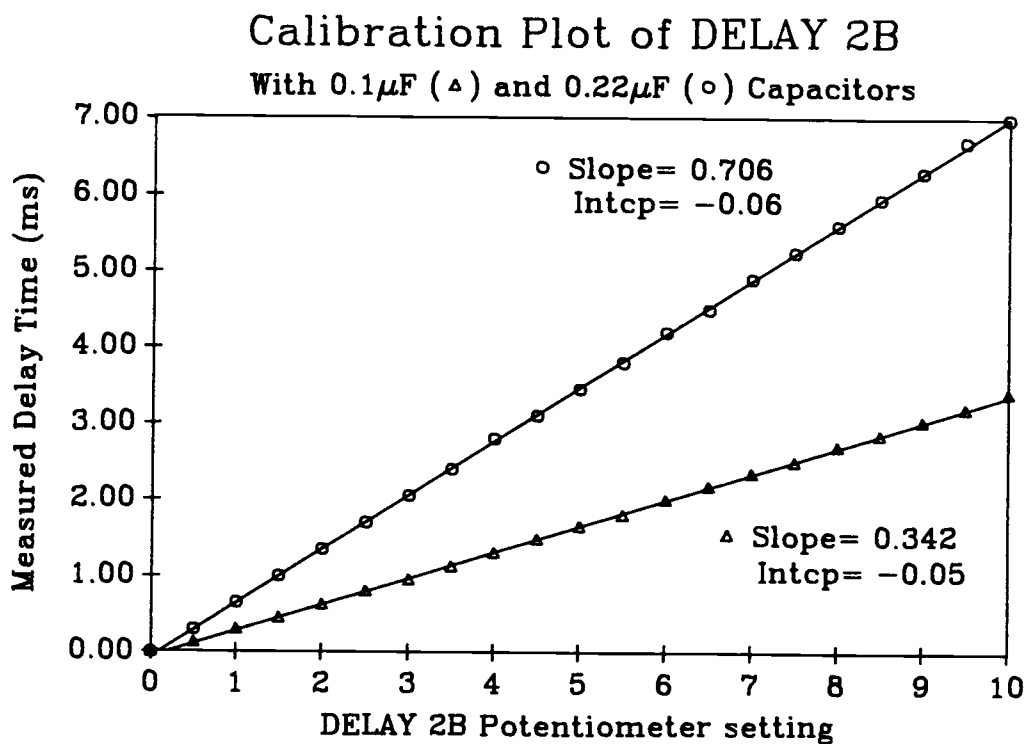


Figure II.27 Calibration plot of the DELAY 2B potentiometer with two different delay capacitors:  $0.1\mu\text{F}$  ( $\Delta$ ) and  $0.22\mu\text{F}$  ( $\circ$ ). Delays were measured by viewing the time difference between the delay 2B trigger pulse and the laser pulse on an oscilloscope.



logic high levels up to the +5V required by certain parts of the synchronization and control circuitry. This is accomplished through the use of open collector AND gates (74LS09 Quad AND gates) whose inputs are tied together. The output of each of these gates is pulled up to +5 V by 150- $\Omega$  or 180- $\Omega$  pull-up resistors. Thus a TTL high (3.5-4.0 V) applied to the inputs of the gate will produce a 4.5-5.0 V high at the output. In addition, these gates also buffer the different parts of the circuitry. The circuitry that accomplishes this interface is located on a Vector wire wrap prototype board, and is described by the schematic circuit diagram shown in Figure II.28. In addition, Table II.12 identifies the inputs and outputs to this board, along with the pin assignments which also correspond to the lettered connectors in the circuit diagram. The interface circuit board is located in a Vector chassis which slides into the synchronization interface panel. Connections to this board are made through two plates located on the back of the interface panel. These two connector panels are depicted in Figure II.29. In order to facilitate additions, modifications, and repairs to the circuitry, the wires which connect the back panel connectors to the circuit board pass through several intermediate connectors (the "Connector Out" column of Table II.12). This provides a means by which both the circuit board and the back panel can be easily removed, modified, and resembles. The connectors labeled "167772" and "167774" remain from the original interface where they were connected to PDP-11 I/O ports with those addresses. The connectors are still identified by these numbers, but the addresses no longer have any meaning.

#### (1) Stepper Motor Interface

The four AND gates labeled A1-A4 in Figure II.28 are used to pull the wavelength control lines of the CMX-4 etalon and birefringent filter, which originate from the second parallel port of

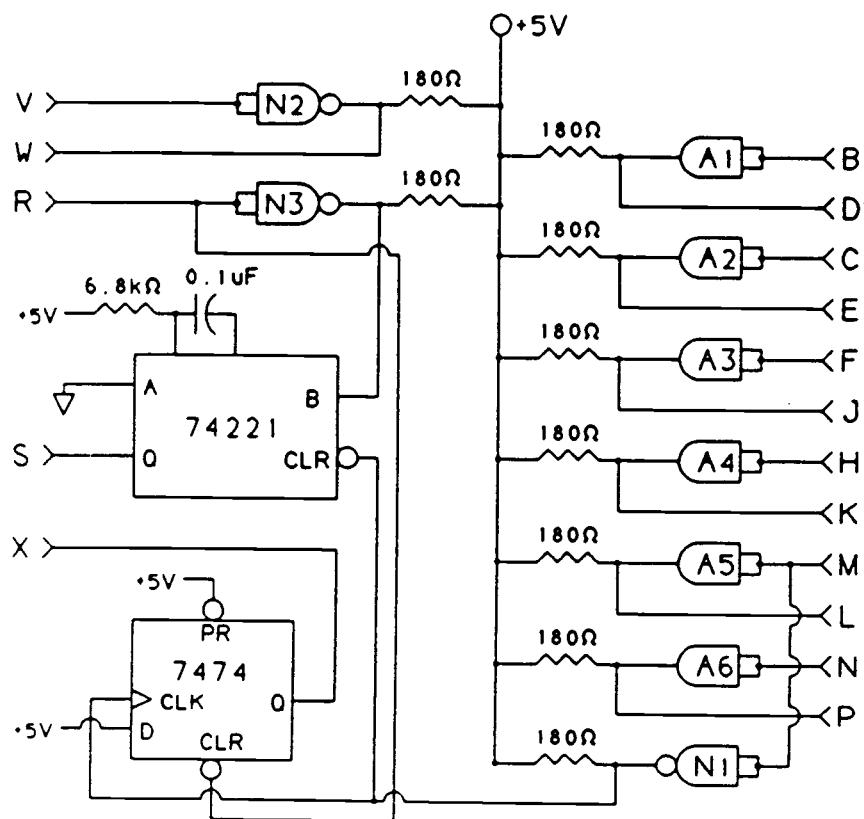


Figure II.28 Schematic circuit diagram of the synchronization interface board.

Table II.12

Corona PC-Synchronization Circuitry  
Interface Circuit Board I/O Pin Assignments

Pin <sup>1</sup> Number	Description	Wire <sup>2</sup> Out	Connector Out <sup>3</sup>	Back Panel Connector
A (1)	N/C			
B (2)	$\lambda$ step [+] fine in	Yellow	AMP1-E	LPT: pin 2
C (3)	$\lambda$ step [-] fine in	Orange	AMP1-A	LPT: pin 3
D (4)	$\lambda$ step [+] fine out	Violet	AMP2-F	167772: 33
E (5)	$\lambda$ step [-] fine out	Orange	AMP2-C	167772: 6
F (6)	$\lambda$ step [+] coarse in	Red	AMP1-H	LPT: pin 4
H (7)	$\lambda$ step [-] coarse in	Violet	AMP1-B	LPT: pin 5
J (8)	$\lambda$ step [+] coarse out	White	AMP2-E	167772: 27
K (9)	$\lambda$ step [-] coarse out	Red	AMP2-D	167772: 8
L (10)	Gate pulse out	White	--	Gate out BNC
M (11)	Delay 4A in (gate in)	White	--	Delay 4A BNC
N (12)	DASH-8 OP2 in (fire D2B)	Purple	AMP3-C	DASH-8: 8
P (13)	Fire delay 2B out	Yellow	AMP2-A	167772: 2
R (14)	Delay 1B in	Blue	AMP2-B	167774: 2
S (15)	Delay 1B out (to IP1)	Red	AMP3-E	DASH-8: 25
T (16)	DASH-8 OP1 in	Orange	AMP3-B	DASH-8: 7
U (17)	Trigger counter 2	White	AMP3-D	DASH-8: 23
V (18)	Counter 2 output in	Yellow	AMP3-A	DASH-8: 6
W (19)	Prog. pulse out	White	Molex2	Pulse Out BNC
X (20)	Gate done (to IP2)	Blue	AMP3-F	DASH-8: 26
Y (21)	+5 Volt power Bus	Red	Molex3	+5 V P.S.
Z (22)	Ground	Black	Molex3	"

<sup>1</sup>The number in parenthesis is the pin number as viewed from the bottom (wire) side of the board.

<sup>2</sup>Wire color refers to the wire which joins the mating edge connector of the circuit board, and the intermediate connector listed in the "Connector Out" column.

<sup>3</sup>The AMP designation refers to Amphenol type connectors, and Molex refers to Molex type connectors.

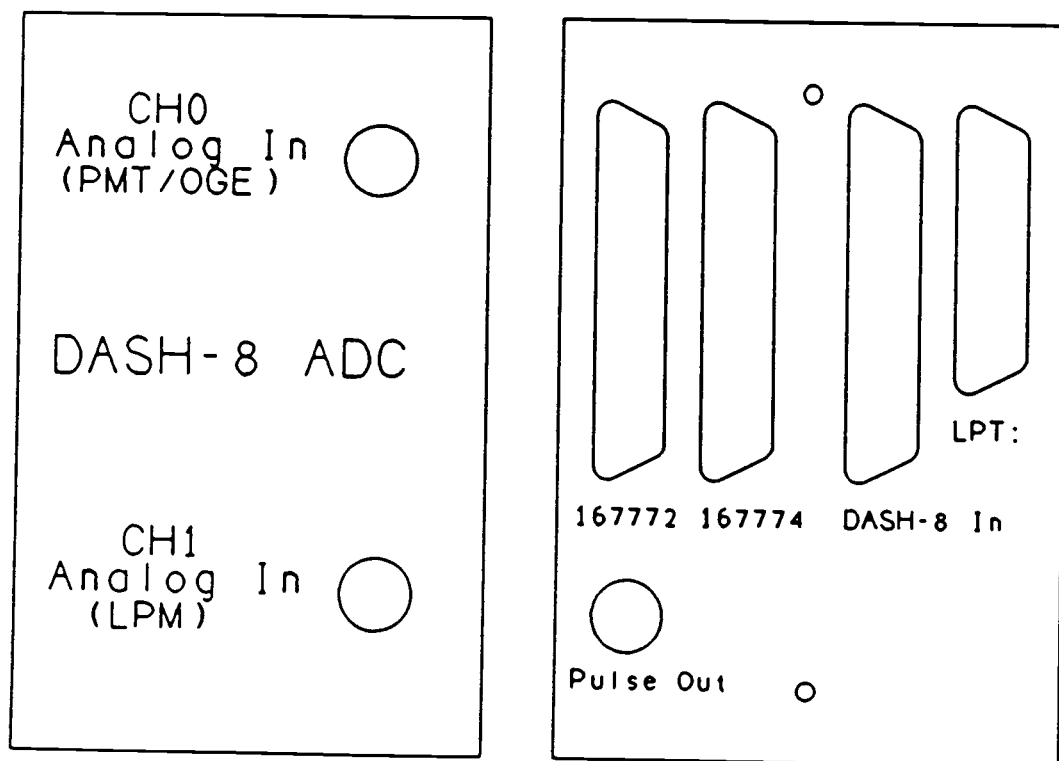


Figure II.29 Diagram of the back panel connections to the synchronization and data acquisition circuitry.

the PC, up to the +5 V required by the stepper motor translators. The UV doubling crystal stepper motor uses a different translator which doesn't require this level conversion.

## (2) Synchronization Interface

In order to facilitate the detection of the DELAY 1B timing pulse by the compiled BASIC control program, the DELAY 1B pulse is first inverted by NAND gate N3, and then is used to trigger a 74221 monostable multivibrator. The resistor and capacitor of the monostable are selected to give a 0.47-msec output pulse which can easily be detected by the control program. Figure II.30 is a timing diagram which illustrates the temporal relationship of the synchronization signals described in this section.

The control program receives the stretched DELAY 1B on the DASH-8 IP1 line and sends out simultaneous pulses on the DASH-8 OP1 and OP2 lines. The pulse on OP1 is jumpered directly back to the DASH-8 counter 2 gate, triggering a high to low pulse with a software programmed pulse width to be output as described earlier. This pulse, which must be inverted by NAND gate N2, is used to fire either the hollow cathode lamp during calibrations, or the Bosch fuel injector during fluorescence experiments. The other pulse, on OP2, is pulled up to +5 V by AND gate A6, and then triggers DELAY 2B, the laser firing delay.

At the conclusion of DELAY 2B, the laser fires, and the rear synchronization photodiode output triggers the gate delay, DELAY 4A. The output of delay 4A, a 1.7- $\mu$ s pulse, is used both to gate the Evans gated integrator, and also as a signal to the software that an analog-to-digital conversion (ADC) can be performed on the analog output of the gated integrator. AND gate A5 pulls the gate pulse up to the +5-V level required by the gate input. In addition, this same pulse, inverted by NAND gate N1, clocks a 7474 D type flip flop. The rising edge of the inverted gate pulse, which corresponds to the end

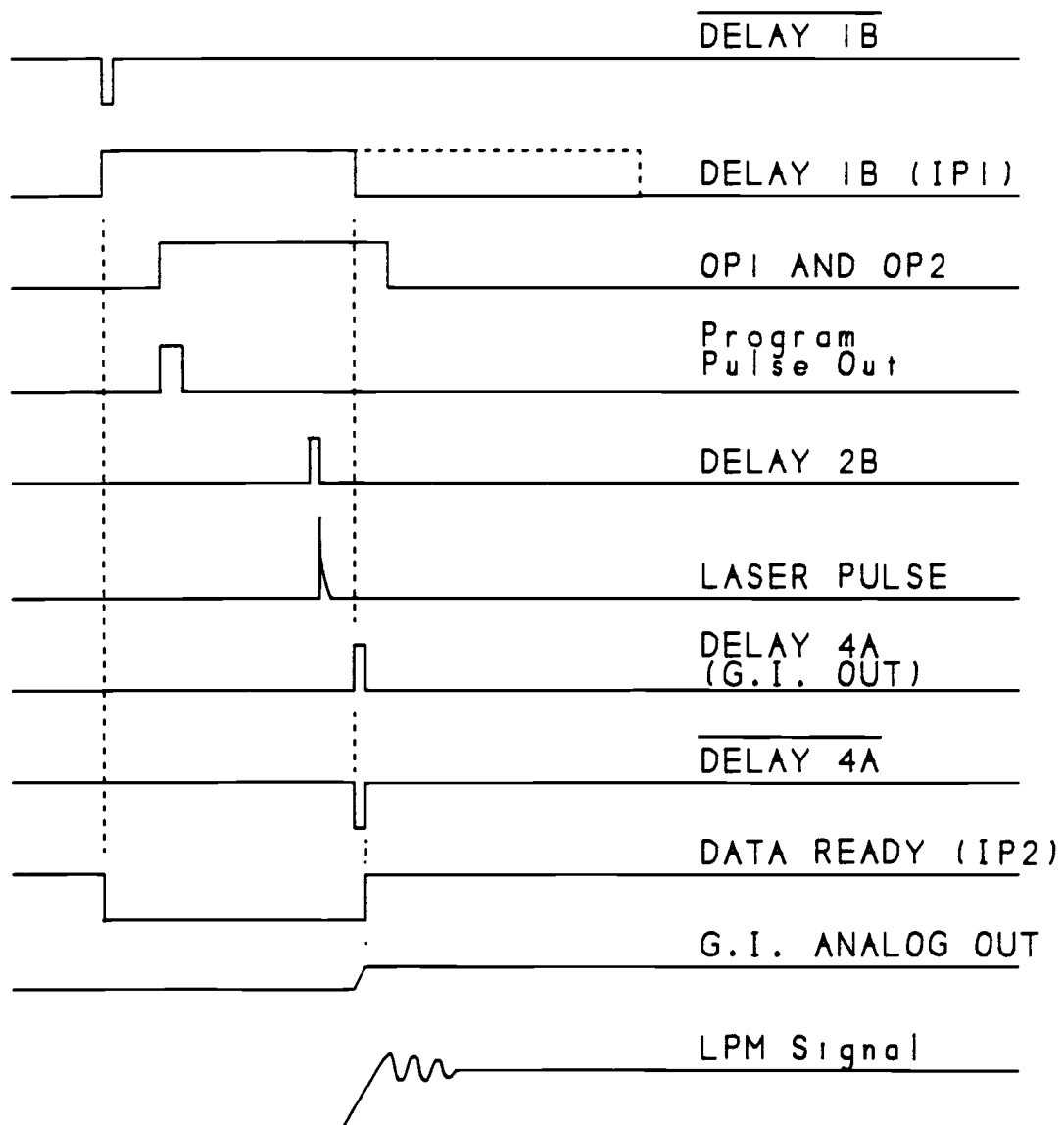


Figure II.30 Timing diagram illustrating the relationship between the various synchronization and data acquisition signals.

of the gate period, causes the flip flop to make a low to high transition. The control program monitors the output of the flip flop (Q) on IP2 of the DASH-8; When the high condition occurs, the gate is finished and an ADC can be performed. After the gated integrator signal has been acquired, the flip flop output must be returned to logic low in preparation for the next laser shot. This is accomplished by connecting the original, unstretched DELAY 1B pulse to the clear (CLR) input of the flip flop. Finally, as a precaution against the occurrence of multiple ADC triggers on a single laser pulse, the inverted gate pulse clears the DELAY 1B 74221 monostable in addition to clocking the 7474 flip flop. This is illustrated clearly by the timing diagram in Figure II.30.

## 5. Acquisition and Control Software

### a. General

When one designs a software scheme for use with an experimental system such as this one, there are basically two options open: buy commercially available software, or write your own. Because software development can be a very time-consuming occupation, it is often in the researcher's best interest to purchase commercial software when possible. Unfortunately, much of the quality low-cost software that has been written for the IBM PC was designed solely with business applications in mind and thus often has severe limitations from the scientists point of view. The scientist must either be satisfied with the limitations of the business software, or pay a premium and buy the usually very expensive scientific software package if it is available. In addition, especially in control and acquisition applications, instrumental configurations are often too complex to allow the adaptation of commercial software. Thus, some combination of commercial and personally developed software is often used. This

is the case with this research; data acquisition and control is accomplished with custom software while data analysis is achieved with commercial packages.

All of the custom, high level programs developed in this work were written with the Microsoft QuickBASIC compiler (version 4.0, Microsoft Corporation, Bellevue WA). BASIC was chosen as the development programming language because it is a language that is easily learned and thus the code will be more easily maintained by those who use it in the future. Fortunately, most of the classic drawbacks to BASIC, that is, slow execution speed, and inability to program in a structured format, have been solved with the release of the new Microsoft BASIC compiler used in this work. In those situations where faster execution speeds are required, assembly language subroutines were developed which are called from the main BASIC program. The assembler used to compile the assembly language subroutines was the Microsoft Macro Assembler (version 5.0, Microsoft Corporation, Bellevue WA). These custom acquisition and control programs and subroutines will be described in detail in the following sections and are summarized in Tables II.13 and II.14. In addition, the commercial packages used for data analysis will also be discussed.

Representative BASIC programs and the important subroutines used in this research are listed in Appendix C. In addition, Appendix B provides important information regarding the compilation of both the BASIC programs and the assembly language subroutines. Additional information concerning the creation of subroutine libraries and their use with QuickBASIC is also provided.

#### b. Assembly Language Acquisition and Control Subroutines

Each of the high level BASIC control programs must interact in some way with the laser or detector system and thus must operate under the synchronization and control constraints mentioned



Table II.13

Custom Data Acquisition and Control  
Programs used in this Research: BASIC Programs

Name	Description
BIFIT.BAS	Least-squares fitting program which fits the birefringent filter and UV crystal calibration data to a quadratic polynomial
CHROM.BAS	Control of the CMX-4 laser system for acquisition of fluorescence excitation gas chromatograms.
CMX4CAL.BAS	CMX-4 laser calibration program: automated acquisition of optogalvanic data for etalon and birefringent filter scans.
GPMENU.BAS	Main menu program for experimental system
PEAK.BAS	Signal peaking utility which provides limited data acquisition capabilities.
REPLOT.BAS	Graphics plotting of fluorescence spectra and chromatograms that allows peak areas and locations to be determined.
SIMPLEX.BAS	Simplex optimization of the etalon parameters, $t$ , "80", $\Delta X$ , and $\cos 2\phi$ , using calibration data.
SPECTRUM.BAS	Acquisition of laser-excited fluorescence excitation spectra: automated control of laser and acquisition of data.
UVCAL.BAS	CMX-4 UV-doubling crystal calibration program: automated acquisition of UV Xtal micrometer calibration data

Table II.14

Custom Data Acquisition and Control Programs  
used in this Research: Assembly Language Subroutines

Name	Description
A2D.ASM	Assembly language subroutine which triggers an ADC on a desired channel and returns the data. Used after DATAQ to obtain the laser power signal.
DATAQ.ASM	Assembly language subroutine which triggers the laser and pulsed valve, and returns the analytical signal from the desired channel (CH0 normally) of the ADC.
DELAY.ASM	Assembly language subroutine delays program execution for a desired number of milliseconds.
MSDELAY.ASM	Core millisecond delay routine used by DELAY, PULSE, and TRAIN to generate delays in 1 millisecond increments. Not callable from BASIC.
PULSE.ASM	Assembly language subroutine sends out a pulse of desired width on an output port.
TRAIN.ASM	Assembly language subroutine which sends a programmed pulse train to an output port.

previously. Since these constraints are the same for each of the control programs, they all must share similar coding of their control and acquisition loops. To ensure consistency and compatibility, a set of generalized data acquisition subroutines were written in assembly language that execute the core acquisition loop. In addition, several other low level control routines were also written in assembly language.

### (1) Data Acquisition Loop

At the lowest level of synchronization associated with simply firing the laser, the program code must follow the flow chart illustrated in Figure II.31. The constraint here is simply that DELAY 1B must be received on line IP1 (IP1 must go high) before the laser and pulsed valve can be fired. The BASIC code which could be used to accomplish this is fairly simple, and is listed below.

```

DO
1      WAIT StatReg, 16      'Wait for IP1 = 1
2      OUT StatReg, 48      'Pulse OP1 & 2 to 1
3      OUT StatReg, 0      'Finish Pulse
      LOOP UNTIL Done

```

This code will simply fire the laser repetitively at whatever rate has been set on the front panel DIP switches.

The complexity of the required code increases rapidly as data acquisition is added into the loop as illustrated by the flowchart in Figure II.32. Here, the program must not only monitor DELAY 1B, but it must also determine when the gate pulse has finished by monitoring the signal on IP2. In addition, for each of the ADCs, it must determine when the conversion is finished by monitoring the EOC flag which is bit 7 of the Status Register (see Table II.11). The equivalent BASIC code required to perform this is illustrated below.

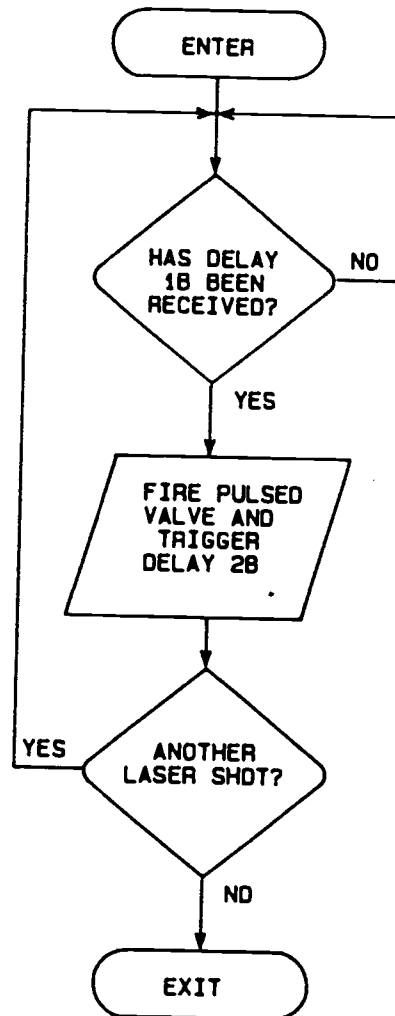


Figure II.31 Flow Chart of the laser synchronization and triggering loop.

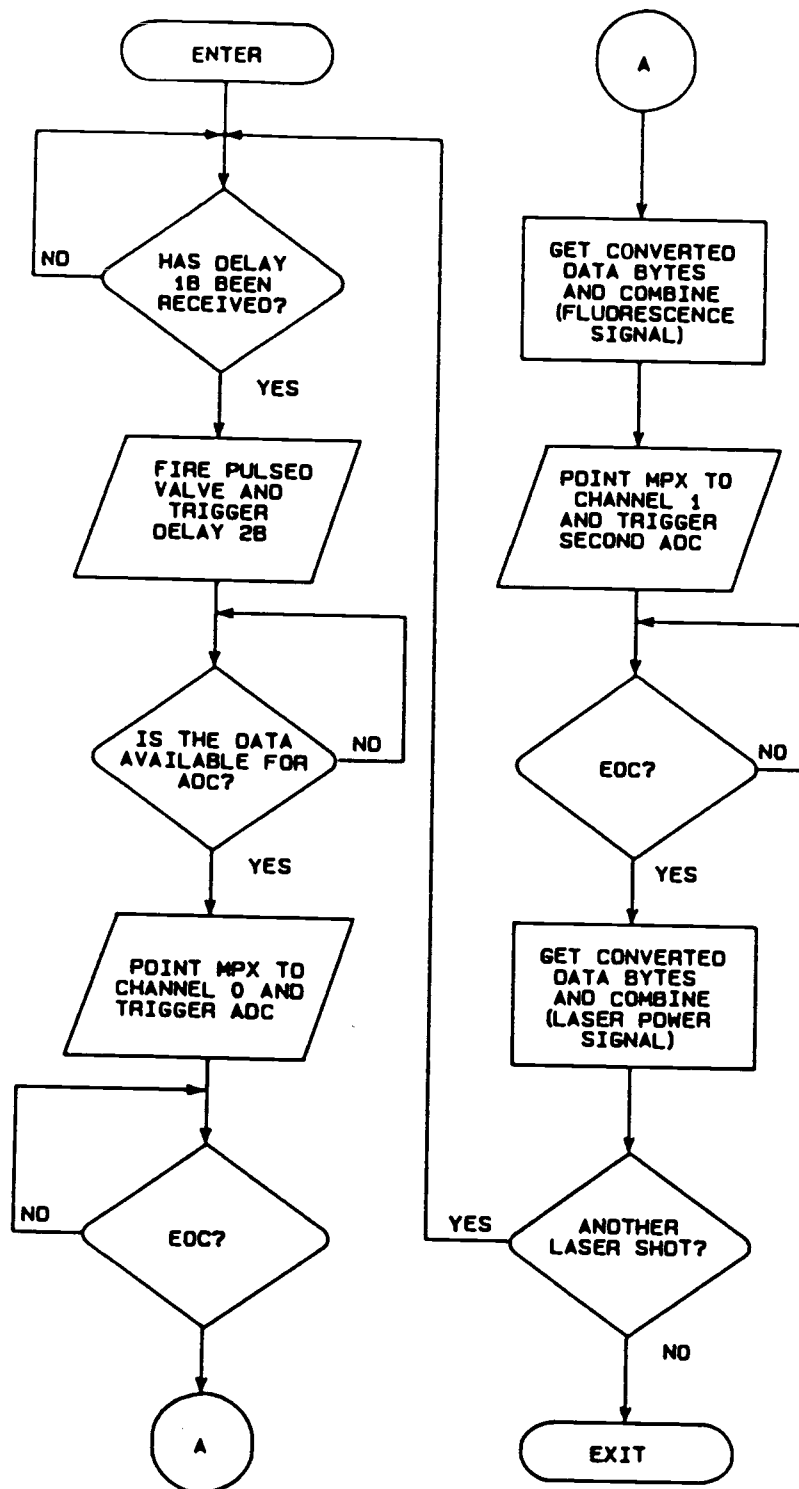


Figure II.32 Flow Chart of the combined synchronization and data acquisition loop used by most of the control programs in this research.

```

DO
1      WAIT StatReg, 16      'Wait for DELAY 1B
2      OUT StatReg, 48      'Fire Valve & Laser
3      OUT StatReg, 0       'Finish Trig. Pulses
4                               'and point MPX to CH0
5      WAIT StatReg, 32     'Wait for Gate Done
6      OUT ADCReg,0         'Trigger ADC on CH0
7      WAIT StatReg, 128    'Wait for EOC
8      Xlow = INP(BaseAdd)  'Get Low Byte
9      Xhigh = INP(ADCReg)  'Get High Byte
10     X0 = Xhigh*16 + Xlow/16 'Combine: Anal. Signal

11     OUT StatReg, 1       'Point MPX to CH1
12     OUT ADCReg,0         'Trigger ADC on CH1
13     WAIT StatReg, 128    'Wait for EOC
14     Xlow = INP(BaseAdd)  'Get Low Byte
15     Xhigh = INP(ADCReg)  'Get High Byte
16     X1 = Xhigh*16 + Xlow/16 'Combine: Laser Power

LOOP UNTIL Done

```

This code can be incorporated directly into any new program to provide the means for correct synchronization of the experimental system and acquisition of the analytical signal and laser power signal. Although this routine will work as written, much of the code was combined into two assembly language subroutines, DATAQ and A2D, which will be discussed in the following sections. The use of the assembly language version of this routine increases execution speed and thus eases any code dependent timing requirements: for example, the DELAY 1B signal is sensed much more quickly by the assembly language routine than by the similar BASIC code, and thus the laser can be fired much earlier in the period in which it must triggered (when its input power is in a positive cycle).

#### (a) DATAQ Acquisition Subroutine

An assembly language subroutine, DATAQ.ASM, was written to execute the core synchronization and acquisition functions required for data collection. This subroutine can be called directly from the main BASIC control program if the steps outlined in Appendix B are

followed. The subprogram is called, passing four integer arguments:

Dataq TrigByte%, Channel%, LoByte%, HiByte%

All four of the integer variables must be included when the subroutine is called. These four variables are defined as follows. TrigByte% is the byte that will be sent to the status register of the DASH-8 to trigger the laser and pulsed valve by setting the DASH8 digital output ports high (see Table II.11). Channel% is also written to the status register and is used both to set the multiplexer channel on which the ADC will occur and to turn off the output port bits that were turned on by TrigByte%. Finally, LoByte% is the low data byte returned from the ADC, and HiByte% is the high data byte returned from the ADC. Dataq replaces lines 1-9 of the BASIC acquisition loop listed previously.

#### (b) A2D Acquisition Subroutine

Since two separate analog-to-digital conversions are required for each laser shot to acquire both the analytical signal and laser power, and since Dataq only returns the analytical signal, a second assembly language subroutine was written to acquire the laser power signal from channel 1 without retriggering the laser. The subroutine A2D simply triggers a conversion on the desired channel, and returns the data. It is used in the same manner as Dataq, and requires three integer parameters. It is called using the following syntax.

A2D Channel%, LoByte%, HiByte%

The three parameters have the same meaning as they did in Dataq above. This subroutine is used to replace lines 11-15 of the previous BASIC language example, but could be used more generally whenever it is desired to trigger an ADC from software. When Dataq

and A2D are combined the previous BASIC acquisition loop is condensed from 16 lines to the following 4 lines.

```

      DO
1      Dataq 48, 0, Xlow, Xhigh
2      X0 = Xhigh*16 + Xlow/16
3      A2D 1, Xlow, Xhigh
4      X1 = Xhigh*16 + Xlow/16
      LOOP UNTIL Done

```

This loop is used, with various values of TrigByte% and Channel%, as the acquisition loop in PEAK.BAS, CMX4CAL.BAS, and SPECTRUM.BAS, CHROM.BAS, and UVCAL.BAS, which are the main data acquisition programs.

## (2) Other Important Subroutines

### (a) DELAY

As described in the section describing the use of the PCs 8253 timer, there are often instances when delays and pulses of known, reproducible duration must be generated. The subroutine DELAY, which was written to generate time delays with millisecond resolution, will be described first since it is the simplest case. After declaring DELAY at the beginning of the main BASIC module as described in Appendix B, it can be called directly from BASIC using the following format.

DELAY Delay%

DELAY requires one integer argument, Delay%, which is the delay time in milliseconds.



## (b) PULSE

A single pulse of desired width can be generated at an output port using the assembly subroutine PULSE. For example, pulse is used to send pulses to the stepper motor translators in the high level BASIC subroutines that control the movement of the stepper motors. This results in one step of the stepper motor for each pulse sent by PULSE. PULSE requires four integer arguments and can be called as follows.

PULSE PWidth%, Port%, ByteOn%, ByteOff%

Where PWidth% is the width of the output pulse in milliseconds, Port% is the output port to which the pulse will be sent, ByteON% is the byte that will be written to PORT% to turn on the desired bits of the port, and ByteOff% is the byte that will be sent to PORT% to turn off the bits turned on by ByteOn%. Note that ByteOff% is normally 0, but can be set to a non-zero value if it is desired to keep some of the output port bits high.

## (c) TRAIN

The logical extension of sending a single pulse to an output port is to send multiple pulses separated by a fixed delay (a pulse train). The subroutine that accomplishes this, TRAIN, is essentially a combination of the PULSE and DELAY subroutines. TRAIN is used in the same manner as previous subroutines, and requires six integer arguments as illustrated below.

TRAIN PWidth%, Delay%, Length%, Port%, ByteOn%, ByteOff%

Four of these arguments, PWidth%, Port%, ByteOn%, and ByteOff%, are identical to those described for PULSE above. Additionally, TRAIN requires an argument, Delay%, defining the delay, in milliseconds, between pulses. Finally, Length% is simply the length of the pulse train; the integer number of pulses to be output.

### c. High Level BASIC Acquisition and Control Programs

#### (1) Overview: Master Control Program, GPMENU

Each of the acquisition and control programs was written so it can be called either directly from DOS, or from a central menu program, GPMENU.BAS. When each program is finished it returns to the environment from which it was called, DOS, or GPMENU. A flowchart illustrating the various options available through GPMENU can be found in Figure II.33. In addition, Figure II.34 is a computer screen dump of the menu. Selection of GPMENU options 1-4, 8-9, "C", and "P" result in transfer of program control to compiled basic programs through the use of the BASIC CHAIN statement. In addition, options 5 and 6 access the Norton Editor (NE, Peter Norton Computing) to allow editing of the two calibration data files BIFILTER.DAT and ETALON.DAT. This is useful when a calibration is being performed and it is desired to add or remove data pairs from the data set. The programs called from GPMENU are described in the following sections in the order they would most likely be used when using the instrument for the first time.

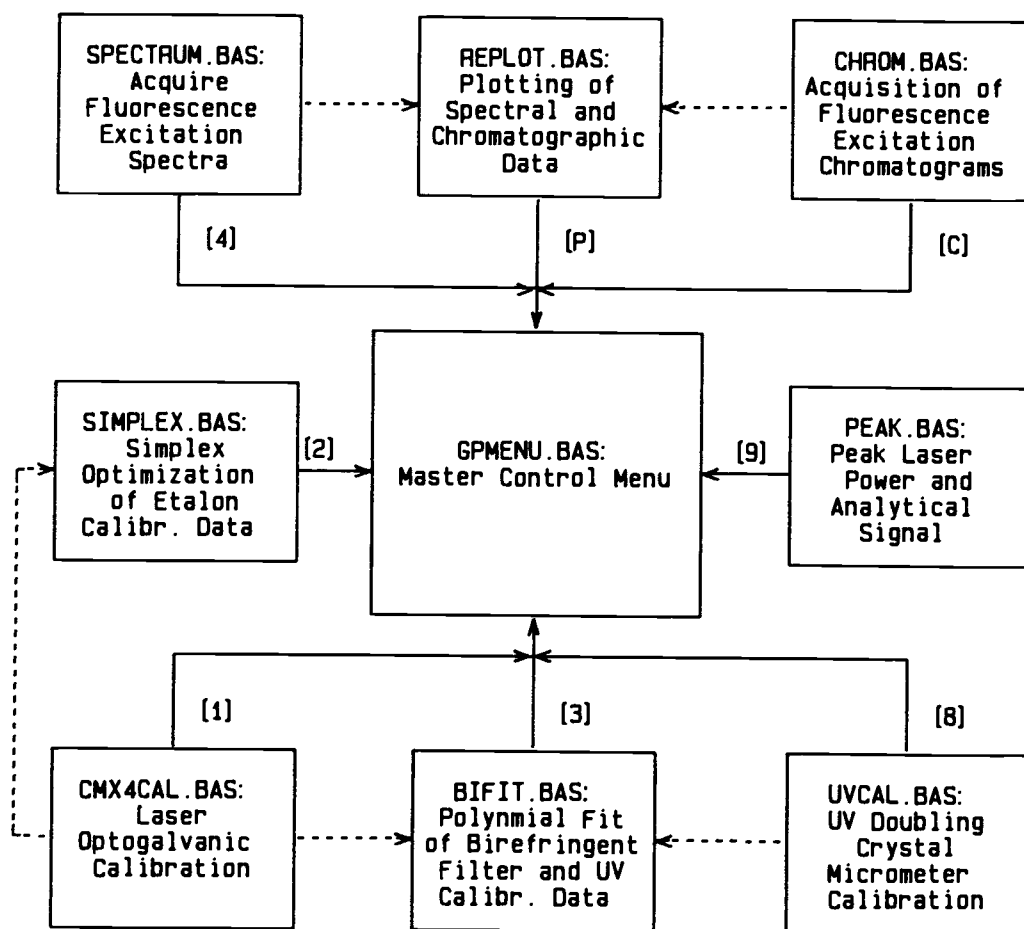


Figure II.33 Flow chart of the master control menu program GPMENU.BAS illustrating the relationship between the various control and acquisition programs. Dotted lines link programs that share common data files.

Data Acquisition and Control Software for the Chromatix CMX-4 Dye Laser: Ver 3.20 (C) 1986, 87, 88 Scott J. Hein		
11 June 1988	MENU OPTIONS	22:24:49
<b>1</b> Calibrate CMX-4	<b>6</b> Edit (NE) ETALON.DAT	
<b>2</b> Simplex Optimization	<b>7</b> DOS Shell (Return via EXIT)	
<b>3</b> Poly Fit of B.F. & UV Data	<b>8</b> Calibrate Doubling Crystal	
<b>4</b> Acquire Fluorescence Spectra	<b>9</b> Peak Laser Power	
<b>5</b> Edit (NE) BIFILTER.DAT	<b>P</b> Plot Fluor. or Chrom. Data	
<b>C</b> Chromatographic Acquisition	<b>Q</b> Quit and Return to DOS	

Figure II.34 A printer screen dump of the GPMENU.BAS menu screen.

## (2) Laser Signal Peaking Utility, PEAK

In order to maximize the power output of the CMX-4, the front mirror micrometers and the UV doubling crystal position must be optimized prior to each experiment. A BASIC program, PEAK, was written to make this process easier. PEAK uses the acquisition loop described in previous sections to acquire the signal from both the laser power monitor and the Evans gated integrator. A moving bar graph is then displayed on the graphics monitor, the height of each bar being proportional to the signal. For reference, the level of the largest acquired signal is displayed as a line across the display window. Since this display is continuous, and the visual representation of the signal level is easy to follow, even from across the room, the optimization of experimental parameters can be accomplished much more readily. A graphics screen dump of PEAK in operation is shown in Figure II.35 which illustrates a partially filled bar graph window as well as the menu options and other information.

By selecting menu options 1-3 it is possible to toggle between viewing the laser power signal, the raw gated integrator signal, and the corrected gated integrator signal, which is the raw signal divided by the laser power. In addition, the pulsed valve can be toggled on and off by selecting menu option 4. This is particularly useful in optimizing the fluorescence signal since the analytical signal (valve on) can easily be differentiated from background scatter (valve off). Other options include the ability to set the valve pulse width (option 5), to scale the display window (options S, +, and -), to block the laser beam (B) and to pause the program (space bar). Pausing the program also resets the running signal average, which is displayed in the upper right corner of the display window, to zero. Finally, the laser can be toggled off and on with the valve pulsing continuously using the "V" (Valve only)

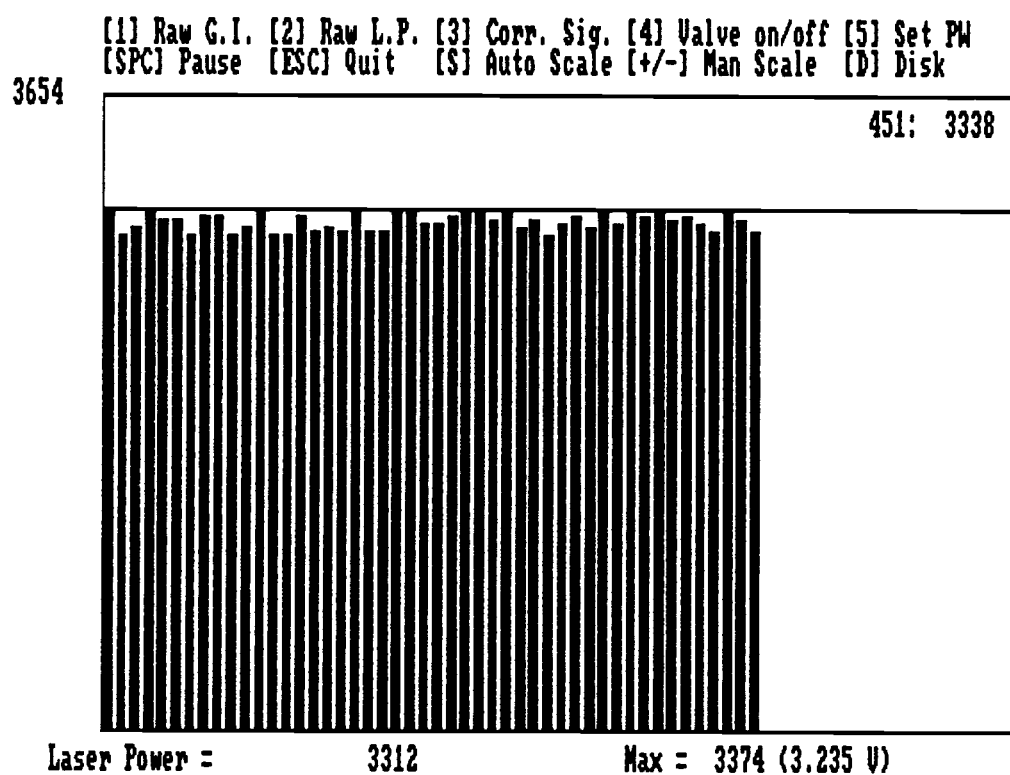


Figure II.35 Graphics screen dump of the program PEAK showing the various menu options and a partially filled bar graph window.

option. This is useful in chromatographic experiments where flow through the column must be maintained even though data collection is not needed.

In addition to the signal maximization functions, PEAK also has limited, low level data acquisition capabilities. Selection of menu option "D" (for Disk) will allow the user to specify an output file for data storage, and the number of laser shots to collect each time acquisition is requested. Subsequently, each time the enter key is pressed, the user will be prompted for an "X" (independent) value and the previously determined number of data points will be collected and written to the data file along with the X value. Selecting option "D" a second time toggles the user out of acquisition mode and closes the data file.

### (3) Laser Wavelength Calibration, CMX4CAL

As described in a previous section, the CMX-4 laser is wavelength calibrated by monitoring the photogalvanic signal from a hollow cathode lamp as a function of etalon and birefringent filter micrometer position for a number of known neon transitions. Because this procedure is very tedious and imprecise when done manually, a program, CMX4CAL.BAS, was written which controls the stepper motor positions and acquires the data for a more precise analysis of the calibration signal.

The program's operation is best described by following the flow chart in Figure II.36. The program uses data from three disk files, CMX4DAT.DAT, ETALON.DAT, and BIFILTER.DAT, which must be present in the same subdirectory as CMX4CAL. The format of these data files is outlined in Table II.15, which also includes sample values for the various parameters. Parameters are placed in these data files in columns separated by spaces; the actual data placed in the file are enclosed in complete boxes in Table II.15. The file CMX4DAT.DAT is shared between all the programs that control the CMX-4 stepper motors

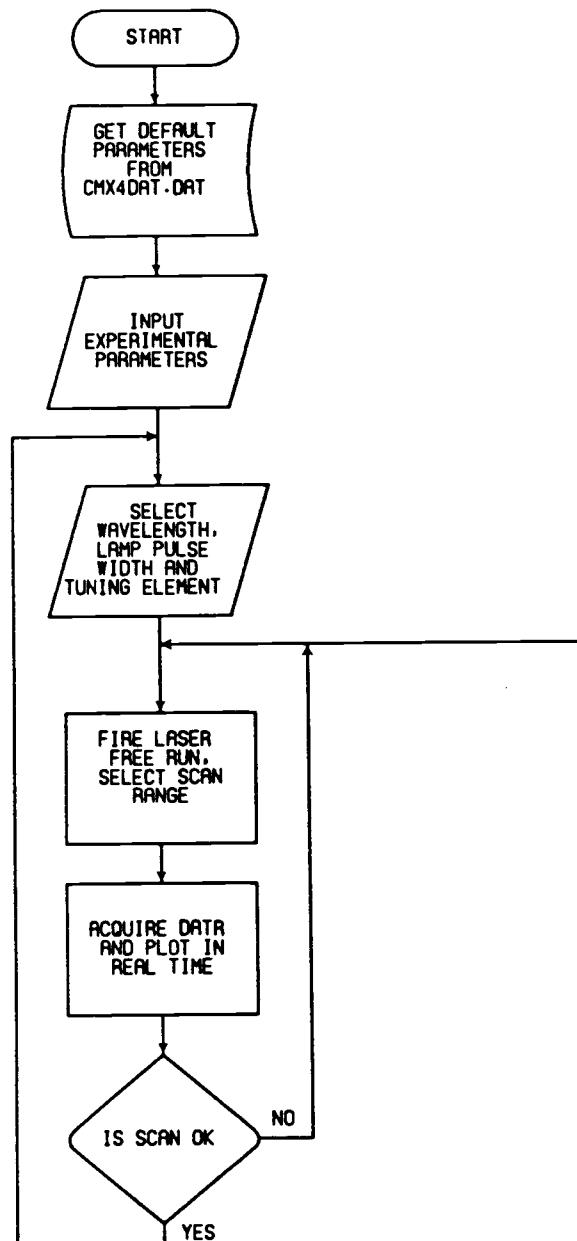


Figure II.36 Flow chart of the laser wavelength calibration program CMX4CAL. Flowchart is continued on the following page.



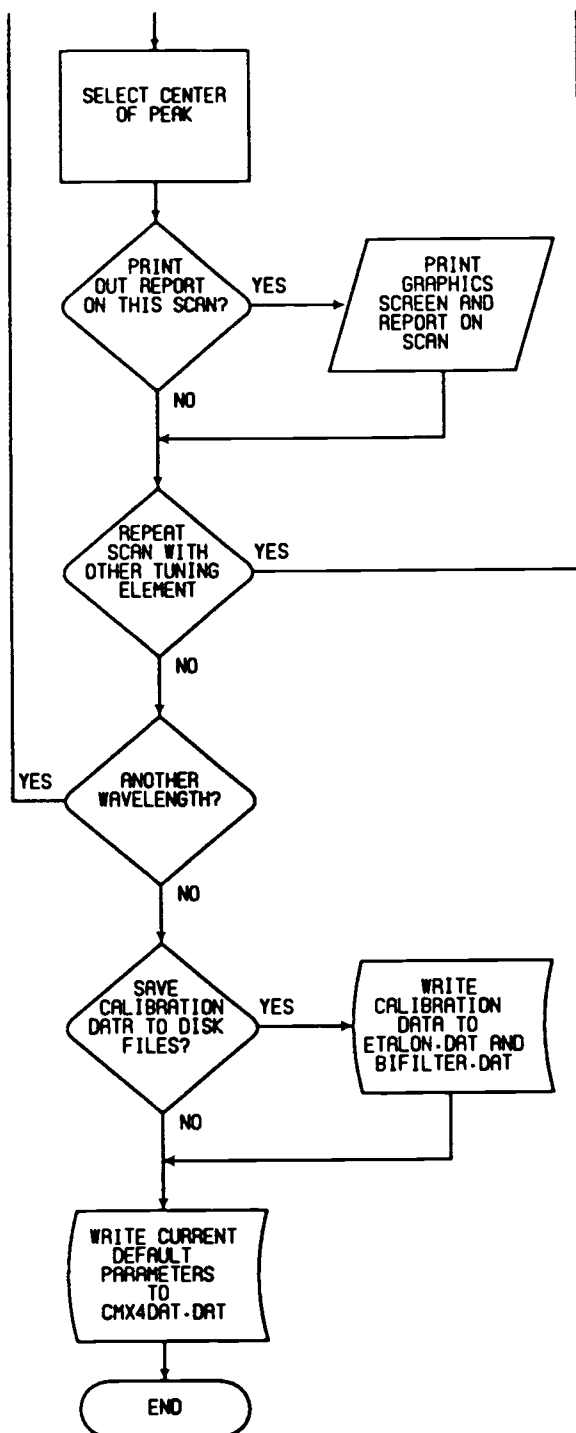


Figure II.36 Continuation.

Table II.15

Format of Data Files Required by  
the Calibration Program CMX4CAL<sup>1</sup>

---

CMX4DAT.DAT: Default CMX-4 Operating Parameters

---

<u>Line</u>	<u>Description</u>	<u>Sample Contents</u>
1	XET: Current Etalon Position	5.255
2	XBI: Current Bi. Filter Pos.	4.616
3	Delay 2B	2.11
4	Delay 4A	0.30
5	Atmospheric Pressure (Torr)	759.2
6	Laboratory Temperature (°C)	25.0
7	XUV: Current UV Crystal Pos.	540.8

<sup>1</sup>The data are stored in ASCII format and, when applicable, columns of data are separated by one or more spaces. Examples of the actual data that are placed in the file are enclosed in a box in each of the file descriptions.

Table II.15 (continuation)

ETALON.DAT: Etalon Wavelength and Micrometer Position  
Data from Previous Calibration.

Etalon Position	Wavelength (Angstroms)	Atmospheric Pressure (Torr)
5.2300	5881.895	753.1
4.4700	5906.429	753.1
5.3650	5913.589	753.1
4.7400	5918.910	753.1
5.0750	5961.630	753.1
5.3750	5965.474	753.1
5.0600	5987.907	753.1
5.4400	5991.670	753.1
5.1700	6000.950	753.1
5.0200	6029.997	753.1

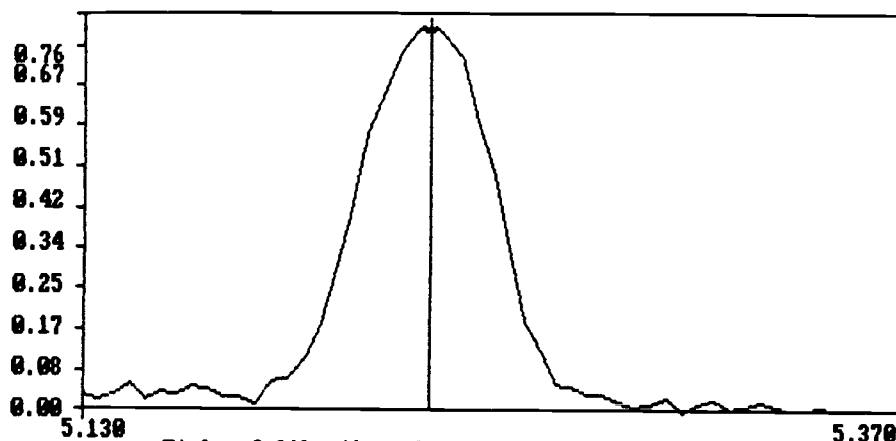
BIFILTER.DAT: Birefringent Filter Wavelength and  
Micrometer Position Data from Previous Calibration

Biref. Filter Position	Wavelength (Angstroms)
4.616	5881.895
4.952	5906.429
5.051	5913.589
5.124	5918.910
5.702	5961.630
5.753	5965.474
6.053	5987.907
6.103	5991.670
6.227	6000.950
6.608	6029.997

and is updated whenever the stepper motor positions (XET, XBI) are changed. The files ETALON.DAT and BIFILTER.DAT are updated by CMX4CAL at the end of the calibration and then are used by the programs SIMPLEX and BIFIT, respectively, to obtain the various calibration parameters. These other programs will be described in subsequent sections.

After initializing the various experimental variables through a series of prompts, the wavelength and tuning element (etalon or birefringent filter) to be calibrated are selected and the program enters a free run mode. In this mode the stepper motor is first stepped to the optimum micrometer position determined from the previous calibration and then the laser is fired free run while the optogalvanic signal is viewed on an oscilloscope. The stepper motor is then stepped to each side of the optogalvanic peak using the right and left arrow keys. The initial and final scan positions are then set by depressing the "I" (Initial) and "F" (Final) keys at the desired stepper motor positions.

Next, the optogalvanic signal is acquired as a function of stepper motor position across the previously determined scan range and the signal is displayed on the computer graphics screen. At the end of the scan the resulting peak is scaled and replotted on the graphics screen. If the scan is acceptable, the center of the peak is selected by moving a cursor using the right and left arrow keys. A graphic screen dump of the peak and a summary report are then printed if desired. An example of one such report is reproduced in Figure II.37. This procedure is then repeated for the other tuning element and again for the remaining wavelengths. After both tuning elements have been calibrated for all ten wavelengths, the new calibration data are written to ETALON.DAT and BIFILTER.DAT. These new data are then used to obtain the calibration parameters for each of the tuning elements using the programs BIFIT.BAS and SIMPLEX.BAS described below.



Etalon Calibration: Lambda= 5881.895  
 SF= 4856 Xmax = 5.2400 Ymax = 0.8433  
 Shift-PrtSc to Print Graphics (Screen 7): <CR> to Print Report

CMX4 ETALON CALIBRATION: LAMBDA= 5881.895

```
=====
07-28-1987    12:41:30
Barometric Pressure (TORR)= 753.1  Lab Temperature = 25
Lamp Used: Hamamatsu Cu HCL
Laser Rep Rate (Hz)= 5
Delay 2B (Laser Trigger Delay) = .99
Delay 4A (Gate Delay) = .9
HCL Pulse Width (mSec)= .4
Neutral Density Filter for Beam Attenuation: None
Neutral Density Filter for Laser Power Monitor: A = 1.5

Initial X for Scan = 5.129996   Final X for Scan = 5.370002
Xcenter = 5.239996
Signal at Xcenter = .8432509 (Raw OGE Signal= 1318 : 1.7812 V)
Maximum Signal = .843251
Background Signal = 1.5786 (Raw Bkg Signal= 1972 : .18544 V)
Final Scale Factor = 4856.206
Number of Shots (raw data points) per X = 5
Average Laser Power = 3161.946 ( 2.718028 V)
=====
```

Figure II.37 Sample wavelength calibration report for a CMX-4 etalon scan of the 5881.895 Å neon transition.

(a) Polynomial Fit of Birefringent Filter Data, BIFIT

The birefringent filter calibration data in the file BIFILTER.DAT consist of ten birefringent filter-neon wavelength pairs. These data are fit to the second order polynomial described by

$$\text{Lambda} = B0 + (B1 * XBI) + (B2 * XBI^2) \quad (\text{II.7})$$

The regression coefficients, B0, B1 and B2, that result from the least-squares polynomial fit, are the desired birefringent filter calibration parameters. These parameters are used by control programs, along with equation II.7, to determine the stepper motor position required to tune the laser to a desired wavelength. The program, BIFIT.BAS, was written to perform this fit. The subprograms that actually perform the fit were converted into BASIC from the FORTRAN subroutines POLFIT.FOR and DETERM.FOR presented by Bevington [88]. An example of the program output illustrating the results of a sample fit can be found in Figure II.38. These data are plotted along with the regression line in Figure II.39.

If the fit is acceptable these three calibration parameters are written to the file CMX4CAL.DAT which contains the most recent calibration parameters for both the etalon, the birefringent filter, and the UV crystal. The format of CMX4CAL.DAT is illustrated in Table II.16 along with sample calibration parameters. It should be noted that BIFIT is also used to fit the UV doubling crystal calibration data and obtain the UV crystal calibration parameters U0, U1, and U2.

Birefringent Filter Calibration: 07-18-1988  
Least Squares Polynomial Fit Results.

=====

Final Regression Coefficients:   B0 =   5564.04839  
                                       B1 =   65.25117028  
                                       B2 =   0.789806354

X (bi)	Lambda	Lambda Calc	Residual
-----	-----	-----	-----
4.6130	5881.895	5881.859	0.03606
4.9500	5906.429	5906.394	0.03509
5.0490	5913.589	5913.636	-0.04661
5.1220	5918.910	5918.985	-0.07536
5.7000	5961.630	5961.641	-0.01087
5.7510	5965.474	5965.430	0.04407
6.0520	5987.907	5987.876	0.03052
6.1020	5991.670	5991.619	0.05100
6.2270	6000.950	6000.993	-0.04259
6.6120	6029.997	6030.018	-0.02131

Sum of the Squared Residuals =   0.01824  
Sum of the Residuals = -0.000000  
Average Residual = -0.000000  
Chi-Square for the Fit =   0.00261

Figure II.38   Example of a birefringent filter calibration report generated by the polynomial fitting program, BIFIT. All wavelengths listed are neon transitions.

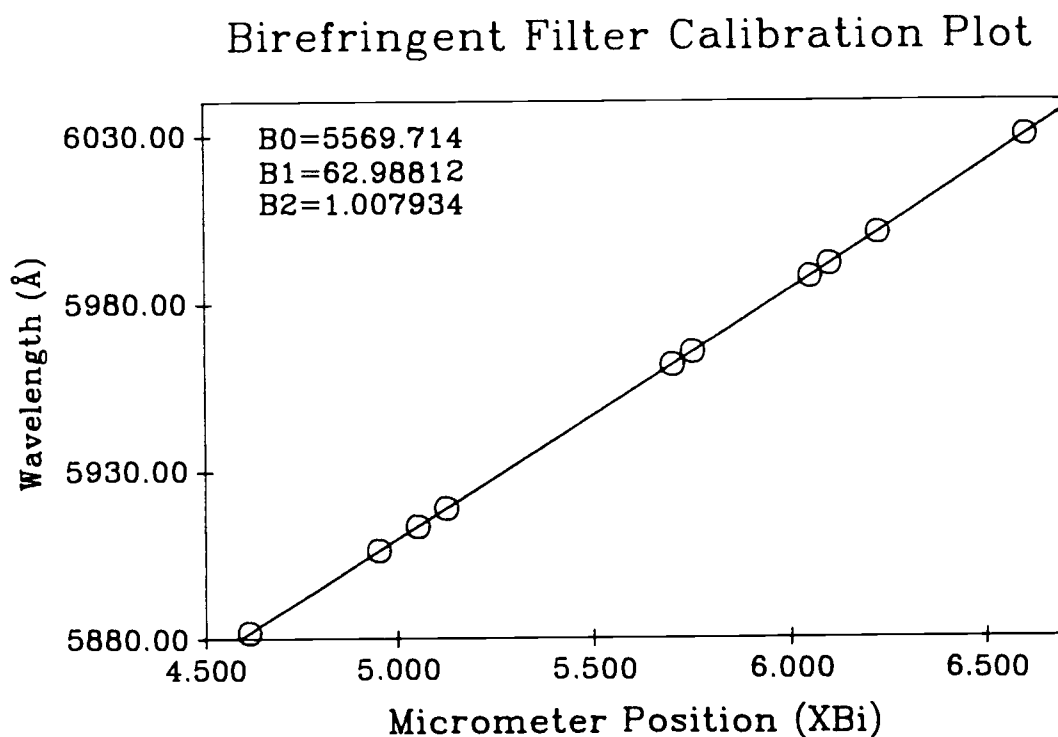


Figure II.39 Calibration plot of the results listed in Figure II.38. The calibration parameters B0, B1, and B2 are used to predict the birefringent filter micrometer position for a desired wavelength.



Table II.16  
Format of the Data File CMX4CAL.DAT

Line	Description	Sample Value
1	Etalon Parameter "t"	5524070
2	Etalon Parameter "Eighty"	79.86003
3	Etalon Parameter "Cos2 $\Phi$ "	0.9995264
4	Etalon Parameter " $\Delta X$ "	-1.340685
5	B.F. Parameter "B0"	5569.7141
6	B.F. Parameter "B1"	62.988125
7	B.F. Parameter "B2"	1.0079339
8	UV Crystal Parameter "U0"	-20642.62
9	UV Crystal Parameter "U1"	6.4049484
10	UV Crystal Parameter "U2"	-4.77D-04

### (b) Simplex Optimization of Etalon Calibration Data, SIMPLEX

The four calibration parameters that are used by control programs to determine the etalon position for a desired wavelength are  $t$ ,  $E_{\text{Eighty}}$ ,  $\cos^2\phi$ , and  $\Delta X$ , as outlined in a previous section. The goal of the etalon calibration is to optimize the value of each of these parameters so that the calculated wavelength they produce is very close to the known wavelength. Unfortunately, as discussed previously, the relationship between the etalon stepper motor position and the resulting wavelength is nonlinear and complex and can not be described precisely by a simple polynomial fit. Consequently, these etalon parameters are obtained by a simplex optimization of the etalon calibration data using the the four etalon parameters as the adjustable parameters of the optimization. The response that is used in determining the path of the simplex is simply the sum of the squared residuals of the calculated and known wavelengths for all ten calibration data points.

After selecting the desired initial parameter values and initial changes, the simplex proceeds, displaying the simplex status as well as the calculated wavelengths, etalon orders, and residuals at each step. The space bar can be pressed to toggle between displaying the individual wavelengths at each step or simply displaying the sum of the squared residuals. The simplex can be terminated at any point by depressing the escape key, otherwise it will continue until the number of steps requested initially has been reached. At this point additional steps can be performed if desired, or the optimized etalon parameters can be saved to CMX4CAL.DAT and a final report printed. A sample simplex report is reproduced in Figure II.40.

FINAL REPORT: ETALON  
 Simplex Optimization of CMX-4 Laser Calibration Parameters  
 =====  
 07-18-1988      15:16:39

Initial Parameters:

Parameter	Initial Value	Initial Change
t	5524083	200
Eighty	79.84628	.1
Cos2Phi	.9995225	.005
Delta X	-1.331426	.4

Final Results:

Total # of simplexes = 63  
 The set of optimal parameters is:

Parameter	Optimum Value	Initial Value	Final Difference
t	5524086	5524083	3
Eighty	79.83986	79.84628	-6.42395E-03
Cos2Phi	.9995228	.9995225	2.980232E-07
Delta X	-1.329187	-1.331426	2.239347E-03
Response	390.2404	384.2345	6.00589
(SOS Resid.)	2.562523E-03		2.602577E-03
-4.005432E-05			

X(etalon)	Lambda	Lambda Calc	m	Residual
5.230	5881.895	5881.865	2737	0.02979
4.450	5906.429	5906.440	2726	-0.01123
5.350	5913.589	5913.625	2722	-0.03564
4.725	5918.910	5918.903	2720	0.00732
5.060	5961.630	5961.623	2700	0.00732
5.360	5965.474	5965.478	2698	-0.00342
5.035	5987.907	5987.916	2688	-0.00830
5.420	5991.670	5991.661	2686	0.00928
5.145	6000.950	6000.948	2682	0.00195
5.010	6029.997	6029.998	2669	-0.00098

Final Sum of Squared Residuals = 0.00256  
 Final Sum of Residuals = -0.00391  
 Average Residual = -0.00039  
 Standard Deviation of Residuals = 0.01687

Figure II.40 Example of an etalon calibration report generated by the simplex optimization program, SIMPLEX.

#### (4) Calibration of the Doubling Crystal, UVCAL

The program PEAK, which was described earlier, was modified to create a program that facilitates the calibration of the UV doubling crystal micrometer. UVCAL has the same general appearance and many of the same functions as PEAK, but in addition, includes the ability to control the birefringent filter and UV doubling crystal stepper motors. The program first prompts the user for the current birefringent filter and UV crystal micrometer settings. Next, the desired scan parameters are input: initial wavelength, final wavelength and the wavelength step size between data points. The final option that is available is to have the UV crystal step to each wavelength based on the previous calibration parameters. The position can then be optimized for the new calibration. This can save a little search time as long as the calibration has not drifted too far since the last calibration was performed. The alternative is to manually adjust the UV crystal position to each point.

The program begins the calibration by stepping the birefringent filter to the initial wavelength for the scan and continuously fires the laser, displaying the laser power as a running bar graph on the computer screen. The UV micrometer can then be stepped forward and backward by one step using the keypad cursor keys (← and →), to optimize the laser power. Depressing the the control key along with the cursor keys (Ctrl ← and Ctrl →) will cause the UV crystal to move 10 steps at a time. It should be noted that there is a dramatic hysteresis problem that occurs when the micrometer is stepped in the reverse direction (to lower counter values). Thus it is best to avoid stepping in the reverse direction unless absolutely necessary.

In any case, if stepping in the reverse direction becomes necessary, it is advised that the micrometer first be stepped several hundred steps past the desired position since all final positions should be approached from the same direction. The hysteresis

correction key (H) can be depressed to accomplish this by stepping the stepper motor rapidly 100 steps back and then 100 steps forward.

Once the laser power has been optimized for a particular wavelength, the carriage return (Enter) key is depressed and the current wavelength and micrometer position are stored. The birefringent filter is then stepped to the next wavelength as determined by the wavelength step size entered previously, and the process is repeated. When the final scan wavelength is reached, the wavelength-micrometer position data pairs are stored in the file UVCAL.DAT for polynomial fitting using the program BIFIT, as described earlier.

#### (5) Acquisition of Fluorescence Excitation Spectra, SPECTRUM

Once the laser has been properly calibrated, it can be used to obtain fluorescence excitation spectra of jet-cooled analyte molecules expanding from the supersonic nozzle. This is accomplished using one of two main acquisition programs: SPECTRUM and CHROM. SPECTRUM controls the CMX-4 laser and detection system, coordinating the simultaneous stepping of all three tuning elements to produce medium (birefringent filter only), or high resolution (etalon and birefringent filter) fluorescence excitation scans in the ultraviolet wavelength range. The data acquired from the fluorescence detection system are displayed graphically in real time to ensure that the experimental parameters have been set properly. If a problem arises, the spectral scan can be aborted at any time by pressing the ESCape key. A description of the operation of the program follows.

SPECTRUM initializes itself by reading the data from three ASCII data files, CMX4DAT.DAT and CMX4CAL.DAT, and SPECTRUM.DEF. The first two of these files have been described previously and contain the CMX-4 position and calibration data, respectively. The third file, SPECTRUM.DEF, contains the operating parameters from the last

spectral scan as listed in Table II.17. These parameters are read in and set as the default values for the next scan. Next, the program prompts for information regarding the current position of the tuning element micrometers, the ambient temperature and atmospheric pressure, and the laser repetition rate. Finally, the remainder of the scan parameters are entered with default values displayed in parenthesis. Pressing the enter key by itself accepts the default value. If any other value is entered, it replaces the default parameter value.

The disk file to which the data will be written is entered next without a file extension. A total of two or three data files, differentiated by their extension, will be created for each spectral scan. Two of these data files will always be created: a scan parameter and information file with an extension of .OUT, and a data file containing the average, corrected fluorescence signal-wavelength data pairs, which has an extension of .DAT. An example of a typical parameter file (.OUT) is reproduced in Figure II.41. A third, optional raw data file may also be produced if desired. The raw data file is updated with each individual data point collected, the laser power for that point, and the average values of each, throughout the run. Since raw data of this type is generated rather quickly, the data must be written to the disk throughout the scan (every 50 wavelength steps). This means that there will occasionally be pauses during the spectral scan while the disk is being accessed. If this pause is unacceptable, or if the raw data are not needed, the user can choose not to produce the raw data file.

Once the scan parameters have been entered and the data files have been initialized, data acquisition can begin. The stepper motors are first stepped to the initial scan wavelength and the laser is fired free running while the laser power is displayed in a PEAK-like moving bar graph at the top of the graphics display. This is illustrated by Figure II.42. The front mirror positions and doubling crystal micrometer position can be adjusted to optimize the laser power at this point. Data acquisition begins with the collection of the dark signal taken with the beam blocker closed,

Table II.17

Format of the Default Parameters File SPECTRUM.DEF

Line	Description	Sample Value
1	Initial Scan Wavelength (Å)	2940
2	Final Scan Wavelength (Å)	2968
3	Wavelength Scan Step Size (Å)	0.1
4	Back Pressure of Diluent Gas (psi)	12
5	Diluent Gas	Helium
6	PMT Voltage (volts)	-725
7	Laser Flashlamp Voltage (kV)	12
8	X: Distance of Beam from Nozzle (mm)	1
9	Emission Spectral Filter Used	None
10	Spectrum ID Number	Fluorene-MR-18-01
11	Data File Path and Name	C:\DATA\FLMR1801
12	Valve Pulse Width (ms)	1
13	Spectrum Title	Fluorene Tc=170
14	Number of laser shots to average	10

FLMR2001.OUT

Saturday, June 11, 1988  
File Created: Sunday, March 20, 1988 at 10:10 am

Page 1

```
1 High Resolution Laser Excited Fluorescence Spectral Data
2 -----
3
4 UV doubled excitation laser beam with
5 Low-resolution wavelength selection using only the B.F.
6
7 Spectrum ID#:          fluorene-MR-20-01          03-20-1988    10:04:14
8
9 Fluorene, Continuous Introduction: Tc = 170, Tf = 130, BP = 12, High Res
10
11 Scan Information:
12 =====
13 Initial Wavelength (Angstroms): 2959
14 Final Wavelength: 2961.49          Scan Length: 2.490234
15 Step Size (Lambda): .025          Total Steps: 101
16 Pulses per Step 10          Total Data Points: 1010
17
18 Experimental Parameters
19 -----
20 Valve Pulsewidth (ms): 1
21 Delay 2B: 2.85
22 Delay 4A: 1.3
23 Backing Pressure (psi): 12
24 Diluent Gas: Argon
25 PMT Voltage (V): -600
26 Laser Flashlamp Voltage (kV): 12
27 X: Beam to Nozzle Distance (mm): 1
28 Emission Filter Used: None (BLank)
29
30 Average Dark Signal: 2071
31 Average 'Valve Off' Background Signal: .9081122
```

Figure II.41 Example of a scan information file (.OUT extension) generated by the program SPECTRUM for a high-resolution fluorescence excitation spectral scan of fluorene.



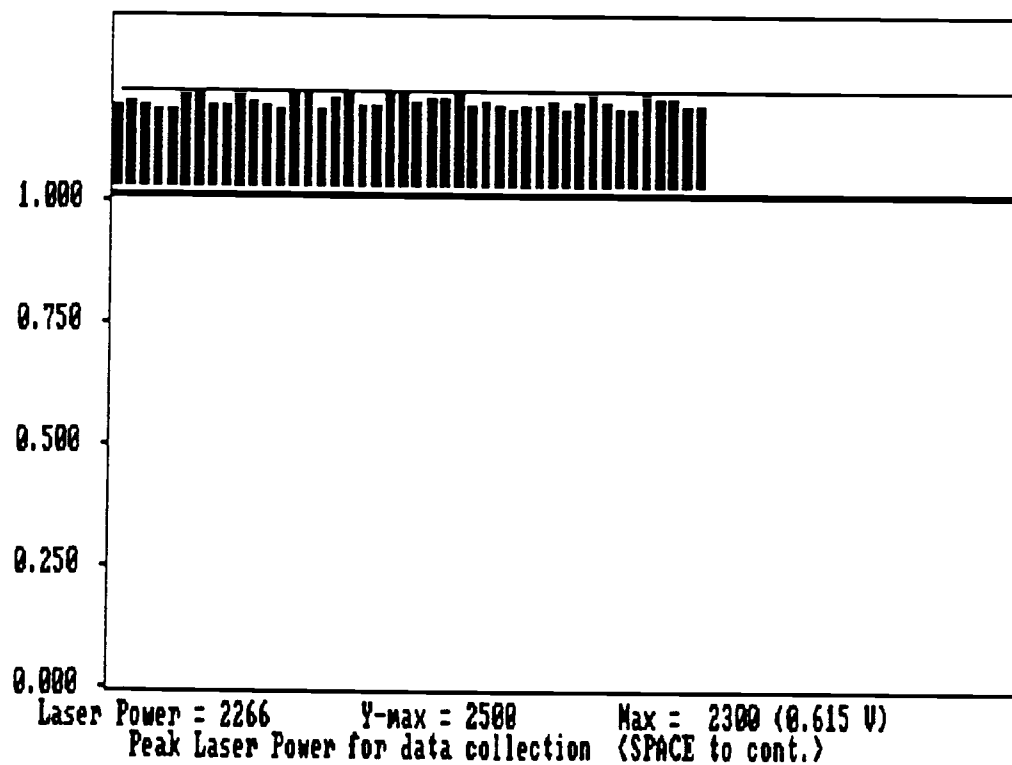


Figure II.42 Graphics screen dump of the SPECTRUM data acquisition screen showing the laser power peaking window viewed when optimizing the laser power prior to a scan.

followed by the background signal taken without the valve pulsing. The average background signal,  $\bar{E}_B$ , is then calculated as

$$\bar{E}_B = \frac{\left[ \sum \frac{E_{B,i}}{E_{Laser,i}} \right]}{PTX} \quad (II.8)$$

where  $E_{B,i}$  and  $E_{Laser,i}$  are a single background signal-laser power data pair, and PTX is the number of data points to average at each wavelength step during the scan. Finally, the spectral scan begins, and the average, corrected fluorescence signal,  $\bar{E}_F$ , is plotted on the graphics screen at each wavelength step throughout the scan:

$$\bar{E}_F = \frac{\left[ \sum \frac{E_{tF,i}}{E_{Laser,i}} \right]}{PTX} - \bar{E}_B$$

where,  $E_{tF,i}$  is the total fluorescence signal, and the remaining terms have already been defined. When the final scan wavelength is reached the entire data set is sorted to determine the smallest and largest signals. The plot window is then rescaled and the spectrum replotted. If the acquired spectrum is satisfactory, the data are saved to the .DAT disk file and the process can be repeated.

#### (6) Acquisition of Fluorescence Excitation Chromatograms, CHROM

The second main data acquisition program used in this work is CHROM. This program is a version of SPECTRUM that has been modified to produce fluorescence excitation chromatograms of PNAs eluting from

a gas chromatograph. A fluorescence excitation chromatogram is the total fluorescence emission plotted as a function of the time elapsed since injection of the sample (retention time). The excitation wavelength is either kept constant throughout the run, or alternatively, can be scanned to the excitation wavelength of several different PNAs during the run. The latter case produces a programmed wavelength fluorescence excitation chromatogram.

CHROM behaves similarly to SPECTRUM except for enhancements related to the chromatographic functions. For example, additional parameter defaults are added to record the conditions of the chromatographic run. The default parameters file for CHROM is CHROM.DEF, an example of which is shown in Table II.18. As is the case with SPECTRUM, a real-time graphic display of the fluorescence signal is plotted on the graphics screen. However, in the case of CHROM, the average corrected fluorescence signal is plotted versus retention time rather than wavelength. If a programmed wavelength chromatogram is desired, a series of retention time, wavelength pairs are entered. The initial wavelength is entered with a retention time of 0 minutes and the system will subsequently scan to any additional wavelengths in the table when the retention time of the run is equal to the time entered in the table for a particular wavelength. Other considerations include the fact that when the GC oven is at a high temperature, carrier gas flow through the column must be maintained constantly to avoid damaging the stationary phase. Thus, either the valve must be pulsing continuously, or the outlet vent must be open at all times. CHROM prompts the user when to open and close the vent, and pulses the valve when the vent is closed.

Because the computer is located several feet away from the chromatograph, a method had to be devised to synchronize injection of the sample and the beginning of data acquisition to ensure reproducible retention times. Since the graphics monitor is easily viewed when standing at the GC, it was decided that a visual countdown signaling the beginning of data acquisition would be a reasonable solution. This is accomplished by displaying 10 large blocks across the graphics screen as illustrated by Figure II.43A.

Table II.18

Format of the Default Parameters File CHROM.DEF

Line	Description	Sample Value
1	Excitation Wavelength (Å)	2960
2	Back Pressure at Column Inlet (psi)	40
3	PMT Voltage (V)	-600
4	Nozzle to Laser Beam Distance (mm)	1
5	Emission Filter Used	(BLank)
6	Data File Path and Name	c:\data\test
7	Valve Pulse Width (ms)	2
8	Scan Title	1 uL of 100 ug/ml Fluorene in CH2CL2
9	Number of Data Points to Average	5
10	Injection Port Temperature (°C)	300
11	Transfer Line Temperature (°C)	300
12	Flange Temperature (°C)	145
13	Temperature Program	100/0-250/16 @32
14	Acquisition Length (min)	10
15	Acquisition Delay (min)	8
16	Number of Excitation Wavelengths	2
17	Program #1: Ret. Time, Wavelength	0        2960
18	Program #2: Ret. Time, Wavelength	5        2947

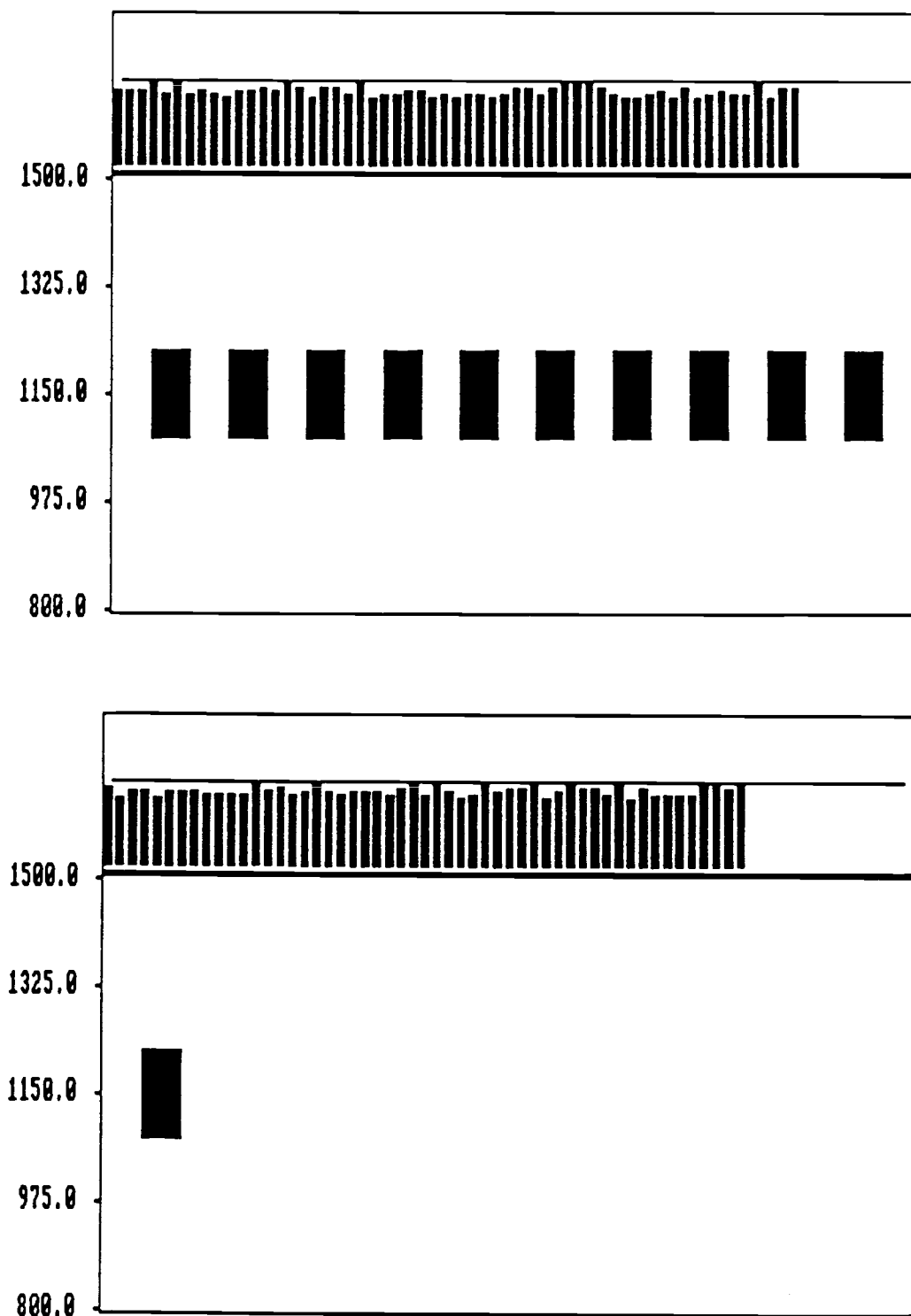


Figure II.43 Graphics screen dumps of the CHROM data acquisition screen showing (A) the ten blocks displayed on the screen prior to the 20 second injection countdown and (B) the one block that remains after 18 seconds, signaling that the injection should be made

Successive blocks are erased from the screen moving from right to left, every 2 seconds. The injection is made when only one block remains on the screen, as depicted in Figures II.43B, allowing the injection time to be reproduced to better than 2 seconds from run to run. Finally, in order to save laser shots, an acquisition delay can be specified. The acquisition delay is the time in minutes that data acquisition is delayed from the injection. During the period that the delay is in effect, the valve is pulsed continuously and the time remaining in the delay is displayed on the graphics screen.

Once the delay time is exceeded, the run begins and the fluorescence signal is collected until the final time is reached. If the results are acceptable the data are written to the .DAT file as retention-time, average-corrected-fluorescence-signal pairs and the process can be repeated.


#### (7) Plotting and Analysis of Data, REPLOT

The final program that was written for this research is a plotting and data analysis program called REPLOT. REPLOT allows the data from the .DAT files generated by SPECTRUM and CHROM to be replotted on a variety of graphics displays. The data files produced by the acquisition programs all have the same format as depicted in Table II.19, and REPLOT requires the data files to be in this format to work properly. Peak locations and peak areas for all spectral or chromatographic peaks in the data file can be calculated and a report generated on the results of these calculations.

When REPLOT is first started, the name of the data file produced by SPECTRUM or CHROM that is to be plotted must be specified. This filename can be entered from within the program, from the command line when the program is called from DOS, or a DOS environment variable, REPLOT, can be set to provide the path to the data file(s). The DOS syntax for the latter case is

Table II.19

Format of the Data Files Required by CHROM

Line #	Description
1	 <p>Lines 1-8 contain arbitrary header information such as the time and date the data file was created. Replot reads these lines into a dummy variable and ignores them.</p>
2	
3	
4	
5	
6	
7	
8	
9	Title of the data set, a 1 line string.
10	X, Y data pairs, in columns separated
11	by a comma.
.	
.	
.	

```
C> SET REPLOT=DRIVE:\PATHNAME\FILENAME
```

which stores the path and file information in the environment space until the computer is rebooted. When REPLOT is first started, the program checks to see if a filename was entered from the command line, in which case the command-line variable is set up as the default filename. If no command-line variable is found, REPLOT next checks to see if there is a DOS environment entry under the name REPLOT. If so, this value is displayed as the default filename. Finally, if neither of the previous cases is true, no default filename is presented and the desired filename must be entered manually. In any case, the selected file is read in from the disk and plotted on the graphics screen.

Data analysis proceeds in the following manner. First, a cross hair is moved along the spectrum or chromatogram to a peak maximum using the right and left cursor keys, alone or in conjunction with the Ctrl key, which moves the cross hair by 10 points instead of 1. The enter key is then pressed and a peak identification number is displayed next to the peak. A short description is then entered. The peak area is calculated by first moving the cursor to the left baseline and pressing "L", and then moving the cursor to the right baseline and pressing "R". A line is automatically drawn between the two baseline points and the area bounded by the peak and the line connecting the baseline points is calculated and displayed in the upper right hand corner of the graphics window. Especially with a noisy data set, the position of the true baseline points may be difficult to determine. To address this problem REPLOT allows several area measurements of a single peak to be calculated. This is accomplished by pressing the "C" key to clear the current area display, and then redefining the left and right baseline points using "L" and "R" as before. This procedure can then be repeated for other peaks in the spectrum or chromatogram by stepping to the next peak maximum and pressing the enter key again. When data analysis is finished the graphics screen can be printed (requiring a graphics



screen dump program of some sort), along with a report on the results of the area measurements. An example of such a screen dump/report is shown in Figure II.44. The report provides information on the independent variable (retention time or wavelength) at the peak maximum, the peak height, which is defined as the peak maximum minus the average baseline signal, the peak area, the baseline width of the peak,  $t_w$ , in minutes or angstroms, and the descriptions entered for each peak. The entire process can then be repeated for another data file.

Whereas SPECTRUM and CHROM are designed for use with the color graphics adaptor (CGA) on the data acquisition computer, and thus are limited to the low resolution (640x200 pixels) provided by the CGA, REPLOT was written to operate on three different graphics adaptors. REPLOT automatically checks for the presence of an enhanced graphics adaptor (EGA), a Hercules graphics controller (HGC), or the color graphics adaptor. Once the installed video adaptors and current video mode have been determined, REPLOT automatically configures itself for the highest resolution mode available. Thus, data files can be viewed and printed on a computer that provides a higher resolution display than that currently available on the laboratory computer.

#### d. Commercial Software Packages Used in This Research

A number of commercial software packages were used for data analysis and presentation in this research and thesis and it is worthwhile identifying those which have been particularly useful. As discussed previously, an electronic spreadsheet, QUATTRO (Borland International, Scotts Valley, CA), was used for some data analysis, in particular the theoretical supersonic expansion characteristics, and occasional plotting. Presentation quality graphs were prepared using the program SigmaPlot (Jandel Scientific, Sausalito, CA) and the liquid-solution spectra of fluorene and 1-methylfluorene in

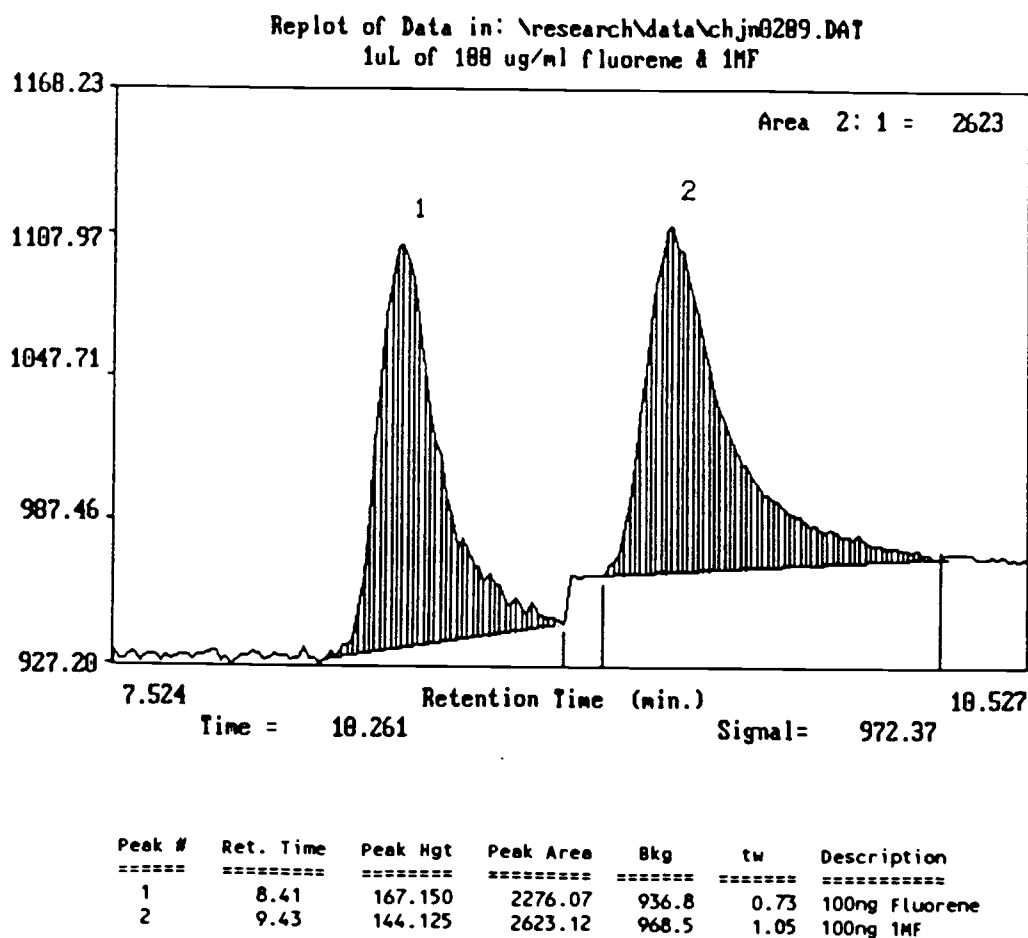


Figure II.44 Example of a REPLOT graphics display showing a programmed wavelength fluorescence excitation chromatogram of fluorene and 1-methylfluorene. Peak areas are calculated and listed in the report below the chromatogram.

Figure I.1 were digitized using Jandel's Digital Paintbrush system. Graphics screen dumps were made with Pizzaz (Application Techniques, Inc., Pepperell, MA) and most of the figures found in this thesis were created using Generic CADD Level 3 (Generic Software, Redmond, WA). In order to manage the excessive amount of data generated by the acquisition programs, the shareware program ARC (version 5.12, System Enhancement Associates, Wayne, NJ) was used to compress and combine all the data files from each day's experiments into a single archive file. This substantially reduced the use of disk space and made organization and backup much easier to manage. Thesis flow charts were constructed using the program Easyflow (HavenTree Software Limited, Thousand Island Park, NY), and finally, the thesis was prepared using MultiMate Advantage II (Ashton Tate, Torrance, CA).

### III. Experimental Procedure and Results

The experiments that were performed using the instrumental system described in the previous sections are divided into two basic groups: experiments to characterize the instrumentation and analytes using continuous sample introduction, and application of the instrumentation to the determination of PNAs by gas chromatography. The procedures required to carry out the various experiments are presented in the following sections along with the results of those experiments.

#### A. General Experimental Procedure

##### 1. Instrument Power-Up Sequence and Signal Optimization

Regardless of the type of experiment being performed, the instrumentation must be powered-up in the proper manner and be allowed to thermally stabilize before measurements begin. The usual instrument power-up sequence and the method used to optimize the fluorescence signal, are outlined in the steps below.

1. The refrigerated circulating bath is turned on at least an hour prior to making measurements. This allows the circulating water that flows through the cooling coils immersed in the dye pot and laser cooling water pot, to be cooled to approximately 15°C. The laser cooling water pump and dye pump are also turned on at this time to ensure that the laser and the laser cavity are thermally stable prior to operation.
2. The heaters used to heat the detection cell, sample heater block, and nozzle flange, as well as the GC injection port and

transfer line heaters, if applicable, must all be turned on at least 45 minutes prior to the experiment. At this same time the PMT cooling water pump must be turned on to prevent overheating the PMT.

3. The laboratory fume hood that is used to draw air through the laser cavity air-flow tube is turned on, along with the nitrogen supply that circulates dry nitrogen through the spark gap during experiments. The laser power supply is also turned on and brought up to its operating voltage just below the red line on the lamp voltage meter ( $> 7$  kV).
4. The computer is booted and the rest of the power supplies are turned on including the synchronization panel 5-V power supply, the 30-V power supply that drives the beam blocker and pulse counter unit, the rear synchronization photodiode, the laser power monitor, the gated integrator module, the 3 stepper motor translators, and finally, the PMT high voltage power supply. These electronic components are allowed to warm-up for at least 45 minutes prior to experimentation.
5. Once the various heaters are stabilized at their operating temperatures, the laser power and fluorescence signal are optimized using the program PEAK. The front mirror micrometers are first adjusted to give the highest stable signal with PEAK continuously displaying the raw laser power signal. Next, PEAK is switched to display the raw gated integrator signal and a valve pulse width of 2 ms is specified. The birefringent filter and doubling crystal are then adjusted to the wavelength of a strong analyte excitation transition: 2960 Å for fluorene or 2947 Å for 1-methylfluorene. With the valve pulsing the PNA sample continuously into the detector cell, the beam position is adjusted to give the maximum fluorescence signal as viewed on the PEAK display. Beam position is changed over the small distances required by rotating the two position adjustment

screws of the corner mirror on the optical table. When the sample is continuously introduced from the heated cell, this optimization is straightforward since the analyte is present in relatively high, constant concentrations. However, in the chromatography experiments, the signal that is used for this optimization is the 'background' signal arising from small amounts of analyte remaining in the nozzle from previous experiments. This makes signal optimization more difficult and it is often necessary to inject a large amount of sample onto the column (*i.e.*, 1-5  $\mu\text{g}$ ) and optimize the signal on the tail of the peak when it elutes from the column. The analyte fluorescence signal is distinguished from the scatter signal by toggling the valve on and off using the "4" key. By optimizing the valve-on/valve-off signal ratio, the signal-to-background ratio is optimized.

6. Finally, the desired data acquisition program, SPECTRUM or CHROM, is called from GPMENU. In both cases, after initialization of several experimental parameters, the program steps to the initial wavelength for the run and enters a laser power peaking mode. This is mainly for re-positioning of the doubling crystal to provide maximum laser power output since it is not unusual for the optimum position to change slightly during the day and from day-to-day. Obviously this drift in the optimum doubling crystal position could be a major problem since it implies that the calibration is not valid. Fortunately, experience has shown that for a relatively recent calibration, this drift is simply an offset, not a change of the calibration slope. Thus, if the UV crystal translator is turned off and the micrometer position is reoptimized at the beginning of the run, the control program can still accurately position the crystal and provide sufficient UV power across a spectral scan (the control program is fooled into assuming it is still on the original calibration by turning off the translator when the adjustments are made).

7. When all experiments are finished, the various heaters and power supplies are turned off, the laser lamp voltage is returned to 0 kV on the meter, and the laser is turned off. In addition, the nitrogen flow is turned off at the pressure regulator and the laser cooling water and dye circulating pumps are also turned off. The PMT cooling water pump and the refrigerated cooling bath, however, are left running until the front flange temperature is below 50°C, the temperature maximum for the PMT.

## 2. Model Compounds Studied

Two PNAs, fluorene and 1-methylfluorene, were used for all studies performed in this research. The reasons for the selection of these compounds are numerous. First, the high-resolution spectrum of jet-cooled fluorene has been published [67,89,90] and exhibits transitions in the middle of the tuning range of the laser dye that has been used most often with our laser system in the past (R590). This meant that the laser system would not have to be re-characterized for calibration and operation using a different dye. In addition, the most intense transition observed in the literature spectrum (2960.2 Å, frequency doubled 5920.4 Å fundamental) occurs near the maximum of the R590 tuning curve, ensuring reasonable sensitivity for fluorene. An additional advantage of the existence of a literature spectrum is that the spectra obtained with the system developed in this project can be compared to the literature spectrum to qualitatively determine instrument performance. Other advantages include the fact that these compounds have not been found to be carcinogenic, which eases handling and disposal requirements. Finally, they are fairly small PNAs with relatively low melting and boiling points. Thus, they would be expected to be more easily vaporized than their larger counterparts, and also be less likely to trap out on the walls of the

pulsed valve, which can only be heated to  $\approx 150^{\circ}\text{C}$ . In addition, their lower boiling points imply a shorter retention time in the gas chromatography experiments, increasing the number of experiments that can be performed over a particular period of time. The structure and important properties of these two compounds are listed in Table III.1.

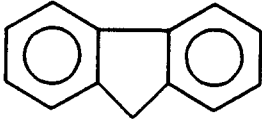
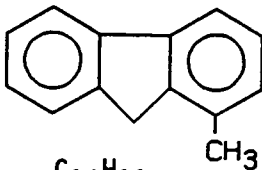
#### B. Characterization of the Instrumentation and Analytes

One of the main goals of this project was to interface the laser-based spectroscopic instrumentation to a gas chromatograph and to apply the system to the determination of PNAs. Consequently, the initial experiments that were performed to characterize the spectroscopic system were designed with the eventual chromatographic interface in mind. Thus, for example, the spectroscopy was examined in terms of the conditions under which sufficiently high-resolution spectra could be obtained while still maintaining the detection sensitivity that is required when analyzing real samples. In addition, experimental variables were examined only over the range that it was anticipated they would be likely to fall into when the gas chromatograph was used for sample introduction.

Experiments were also carried out to determine the feasibility of utilizing the simplest instrumental components possible. For example, it was hoped that the expansion could be maintained using only a low-volume mechanical rotary vacuum pump rather than the more complicated pumping systems used by other researchers [61,63]. If high-resolution spectra could still be obtained with the low-volume mechanical pump, instrument complexity could be greatly reduced. In addition, it was desired that the laser be operated with the birefringent filter as the only wavelength selection device since the etalon significantly reduces laser output power, decreasing detection sensitivity. The etalon also complicates wavelength scans due to the complex relationship between etalon dial reading and wavelength.



Table III.1  
Properties of the Model Compounds  
Used in this Research

Property	Compound:	
	Fluorene	1-Methylfluorene
Structure		
Formula	$C_{13}H_{10}$	$C_{14}H_{12}$
Registry #	86-73-7	1730-37-6
Molecular Weight	166.23	180.25
Boiling Pt. ( $^{\circ}C$ )	298	318
Melting Pt. ( $^{\circ}C$ )	112-115	84-86
Source	Aldrich <sup>1</sup>	Aldrich <sup>1</sup>
Purity	98%	99%

<sup>1</sup>Aldrich Chemical Company, Milwaukee, WI.

Furthermore, as described in the instrumentation section, the detection cell was designed to filter spatially and eliminate scattered and stray light using a variety of baffles, a beam stop, and a detector aperture plate. Thus it was hoped that the total fluorescence emission signal could be collected without the need for emission wavelength selection using an emission monochromator or bandpass filters. This would potentially increase the throughput of the fluorescence emission to the detector while simplifying the instrumentation.

Finally some mention should be made regarding the units used to report wavelengths in the following studies. Although the modern convention is to report wavelengths in nm, units of Angstroms ( $\text{\AA}$ ,  $10^{-10} \text{ m}$ ) were used throughout this project. This convention was adopted because all of the original CMX-4 laser wavelength calibration studies that were performed in previous projects [75,80], were based on the Angstrom unit. Thus, the wavelength calibration routines that were developed in this project were also based on the Angstrom. Consequently, in order to remain consistent, the Angstrom was used to report wavelengths throughout this thesis.

In order to facilitate these investigations, a continuous sample introduction system was developed as described in a previous section. The PNA sample is placed in a glass thimble and heated above its melting point, typically to  $200^{\circ}\text{C}$ . The diluent gas then mixes with the analyte vapor and the mixture flows through the nozzle into the vacuum. The concentration of analyte in the nozzle is thus determined by both its vapor pressure and the stagnation pressure of the diluent gas. It is worthwhile calculating the vapor pressure of fluorene at several temperatures to get a rough of idea of the analyte number density used in these experiments.

The Clausius-Clapeyron equation relates the temperature of a material to its vapor pressure. In its general form, this equation can be expressed as

$$\text{Log } P = -A(1/T) + B \quad (\text{III.1})$$

where  $P$  is the vapor pressure at temperature  $T$ ,  $A$  is a constant that is related to the enthalpy of vaporization, and  $B$  is a second constant. Thus, a plot of  $1/T$  versus  $\log P$  should be linear with a slope of  $-A$  and an intercept of  $B$ . The vapor pressure of fluorene has been measured at several temperatures [91]. These vapor pressures are summarized in Table III.2 and are plotted in Figure III.1. A linear regression performed on these data produces the desired constants which can then be used to predict the vapor pressure of fluorene at a number of other temperatures as listed in Table III.3. Diluent gas pressures used in these experiments range from 7 to 20 psi as read off the second stage of the regulator, while the sample heater block is maintained at 170 to 200°C and the nozzle flange is held at 125 to 145°C. For a back pressure of 10 psi, a sample block temperature of 200°C, and a flange temperature of 145°C, fluorene is predicted to be present in the diluent gas at levels ranging from 0.9 to 5% depending on the influence of the thermal gradient that exists between the 200°C sample cell and the 145°C nozzle.

## 1. Preliminary Studies

With these considerations in mind it is worthwhile examining one of the first fluorescence excitation spectra produced with this system. Figure III.2 is a comparison of the conventional liquid-solution absorbance spectrum of 5  $\mu\text{g/ml}$  fluorene in cyclohexane, and the fluorescence excitation spectrum of fluorene in an argon supersonic expansion. The jet-cooled fluorescence excitation spectrum was obtained with an argon back pressure of 10 psi, a sample temperature of 200°C, a flange temperature of 140°C, a valve pulse width of 2 ms, and a wavelength step size of 0.1 Å using only the birefringent filter for wavelength selection. The laser beam was positioned directly off the nozzle tip (within 1 mm of the orifice) for this experiment and all remaining experiments unless

Table III.2

Vapor Pressure<sup>1</sup> of Fluorene at Several  
Temperatures for Calculation of the A and B  
Constants of the Clausius-Clapeyron Equation

T (°C)	T (K)	1/T (K)	P (mm Hg)	Log P
146	419	0.00239	10	1.00
185.2	458.4	0.002182	40	1.60
214.72	487.17	0.002050	100	2.00
268	541	0.00185	400	2.60
295	568	0.00176	760	2.88

<sup>1</sup>Vapor pressure data was taken from the CRC handbook [91].

Table III.3

Vapor Pressure of Fluorene  
Calculated at Several Different Temperatures  
Using the Clausius-Clapeyron Equation

T (°C)	P (mm Hg)
100	1
125	4
130	5
150	11
170	23
200	64
250	260
280	550
300	818

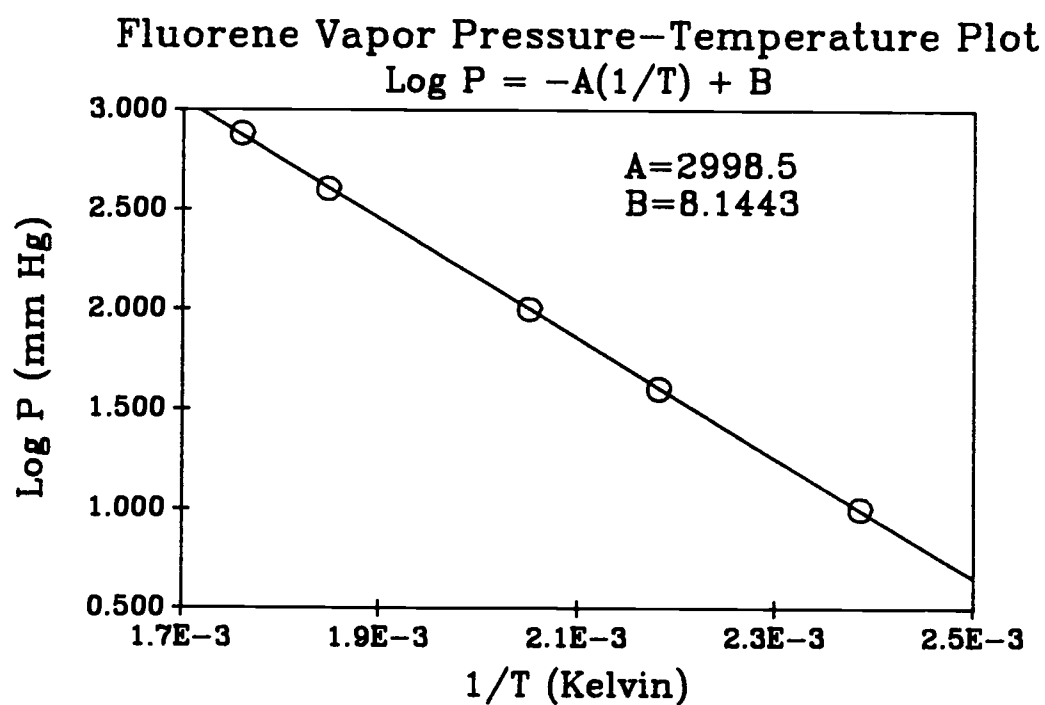


Figure III.1 Plot of log vapor pressure versus  $1/T$  used to obtain the Clausius-Clapeyron A and B parameters for fluorene.

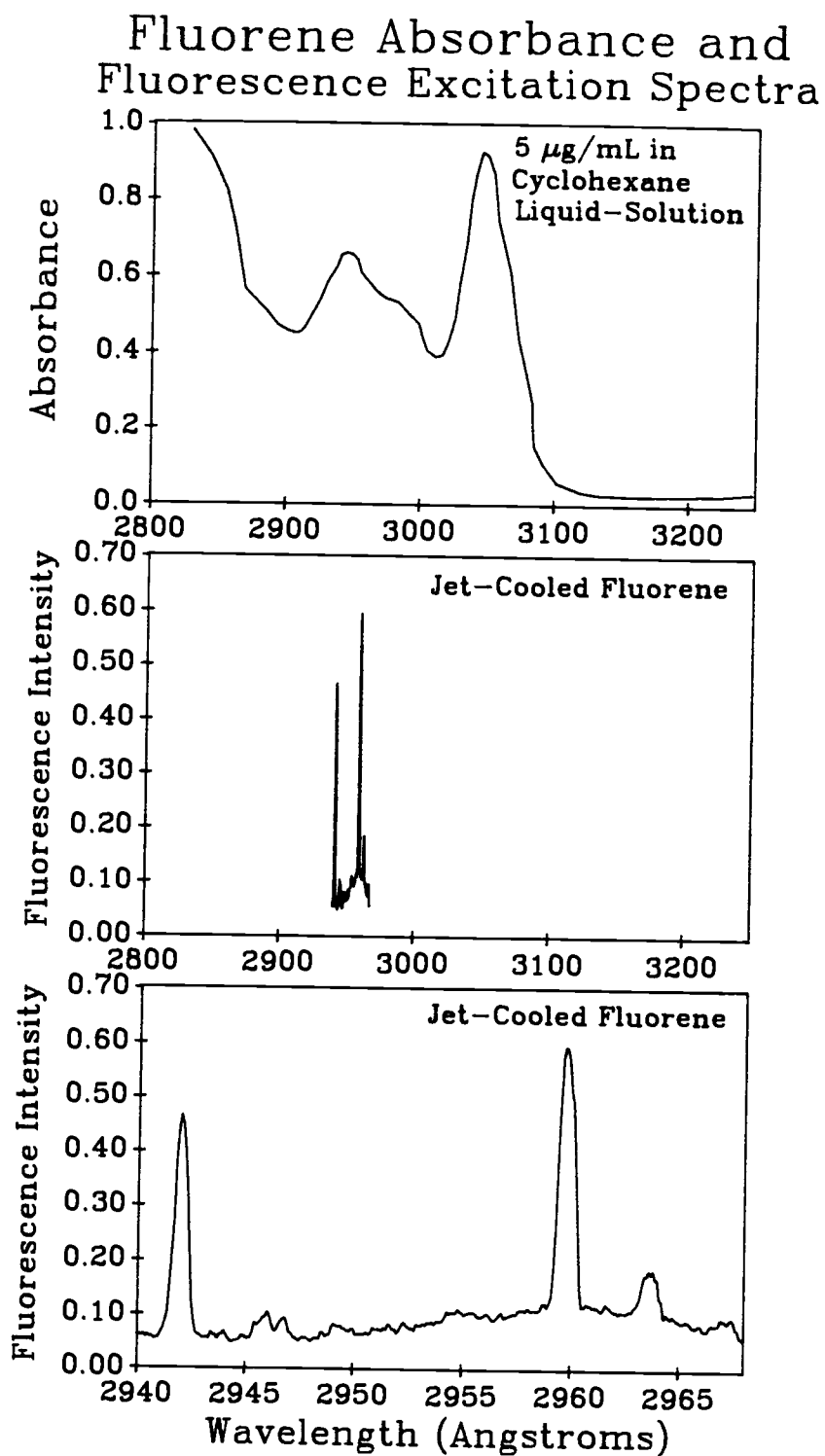


Figure III.2 Comparison of the conventional liquid-solution absorbance spectrum of fluorene (top), and the fluorescence excitation spectrum of fluorene in an argon supersonic expansion on the same wavelength scale (middle), and an expanded scale (bottom).

otherwise indicated. Typical experimental conditions used to acquire fluorescence excitation spectra in this research are listed in Table III.4. It is important to note that throughout these experiments the diluent gas pressures were set using the second stage of the main gas cylinder regulator. This particular regulator is not designed to regulate gas at subambient pressures and thus all diluent gas pressures that are reported should be interpreted as the pressure above 1 atmosphere (*i.e.*, 7 psi helium represents a 1.5 atm stagnation pressure).

Regarding the spectra in Figure III.2, the 2960-Å peak, which is the most intense in the jet-cooled spectrum, has a width of slightly less than 1 Å (FWHM) compared to the narrowest peak in the liquid-solution spectrum, which has a half width of about 50 Å and is not resolved from adjacent spectral features. Thus, the dramatic gains in spectral resolution that can be obtained from a system such as this are immediately obvious. Further, this resolution can be attained without requiring the use of massive pumping systems and extremely narrow bandwidth lasers. Since the width of the peaks in the jet-cooled spectrum ( $\approx 1$  Å) are slightly wider than the bandwidth of the laser using only the birefringent filter for wavelength selection (0.25 Å), the birefringent filter would seem to provide a sufficiently narrow excitation bandwidth for this application.

However, it is still possible that there are unresolved spectral features underneath the peaks that might be at least partially resolved if a higher resolution etalon scan were made. The result of such an etalon fluorescence excitation scan of the 2960 Å peak of fluorene is illustrated in Figure III.3. This excitation scan was taken under conditions similar to the previous spectrum, however in this case the wavelength step size was reduced to 0.025 Å to take advantage of the narrower excitation bandwidth provided by the etalon. It is apparent from Figure III.3 that there is indeed some structure observed underneath the transition when excited under these higher resolution conditions. This underlying structure is due possibly to a combination of vibrational hot-band transitions and unresolved rotational structure arising from incomplete cooling of

Table III.4

Typical Experimental Conditions for the Acquisition of  
High-Resolution Fluorescence Excitation Spectra  
of Fluorene and 1-Methylfluorene

Parameter	Typical Value or Range
Diluent Gas	Helium or Argon
Sample block temperature	170 to 200°C
Nozzle flange temperature	125 to 145°C
Diluent gas stagnation pressure	7 to 20 psi
PMT voltage	-600 to -725 V
Delay 2B <sup>1</sup>	2.0 to 3.4
Delay 4A <sup>1</sup>	1.3
Number of laser shots averaged for each wavelength step	5 or 10
Nozzle diameter (D)	0.33 mm
Beam to nozzle distance (X)	1 to 6 mm
X/D	3 to 20

<sup>1</sup>As measured off the synchronization panel potentiometer dial.



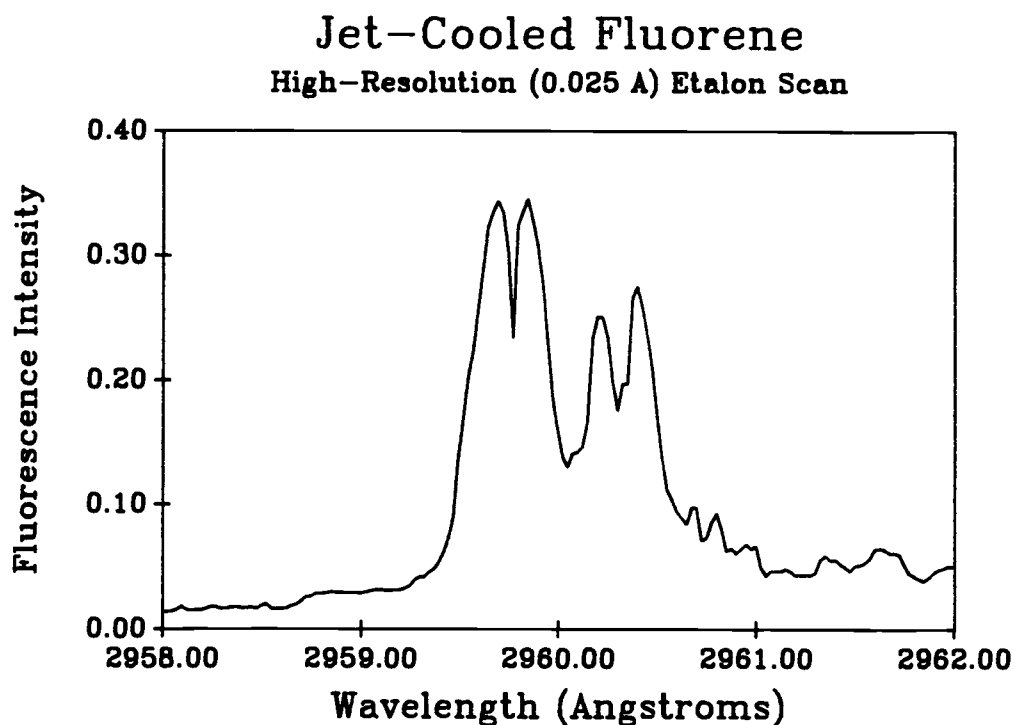


Figure III.3 A high-resolution fluorescence excitation spectrum of the 2960-Å fluorene transition in an argon supersonic expansion. The etalon was rotated into the laser cavity and stepped in 0.025-Å increments synchronously with the birefringent filter to produce the spectrum.

the rotational and vibrational energy levels in the expansion. However, since one of the goals of this research is to maximize the sensitivity of the method even at the expense of some spectral resolution, and since the birefringent filter provides a sufficiently narrow excitation bandwidth as evidenced by the previous spectrum (Figure III.2), all subsequent spectral scans and experiments were performed using only the birefringent filter.

## 2. Pulsed Valve Characteristics

Once it was determined that the experimental system was capable of producing the desired high-resolution spectra, additional studies were performed to further characterize the instrumentation. The first of these experiments involved the study of the pulse characteristics of the pulsed valve used as a supersonic nozzle. The impetus for this study was the need to verify proper operation of the valve; to ensure that a 1-ms trigger pulse indeed results in a 1-ms pulse of gas into the vacuum chamber. In addition, information regarding any changes in the fluorescence signal during the period that the valve is open was also of interest.

The 2960 Å fluorene fluorescence signal was monitored as a function of delay 2B (D2B), the laser trigger delay, using the program PEAK and its data acquisition functions. Since delay 2B and the pulsed valve trigger pulse are initiated simultaneously by the software, increasing delay 2B will delay the firing of the laser relative to the start of the valve pulse which is fixed in time. Thus, by increasing delay 2B, the fluorescence signal arising from different temporal parts of the valve pulse can be examined, with a resolution determined by the width of the laser pulse ( $\approx 1.2 \mu\text{s}$ ), the laser trigger jitter ( $< 1 \mu\text{s}$ ), and the accuracy of setting the delay 2B potentiometer ( $\approx 10 \mu\text{s}$ ). For each valve pulse width examined delay 2B was varied over a range of 1 to 10 units as read off the potentiometer scale, corresponding to delay times of 0.3 to 3.4 ms.

At each value of delay 2B the fluorescence signal from 30 consecutive laser shots was acquired and averaged. The results of these measurements for valve trigger pulses of 0.5, 1.0, and 1.5 ms are shown in Figure III.4.

The most prominent feature of these plots is the apparent "bounce" of the valve upon closing as evidenced by the second, smaller pulse occurring at the end of each of the main pulses. This result is reasonable if the mechanical operation of the valve is considered. When the driver circuit sends current through the solenoid windings, the plunger is forced backwards, breaking the vacuum seal formed by the metal-metal contact of the plunger tip and the inside of the nozzle tip. While in this open position the plunger rests upon and compresses a spring. When the input trigger pulse returns to ground potential, the current through the windings ceases to flow and the force holding the plunger relaxes. The spring then expands slamming the metal plunger into the face of the nozzle tip. It is likely that this metal on metal collision results in the plunger bouncing back against the spring again before finally coming to rest in the desired sealing position. The fact that this bounce is smaller for the 0.5-ms input pulse is probably due to the fact that this pulse is close to the minimum pulse width for the valve and consequently the plunger does not fully compress the spring and thus achieves a lower momentum when returning to seal against the nozzle tip. For an input trigger pulse that completely opens the valve, this bounce appears to be slightly less than 0.5 ms wide, which is a significant fraction of the total pulse width. Thus, if an experiment requires precise control of the actual gas pulse and knowledge of its true width, the bounce would either have to be taken into account or eliminated.

It is also worth noting that if the falling edge of the main body of each of the three pulses is extended to the baseline and if the bounce is ignored, the resulting pulse width agrees with the width of the input trigger pulse. Thus, the driver circuit appears to be able to open and close the valve properly. In addition, once the valve opens, the fluorescence signal remains relatively constant

### Bosch Valve Pulse Characteristics

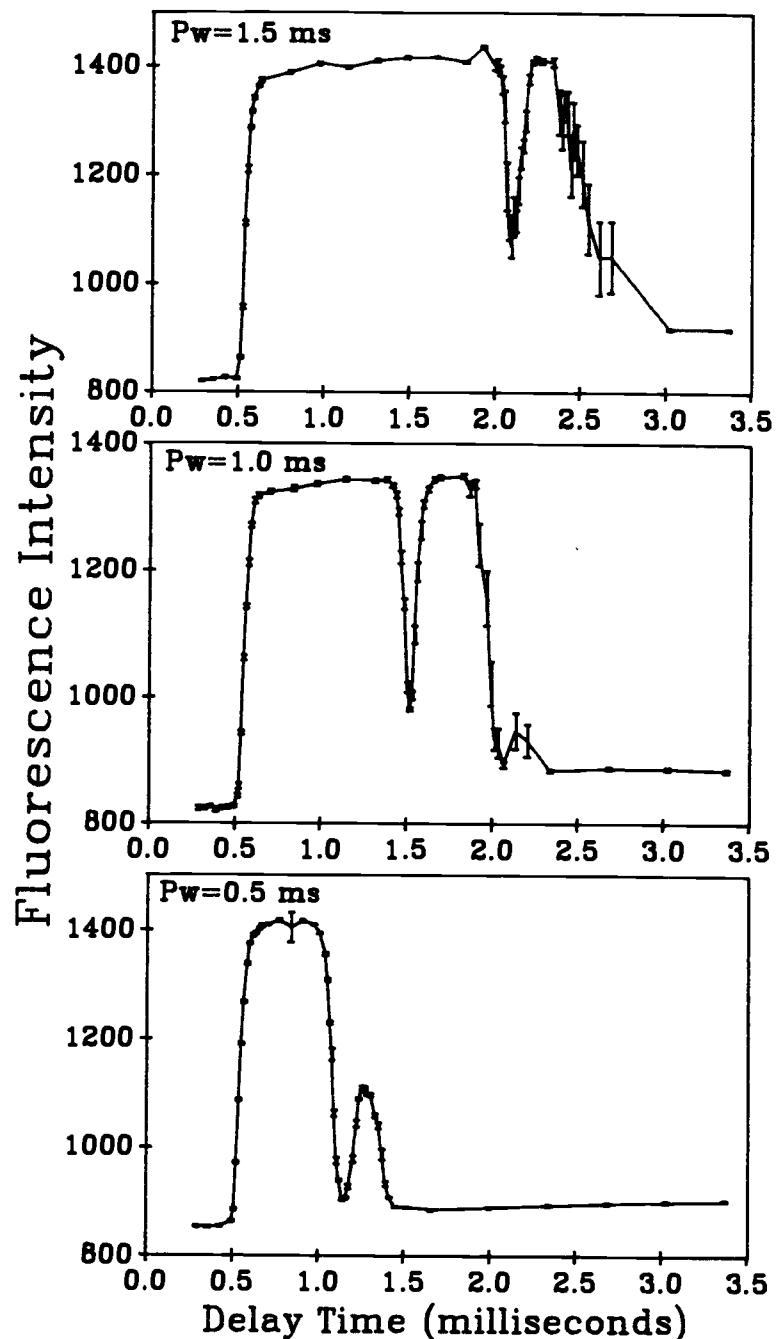


Figure III.4 Pulse characteristics of the Bosch valve measured by monitoring the 2960-Å fluorene fluorescence signal as a function of Delay 2B, the laser firing delay. Each data point is the average of 30 consecutive laser shots and the error bars represent the 99% confidence interval.

with only a slight increase in intensity towards the end of each pulse. Thus, the actual value of delay 2B is not critically important as long as it is set to trigger the laser during the period the valve is open. This observation was substantiated by acquiring the fluorescence excitation spectrum of fluorene at both  $D2B = 2.00$  (0.6 ms) which is near the beginning of the 1 ms valve pulse, and at  $D2B = 3.40$  (1.1 ms) which is near the end of the valve pulse. These spectra are compared in Figure III.5 and are almost identical in terms of the observed transitions and their relative intensities; the only difference is a slight increase in the overall intensity of the second spectrum. Therefore, Delay 2B was set to 3.4, which corresponds to the second of the two spectra in Figure III.5, for all remaining experiments. It should be noted that the diluent gas used for these last two spectra was helium, the effects of which will be examined in a subsequent section. Finally, the rise time of the opening of the valve as calculated from these data is approximately 120  $\mu s$ .

### 3. Influence of Diluent Gas on Spectra

Many of the initial spectral characterization experiments were carried out using argon as the diluent gas. It was hoped, however, that helium could be used as both the diluent gas and as the gas chromatography carrier gas. Helium is favored as a carrier gas since it can be used at higher flow rates to decrease analysis times with only small sacrifices in chromatographic resolution as compared to higher molecular weight gases like argon. Consequently, if sufficiently high resolution spectra could be obtained using helium diluent gas, the GC carrier gas and diluent gas could be the same, thereby easing interfacing requirements. Thus, comparisons of the spectra produced by cooling in an argon expansion and a helium expansion are of interest.

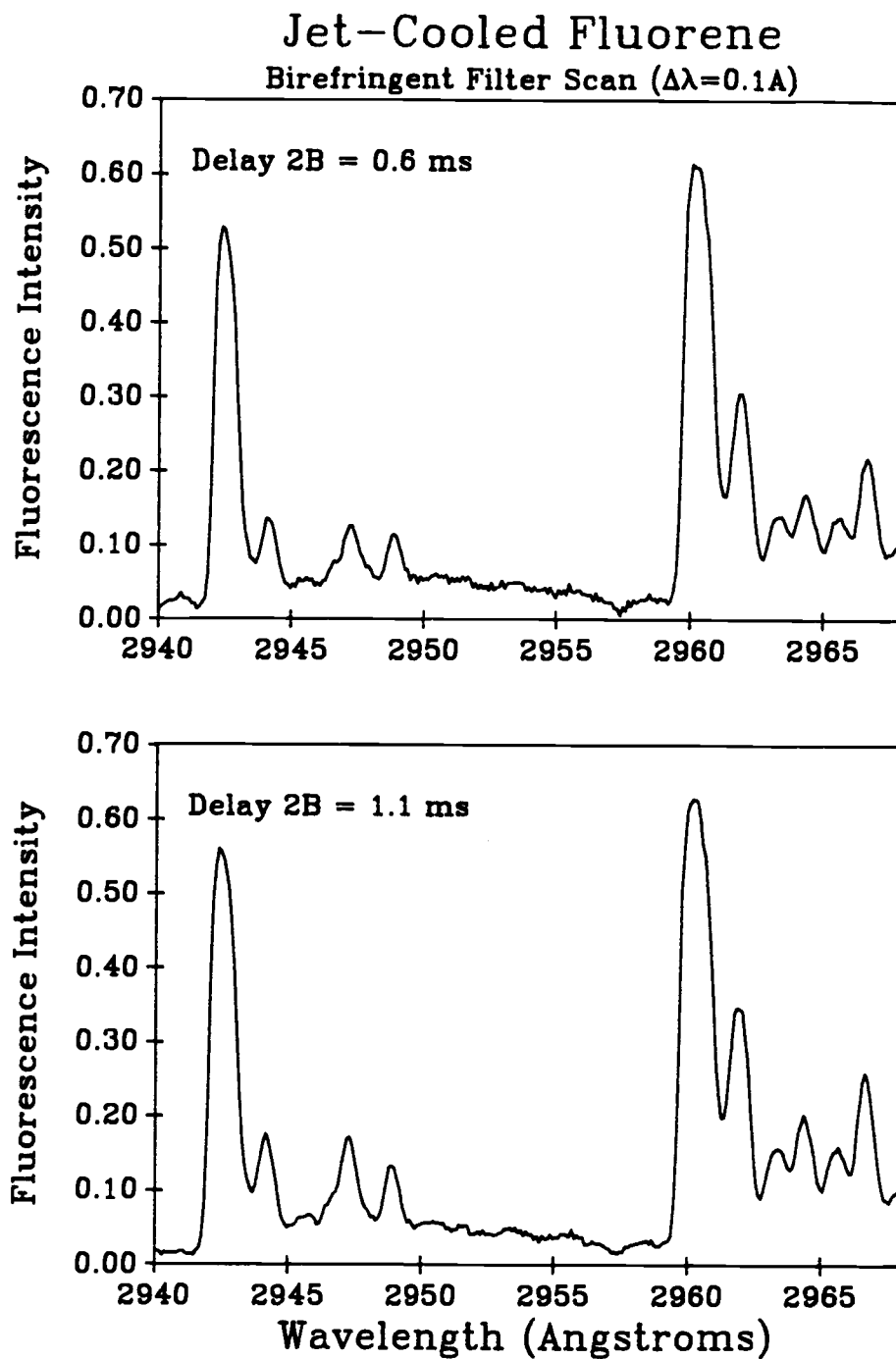


Figure III.5 Fluorescence excitation spectra of fluorene in a helium supersonic expansion measured at delays of 0.6 ms and 1.1 ms relative to the pulsed valve trigger pulse.

Examples of two such spectra are found in Figure III.6. These spectra were obtained in the following manner. First, the spectrum of fluorene was acquired with a back pressure of 7 psi argon as measured off the pressure gauge on the second stage of the regulator. Other experimental conditions were similar to those used for the previous spectra: a valve pulse width of 1 ms, the laser beam focused 1 mm from the tip of the nozzle, a sample cell temperature of 170 °C and a flange temperature of 130 °C. Once this spectrum was acquired, the regulator was removed from the argon gas cylinder and was mounted on the helium cylinder without changing the regulator setting. The pulsed valve driver was then switched to continuous operation for several seconds to purge any residual argon from the system, and the spectrum of fluorene in 7 psi of helium was acquired.

The initially surprising result of this experiment is that the helium diluent appears to produce spectra exhibiting higher resolution with a lower overall background signal. Normally, the higher molecular weight argon molecule is able to cool these analyte molecules more efficiently than helium as discussed in the introduction. However, in the case of the argon-fluorene spectrum the overall background signal increases toward the 2960 Å peak, resulting in a loss of spectral resolution in that region of the spectrum. In addition, the intensity of the 2960 Å peak is also reduced relative to the helium-fluorene spectrum.

These observations are consistent with the formation of fluorene-Argon van der Waals (vdW) complexes. Complexes, or clusters, of rare gas atoms with large polyatomic molecules have been widely observed in supersonic expansions [65,66,89,90,92-95]. These clusters are formed in the high-density, high-pressure region that occurs early in the expansion where the required three-body collisions are most likely to occur. For large molecules (*i.e.*, PNAs) the formation of clusters depends on both the nozzle diameter,  $D$ , and the stagnation pressure,  $p_0$ ; cluster formation has been shown to scale roughly with  $p_0^{2n} \cdot D$  where  $n$  is the coordination number of the complex [92]. In addition, larger inert gas atoms (Ar,

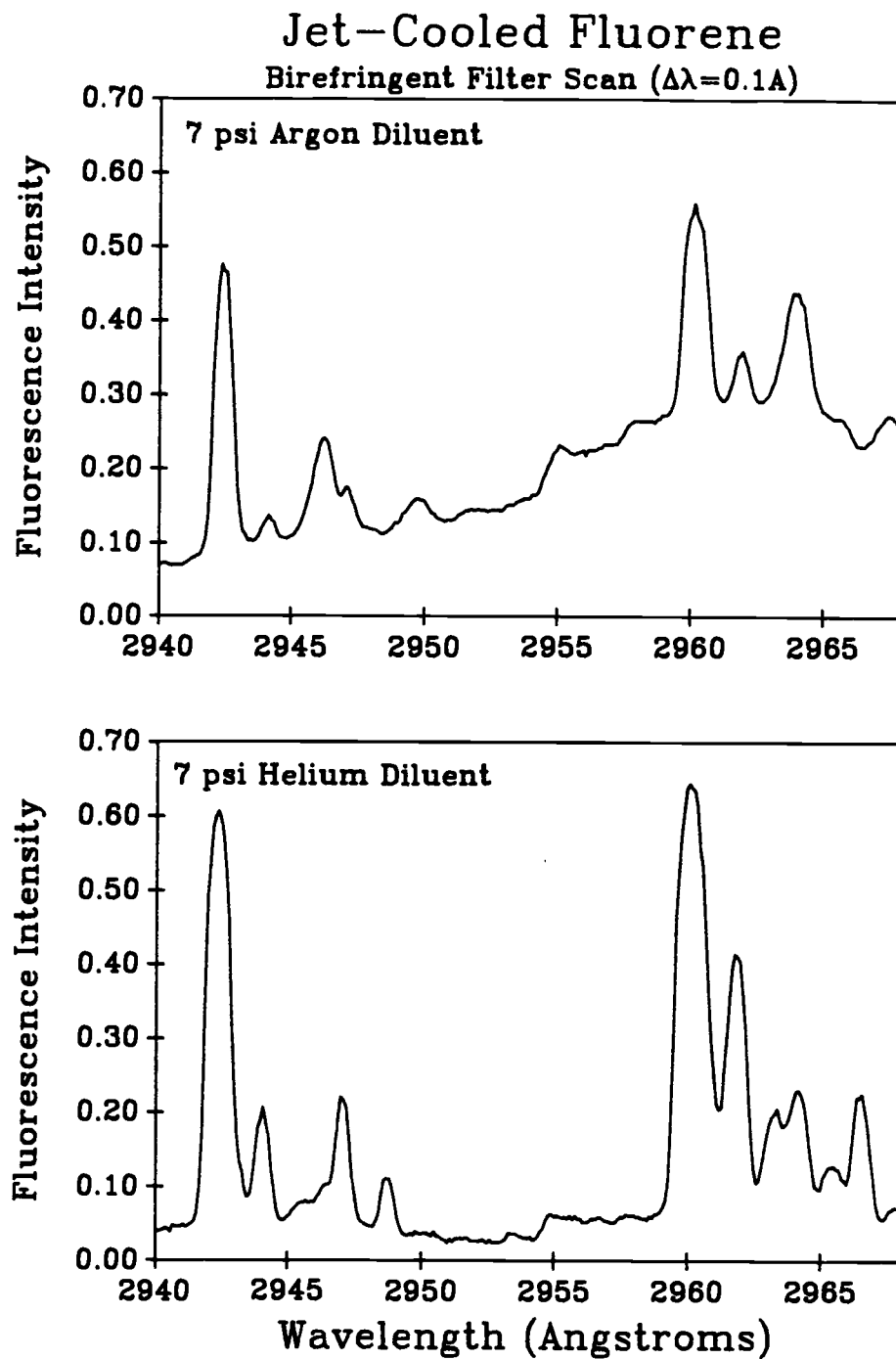


Figure III.6 Comparison of the fluorescence excitation spectra of fluorene produced in argon and helium supersonic expansions.



Kr, Xe) are more likely to form complexes than are the smaller gases (He, Ne). This is due to the fact that the larger atoms are more polarizable and thus can form these very weak van der Waals bonds more easily. Expansion of large, heavy molecules in a light diluent gas such as helium also results in significant "velocity slip"; the light diluent gas atoms are unable to accelerate the heavier molecules to the same velocity and thus a significant velocity difference exists between the diluent gas and the heavier molecules. Since the inert gas atoms are traveling at velocities that are significantly higher than the molecular velocities, collisions between the two will be less likely to result in the diluent gas atoms "sticking" to the molecule.

The van der Waals complexes of argon with fluorene have been studied in supersonic expansions [89,90,94]. In one study, the fluorene sample was heated to 100°C and was expanded through a 0.2-mm by 70-mm slit-shaped nozzle. Significant fluorene-Ar<sub>n</sub> clustering was observed beginning at the relatively low stagnation pressure of 53 torr. In addition, spectral shifts of 4 Å, and 7 Å, were observed for cluster coordination numbers of n=1 and n=2, respectively.

Another PNA-rare gas complex that has been studied in detail is the tetracene-Ar, Kr, Xe system [92,65]. Tetracene-Ar<sub>n</sub> (T-Ar<sub>n</sub>) clusters with coordination numbers, n, of 1 to 7 were identified by observing shifts in the wavelength of the 0-0 transition as each additional argon atom was added to the cluster. These shifts ranged from +7 Å for the T-Ar<sub>1</sub> cluster to +50 Å for the T-Ar<sub>7</sub> cluster. Using a continuous nozzle with a diameter of 150 μm, significant T-Ar clustering was observed at stagnation pressures of 478 torr and greater. In addition, conservation of fluorescence intensity was observed: *i.e.*, as the stagnation pressure and thus the number of clusters was increased, the intensity of the T-Ar<sub>0</sub> (uncomplexed tetracene) 0-0 transition decreased proportionally to the combined increase in the intensities of all the cluster bands in the spectrum. Thus, cluster formation results in a wavelength shift, possibly dramatic, and a decrease in the intensity of uncomplexed spectral transitions. In addition, significant cluster formation

also initiates condensation which results in a warming of the expansion and a resultant increase in the number of vibrational and rotational states that are populated.

It is thus reasonable to attribute the loss of spectral resolution and decrease in the intensity of the 0-0 transition peak observed in the fluorene-argon spectrum of Figure III.6 to cluster formation. The observation of clusters in the fluorene-argon expansion is likely due to the moderately large nozzle diameter used (330  $\mu\text{m}$ ), fairly high stagnation pressures ( $> 1000$  torr) and the necessity of operating the pulsed valve at temperatures well below the boiling point of fluorene. Additional data supporting the formation of PNA-argon clusters will also be presented in a subsequent section. Clustering in the fluorene-helium expansion is less likely due to velocity slip effects and the low polarizability of helium, and in the case of the tetracene studies [92] no tetracene-He clusters were observed at stagnation pressures up to 8000 torr.

The final point to make regarding these results is that under these conditions, nothing is sacrificed in using helium rather than argon as the diluent gas. Helium provides sufficient cooling while minimizing the formation of the clusters that warm the expansion and complicate the spectra. This means that helium can be used as both the GC carrier gas and as the diluent gas for the expansion, making the interfacing of the two systems more straightforward.

#### 4. Comparison of Fluorene and 1-Methylfluorene Excitation Spectra

All experiments described to this point have used fluorene as the model compound for the studies. One of the goals of this research is to develop instrumentation that is not only selective for PNAs, but also, exhibits selectivity among the various PNAs. Thus, spectroscopic properties of a closely related compound, 1-methylfluorene (1MF), were examined using this system.

Because the pulsed valve had been used in the fluorene studies for several months and had been operated at temperatures well below the boiling point of fluorene, it was anticipated that there would be "memory" problems arising from condensation of fluorene onto the exposed surfaces in the interior of the valve. In order to minimize these memory effects, the valve was disassembled and the plunger, washer, spring, and nozzle tip were washed with both dichloromethane and methanol. Unfortunately, the plastic spacer used to support the solenoid windings of the valve would be dissolved by a strong solvent such as dichloromethane. In addition, it was not known if there were any glues or other valve components that would be damaged by excessive exposure to organic solvents. Thus, only the metal surfaces inside the valve were washed using a solvent soaked cotton swab, with care taken to minimize exposure of the plastic surfaces to direct contact with the solvent. The result of these factors was that the valve could only be partially cleaned of residual fluorene. As it turned out, however, the fluorene remaining in the valve, which was a rather significant amount as we will see, allowed the spectrum of a mixture of both fluorene and 1-methylfluorene to be obtained.

The pure IMF sample was placed in a clean glass thimble which was then installed in the sample block Swagelok tee. The tee had also been cleaned with dichloromethane-methanol rinses as had all tubing and fittings located between the tee and the valve. Fluorescence excitation spectra of IMF were then obtained under conditions similar to the previous fluorene spectra. A series of fluorescence excitation spectra taken over a one hour period of time after the sample change are exhibited in Figure III.7. The first spectrum displayed in this series (A) is the fluorene spectrum taken just before changing the sample and is included for comparison to subsequent spectra. The remaining spectra (B to F) were taken at approximately 12 minute intervals. The main details to observe from these spectra are that the peaks due to fluorene decrease with time as the supply of fluorene is slowly used up, and consequently the peaks due to 1-methylfluorene gradually become more prominent. In addition, it is also important to notice that the peaks due to each

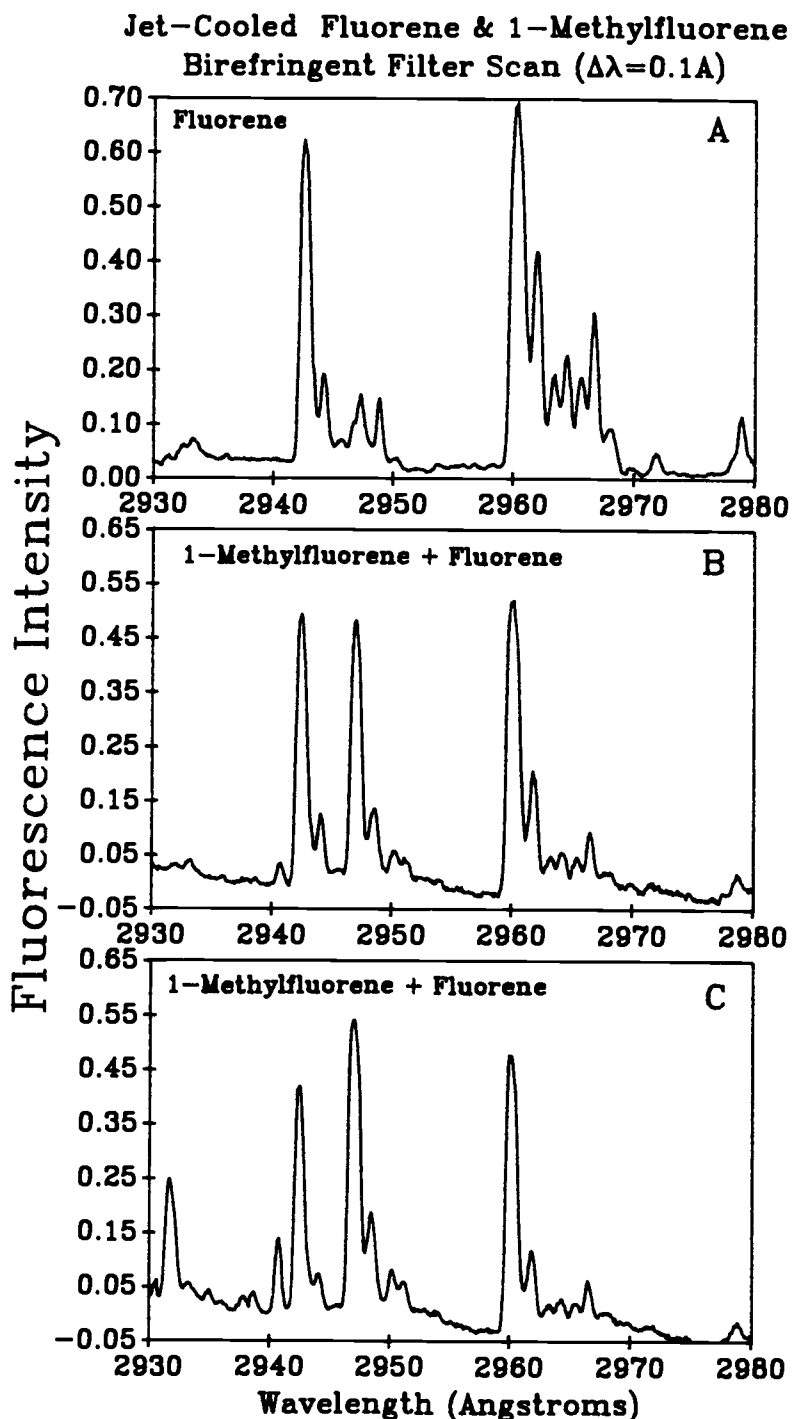


Figure III.7 The fluorescence excitation spectra of (A) fluorene in helium, (B) IMF and residual fluorene immediately after replacing the fluorene in the sample thimble with IMF, (C) IMF and residual fluorene after approximately 24 min. (continued)

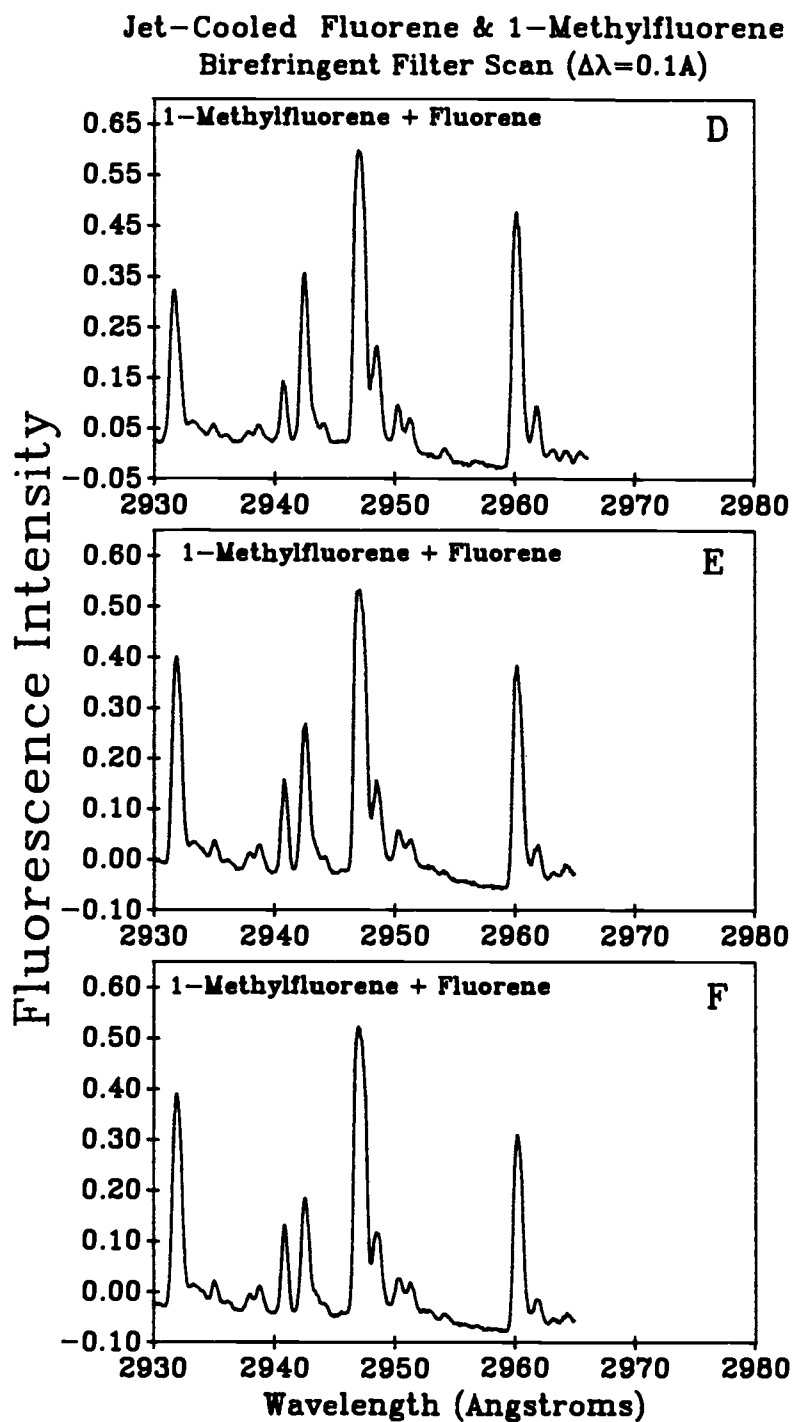


Figure III.7 (continuation) 1MF and residual fluorene after approximately (D) 36 min., (E) 48 min, and (F) 60 min.

of these closely-related compounds are baseline resolved and easily distinguished from each other. This fact further demonstrates the excellent selectivity of the method and its utility in determining the components of complex mixtures.

Finally, the fact that the spectrum of a "pure" sample of IMF is observed as a mixed spectrum of fluorene and 1-methylfluorene for hours, and even days after changing the sample, indicates that problems with analyte condensation (cold-trapping) in the valve will most likely be observed in the chromatography experiments. This effect is likely to be viewed as tailing of the chromatographic peaks and as a significant background signal. It should be noted, however, that these continuous sample introduction experiments were performed over a period of several months and thus the analyte had ample opportunity to seek out all the surfaces inside the valve and condense upon them. In the case of the chromatography experiments, the analyte is only present in the valve a small fraction of the time when the peak elutes and thus contamination is expected to be less of a problem. The tailing and increased background effects are indeed observed experimentally, and are discussed in a subsequent section, but are not so great as to detract significantly from the results.

## 5. Axial Expansion Characteristics

In order to maximize the sensitivity of the previous measurements in anticipation of the need to obtain reasonable chromatographic detection limits, the laser beam was aligned a millimeter from the nozzle tip where the analyte density would be expected to be greatest. It is of some interest, however, to examine the characteristics of the expansion downstream from the nozzle to determine just how much sensitivity is sacrificed for additional selectivity when the expansion is sampled in the colder, less dense regions.

Unfortunately, the instrumentation developed in this work does

not lend itself particularly well to such an experiment. As discussed previously, the only way to change the laser beam-expansion intersection point over distances greater than a few millimeters is to open the vacuum chamber, remove the nozzle flange and insert a spacer between the nozzle flange and the detection cell. Since this procedure takes a fair amount of time and has a tendency to disrupt the alignment of the system, the expansion was sampled at only 4 different axial positions by using various combinations of the spacers: at  $X = 0$  (at the nozzle tip),  $X = 1.9$  mm,  $X = 3.5$  mm, and  $X = 6.4$  mm. It should be noted that due to the design of the detection cell, it is also difficult to measure the actual nozzle-laser beam intersection distance precisely. To minimize this source of error, the beam was first visually centered as close as possible to the nozzle tip to set the  $X = 0$  position. When subsequent measurements were made using the different spacers, no additional adjustment of the laser beam position was made. Consequently, the values of  $X$  that are reported are the distance downstream from the  $X = 0$  position and are determined by the width of the spacer.

Measurements were made starting at  $X=6.4$  mm and progressed inward towards the nozzle to the  $X=0$  position. In addition, at each axial position a spectrum was obtained for both helium- and argon-cooled IMF for comparison. The helium-cooled IMF spectra that were acquired at each of the different axial positions are presented in Figure III.8 and the characteristics of the 2947-Å IMF transition at each of these positions are summarized in Table III.5. Each spectrum was acquired with a helium stagnation pressure of 7 psi and a valve pulse width of 1 ms. It is apparent from these data that indeed, the spectrum acquired the farthest distance away from the nozzle at  $X/D = 19$ , exhibits the narrowest, least intense 2947-Å peak, and a very clean baseline with little other structure. The spectra measured at distances closer to the nozzle exhibit spectral peaks that are more intense, but wider, and in the case of the  $X = 0$  spectrum, exhibit hot band transitions on the long wavelength side of the 2947-Å peak, indicating that less complete cooling has been

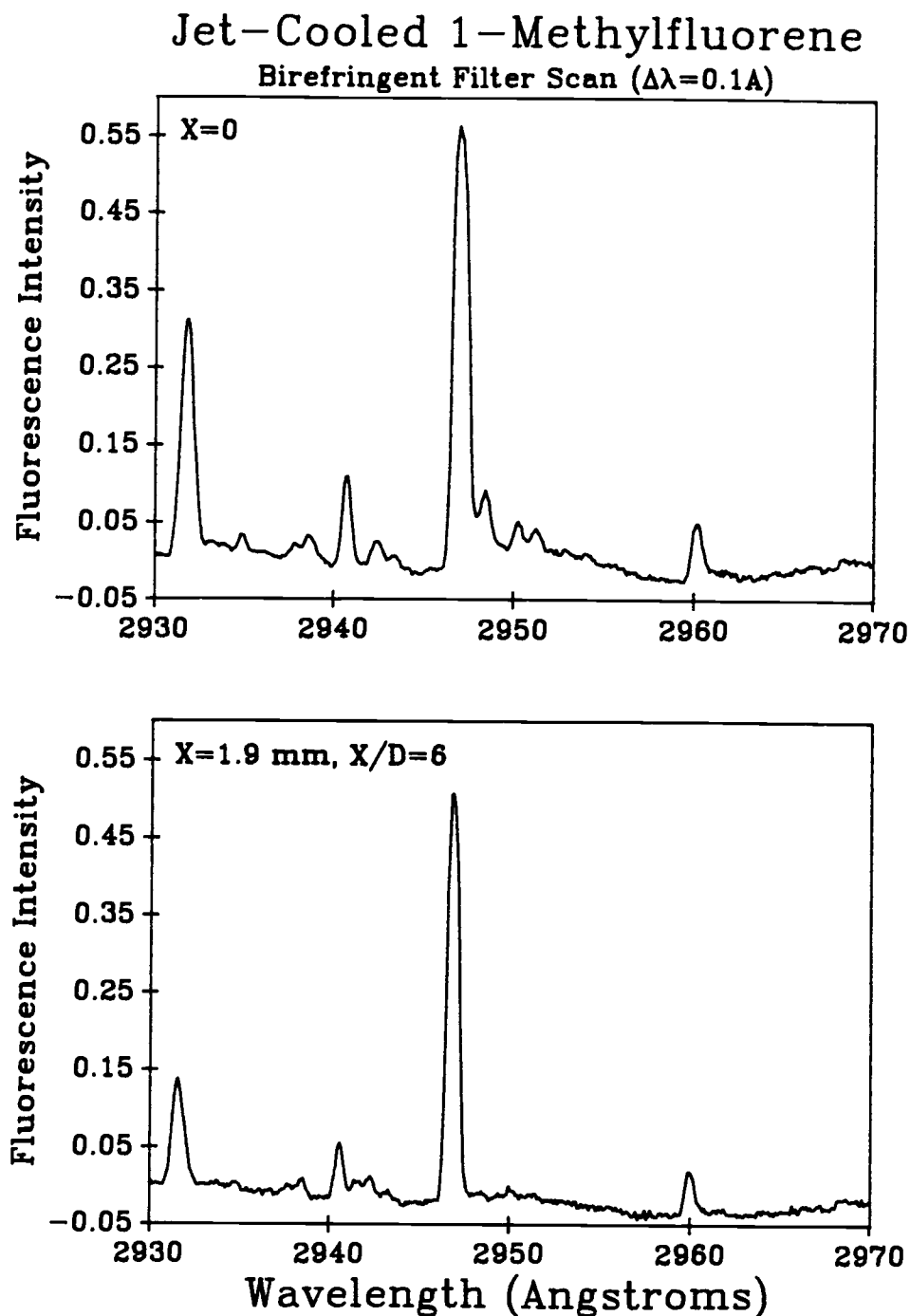


Figure III.8 Fluorescence excitation spectra of 1MF in helium (top) with the laser beam focused approximately 1 mm from the nozzle tip at  $X=0$ , and (bottom) with the beam focused 1.9 mm downstream from  $X=0$  (continued).



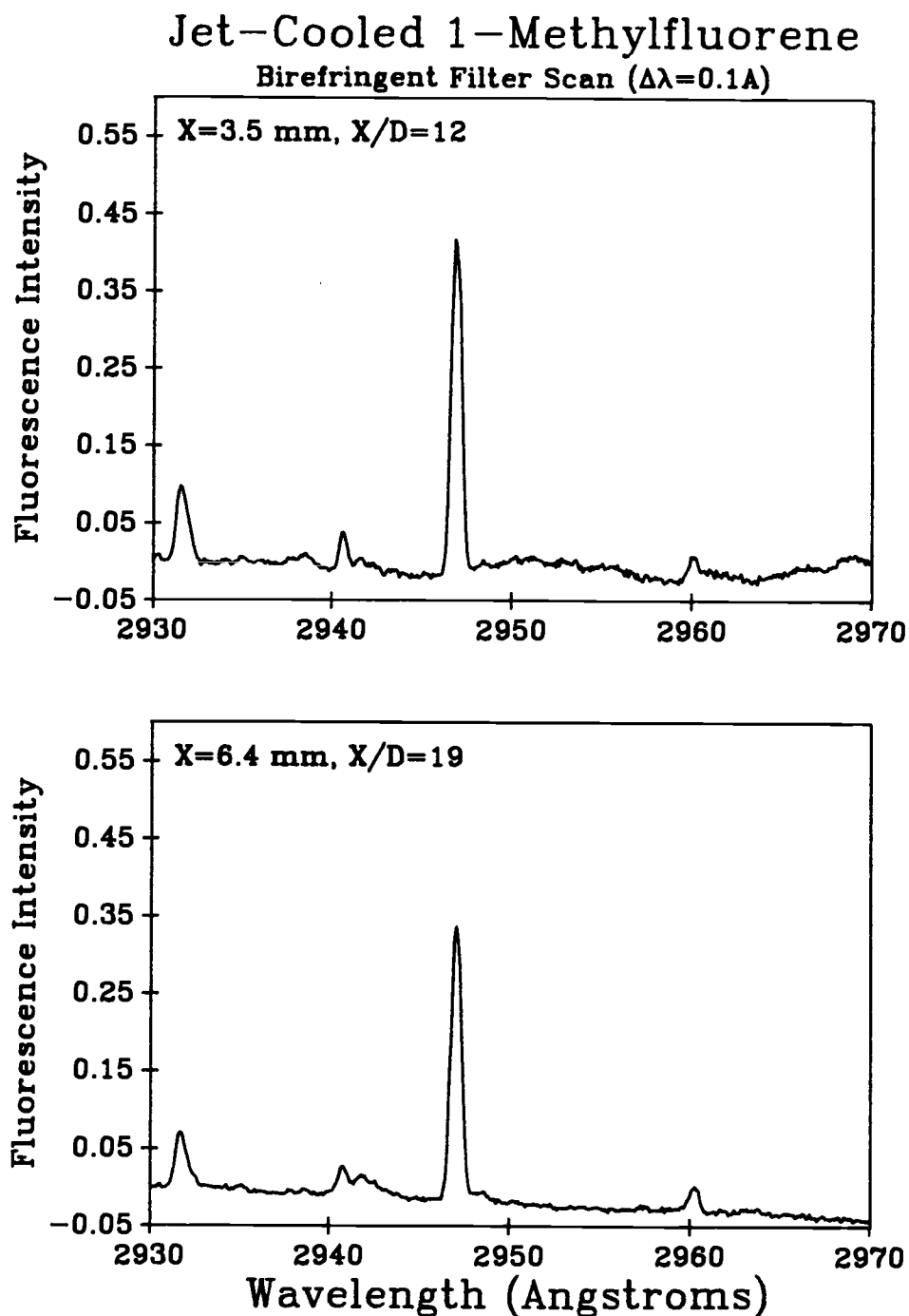


Figure III.8 (continuation) Spectra produced with the laser focused (top) 3.5 mm downstream from  $X=0$ , and (bottom) 6.4 mm downstream from  $X=0$ .

Table III.5  
 2947 Å 1-Methylfluorene Fluorescence  
 as a Function of the Axial Distance of the  
 Laser Beam from the Nozzle Tip

X (mm)	X/D	$\Delta\lambda^1$ (Å)	Intensity <sup>2</sup>
X = 0	0	1.1	0.564
1.9	5.8	0.75	0.508
3.5	11	0.7	0.418
6.4	19	0.7	0.338

<sup>1</sup>Peak width (FWHM) of the 2947 Å transition.

<sup>2</sup>Relative peak fluorescence intensity of the 2947 Å transition.

achieved. Thus, if additional spectral selectivity is required by a particular analysis, simply moving the laser beam intersection point downstream a few millimeters can provide narrower, cooler spectra with a resultant sacrifice in fluorescence signal intensity of approximately 10 to 40%.

The argon-cooled IMF spectra acquired at each of the three axial positions closest to the nozzle are presented in Figure III.9. It should be noted that again, the effects of clustering are observed in these spectra. Downstream from the nozzle tip the intensity of the uncomplexed transition is dramatically decreased, possibly as a result of substantial clustering. Also, since no additional spectral peaks are observed in this region of the spectrum, the peaks due to IMF-Ar<sub>n</sub> clusters appear to have been shifted outside the scan range of this spectrum. These results help to reinforce the choice of helium as the diluent gas for subsequent experiments.

## 6. Miscellaneous Characterization Experiments

A few additional experiments were performed to determine the influence of factors such as stagnation pressure, and vacuum chamber pressure on the excitation spectra. These studies were undertaken simply to get a rough idea if any consideration should be paid to these variables when interfacing the system to the chromatographic system.

### a. Influence of Stagnation Pressure on Spectra

The influence of diluent gas stagnation pressure was investigated by acquiring fluorescence excitation spectra of IMF with back pressures of 7- and 20-psi helium (1120 and 1800 Torr). These spectra are displayed in Figure III.10. The main point to note is

Jet-Cooled 1-Methylfluorene in Ar  
Birefringent Filter Scan ( $\Delta\lambda=0.1\text{\AA}$ )

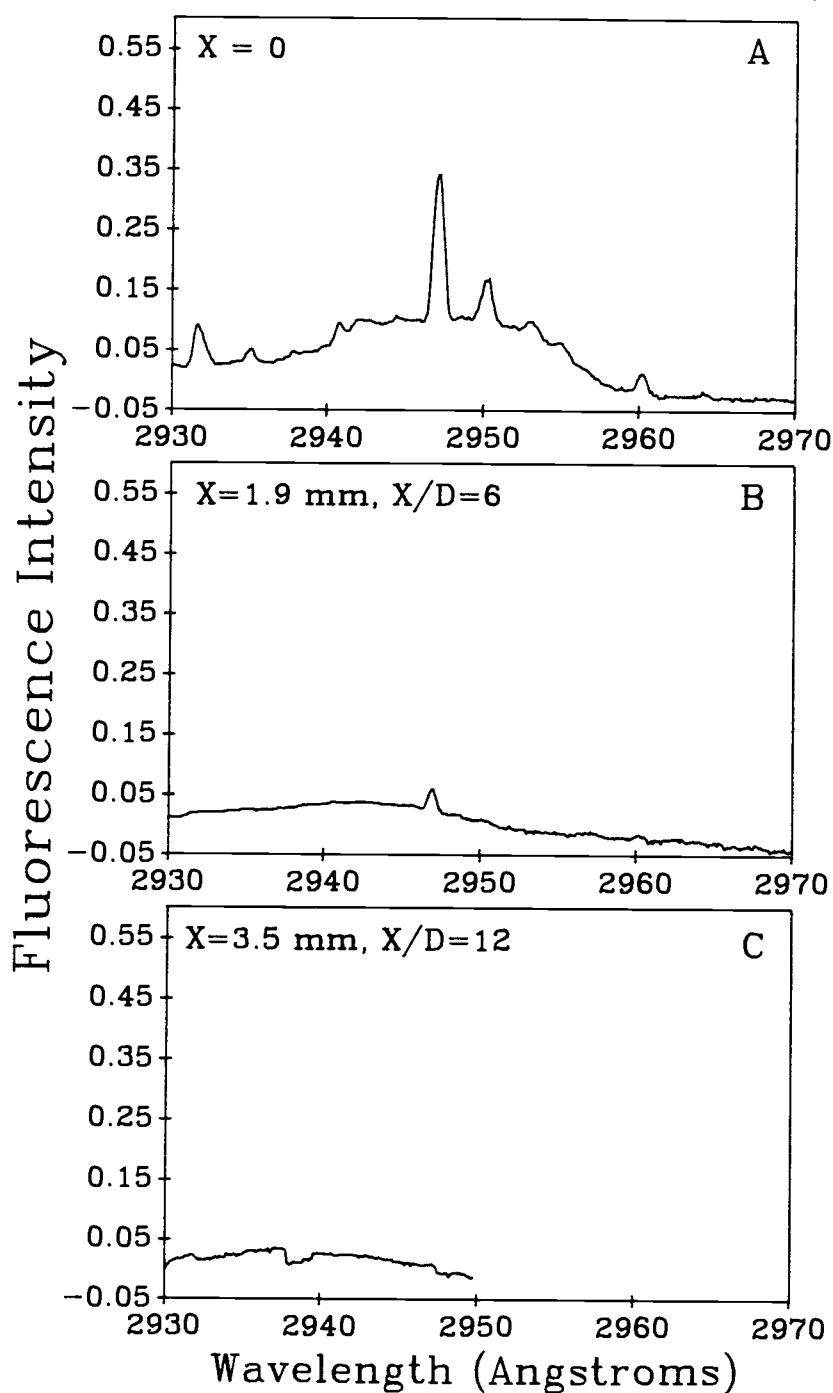


Figure III.9 Fluorescence excitation spectra of IMF in argon with the laser focused approximately (A) 1 mm, (B) 1.9 mm, and (C) 3.5 mm downstream from the nozzle tip.

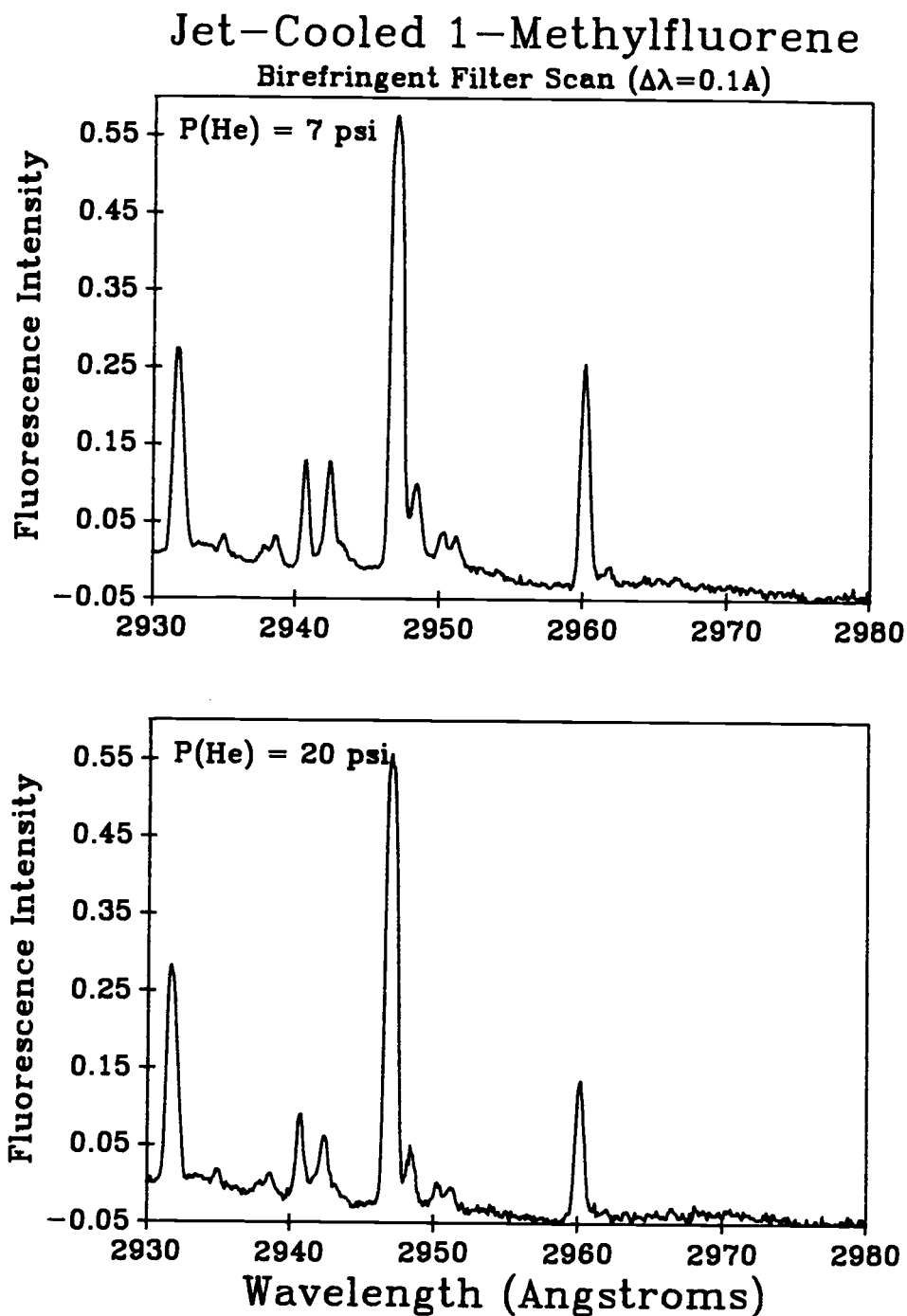


Figure III.10 Fluorescence excitation spectra of IMF in helium obtained with stagnation pressures of (top) 7 psi and (bottom) 20 psi as read from the second stage of the high-pressure regulator.

that there are no dramatic changes in the spectra as the diluent gas pressure is changed over this range.

#### b. Influence of the Vacuum Cell Pressure on Spectra

In order to determine if there was any benefit to be gained by reducing the overall vacuum chamber pressure, data acquisition was delayed between each wavelength step in a series of spectral scans. This provided the vacuum pump with more time to evacuate the gas that was released into the chamber during the previous set of pulses. The average vacuum chamber pressure could thus be adjusted by changing the length of the delay between wavelength steps. It was anticipated that the main influence the absolute chamber pressure would have on the expansion would be to change the location and size of the Mach disk (see equation I.9). Since the expansion was probed within a few millimeters of the nozzle tip during most of the experiments, the chamber pressure should have little effect on the quality of the spectra.

Fluorescence excitation spectra of IMF were acquired using delays of 0, 1, and 5 seconds, resulting in detector cell vacuum pressures of 30, 20, and 10 mTorr respectively. These spectra are displayed in Figure III.11 and it can be seen that there are no drastic differences between the features in each of these spectra.

#### C. Combined High Spectral-Resolution Laser-Excited Fluorescence Spectroscopy and Gas Chromatography.

Once the initial experiments were completed and the spectroscopic system was reasonably well characterized, the continuous sample introduction system, which was used in the studies described above, was replaced by a packed-column gas chromatograph.

# Jet-Cooled 1-Methylfluorene Birefringent Filter Scan ( $\Delta\lambda=0.1\text{\AA}$ )

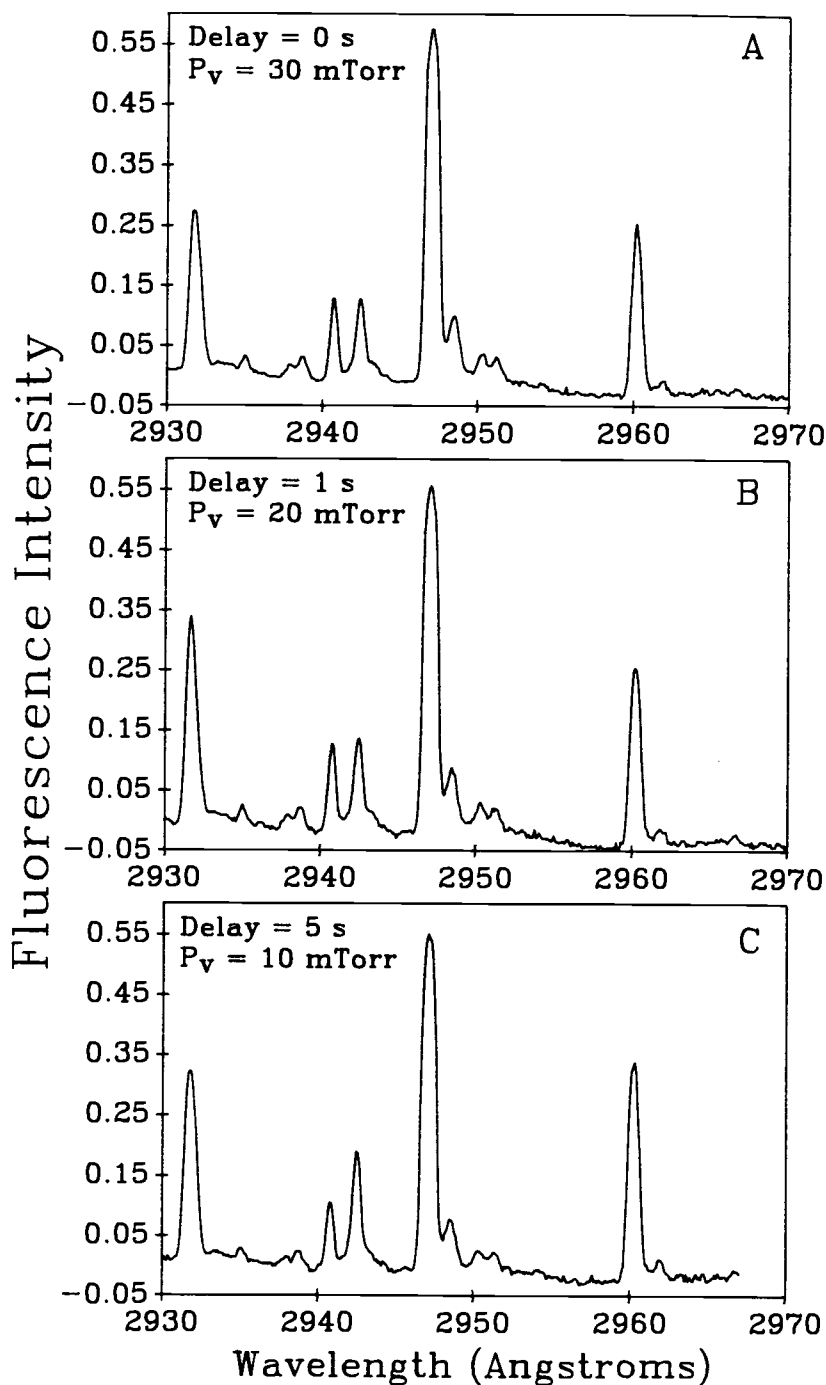


Figure III.11 Fluorescence excitation spectra of 1MF in helium obtained with delays of (A) 0 s, (B) 1 s, and (C) 5 s between each wavelength step. This delay gives the vacuum pump additional time to evacuate the detector cell and thus reduces the cell pressure,  $P_v$ .

The gas chromatograph has already been described in a previous section and is depicted in Figure III.12, which also illustrates the interface between the GC and the pulsed valve used as a supersonic nozzle. One important feature to notice from this figure is the fact that the GC column outlet is connected directly to the pulsed valve through a heated transfer line. Thus, the GC column effluent must exit entirely through the pulsed valve, which pulses the gas non-continuously into a vacuum rather than the usual chromatographic configuration where the effluent exits continuously to the atmosphere. Consequently, the interaction between the column flow and the valve flow must be considered prior to examining the actual chromatographic results to determine if the two systems can be interfaced without any major sacrifices.

#### 1. Description of the GC-Pulsed Nozzle Interface

In order to examine the interface between the GC and the supersonic nozzle, the factors that influence the gas flow through the GC column and the pulsed valve orifice must first be described. Once the variables that affect the flow through each of these systems are understood, their interaction can be examined when the outlet of the GC column is connected to the inlet of the pulsed valve through the flow interface volume defined by the transfer line.

##### a. Flow Through a Packed GC Column

The flow of a compressible gas through a porous bed is governed by Darcy's Law [96] and can be expressed in terms of a packed gas chromatography column by [97,98]:



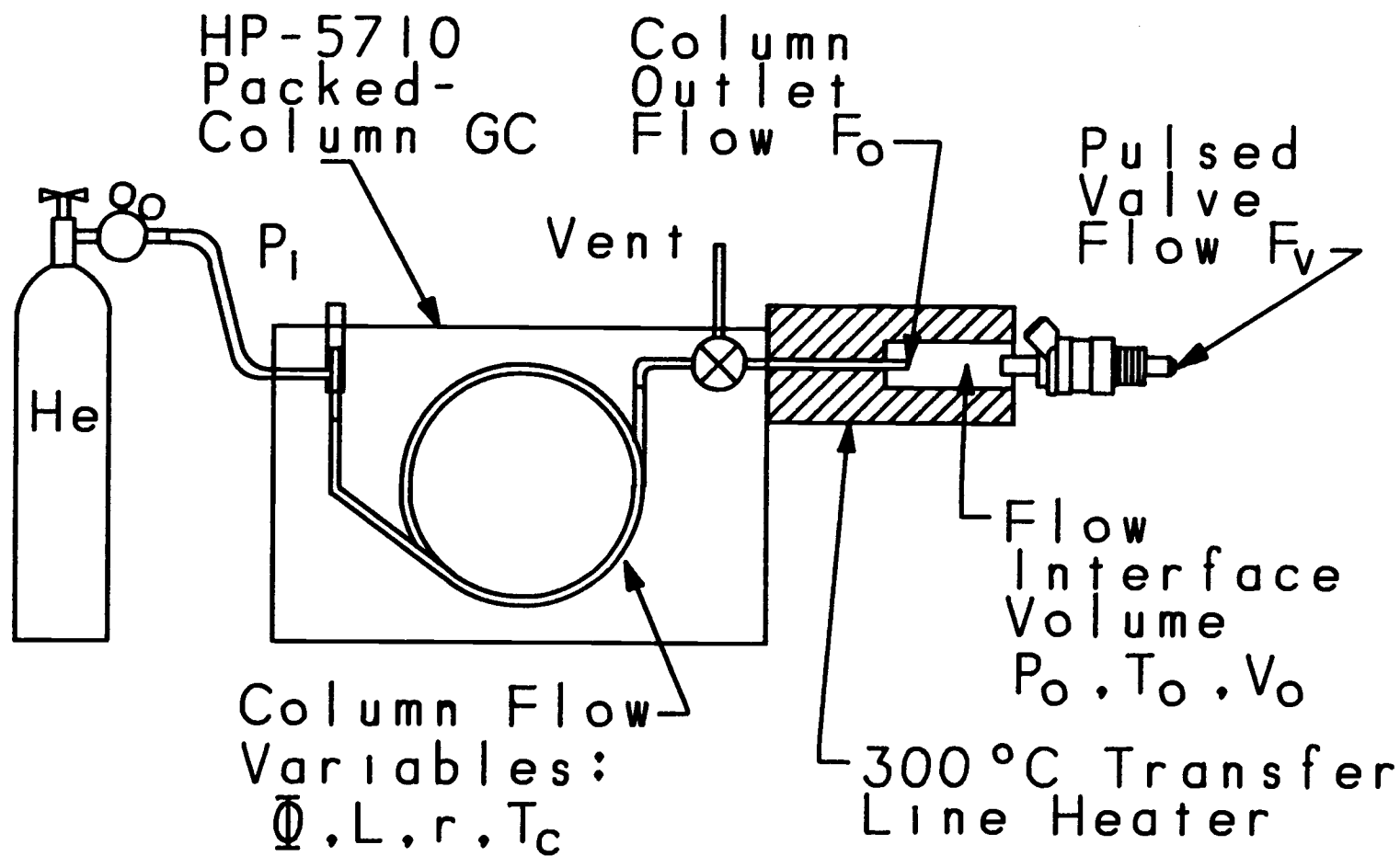


Figure III.12 Diagram of the configuration used when a packed-column gas chromatograph is used for sample introduction.

$$u_0 = \frac{\Phi}{\eta L} \cdot \frac{(p_i^2 - p_o^2)}{2p_o} \quad (\text{III.2})$$

where  $u_0$  is the linear velocity of the gas at the column outlet, expressed in  $\text{m}\cdot\text{s}^{-1}$ ;  $\Phi = B_0/\epsilon$ , where  $B_0$  is the specific permeability coefficient, which is related to the surface area and geometry of the column packing and has units of  $\text{m}^2$ , and  $\epsilon$  is the unitless porosity of the column packing;  $L$  is the packed length of the column in m;  $\eta$  is the viscosity of the gas in the column, which has units of  $\text{kg}\cdot\text{m}^{-1}\cdot\text{s}^{-1}$  and depends on the square root of the column temperature; and  $p_i$  and  $p_o$  are the column inlet and outlet pressures in  $\text{kg}\cdot\text{m}^{-1}\cdot\text{s}^{-2}$  (Pascals). The outlet velocity is of interest when considering the interface between the column and the pulsed valve. However, the chromatographic separation efficiency depends more on the average linear velocity than the outlet velocity.

Because gases are compressible and since a pressure gradient is required between the column inlet and outlet for gas to flow, the gas velocity changes continuously along the length of the column. Thus, the average linear velocity is always less than the outlet velocity described by equation III.2. The average flow velocity,  $\bar{u}$ , is related to the outlet velocity,  $u_0$ , by the compressibility correction factor,  $j$ , which depends on the inlet and outlet pressures [99]:

$$j = \frac{3 (\bar{p}^2 - 1)}{2 (\bar{p}^3 - 1)} \quad (\text{III.3})$$

where  $\bar{p} = P_i/P_o$ . This factor is then used to calculate the average linear flow velocity:

$$\bar{u} = j \cdot u_0 \quad (\text{III.4})$$

The volumetric and mass flow rate of the carrier gas through the column outlet,  $F_o^{\text{vol}}$  and  $F_o^{\text{mass}}$ , are calculated from the linear flow velocity,  $u_0$ :

$$F_0^{\text{vol}} = u_0 \cdot \pi r^2 \quad (\text{III.5})$$

and,

$$F_0^{\text{mass}} = F_0^{\text{vol}} \cdot P_0/R \cdot T_c \quad (\text{III.6})$$

where  $r$  is the inside radius of the column,  $T_c$  is the temperature of the column, and  $R$  is the ideal gas constant. Each of these flow rates can also be converted to their average values by multiplication with the compressibility correction factor,  $j$ .

Thus, assuming that  $L$ ,  $r$ ,  $\Phi$ , and  $P_i$  remain constant through an experiment, the flow rate thorough the column will be determined by the outlet pressure,  $P_0$ , and the column temperature,  $T_c$ , which influences the gas viscosity (the viscosity is not influenced significantly by these relatively small changes in pressure). The fact that the flow rate through the column depends on the outlet pressure is of particular importance in this project since the column outlet is connected to a vacuum chamber through a pulsed valve. This configuration could degrade the chromatography in several ways. First, since the gas is only allowed to flow through the orifice during the small period of time that the valve is open, it is possible that the carrier gas flow rate might fluctuate dramatically as the valve opens and closes and the column is exposed to a vacuum for a brief period of time. Similarly, if the average flow through the pulsed valve is dramatically different than the flow through the column outlet, the pressure in the interface volume between the column and valve,  $P_0$ , will either increase or decrease. This would also influence the flow through the column. In either case, changing the average linear velocity through the column changes the column efficiency and thus the resolution of the chromatographic separation. In order to understand this interaction between the column flow and the flow through the pulsed valve, the variables that influence supersonic nozzle flow must next be examined.

### b. Supersonic Nozzle Flow

The flow rate of gas,  $F_{noz}$ , from a stagnation reservoir at high pressure, through a nozzle orifice into a region of much lower pressure can be described by [100,101],

$$F_{noz} = \alpha A_t a_0 n_0 \quad (III. 7)$$

where  $\alpha = \frac{1}{2}(\gamma+1)^{-\frac{1}{2}}(\gamma+1)/(\gamma-1)$ ,  $\gamma$  is the ratio of specific heats at constant pressure and volume,  $C_p/C_v$ , as described in an earlier section;  $A_t$  is the cross-sectional area of the nozzle throat;  $a_0$  is the sonic velocity of the gas entering the nozzle; and  $n_0$  is the number density of the gas in the stagnation chamber. If  $\alpha$  is solved for  $\gamma=5/3$ , the specific heat ratio for monatomic ideal gases, and the expressions for each of the other terms are substituted, Equation III.7 becomes [49],

$$F_{noz} = 0.562 \cdot (\frac{1}{4}\pi D^2) \cdot (\gamma R_a T_v / M)^{\frac{1}{2}} \cdot (P_0 / R_n \cdot T_v) \quad (III.8)$$

where  $D$  is the nozzle orifice diameter in m;  $T_v$  is the nozzle temperature in K;  $M$  is the atomic weight of the gas;  $P_0$  is the stagnation pressure in atm;  $R_a$  and  $R_n$  are ideal gas constants expressed as  $8314 \text{ m}^2 \cdot \text{g} \cdot \text{s}^{-2} \cdot \text{mole}^{-1} \cdot \text{K}^{-1}$ , and  $8.21 \times 10^{-5} \text{ m}^3 \cdot \text{atm} \cdot \text{mole}^{-1} \cdot \text{K}^{-1}$ , respectively; and  $F_{noz}$  is in units of  $\text{moles} \cdot \text{s}^{-1}$ . Thus, for a particular nozzle diameter and temperature, the flow rate through the nozzle will be determined by the stagnation pressure,  $P_0$ . The situation in this project is slightly more complicated since a pulsed nozzle is used to form the expansion. It has been shown, however, that the expansion is completely formed within 1-10  $\mu\text{s}$  of the opening of the valve [102]. Since pulse widths greater than 500  $\mu\text{s}$  are used in this work, the expansion can be considered to behave completely as a continuous expansion while the

valve is open. Thus, the average mass flow rate through the pulsed valve,  $F_v$ , can be estimated by multiplying the flow rate calculated using Equation III.8,  $F_{noz}$  with the duty cycle of the valve, which is calculated as,

$$\text{Duty Cycle} = t_w \cdot R_v \quad (\text{III.9})$$

where  $t_w$  is the pulse width of the valve, and  $R_v$  is the repetition rate at which the valve is fired.

### c. Flow Through the GC-Nozzle Interface Volume

It is apparent from the previous discussions that both the GC carrier gas flow rate, and the pulsed valve flow rate depend on the pressure of the interface volume that connects the two. However, while the GC flow rate decreases with increasing outlet pressure, the nozzle flow will increase with an increase in stagnation pressure. Thus, the change in the pressure of the interface volume as a function of the column outlet flow and the nozzle flow is of interest. Figure III.12 illustrates the overall configuration of the interface, while the diagram in Figure III.13 focuses on the interface volume.

The principle of the conservation of mass flow can be used to describe the flow through a system such as this one [103]. The total number of particles of gaseous material (*i.e.*,  $n$ , the number of moles) that enter and exit an arbitrary volume must be conserved. Thus, the particles that flow into the volume must be equal to the particles contained within the volume plus the number of particles that flow out of the volume. This means that if there is a difference in the flow rate of particles into and out of the volume, the number of particles contained within that volume must change. This conservation principle can be expressed mathematically in terms

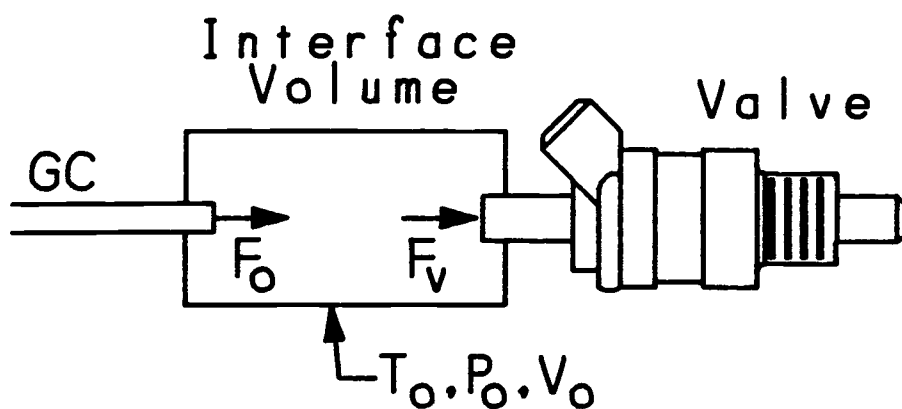


Figure III.13 Diagram of the GC-nozzle flow interface volume.  $F_o$  represents the mass flow of the carrier gas through the GC column outlet and into the interface volume, and  $F_v$  is the mass flow from the interface volume and through the supersonic nozzle.  $T_o$ ,  $V_o$ , and  $P_o$  are the temperature, volume, and pressure of the interface volume, respectively.

of the variables in Figure III.13 as,

$$F_o = \partial n_o / \partial t + F_v \quad (\text{III.10a})$$

If the interface volume,  $V_o$ , and temperature,  $T_o$ , remain constant, then according to the ideal gas law, a change in the number of moles of gas contained within the volume must manifest itself as a change in the interface pressure,  $P_o$ . Thus,

$$F_o = V_o / R \cdot T_o \partial P_o / \partial t + F_v \quad (\text{III.10b})$$

or, rearranging,

$$(\partial P_o / \partial t) = (F_o - F_v) \cdot R T_o / V_o \quad (\text{III.10c})$$

Thus, differences in the flow rates into and out of the interface volume will cause a change in the pressure of the gas in the volume with time.

Fortunately, the carrier gas flow rate through the GC column and the flow rate through the nozzle react in opposite directions to changes in the interface pressure. This means that if there are initially differences in flow between the GC outlet and nozzle ( $F_o - F_v \neq 0$ ), the resultant change in interface pressure will tend to bring the flow rates back to an equilibrium where  $\partial P_o / \partial t$  is zero. For example, if the GC flow rate is initially greater than the nozzle flow rate,  $\partial P_o / \partial t$  is positive and the interface pressure increases. This causes the GC flow rate to decrease and the nozzle flow to increase, which reduces the magnitude of the flow difference and thus the value of  $\partial P_o / \partial t$ . As the flow rates converge,  $\partial P_o / \partial t$  will decrease until flow equilibrium is reached.

In order to represent these flow processes in a more quantitative manner, the various flow equations described above were programmed into a Quattro spreadsheet and flow parameters were calculated for several valve pulse widths. It is assumed that the system is set initially with the outlet vent depicted in Figure

III.12 open to the atmosphere and with the valve sealed and not pulsing. At time  $t=0$ , the vent is closed and the pulsed valve simultaneously begins pulsing. The relaxation of the system to equilibrium conditions is then followed by recalculating  $\partial P_0/\partial t$ ,  $P_0$ ,  $F_0$ , and  $F_V$  at 10-ms intervals over a period of 5 s.

The various experimental parameters required by these calculations were modeled after the GC system used in this research project. These parameters are summarized in Table III.6 and are described below. A column length,  $L$ , of 1.83 m (6 ft), inside radius of 1 mm, and temperature of 298 K were used in the calculations. The carrier gas was assumed to be helium (atomic weight = 4.002 g·mole<sup>-1</sup>) at an inlet pressure,  $P_i$ , of 40 psi, and the column packing was modeled after a 100/120-mesh solid support with an average particle diameter,  $\bar{d}_p$ , of 140  $\mu\text{m}$ . In addition, the interface volume was assumed to be the combined dead volume of the transfer line and the pulsed valve (750  $\mu\text{L}$ ), and the temperature of the interface volume was assumed to be 598 K as determined by the temperature setting of the transfer line heater used for all experiments. In addition, the column packing porosity,  $\epsilon$ , was assumed to be 0.41, which is a reasonable value for many types of solid supports [98]. The specific permeability,  $B_0$ , was calculated from  $\epsilon$  and  $d_p$  using a form of the Kozeny-Carman equation [97]:

$$B_0 = \frac{d_p^2 \epsilon^3}{180(1 - \epsilon)^2} \quad (\text{III.11})$$

Finally, known helium viscosity-temperature data [104] were fit to a second-order polynomial and the resulting regression coefficients were used to predict the carrier gas viscosity at the desired column temperature,  $T_C$ . The helium viscosity-temperature equation derived from the polynomial fit is,

$$\eta \text{ (}\mu\text{poise)} = 53.28 + 0.5303 \cdot T - 1.654 \times 10^{-4} \cdot T^2 \quad (\text{III.12})$$

which is valid over the temperature range  $273 \text{ K} \leq T_C \leq 523 \text{ K}$ .



Table III.6

Experimental GC and Pulsed Valve Parameters  
used in the GC-Nozzle Interface Calculations

Parameter	Value
<u>Gas Chromatograph</u>	
Carrier Gas	Helium
$P_i$ , Inlet Pressure	40 psig (2.7 atm)
$T_c$ , Column Temperature	298 K
$L$ , Column Length	1.83 m (6 feet)
$r$ , Column Inside Radius	1 mm
$\epsilon$ , Packing Porosity	0.41
$\bar{d}_p$ , Average Particle Dia.	140 $\mu\text{m}$ (100/120 mesh)
$B_0$ , Specific Permeability	$2.06 \times 10^{-11} \text{ m}^2$
$\eta$ , Carrier Gas Viscosity	$1.966 \times 10^{-5} \text{ kg/m/s}$ @298K
$j$ , Compressibility Correction	0.501 @ $P_0 = 1 \text{ atm}$
$R$ , Gas Constant	82.3 mL·atm/mol·K
<u>Interface Volume</u>	
$V_0$ , Interface Volume	0.75 mL
$T_0$ , Interface Temperature	598 K
<u>Pulsed Valve</u>	
$D$ , Orifice Diameter	330 $\mu\text{m}$
$\gamma$ , $C_p/C_v$	1.667
$t_w$ , Valve Pulse Width	1, 2, 3, 4 ms
$R_v$ , Valve Rep. Rate	$5 \text{ s}^{-1}$
$T_v$ , Valve Temperature	418 K

The results of these calculations are plotted in Figures III.14 and III.15, and are summarized in Table III.7. Several important points can be made concerning these theoretical results. First, in each case presented the steady-state conditions are reached within 5 seconds of starting the valve pulsing. This means that as long as the vent valve is closed and the valve is started pulsing prior to injection of the analyte, the analyte will most likely experience the steady-state flow conditions.

In addition, because of the compressible nature of the carrier gas, the average carrier gas velocity in the GC column,  $\bar{u}$ , is influenced much less by changes in the outlet pressure than is the outlet velocity,  $u_o$ . This is illustrated by the much smaller %-change values exhibited by the average velocities in Table III.7 than are exhibited by the outlet velocities. This property is of particular interest in terms of the fluctuations in average carrier gas velocity that occur when the pulsed valve opens and closes. The data presented in Figure III.15 and Table III.7 are calculated using the average pulsed-valve mass flow rate of helium,  $F_v$ , which is the product of the true continuous nozzle mass flow rate,  $F_{noz}$  and the valve duty cycle. The average pulsed valve mass flow rate calculated in this manner is thus equivalent to the mass flow rate through a continuous nozzle with an orifice diameter that is reduced by a factor equal to the square root of the duty cycle of the valve (since  $F_{noz} \propto D^2$ ). Although this allows easier calculation of the various flow parameters as they relax towards a steady state, it ignores the fact that in reality the nozzle mass flow rate,  $F_{noz}$  fluctuates from very high values while the valve is open, to zero flow while the valve is closed. Thus, it is worthwhile examining the influence of these large fluctuations in nozzle mass flow on the other flow parameters.

The spreadsheet that was used to calculate the flow parameters using the average valve flow rate was reprogrammed to calculate the flow parameters for a 2-ms valve pulse width using the true nozzle mass flow rate as it oscillates with time. The results of these

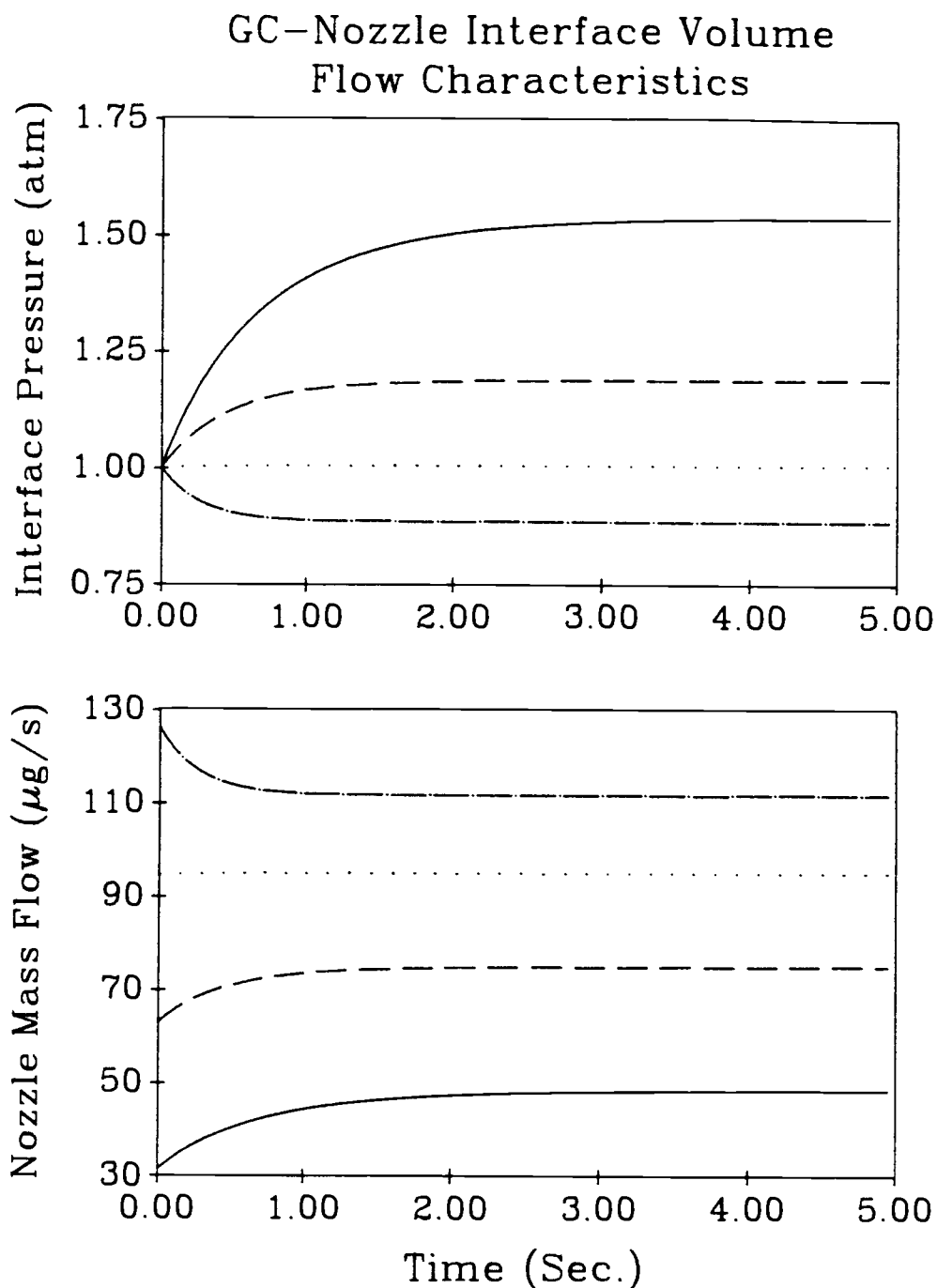


Figure III.14 Theoretical flow characteristics of the GC-nozzle interface illustrating the change in  $P_0$ , the interface pressure (top), and  $F_v$ , the average mass flow of helium through the nozzle (bottom), as a function of the time elapsed after starting the valve pulsing. Data for valve pulse widths of (—) 1 ms, (----) 2 ms, (.....) 3 ms, and (-·-·-) 4 ms, at a 5 Hz repetition rate are shown.

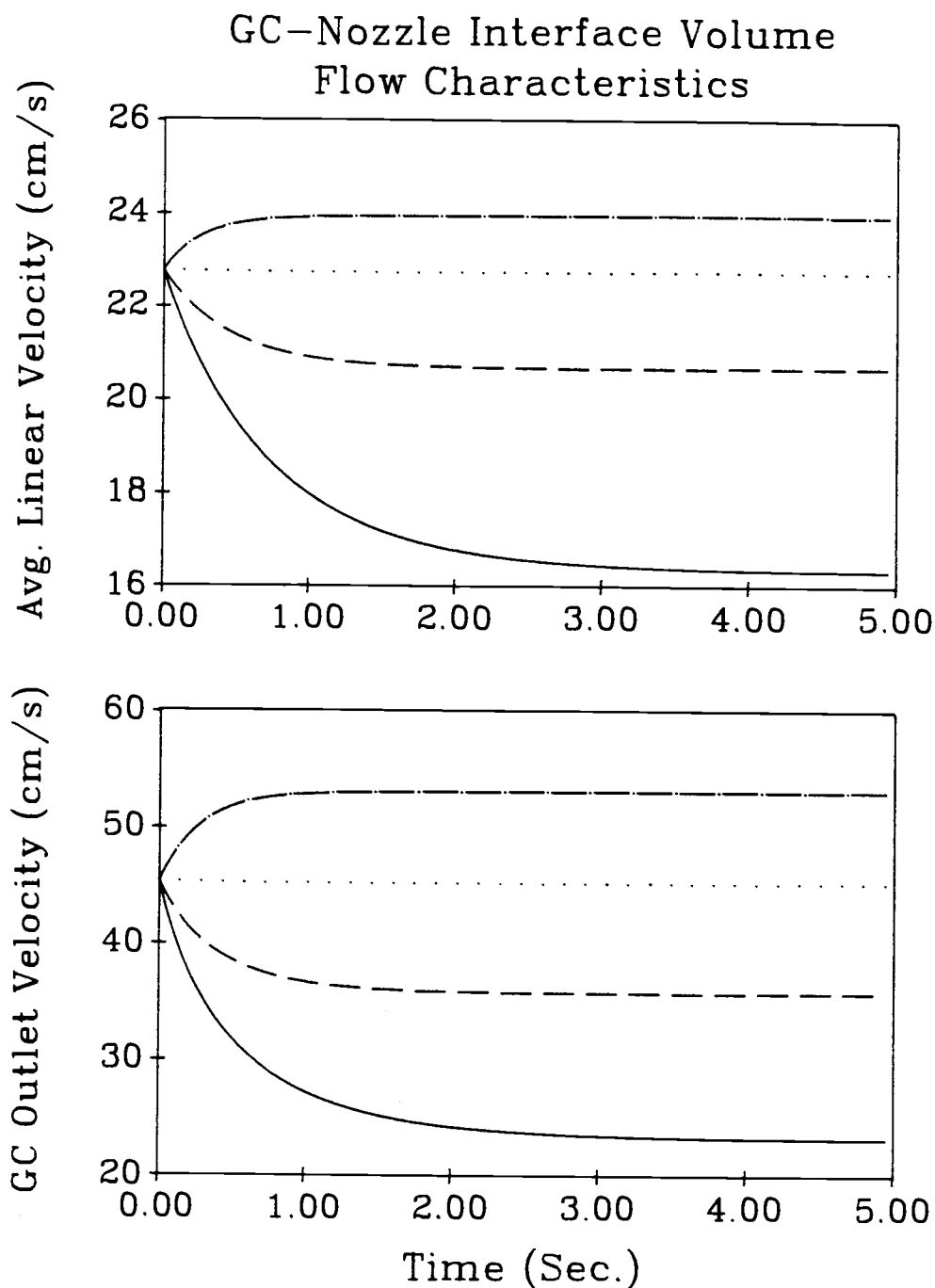


Figure III.15 Theoretical flow characteristics of the GC-nozzle interface illustrating the change in  $\bar{u}$ , the average linear velocity of the carrier gas (top), and  $u_0$ , the velocity of the carrier gas at the column outlet (bottom), as a function of the time elapsed after starting the valve pulsing. Data for (—) 1 ms, (---) 2 ms, (....) 3 ms, and (-.-.) 4 ms valve pulse widths are shown.

Table III.7  
Theoretical Flow Characteristics  
of the GC-Supersonic Nozzle Flow Interface

<sup>1</sup> Pulse Width (ms)	$P_o$ (atm)	$u_o$ , (cm/s)	$\bar{u}$ (cm/s)	$F_o$ ( $\mu\text{g/s}$ )	<sup>4</sup> $F_v$ ( $\mu\text{g/s}$ )
1.0	<sup>1</sup> t=0: 1.0 <sup>2</sup> t=5 s: 1.54 <sup>3</sup> %Change: 35%	45.4 23.2 -49%	22.8 16.3 -28%	95.0 48.3 -49%	31.7 48.3 35%
2.0	t=0: 1.0 t=5 s: 1.2 %Change: 16%	45.4 35.7 -21%	22.8 20.7 -9.3%	95.0 75.0 -21%	63.3 75.0 16%
3.0	t=0: 1.0 t=5 s: 1.0 %Change: 0.4%	45.4 45.2 -0.5%	22.8 22.7 -0.2%	95.0 94.5 -0.5%	94.7 95.0 0.4%
4.0	t=0: 1.0 t=5 s: 0.88 %Change: -12%	45.4 53.1 14%	22.8 24.0 5%	95.0 111.7 14%	126.7 111.7 -12%

<sup>1</sup>The data presented in this row are the flow parameters at time t=0, the point at which the outlet vent is closed and the valve is started pulsing.

<sup>2</sup>The data presented in this row are the flow parameters at time t=5 s, the point at which it is assumed the system has reached steady-state flow .

<sup>3</sup>The data presented in this row are the percent change in each of the flow parameters from time t=0 to time t=5 s.

<sup>4</sup>The mass flow through the nozzle is the average flow, i.e., the continuous mass flow rate times the valve duty cycle.

calculations are plotted in Figure III.16. It is clear that  $P_0$ ,  $u_0$ , and  $\bar{u}$  are influenced by the pulsed nature of the nozzle as demonstrated by the oscillations of each of these variables with time. These oscillations directly follow the valve pulses: *i.e.*, when the valve opens,  $u_0$  and  $\bar{u}$  immediately increase, and  $P_0$  decreases for the duration of the 2-ms valve pulse. When the valve closes each of these parameters relax for the remaining 198 ms of the duty cycle until the valve opens again. Since the oscillations arise directly from the pulsed nature of the valve, and since the flow parameters change rapidly during the time the valve is open, longer pulse widths would be expected to increase the oscillation amplitude. This is seen to be true when similar data for a 3-ms valve pulse width are examined. These data are shown in Figure III.17, and the data for the 2- and 3-ms pulse widths are compared in Table III.8. The average value of the peak-to-peak oscillations of  $P_0$ ,  $u_0$ , and  $\bar{u}$ , are listed in Table III.8, along with the peak-to-peak differences in their value (the amplitude of the oscillations), and the relative percent change in the value of the parameter over the oscillation. It can be seen from these data that the amplitudes of the oscillations in the flow parameters are indeed greater for the 3-ms pulse than for the 2-ms pulse.

Since it is desirable to maintain the average linear carrier gas velocity at its optimum value to ensure the highest separation efficiency, large oscillations in  $\bar{u}$  are undesirable. This would seem to suggest that short pulse widths should be used. Very short pulse widths, however, decrease  $\bar{u}$  to low values that might also degrade separation efficiency, and thus are also undesirable. Consequently, a valve pulse width must be selected that is long enough to provide reasonable average values of  $\bar{u}$ , but not so long that the oscillations becomes too large. In this case, although the 3-ms pulse width appears to best match the GC carrier gas flow rate, as demonstrated by the small "%Changes" listed in Table III.7, a better choice for pulse width might be 2 ms. The 2-ms pulse width produces smaller oscillations in  $\bar{u}$  while still providing reasonable linear velocities. Regardless of the choice of pulse width there

# GC-Nozzle Interface Volume Flow Characteristics

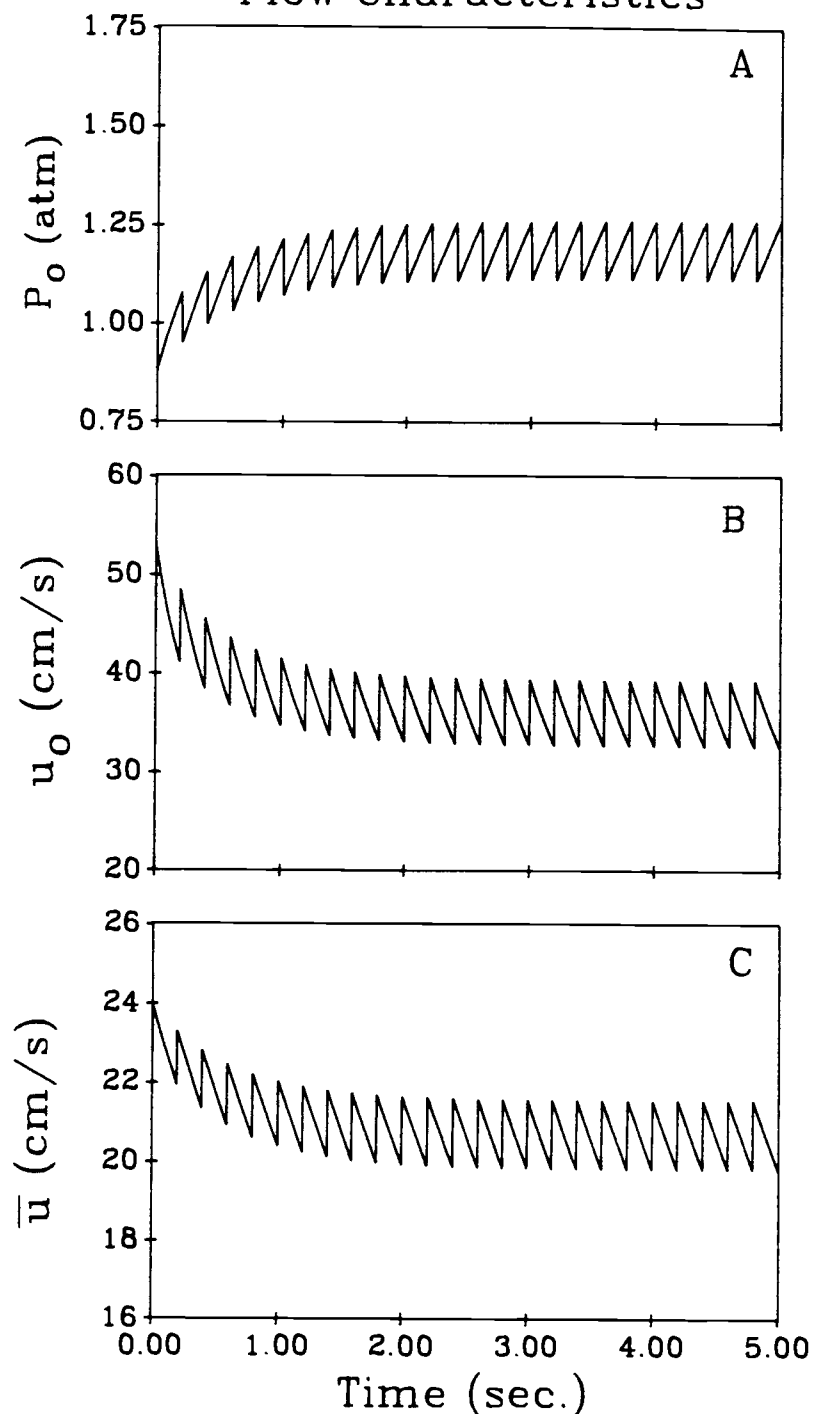


Figure III.16 Theoretical flow characteristics of the GC column and interface volume using the true mass flow of He through the nozzle,  $F_{noz}$ , with a 2-ms pulse width, and 5 Hz rep. rate. The A) interface pressure, B) carrier gas velocity at the column outlet, and C) average carrier gas velocity in the column are presented.

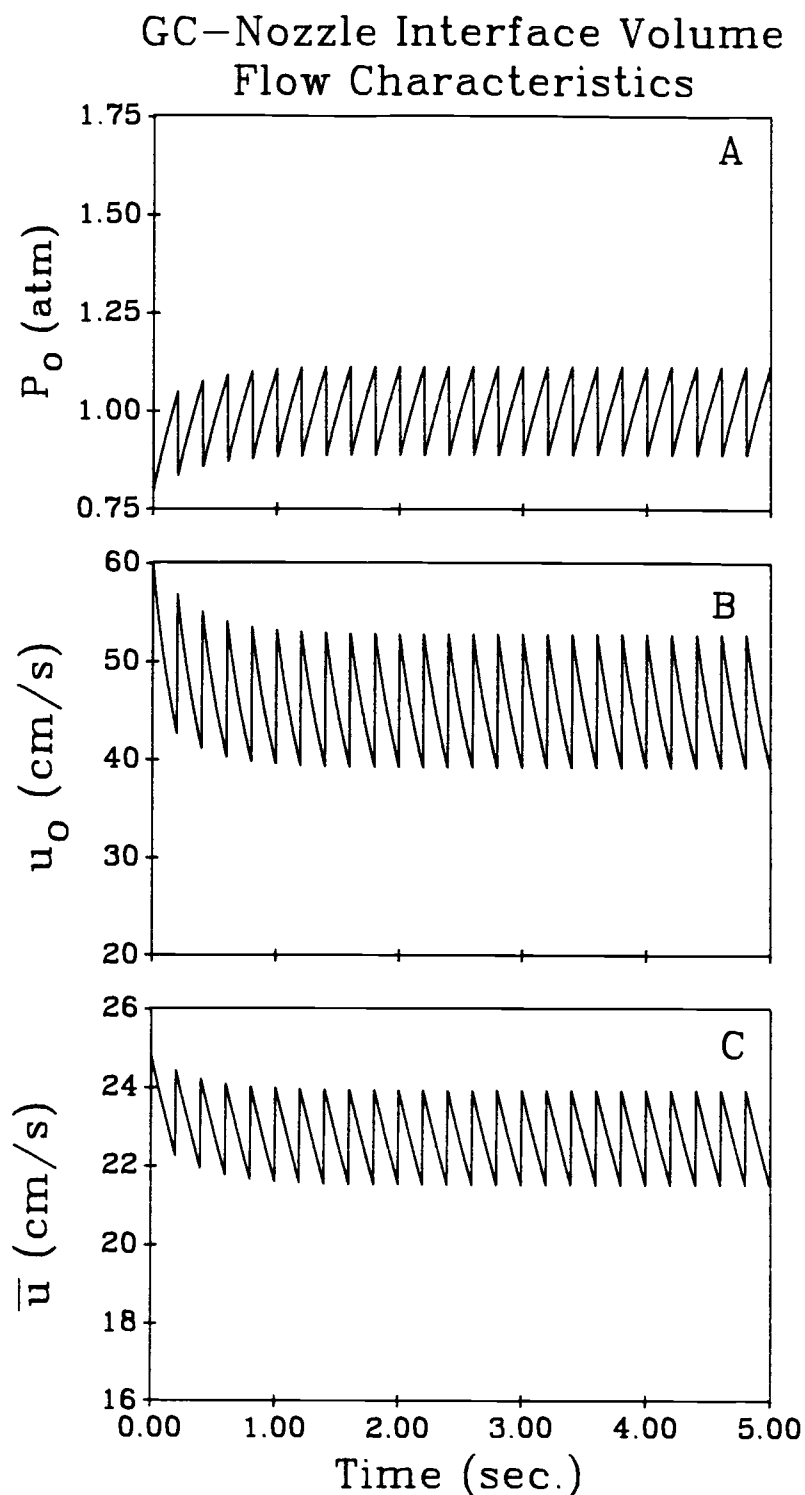


Figure III.17 Theoretical flow characteristics of the GC column and interface volume using the true mass flow of the nozzle,  $F_{noz}$ , with a 3-ms pulse width in the calculations. The (A) interface pressure,  $P_o$ , (B) carrier gas velocity at the column outlet,  $u_o$ , and (C) average carrier gas velocity  $\bar{u}$ , are presented.



Table III.8

Theoretical Flow Characteristics of the  
GC-Nozzle Interface: Oscillations of  $P_0$ ,  $u_0$ , and  $\bar{u}$   
During Nozzle Pulses

Parameter	Pulse Width	
	2 ms	3 ms
<sup>1</sup> $P_0$ (atm)	1.18	1.00
<sup>2</sup> $\Delta P_0$ (atm)	0.15	0.23
<sup>3</sup> Relative %	12.9%	23%
$u_0$ (cm/s)	36.0	46.0
$\Delta u_0$ (cm/s)	6.8	13.8
Relative %	18.8%	30%
$\bar{u}$ (cm/s)	20.7	22.7
$\Delta \bar{u}$ (cm/s)	1.8	2.5
Relative %	8.6%	11%

<sup>1</sup>The numbers in this row are the average values of each flow parameter over 1 oscillation (*i.e.*, over the 2-, or 3-ms valve pulse).

<sup>2</sup>The numbers in this row are the changes in the magnitude of each parameter over the period of time the valve is open (*i.e.*, the amplitude of 1 oscillation).

<sup>3</sup>The Relative % value is the percent change in the parameter over 1 oscillation relative to its average value.

will always be some oscillation in  $\bar{u}$ . Since separation efficiency is affected less by changes in  $\bar{u}$  when lighter gases are used as the mobile phase, helium is again a good carrier gas choice for this application.

## 2. Additional Experimental Details

Although some of the experimental conditions utilized in the chromatography experiments were presented previously in Table III.6, additional details are provided in the following sections, and in Table III.9.

### a. General Chromatography Conditions

The column used for all separations was a 6-ft x  $\frac{1}{4}$ -in o.d. x 2-mm i.d., glass column packed with 3% SP-2250 stationary phase on 100/120 mesh Supelcoport solid support (Supelco Inc., Bellefonte, PA). The carrier gas was Airco grade 4.5, 99.995 % pure helium (Airco, Vancouver, WA), maintained at an inlet pressure of 40 psi. The carrier gas flow rate was set to 30 mL/min as measured at 25 °C and 1 atm using a soap-bubble flowmeter connected to the transfer line outlet. The flow rate was measured prior to connecting the transfer line to the pulsed valve. Since a pulsed valve pulse width of 2 ms was used for all experiments, the interface pressure would be expected to be slightly higher than atmospheric pressure based on the discussions of the previous section. This means the actual flow rate would be expected to be slightly less than 30 mL/min with the GC interfaced to the pulsed valve.

The fact that the interface pressure is higher than atmospheric pressure is advantageous since leaks in the GC-valve interface can be recognized by a drop in the detector cell vacuum pressure. In the

Table III.9  
Representative Experimental Conditions  
Used in the Acquisition of Chromatographic Data

Parameter	Typical Value or Range
Carrier Gas	Helium
P <sub>i</sub> , Inlet Pressure	40 psig
L, Column Length	6 feet
Packing Material	3% SP-2250 on 100/120 Supelcoport
Temperature Program	100°C/0 min-250°C/16 min @16°C/min
Injection Port Temperature	300°C
Transfer Line Temperature	300°C
Carrier Gas Volumetric Flow	30 mL/min
Rate at STP	
Injection Volume	0.1 - 2 $\mu$ L
Valve Pulse Width	2 ms
Nozzle Flange Temperature	145°C
PMT Voltage	-725 V
Delay 2B	3.4
Delay 4A	1.3
X: Nozzle-Beam Distance	1 mm
Acquisition Delay	5 to 8 minutes
Length of Analysis	12 min
Pulses Averaged per Datum	5

absence of leaks, with the GC column at 100°C, and with the valve pulsing continuously at 5 Hz with 2-ms pulse widths, the vacuum pump was able to maintain a consistent detector cell pressure of 80 mTorr. If a leak was present in the fittings connecting the GC to the valve, the interface pressure was reduced, less gas entered the detector cell, and the detector cell pressure dropped to 65 to 70 mTorr, depending on the size of the leak.

The temperature program used for the GC separations typically consisted of an initial temperature of 100 °C with no initial wait, followed by a linear ramp at 16 °C/min to a final temperature of 250 °C which was held for 10 to 30 minutes (shorthand: 100/0-250/10 @16). It should be noted that the detector cell vacuum chamber pressure decreases from 80 mTorr with the GC oven at 100 °C, to 60 mTorr with the oven at 250 °C. This observation is consistent with the decrease in carrier gas flow rate that occurs when the carrier gas viscosity is increased due to an increase in the column temperature. Finally, the injection port and transfer line were maintained at 300°C, while the pulsed nozzle flange was maintained at 145°C.

#### b. Pulsed Valve Dead Volume

An important characteristic of any chromatographic detector is the dead volume. In order to maintain the highest chromatographic resolution possible, the total unpacked volume through which the carrier gas flows must be minimized. Thus, any tube fitting, transfer line, or even detector design that adds significantly to the overall volume of the system is undesirable and should be removed by redesign. In the case of this detector, the pulsed valve is one such source of dead volume. The dead volume of the Bosch fuel injector in the configuration normally used is approximately 600  $\mu\text{L}$ . Fortunately, 400  $\mu\text{L}$  of this volume is due to the 0.6-cm i.d. x 1.5-cm long connecting tube at the rear of the valve. In order to reduce

this dead volume, a teflon insert was constructed to slide inside the connecting tube. The insert has a 0.25-cm hole drilled down its center and is slightly longer than the connecting tube so that it extends into, and butts against the inside of the reducing union that connects the transfer line to the valve. This, in turn, reduces the dead volume of the reducing union fitting. The insert reduces the valve dead volume from 400  $\mu\text{L}$  to approximately 100  $\mu\text{L}$ , which is still large for capillary chromatography, but is acceptable for packed-column chromatography.

#### c. Additional Gas Chromatograph Details

Although the GC itself was described in the instrumental section of this thesis, a few additional details are worth mentioning. First, because the response of the fluorescence system is sensitive to any vibrations of the detector cell due to vibration of the laser beam-supersonic expansion intersection, and since the GC is connected directly to the cell, vibrations of the GC due to the oven fan had to be considered as a source of noise. These vibrations were reduced by placing a 40-pound lead ingot on top of the GC, while a smaller lead ingot was placed directly above the transfer line. In addition, when the GC was attached to the pulsed valve, care was taken to align the GC so that coupling of vibrations through the transfer line to the detector were minimized. This was accomplished by physically feeling the detector cell vibrations while orienting the position of the GC. Even with these precautions, vibrations due to the GC fan are still a major component of the signal noise.

#### d. Preparation and Storage of Standard Solutions

Standard solutions of fluorene and 1-methylfluorene were

prepared from the solid reagent in acid-washed class A volumetric flasks using pesticide-grade dichloromethane as a solvent. Solutions containing 100  $\mu\text{g/mL}$  FL, 100  $\mu\text{g/mL}$  IMF, and a mixture of 100  $\mu\text{g/mL}$  FL+IMF were prepared from stock solutions of 1000  $\mu\text{g/mL}$  FL and 1000  $\mu\text{g/mL}$  IMF. A 2-mL portion of each of these solutions was then decanted into smaller vials with Teflon-lined, gas-tight, rubber-lined screw caps. Liquid levels in these vials were marked with indelible ink to monitor evaporation of the solvent. In order to minimize evaporation and sample degradation, all standard solutions were stored in a dark refrigerator. In addition, all volumetric flask stopper joints and vial screw caps were sealed with multiple wraps of Teflon tape.

Standard solutions were injected onto the GC column using a 10- $\mu\text{L}$  syringe with 0.1- $\mu\text{L}$  graduations (Model 701-N, Hamilton Co., Reno, NV). All injections were made using the "solvent-wash" method, and the syringe was rinsed with multiple volumes of solvent both before and after an injection. Using injection volumes ranging from 0.1 to 2  $\mu\text{L}$ , along with the standard solutions described above, sample masses varying from 10 ng to 2  $\mu\text{g}$  could be injected onto the column.

#### e. Chromatographic Experimental Procedure

The BASIC program CHROM was used to acquire all chromatographic data presented in this thesis. CHROM controls all aspects of the data acquisition and also prompts the user when to open and close the GC outlet vent, when to optimize the doubling crystal position, as well as when to make an injection. The steps taken in performing a typical chromatographic analysis using this equipment and the CHROM software are outlined below.

- 1) The laser is aligned, and the fluorescence signal and laser power are optimized as described at the beginning of this thesis chapter.
- 2) CHROM starts the valve pulsing continuously and prompts the user to close the GC vent. This should be done several minutes before the injection of sample to ensure the column has reached steady-state flow conditions.
- 3) The desired temperature program is set-up on the GC using the oven temperature control slide switches, and the "Cycle to Temp 1" button is depressed to initialize the program. Pressing this button also aborts any previous program and recycles the oven temperature to the initial set-point temperature.
- 4) When the oven temperature drops several degrees below the initial setpoint, the compressed-air actuated oven door automatically closes and the oven heater turns on. The status of the oven heater is monitored by viewing a small indicator light on the front of the GC. Sample injection should only be made when the oven indicator light is flickering steadily. In all cases, the GC oven temperature controller overshoots the initial set point after the oven door first closes. Thus, the user must wait for the oven temperature to drop below, and then return to the set point. When the oven temperature is correctly maintained at the initial temperature, a small "Ready" light is illuminated, indicating that the temperature program can be started. When this light is off, the oven temperature programmer will not respond to attempts to start the program.
- 5) When the "Ready" light is on and the oven heater light is flickering steadily, the desired sample volume is drawn

into the syringe, and the CHROM injection delay is started. At the end of the delay, when the last block disappears from the computer screen, the sample is injected, and the "Start" button on the GC is simultaneously depressed to start the oven temperature program.

- 6) After acquisition of the chromatogram, CHROM prompts the user to open the GC outlet vent, after which the valve ceases to pulse. The GC oven, presumably at the final temperature of the program, is returned to the initial temperature by depressing the "Cycle to Temp 1" button on the oven temperature programmer, and another analysis can be performed.

Experience has shown that most of the problems with the instrumentation arise from one of three sources. Poor detector sensitivity can most often be traced to improper setting of the excitation wavelength or alignment of the beam with the supersonic expansion. Long retention times and loss of chromatographic resolution, which also degrade detection sensitivity, are most often due to a leak in the chromatographic system. During many of the earlier studies, leaks occurred most often at the Teflon ferrule that seals the transfer line fitting to the pulsed valve. To eliminate this problem the Teflon ferrule was eventually replaced with a permanent stainless steel ferrule set. Unfortunately, stainless steel ferrules attach the fitting permanently to the valve. Consequently, it is recommended that graphite or Vespel ferrules be acquired and used in the future. Leaks can also occur when the injection port septum has been used for too many injections. To minimize this possibility, the septum was replaced after every ten injections and care was taken not to over-tighten the septum retainer.



### 3. Preliminary Discussion of Chromatographic Results

With the previous discussions in mind it is worthwhile examining representative fluorescence-excitation chromatograms of fluorene and 1-methylfluorene. Such chromatograms are presented in Figure III.18. Data was only acquired over the period of time that the analyte was expected to elute in order to save laser shots. The main points to notice concerning these peaks are, first, the peak shapes are quite acceptable: the fluorene peak is 10.2 s wide (FWHM), while the 1-methylfluorene peak is 12.6 s wide. The peak tailing that is observed is due to the low temperature at which the pulsed valve must be kept (145°C) due to internal plastic parts. Since the valve is maintained at temperatures well below the boiling point of the analyte, some of the sample will condense onto the valve as the peak passes through. The material that condenses will be more slowly removed than the material that passes directly through, resulting in a tail on the peak. The only way to eliminate this problem would be to follow Ishibashi's suggestion [61], and disassemble the commercial Bosch valve, replacing all plastic parts with Teflon, and all silicone O-rings with similar Viton parts. This procedure was not attempted as a part of this project since it would have required the valve to be redesigned and reconstructed, but is highly recommended if the project is continued in the future.

A second, related point to make concerning the chromatograms in Figure III.18 is that the background signal of the 1MF peak is substantially higher than that of the FL peak. At the time these chromatograms were acquired, the valve had been used for several months in the 1MF continuous sample introduction experiments, and thus, a substantial amount of 1MF had condensed out on the inside of the valve. The background signal arises from the condensed 1MF slowly revaporizing during the chromatographic analysis. Although in theory this background signal is undesirable, in practice it was

## Fluorescence Excitation Chromatogram

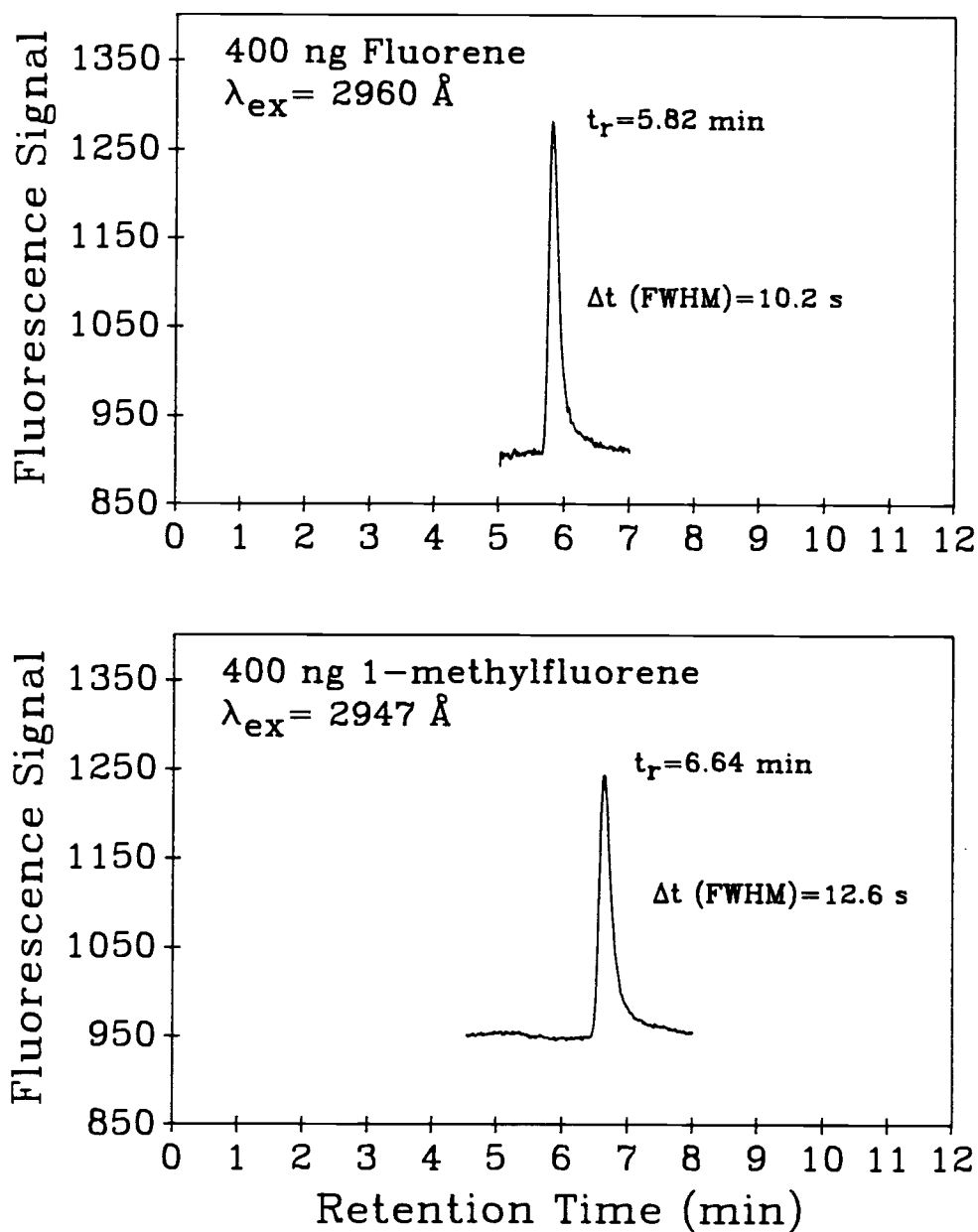


Figure III.18 Fluorescence excitation chromatograms produced by 0.4- $\mu\text{L}$  injections of 1000  $\mu\text{g/mL}$  solutions of fluorene and 1-methylfluorene. The temperature program used was, 100°C to 250°C at 32°C/min.

actually quite useful as a signal that could be monitored to align the laser beam with the expansion. In spite of this usefulness, however, it was decided that this source of background signal, and related background noise should be eliminated. Since previous attempts at cleaning the valve had proved ineffective, the main body of the valve was replaced with a new valve that had never been exposed to a sample. The same plunger, washer, and nozzle tip, however, were washed, and used in the new valve body. This procedure substantially reduced the background signal for IMF. In addition, since changing the valve, the background signal has not increased significantly. This means that during the elution of a chromatographic peak through the valve, in spite of the observed tailing, additional analyte is not permanently condensed inside the valve.

#### 4. Detector Figures-of-Merit

In order to allow comparison of this system to other similar configurations, figures-of-merit such as the limit-of-detection (LOD), are usually cited. However, it should be realized, especially in an instrumental configuration such as this, that the LOD is really a day-to-day proposition that depends on optical alignment, laser power, electrical noise present in the laboratory, and a number of other factors. Thus, because of these variables and the statistical uncertainty associated with determining the background noise level, the LOD should only be used as a rough guideline to evaluate instrument performance and should be considered accurate to only an order of magnitude.

In order to calculate the detection limit, a calibration curve must first be constructed in order to obtain the calibration slope. Three injections each of volumes containing 20, 40, 60, 80, 100, and 200 ng of IMF were made, and the area under each of the resulting peaks was calculated using the program REPLOT. Representative

fluorescence excitation chromatograms for each mass injected are presented in Figure III.19. Because there can be uncertainty in placing the integration baseline due to baseline noise, the area under each peak was calculated three separate times. The resulting calibration plot can be found in Figure III.20. Each point in this plot is thus the average of nine area-concentration measurements taken from three replicate injections, each with three replicate area measurements. The error bars represent the 99% confidence interval calculated from the nine area measurements. A linear regression was then performed on these data and the slope of the resulting best-fit line is  $24.4 \pm 0.7$  area units/ng (95% confidence interval).

The equation used to calculate the area LOD is,

$$\text{LOD} = 3 \cdot \sigma_{bk} \cdot \Delta t / S \quad (\text{III.13})$$

where  $\sigma_{bk}$  is standard deviation of the background signal in fluorescence units,  $\Delta t$  is the estimated width (FWHM) of the chromatographic peak at the detection limit in seconds, and  $S$  is the slope of the calibration curve in fluorescence units  $\cdot$  seconds.  $\sigma_{bk}$ , and  $\Delta t$  were estimated from a 20-ng IMF chromatogram to be 2.3 fluorescence units, and 20 seconds, respectively. The resulting LOD is 6 ng.

Compared to the LODs reported by other investigators, as presented previously in Table I.7, it can be seen that a LOD of 6 ng is competitive. In addition, improvements in the LOD are surely attainable. If equation III.13 is examined, it is clear that the detection limit decreases with a decrease the background noise,  $\sigma_{bk}$  and peak width,  $\Delta t$ , and with an increase in the calibration slope,  $S$ . The background noise,  $\sigma_{bk}$ , could be reduced by better vibration isolation of the detector cell from the GC fan and the vacuum pump. This might be accomplished by removing the GC from the cart it is currently mounted on, which rolls on castors, and securing it more firmly to the laboratory floor. It might also be necessary to dynamically balance the fan or completely remove the fan motor from the GC and make the connection to the fan spindle through a flexible

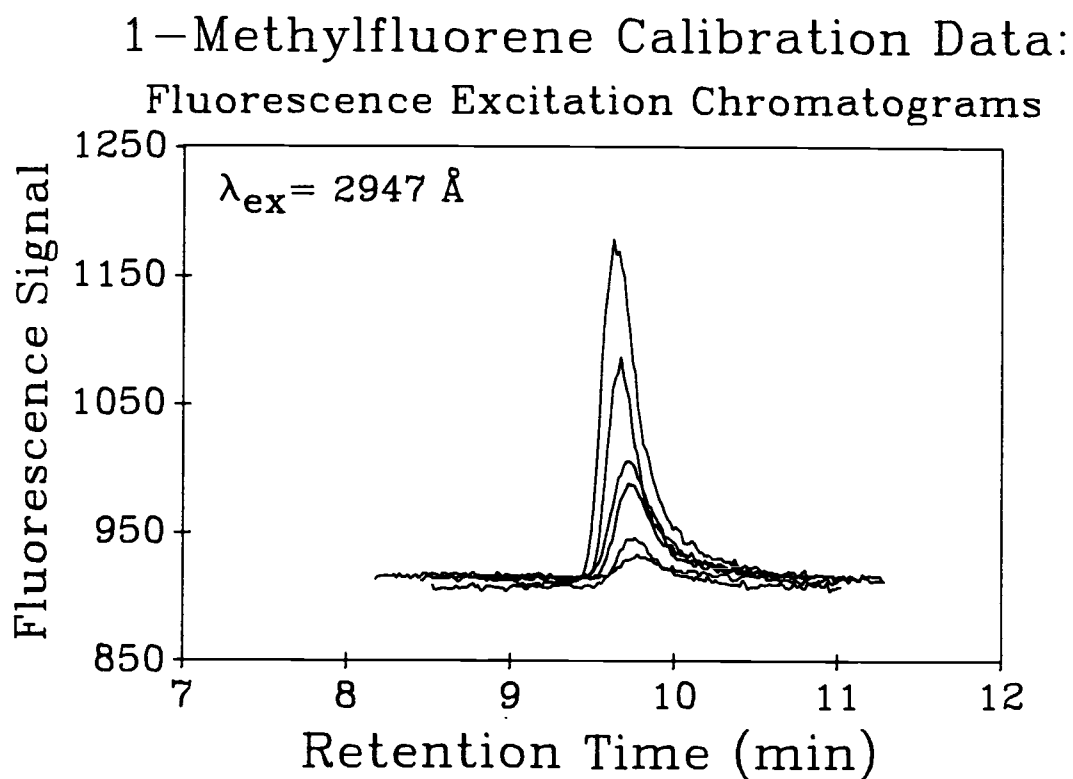


Figure III.19 Representative fluorescence excitation chromatograms used in the preparation of the 1-methylfluorene calibration plot. These chromatograms were produced by injections of 20, 40, 60, 80, 100, and 200 ng 1MF, using a temperature program of 100°C/0 min-250°C/16 min @16°C/min.

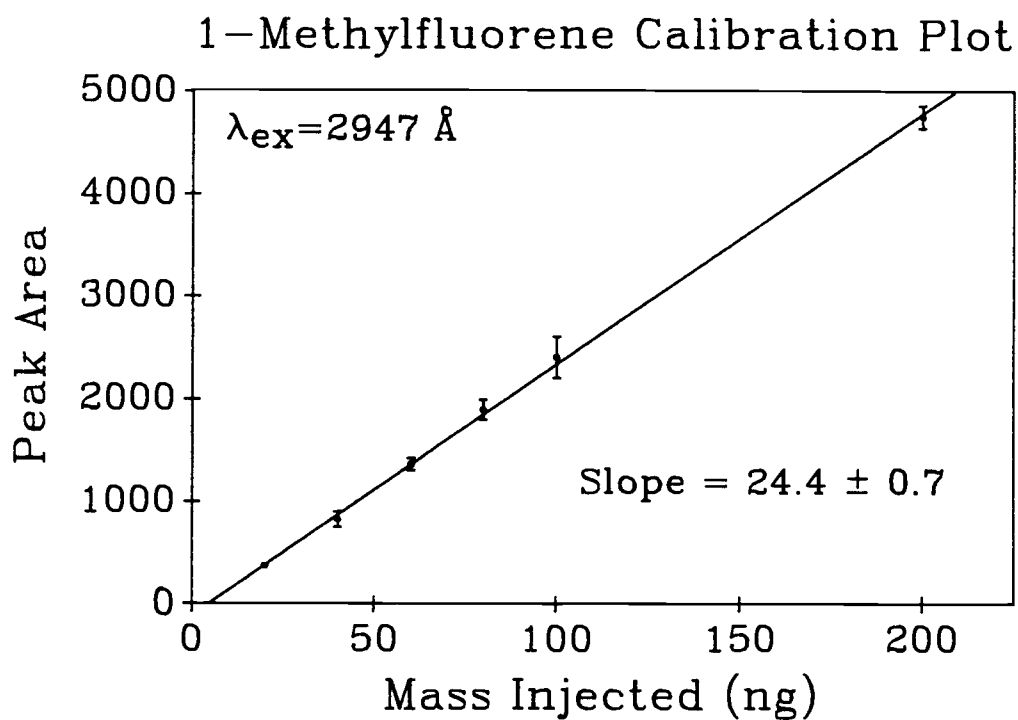


Figure III.20 Calibration plot of 1-methylfluorene. Error bars represent the 99% confidence interval arising from the average of 9 area measurements for each of the masses injected.

coupling. The peak width,  $\Delta t$ , could be decreased by eliminating cold trapping of the analyte in the valve, and thus, peak tailing. In addition, further optimization of the carrier gas flow rate might also improve chromatographic resolution and decrease peak widths. Finally, since the fluorescence signal is proportional to the power of the optical source in the absence of optical saturation, it would be possible (but not practical) to increase the calibration slope through the use of a more powerful laser.

## 5. Detector Selectivity

Detection limits as calculated in the previous section using standard solutions are useful guidelines in comparing instrument performance. When real, complex samples are analyzed, however, these detection limits may lose some of their relevance due to the large number of sample components that could potentially interfere with the quantitative determination of the analyte. If the components of the sample are unable to be resolved chromatographically, then a selective detector that responds only to the analyte or other closely related compounds, can dramatically reduce interferences. Thus, selectivity is an important consideration when examining a new GC detector. It should be noted that although selectivity is often a desirable trait, high selectivity also limits the number of different kinds of compounds that can be detected. In the case of this project, the selectivity of fluorescence detectors for PNAs is considered an advantage due to the very complex matrices in which they are usually found.

The selectivity of this system has already been demonstrated in a previous section (*i.e.*, Figure III.7). It is worthwhile, however, examining the selectivity further in terms of the chromatographic application. Figure III.21 contains the fluorescence excitation chromatograms arising from the injection of a mixture of

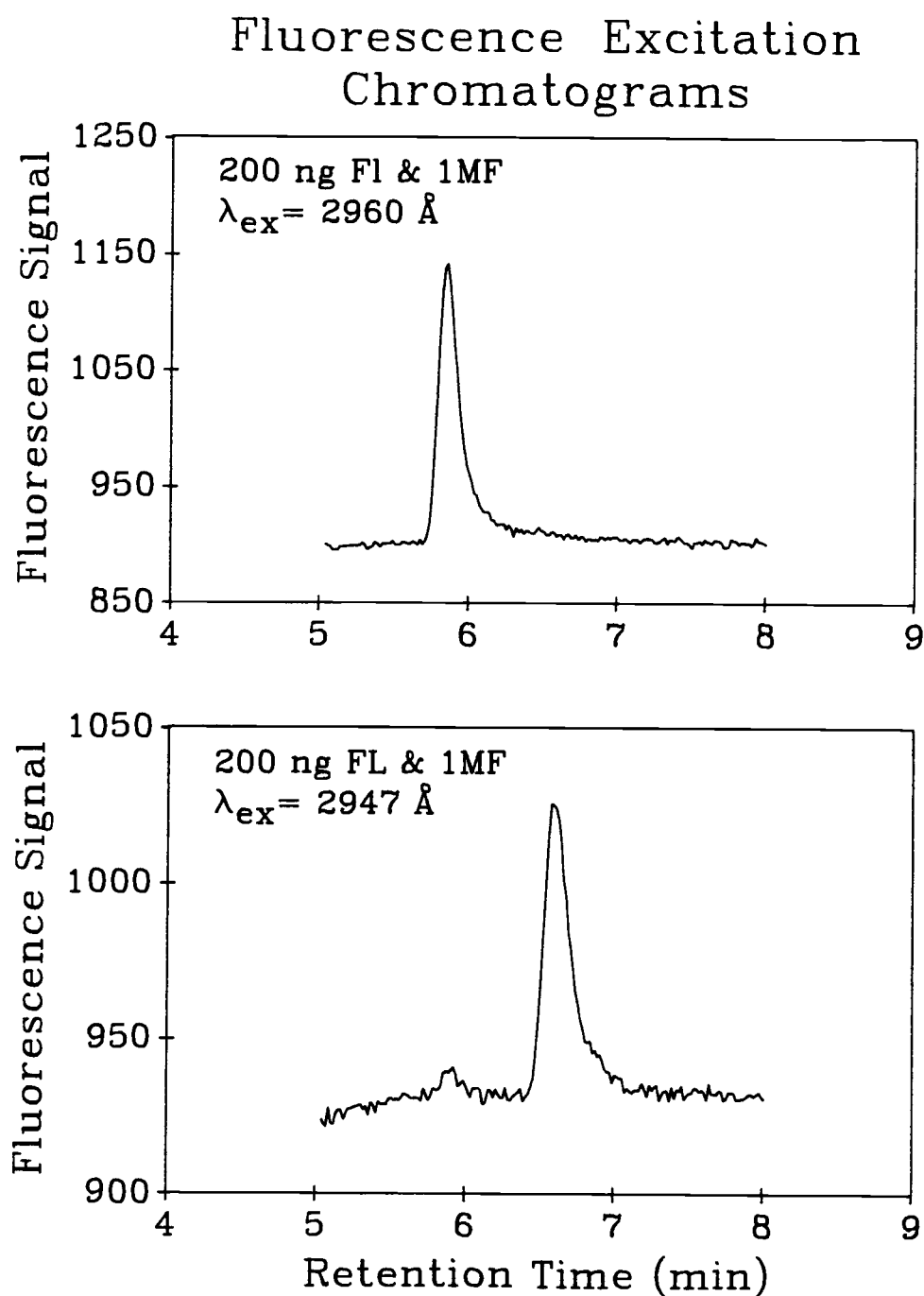


Figure III.21 Fluorescence excitation chromatograms of a mixture of 200 ng each of fluorene and 1-methylfluorene using two different excitation wavelengths.



200 ng each of fluorene and 1-methylfluorene at two different excitation wavelengths. When the excitation wavelength is set to the 2960-Å fluorene transition, only the peak due to fluorene is present in the chromatogram. Similarly, when the excitation wavelength is set to the 2947-Å transition of IMF, the peak due to IMF is the major peak in the chromatogram. In this case, however, it can be seen that fluorene does seem to respond somewhat at 2947 Å as demonstrated by the very small peak occurring in the IMF chromatogram at the fluorene retention time. The response of fluorene upon excitation at 2947 Å can be explained by examining the small spectral peak that occurs near 2947 Å in any of the pure fluorene spectra found in Figures III.5-III.6.

Further demonstration of the selectivity of this system can be accomplished by examining its response (actually the lack of response) to the injection of a complex, PNA-containing sample. An extract of a Columbia River sediment sample was obtained from Dr. Fred Prahl of the Department of Oceanography at Oregon State University. This extract had previously been analyzed, and the PNAs identified and quantitated [105]. The sample consists of approximately 100 components, including PNAs ranging in size from anthracene (3 rings) to much larger, 6-ring species. Sample constituents are present in the extract at concentrations ranging from 1 to 20 ng/μL. It should be noted that, although this sample contains a variety of PNAs, fluorene and 1-methylfluorene were not detected in the original analysis. Figure III.22 shows the fluorescence excitation chromatograms produced by 2-μL injections of this sample with the excitation wavelength set to 2947 and 2960 Å. The top two chromatograms were produced by injections of the sediment extract alone, while the bottom chromatogram consists of a co-injection of 40 ng of the IMF standard, and 2 μL of the sediment extract. It is clear that no fluorene or IMF is present in the sample at detectable concentration levels, and none of the other constituents present respond to the detector over the range acquired. Thus, it is clear that with proper choice of excitation wavelength, this system can provide excellent selectivity for the

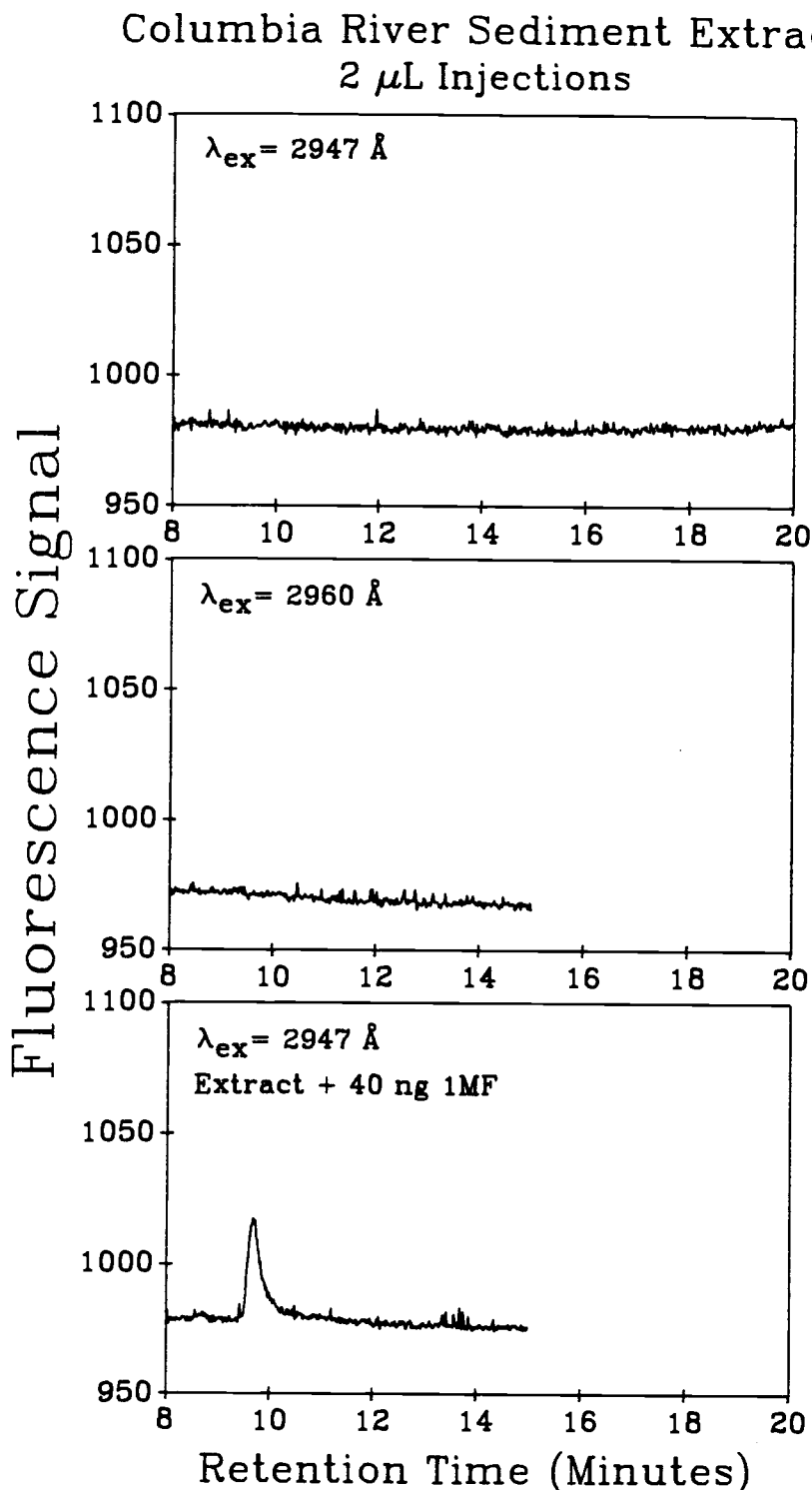


Figure III.22 Fluorescence excitation chromatograms of 2- $\mu$ L injections of a Columbia River sediment extract at the excitation wavelengths of FL and 1MF. The bottom chromatogram includes a co-injection of 40 ng of a 1MF standard.

analysis of individual PNAs. Unfortunately, because fluorene and 1MF are not present in this sample, no actual quantitative analysis could be performed.

In order to illustrate the response of this system to analytes present in a complex environmental matrix, another "real" sample was acquired from Orest Kawka of the Department of Oceanography at Oregon State University. This second sample is a hydrothermal oil extract taken from a deep-ocean hydrothermal vent in the Guyamas Basin of the Gulf of California. The extract had been analyzed previously by GC and GC-MS and was determined to be very complex, containing a variety of both methylated and parent PNAs including both fluorene and four methylfluorene isomers [106]. The fluorescence excitation chromatograms resulting from 2  $\mu$ L injections of this sample, acquired using excitation wavelengths of 2960 and 2947 Å are shown in Figure III.23. Significant response is observed at both excitation wavelengths indicating the presence of fluorene and 1MF in the sample.

Because both fluorene and 1MF are present in the sample, the external standard method had to be used for quantitation. The reasons for, and problems imposed by this limitation will be discussed in the next section. The results of this quantitative analysis are presented in Table III.10 with analyte amounts listed as the total mass of analyte present in the 7.5-mL sample. This table also lists the results of the quantitative analysis performed by Orest Kawka using GC-MS with internal standard quantitation. Although the values obtained for fluorene by the two methods agree fairly well (within 20%), the 1-methylfluorene results compare less favorably. This discrepancy might be due to the fact that 1- and 2-methylfluorene are unresolved chromatographically even by the high resolution capillary chromatography used in the GC-MS analysis. If there was also significant spectral overlap of the 1- and 2-methylfluorene fluorescence excitation spectra at 2947 Å, the chromatographic peak resulting from the unresolved components would be greater than that produced by either component alone. This problem could be solved by acquiring a fluorescence excitation

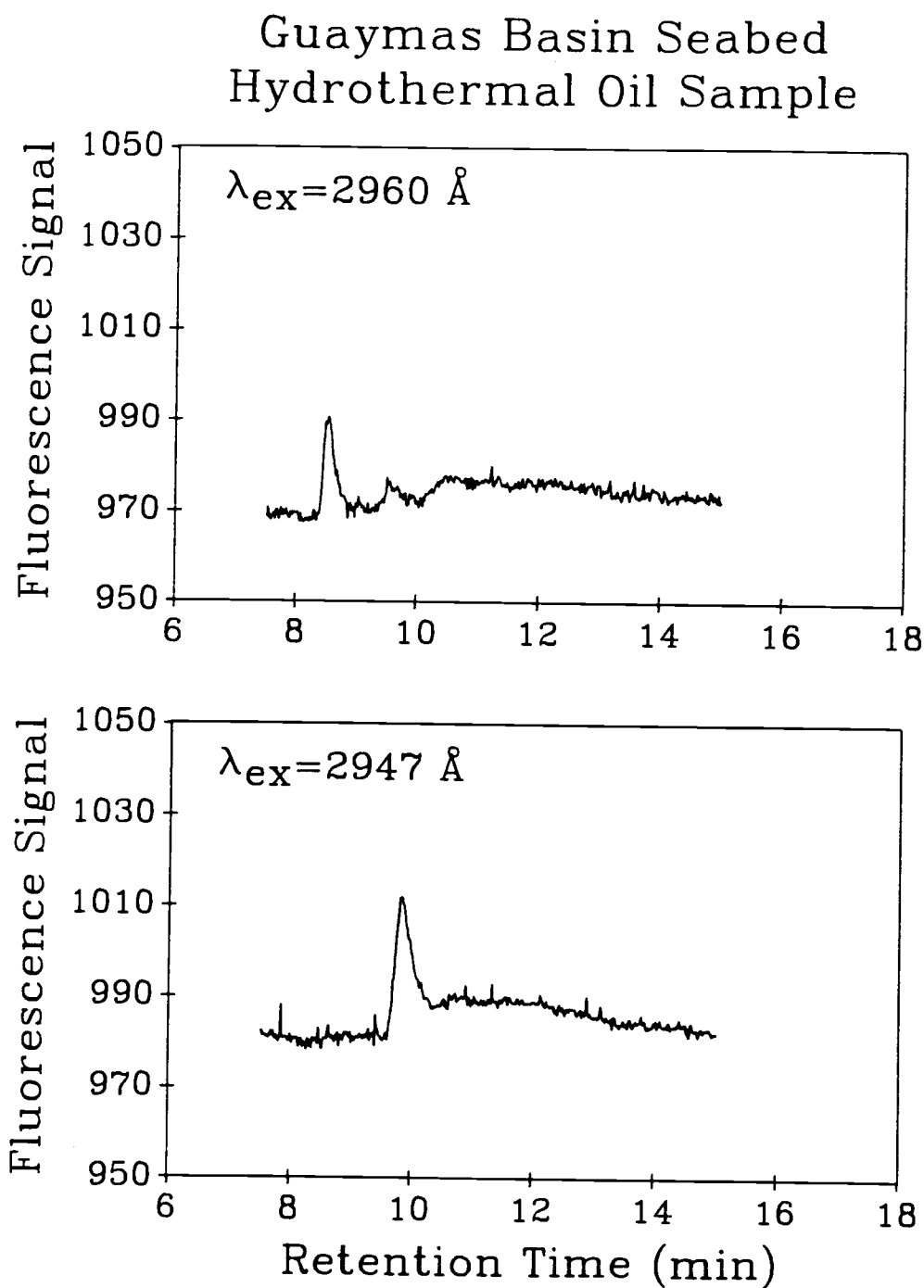


Figure III.23 Fluorescence excitation chromatograms resulting from 2- $\mu$ L injections of a hydrothermal oil sample taken from the Guaymas Basin seabed in the Gulf of California.

Table III.10  
Quantitative Analysis of Guyamas Basin  
Hydrothermal Oil Sample

Analyte <sup>1</sup>	Total Mass <sup>2</sup> via GC-MS ( $\mu\text{g}$ )	Total Mass <sup>3</sup> via Supersonic Jet Fluorescence ( $\mu\text{g}$ )
Fluorene and Substituted Fluorene		
Fluorene	13.2	16
1-MF	12.4	20
2-MF	12.0	
3-MF	25.3	
4-MF	12.0	
Other PNAs		
Phenanthrene	64.1	
Anthracene	14.4	
Fluoranthene	15.4	
Pyrene	78.2	
Benzo[e]pyrene	47.5	
Benzo[a]pyrene	31.1	
Perylene	12.2	
Benzo[ghi]perylene	69.2	
Coronene	38.2	

<sup>1</sup>This is a partial list of the analytes determined by Orest Kawka [106].

<sup>2</sup>Total mass of the analyte present in the 7.5 mL sample as determined by GC-MS [106] using internal standard quantitation with  $\text{d}_{10}$ -anthracene and 4-Bromobiphenyl used as internal standards.

<sup>3</sup>Total mass of analyte present in the 7.5 mL sample as determined by supersonic-jet fluorescence detection using external standard quantitation.

spectrum of 2-methylfluorene and choosing a 1-methylfluorene excitation wavelength that is well resolved from any 2MF transitions.

## 6. Programmed-Wavelength Fluorescence Excitation Chromatograms

The excellent selectivity demonstrated by this system is, in most cases, highly advantageous. In certain situations, however, this selectivity can be "too much of a good thing". This is particularly true when one considers the requirements for performing an accurate quantitative analysis. With the excitation wavelength fixed for the full duration of the chromatogram, as was the case in the studies presented above, only a single analyte is likely to respond significantly. This means that quantitation must necessarily be performed through the use of an external standard evaluated in a subsequent injection. Because detector response and chromatography conditions can change from run to run, and since the sample mass injected can also vary due to irreproducibilities in the injection technique, external standard quantitation is not recommended if high accuracy and precision are required in a quantitative analysis.

The method most commonly used for accurate quantitative analysis in chromatographic applications is the internal standard method [107]. In this case, a standard reference substance is selected that is similar to the analyte, but is not present in the sample and is completely resolved from the analyte upon chromatographic separation. For instance, 1-methylfluorene might be used as an internal standard for the determination of fluorene in a sample containing no 1MF. An accurately known mass of this "internal standard" is then added to the sample solution so that it is present at a concentration similar to that of the analyte. Next, a standard solution containing known concentrations of both the analyte and the internal standard is injected and a separation performed. From the

resulting chromatogram a response factor (RF) can be calculated that is used to compensate for differences in the detector response to the analyte and the internal standard:

$$\frac{A_a}{C_a} = RF \cdot \frac{A_{IS}}{C_{IS}} \quad (\text{III.14})$$

where  $A_a$  and  $C_a$  are the peak area and concentration of the analyte, respectively, and  $A_{IS}$  and  $C_{IS}$  are the peak area and concentration of the internal standard, respectively. Once the RF has been calculated using the data from the standard solution, the unknown concentration of the analyte in the sample can be determined using the known peak area and concentration of the internal standard in the sample, and the peak area of the analyte, along with RF and equation III.14. Since the internal standard and analyte experience the same injection and chromatography conditions, quantitative precision is improved.

The use of this method requires two additional assumptions: that the analyte and internal standard both show significant detector response, and that the response factor does not change between successive runs. In the case of many conventional detectors, these conditions may be assumed to be true without a great deal of further consideration. With the system developed in this project, however, these concerns are non-trivial. In order to perform an internal standard quantitation using this instrumentation, while taking advantage of the full response of the detector for both components, the excitation wavelength must be changed during the course of the separation. This means that the birefringent filter and doubling crystal stepper motors must be rapidly scanned from one excitation wavelength to the the other during the period between elution of each of the substances. In the case of FL and IMF, this means the excitation wavelength must be scanned from 2960 to 2947 Å (approximately 400 birefringent filter steps) during the short, 20 second period of time between the end of the tail of the FL peak and the beginning of the IMF peak. In addition, this wavelength scan

must be reproducible since any variation in positioning the peak wavelength or doubling crystal will be reflected in a change in signal intensity thus, a change in the response factor.

If the birefringent filter were the only wavelength tuning element that had to be scanned between chromatographic peaks, the situation would be fairly straightforward. Unfortunately, the doubling crystal must also be scanned. As discussed in a previous section, the doubling crystal micrometer is subject to hysteresis problems when it is scanned in opposite directions. To compensate for this problem, whenever the doubling crystal is scanned to lower counter values (lower wavelengths), it is scanned 200 stepper motor steps beyond the desired position and then is stepped back in the positive direction. This procedure is necessary, but adds extra overhead to the time required to scan between excitation wavelengths.

A comparison of the fluorescence excitation chromatograms of a mixture of 100 ng of FL and IMF acquired with fixed excitation wavelengths and with programmed excitation wavelength changes can be found in Figure III.24. It is worth noting that the wavelength scan required in this situation is the worst case circumstance; the excitation transition of the first substance to elute is at a longer wavelength than the transition of substance that elutes at the longer retention time. This means that the doubling crystal must be scanned in the negative direction, and thus hysteresis must be considered. Since this is the worst-case situation, it is useful in evaluating the worst-case performance of the scanning system. This evaluation was executed by making multiple injections of the FL-IMF standard solution and calculating the response factor for FL and IMF. If the bottom chromatogram in Figure III.24 is examined, it is clear that the FL peak at 2960 Å does not completely return to the baseline before the excitation wavelength is scanned. This means that peak heights rather than peak areas must be used to calculate the response factor. The peak height was calculated as the average peak signal minus the average baseline signal immediately prior to elution of the peak. The results of these measurements are listed in Table III.11.



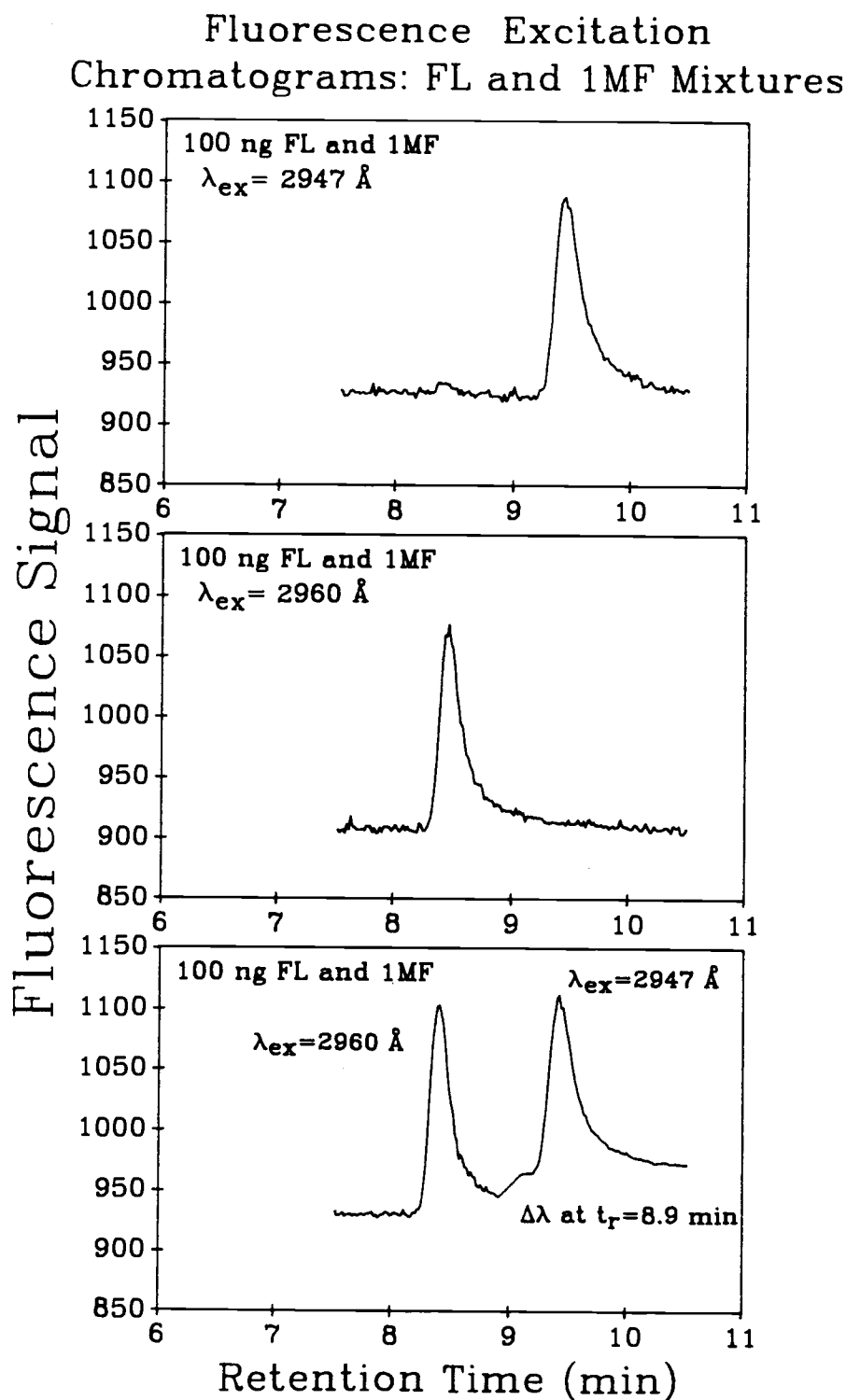


Figure III.24 Fluorescence excitation chromatograms (top and middle) of a mixture of 100 ng each of FL and 1MF, and (bottom) the chromatogram of the same mixture produced by a programmed excitation wavelength scan.



It is evident from these results that reproducible programmed-wavelength scans can be performed using this instrumentation, and that the response factor resulting from such scans remains constant, with a relative standard deviation (RSD) of less than 2%. It can also be seen that this reproducibility is only possible when the doubling crystal position is not reset between runs as demonstrated by the change in RF seen in Table III.11 when the doubling crystal was retuned to increase the laser power.

A few final points should be made concerning the selection of an internal standard for an analysis using this system. Obviously, the internal standard must be similar enough to the analyte that it will exhibit excitation transitions within a fairly narrow wavelength range from the analyte. In this case, IMF would be a good choice as an internal standard for FL as long as it is not also present in the sample. In very complex samples containing a variety of small PNAs, however, it might be difficult selecting an internal standard not present in the sample. An interesting solution to such a dilemma that has been used successfully in GC-MS analyses [108], might be to use a deuterium-labeled isomer of the analyte (*i.e.*,  $d_{10}$ -fluorene) as the internal standard. This would satisfy two of the requirements for the internal standard: the deuterium-labeled standard would not be present in the sample, and it would have spectral transitions that lie close to the analyte transitions. In addition, if there was significant overlap of the spectral transitions of the analyte and deuterium-labeled internal standard, it might be possible to perform the quantitation without scanning the excitation wavelength. The only problem that might arise is whether the chromatographic resolution of the system is great enough to separate the analyte from the labeled analyte. This proposal might prove to be an interesting topic for future studies using this system.

#### IV. Conclusion

As our knowledge regarding the impact of environmental toxicants on living organisms increases, so does the need to improve our ability to determine trace amounts of such analytes in the very complex samples in which they are often found. Although GC and GC-MS are analytical methods that have proven to be invaluable tools for such analyses, there are situations where samples are so complex that chromatographic resolution alone is insufficient to allow unambiguous determination of important analytes. In those cases, a highly selective detector can greatly simplify the situation by responding only to the analytes of interest. In addition, high selectivity can also reduce the need for time-consuming, and often expensive pretreatment of samples. The instrumental system developed in this research is an example of just such a detector. In fact, with the proper choice of excitation wavelength, detection can almost be limited to a specific PNA, with detector response due to even other closely-related PNAs highly attenuated.

The unique features of this system when compared to other combined GC-supersonic jet systems revolve around the use of the modified automobile fuel injector as a supersonic nozzle. The Bosch fuel injector has the advantages of being fairly inexpensive to procure, allows easy substitution of the nozzle tip to change orifice sizes, and is robust, being designed to operate at elevated temperatures over long periods of time in an automobile. In addition, since the duty cycle of the valve can be changed by simply altering the trigger pulse width and repetition rate, the valve can be adapted to a variety of different experimental requirements.

Ishibashi has also used a modified automobile fuel injector in a GC-supersonic jet fluorescence system [61]. However his chromatographic results were poor, with peak widths of several minutes, and no detection limits were reported. In addition, his system required a 6-inch diffusion pump backed by both a 1500-LPM

mechanical booster pump and a 300-LPM rotary pump to maintain the supersonic expansion.

It was realized during the course of this research that one of the main advantages of using a pulsed nozzle lies in reducing the need for such complicated pumping plants. Since the valve can be operated with a low duty cycle (e.g., open 1% of the time) the requirements for the vacuum system are reduced. In this project a single, low-volume 200-LPM rotary pump provided sufficient pumping power to maintain the supersonic expansion, as demonstrated by the spectral bandwidths of less than 0.1 nm that were observed in the fluorescence excitation spectra. In addition, since the mechanical pump can be operated at relatively high vacuum pressures, the mass flow rate through the nozzle can be increased, which improves detection sensitivity, as demonstrated by the detection limit of 6 ng that was calculated for IMF. This detection limit is comparable to those reported by Callis for a high-resolution capillary GC system that used a diffusion pump to maintain the supersonic expansion (see Table I.7).

In addition, although Small and Callis have demonstrated quantitative analyses with GC-supersonic expansion systems [21,23], no mention was made of the method of quantitation used, and in both cases only a single excitation wavelength was monitored during the chromatographic elution. The programmed-excitation wavelength scanning method described in this thesis allows multiple analytes to be determined in a single chromatographic elution. Thus, internal standard quantitation can be performed, thereby improving the precision of quantitative analyses.

The microcomputer control, synchronization, and data acquisition system was also unique, and performed several important functions for this project. In addition to instrument synchronization and control functions, the data acquisition system was designed to provide real-time feedback of the experimental results. This is a particularly significant function since it can save the researcher substantial amounts of wasted time. If analysis of the data is postponed until after the completion of an experiment,

problems that could otherwise have been fixed go unnoticed, and a large amount of useless data might be generated. By plotting the data as it is acquired, problems can easily be recognized and fixed, or the experiment can be aborted before completion.

Many of the drawbacks to the use of this system commercially or routinely, are common to all laser-based instruments, that is, the requirement that a tunable laser be used as the source of excitation radiation. Lasers are expensive to procure, expensive to maintain, and require a great deal of patience to operate. In the case of the CMX-4, flashlamps have a useful lifetime of 600,000 shots, which at a repetition rate of 5 Hz, is only 33 hours, or 4, 8-hour days of continuous operation. When the \$200 flashlamp finally shatters, the optical cavity must be disassembled to remove all shards of glass, and to inspect the air-, and dye-flow tubes for any deposits, scratches, or cracks. After reassembling the cavity, the laser must usually be recalibrated, which requires several additional hours. Similarly, the laser dye used in this experiment, R590, which has a relatively long lifetime compared to many other dyes, usually requires replacing after 100,000 laser shots, which is 6 hours of continuous operation at 5 Hz. Thus, a laser such as the CMX-4 would be difficult and expensive to use in a routine manner where samples are analyzed continuously throughout the day. Until laser technology advances to the point that low-cost, reliable, tunable lasers become widely available, many powerful analytical systems such as this will remain as developmental research instruments in the laboratory, not available widely to those analytical chemists who could apply them to routine problems and utilize their important capabilities in the most effective manner.

#### A. Suggested Instrumental Improvements

As discussed above, the fuel injector must be redesigned for use at higher temperatures. Improvement of chromatographic

resolution by elimination of the peak tailing should improve detection limits. Replacement of plastic parts with a high-temperature material is recommended and in the process, redesign might also allow the interior dead volume of the valve to be reduced.

Better vibration isolation of the detector cell from the GC is also a recommended way to improve detection limits. This could be accomplished by removing the GC from the unstable cart it currently sits upon and mounting it more stably on a permanent platform that is anchored firmly to the floor. In addition, the GC fan motor, which is the source of these vibrations, could be removed from the GC itself, and a flexible coupling could be used to connect the motor to the fan.

Finally, improvements in the ability to more accurately align the laser beam with the expansion are recommended. The method used in this project was awkward; the two adjusting screws on the corner mirror located on the optical table were rotated to move the beam over the short distances required. It might be possible to place the detector cell and mounting bracket on a large X-Y translation stage attached to the optical table. The system could then be aligned by adjusting the calibrated micrometers of the translation stage, rather than the beam itself. The micrometer readings could then be recorded for easier re-alignment of the system and allow for more precise characterization of the axial properties of the expansion.

## B. Suggested Future Studies

Several additional studies are recommended to further characterize this system. First, the high-resolution fluorescence excitation spectra of additional PNAs need to be acquired to help expand the high-resolution spectral library, and to improve the applicability of the instrumentation. PNAs such as carbazole, acenaphthene, acenaphthylene, and additional substituted fluorenes should exhibit transitions in the tuning range of the laser using

R590 dye. In addition, by changing laser dyes it would be possible to examine larger PNAs such as anthracene and phenanthrene. Other interesting possibilities include the analysis of usually nonfluorescent species that have been derivitized to a fluorescent product.

Additional studies are also recommended to improve methods of quantitation when using highly selective methods of detection such as this. The most intriguing possibility is to utilize deuterated isomers of the analyte as internal standards for quantitative analyses. Several possibilities can be imagined for this configuration. If the deuterated isomer is substantially separated from the analyte by the chromatographic separation then the programmed-excitation-wavelength scanning method described in this thesis could be used to acquire the signal from both species. If, however, there is substantial overlap of the spectral transitions originating from the analyte and internal standard, there is another possibility. In this case, the excitation wavelength could be fixed to a transition maximum of the analyte for the duration of the elution, and the signal due to internal standard, arising from the spectral overlap, could easily be matched to the analyte signal by increasing the mass of internal standard added to the sample.

A final possibility might arise in the case where the internal standard is unresolved chromatographically, but well resolved spectroscopically from the analyte. Internal standard quantitation normally requires the internal standard to be completely resolved from the analyte by the separation. In this case, however, the excitation wavelength could be quickly alternated between the analyte and internal standard transitions throughout the elution. Thus, even though the analyte and internal standard were not chromatographically resolved, the signal taken at each wavelength across the chromatographic peak would be due only to the species that was alternately excited. Thus, the peak heights and areas acquired from the chromatogram, despite originating from an unresolved mixture, would still represent the concentration of the individual species, and the internal standard method could be applied.



### V. References

1. J. W. Nibler and G. V. Knighten, in "Topics in Current Physics", A. Weber, Ed., Springer, Berlin, 1979, Vol. 11, Chapter 7.
2. J. C. Travis, G. Turk and R. B. Green, Anal. Chem., **54**, 1006A (1982).
3. E. H. Piepmeier, Ed., "Analytical Applications of Lasers", Wiley, New York, 1986.
4. S. J. Hein and E. H. Piepmeier, Trends in Analytical Chemistry, **7**, 137 (1988).
5. H. Moenke, L. Moenke-Blankenburg, "Laser Micro-Spectrochemical Analysis", Crane, Russak and Co., New York, 1967.
6. N. Omenetto, Ed., "Analytical Laser Spectroscopy", Wiley, New York, 1979.
7. G. M. Hietfje, J. C. Travis and F. E. Lytle, Eds., "Lasers in Chemical Analysis", Humana Press, Clifton NJ, 1981.
8. G. M. Hietfje, American Lab., May 1983, 66.
9. B. Josefsson, in "Handbook of Polycyclic Aromatic Hydrocarbons", A. Bjørseth, Ed., Marcel Dekker, New York, 1983, Chapter 7.
10. N. T. Edwards, J. Env. Qual., **12**, 427 (1983)
11. R. E. LaFlamme and R. A. Hites, Geochim. Cosmochim. Acta, **42**, 289 (1978).
12. L. C. Thomas and A. K. Adams, Anal. Chem., **54**, 2597 (1982).
13. A. K. Adams, D. L. Van Engelen and L. C. Thomas, J. Chromatog., **303**, 341 (1984).
14. D. L. Van Engelen, A. K. Adams and L. C. Thomas, J. Chromatog., **331**, 77 (1985).
15. D. L. Van Engelen, Ph.D. Thesis, Oregon State University, Corvallis, OR (1986).
16. J. F. Lawrence, "Organic Trace Analysis by Liquid Chromatography", Academic Press, New York, 1981, Chapter 5.

17. A. T. Rhys Williams, "Fluorescence Detection in Liquid Chromatography", Perkin Elmer, Beaconsfield, Buckinghamshire, England, 1980.
18. E. L. Wehry, in "Analytical Applications of Lasers", E. H. Piepmeier, Ed., Wiley, New York, 1986, Chapter 7.
19. J. A. Warren, J. M. Hayes and G. J. Small, Anal. Chem., **54**, 138 (1982).
20. J. D. Winefordner and N. Omenetto, in "Analytical Applications of Lasers", E. H. Piepmeier, Ed., Wiley, New York, 1986, p. 40.
21. J. M. Hayes, G. J. Small, Anal. Chem., **54**, 1202 (1982).
22. A. Kantrowitz and J. Grey, Rev. Sci. Instrum., **22**, 328 and 333 (1951).
23. B. V. Pepich, J. B. Callis, D. H. Burns, M. Gouterman and D. A. Kalman, Anal. Chem., **58**, 2825 (1986).
24. S. W. Stiller and M. V. Johnston, Anal. Chem., **59**, 567 (1987).
25. B. D. Anderson and M. V. Johnston, Appl. Spectrosc., **41**, 1358 (1987).
26. P. Pott, "Chirurgical Observations" (1775), reprinted in Natl. Cancer Inst. Monogr., **10**, 7 (1963).
27. H. V. Gelboin, P.O.P. Ts'o, Eds., "Polycyclic Hydrocarbons and Cancer", Vol. 2, Academic Press, New York, 1978.
28. C. E. Searle, Ed., "Chemical Carcinogens", Vols. 1 and 2, 2nd Ed., American Chemical Society, Washington DC, 1984.
29. I. Schmeltz and D. Hoffman, in "Carcinogenesis, Vol. 1: Polynuclear Aromatic Hydrocarbons", R.I. Freudenthal and P.W. Jones, Eds., Raven Press, New York, 1976.
30. P. W. Jones and R.I. Freudenthal, Eds., "Carcinogenesis, Vol. 3: Polynuclear Aromatic Hydrocarbons", Raven Press, New York, 1978.
31. M. L. Lee, M. V. Novotny and K. D. Bartle, "Analytical Chemistry of Polycyclic Aromatic Compounds", Academic Press, New York, 1981, Appendix 5.
32. H. S. Rosenkranz and R. Mermelstein, in "Nitrated Polycyclic Aromatic Hydrocarbons", C. M. White, Ed., Huethig, New York, 1985, Chapter 6.

33. J. G. Windsor Jr. and R. A. Hites, Geochim. Cosmochim. Acta, **43**, 27 (1979).
34. M. L. Lee, M. V. Novotny and K. D. Bartle, "Analytical Chemistry of Polycyclic Aromatic Compounds", Academic Press, New York, 1981, Chapter 2.
35. R. A. Hites, R. E. Laflamme and J. W. Farrington, Science, **198**, 829 (1977).
36. R. A. Hites, R. E. Laflamme, J. G. Windsor Jr., J. W. Farrington and W. G. Deuser, Geochim. Cosmochim. Acta, **44**, 873 (1980).
37. J. A. Robbins and D. N. Edgington, Geochim. Cosmochim. Acta, **39**, 285 (1975).
38. J. G. Farmer, Can. J. Earth Sci., **15**, 431 (1978).
39. I. B. Berlman, "Handbook of Fluorescence Spectra of Aromatic Molecules", Academic Press, New York, 1965.
40. J. P. Byrne and I. G. Ross, Aust. J. Chem., **24**, 1107 (1971).
41. S. M. George, H. Auweter and C. B. Harris, J. Chem. Phys., **73**, 5573 (1980).
42. N. S. Baylis and E. G. McRae, J. Phys. Chem., **58**, 1002 (1954).
43. J. P. Byrne and I. G. Ross, Canad. J. Chem., **43**, 3253 (1965).
44. A. Nakajima, Bull. Chem. Soc. Japan, **45**, 1687 (1972).
45. R. E. Smalley, L. Wharton and D. H. Levy, Accts. Chem. Res., **10**, 139 (1977).
46. G. N. Patterson, "Molecular Flow of Gases", Wiley, New York, 1956.
47. J. D. Lambert, "Vibrational and Rotational Relaxation in Gases", Clarendon Press, Oxford, 1977.
48. R. Campargue, A. Lebehot, J.C. Lemonnier, D. Marette and J. Pebay, "Comptes Rendus 5e Symposium International sur les Jets Moleculaires", April 7-11, 1975, Nice, France.
49. P. Huber-Walchli and J. W. Nibler, J. Chem. Phys., **76**, 273 (1982).

50. H. Ashkenas and F. S. Sherman, in "Rarefied Gas Dynamics, 4th Symposium", J. H. de Leeuw Ed., Academic Press, New York, 1966, Vol II, p84.
51. D. H. Levy, Ann. Rev. Phys. Chem., **31**, 197 (1980).
52. D. H. Levy, L. Wharton, and R. E. Smalley, in "Chemical and Biochemical Applications of Lasers", C. B. Moore, Ed., Academic Press, New York, 1977, Vol. 2, pl.
53. J. B. Anderson and J. B. Fenn, Phys. Fluids, **8**, 780 (1965).
54. O. F. Hagena and W. Obert, J. Chem. Phys., **56**, 1793 (1972).
55. R. Campargue, J. Chem. Phys., **52**, 1795 (1970).
56. R. Campargue, Rev. Sci. Instrum., **35**, 111 (1964).
57. M. Sulkes, C. Jouvet and S. A. Rice, Chem. Phys. Lett., **87**, 515 (1982).
58. A. Amirav, U. Even and J. Jortner, Chem. Phys. Lett., **83**, 1 (1981).
59. F. M. Behlen, N. Mikami and S. A. Rice, Chem. Phys. Lett., **60**, 364 (1979).
60. I. Y. Chan and M. Dantus, J. Chem. Phys., **82**, 4771 (1982).
61. T. Imasaka, T. Okamura and N. Ishibashi, Anal. Chem., **58**, 2152 (1986).
62. W. R. Gentry and C. F. Giese, Rev. Sci. Instrum., **49**, 595 (1978).
63. B. V. Pepich, J. B. Callis, J. D. Sheldon Danielson, M. Gouterman, Rev. Sci. Instrum., **57**, 878, (1986).
64. J. W. Nibler, Dept. of Chemistry, Oregon State University, Personal Communication.
65. A. Amirav, U. Even and J. Jortner, Chem. Phys., **51**, 31 (1980).
66. D. H. Levy, C. A. Haynam and D. V. Brumbaugh, Faraday Discuss. Chem. Soc., **73**, 137 (1982).
67. A. Amirav, U. Even and J. Jortner, Anal. Chem., **54**, 1666 (1982).
68. J. M. Hayes and G. J. Small, Anal. Chem., **55**, 565A (1983).

69. M. V. Johnston, Trends Anal. Chem., 3, 58 (1984).
70. T. Imasaka, H. Fukuoka, T. Hayashi and N. Ishibashi, Anal. Chim. Acta, 156, 111 (1984).
71. J. W. Hofstraat, G. Ph. Hoornweg, C. Gooijer and N. H. Velthorst, Anal. Chim. Acta, 169, 125 (1985).
72. L. Li. and D. M. Lubman, Anal. Chem., 59, 2538 (1987).
73. S. W. Stiller and M. V. Johnston, Appl. Spectrosc., 41, 1351 (1987).
74. E. S. Yeung, in "Analytical Applications of Lasers", E. H. Piepmeier, Ed., Wiley, New York, 1986, Chapter 17.
75. G. J. Beenen, Ph.D. Thesis, Oregon State University, Corvallis, OR (1981).
76. G. J. Beenen, J. W. Hosch and E. H. Piepmeier, Appl. Spectrosc., 35, 593 (1981).
77. G. J. Beenen, B. P. Lessard and E. H. Piepmeier, Anal. Chem., 51, 239 (1981).
78. E. H. Piepmeier, in "Analytical Applications of Lasers", E. H. Piepmeier, Ed., Wiley, New York, 1986, p.22.
79. J. R. FitzPatrick and E. H. Piepmeier, Anal. Chem., 50, 1936 (1978).
80. A. L. Lewis II, Ph.D. Thesis, Oregon State University, Corvallis, OR (1981).
81. G. Hopkins, Masters Thesis, Oregon State University, Corvallis, OR (1985).
82. "Microprocessors and Peripherals Handbook", Vol. II, Intel Corp., Hillsboro, OR., 1983.
83. A. Hansen, PC Tech Journal, 5(1), 173 (1987).
84. B. Sheppard, BYTE, January, 157 (1987).
85. B. Smith and T. Puckett, PC Tech Journal, April, 63 (1984).
86. P. Norton, "Programmer's Guide to the IBM PC", Microsoft Press, Bellevue WA, 1985, Chapter 7.
87. W.L. Pesklak, M.S. Thesis, Oregon State University, Corvallis, OR (1983).

88. P.R. Bevington, "Data Reduction and Error Analysis for the Physical Sciences", McGraw-Hill, New York, 1969, Program listings 8-1 and B-1.
89. A. Amirav, U. Even and J. Jortner, Chem. Phys., 67, 1 (1982).
90. W. L. Meerts, W. A. Majewski and W. M. van Herpen, Can. J. Phys., 62, 1293 (1984).
91. "CRC Handbook of Chemistry and Physics", R. C. Weast, Ed, CRC Press, Boca Raton, FL, 63rd edition, p. D-216.
92. A. Amirav, U. Even and J. Jortner, J. Chem. Phys., 75, 2489 (1981).
93. T. S. Zwier, E. Carrasquillo and D. H. Levy, J. Chem. Phys., 78, 5493 (1983).
94. S. Leutwyler, U. Even and J. Jortner, Chem. Phys. Lett., 5, 439 (1982).
95. H. Saigusa and M. Itoh, J. Chem. Phys., 89, 5486 (1985).
96. P. C. Carman, "Flow of Gases Through Porous Media", Academic Press, New York, 1956.
97. H. Purnell, "Gas Chromatography", Wiley, New York, 1962, Chapter 5.
98. S. J. Hawkes, in "Recent Advances in Gas Chromatography", I. I. Domskey and J. A. Perry, Eds., Dekker, New York, 1971, Chapter 2.
99. L. S. Ettre, L. Mazor, and J. Takacs, in "Advances in Chromatography", J. C. Giddings and R. A. Keller, Eds., Dekker, New York, 1969, Vol. 8, p 271.
100. H. W. Liepmann, J. Fluid Mech., 10, 65 (1961).
101. J. A. Anderson, in "Molecular Beams and Low Density Gasdynamics", P. P. Wegener, Ed., Dekker, New York, 1974, p.1.
102. K. L. Saenger, J. Chem. Phys., 75, 2467 (1981).
103. S. Wicar, J. Chromatogr., 298, 373 (1984).
104. "CRC Handbook of Chemistry and Physics", R. C. Weast, Ed, CRC Press, Boca Raton, FL, 63rd edition, p. F-48.

105. F. Prahl, Unpublished Results, Dept. of Oceanography, Oregon State University, Corvallis, OR.
106. O. Kawka, Unpublished Results, Dept. of Oceanography, Oregon State University, Corvallis, OR.
107. C. J. Kirchmer, M. C. Winter and B. A. Kelly, Environ. Sci. Technol., 17, 396 (1983).
108. V. Lopez-Avila, R. Northcutt, J. Onstot and M. Wickham, Anal. Chem., 55, 881 (1983).

## **VI. Appendices**



### A. Supersonic Expansion Calculations

This appendix lists the equations used in the calculation of theoretical supersonic expansion parameters. The equations were obtained from references 46-48 and were programmed into a QUATTRO spreadsheet as described in the introduction.

---

Calculation of the Mach Number,  
 $M_a$ , as a Function of Distance  
 From the Nozzle

---

$$M_a(x) = A \left[ \frac{x_i - x_0}{D} \right]^{\gamma-1} - B \left[ \frac{x_i - x_0}{D} \right]^{\gamma-1} \quad (A.1)$$

Where, A = Fitting Parameter = 3.26 for monatomic noble gases

B = Fitting Parameter = 0.613 for monatomic noble gases

$\gamma = C_p/C_v$ , the ratio of constant-pressure and  
 constant-volume heat capacities= 1.667 for monatomic  
 noble gases

$x_0 = 0.075$  (cm)

$x_i$  = distance from the nozzle (cm)

D = nozzle diameter (cm)

---

$T_i/T_0$ : The Ratio of the  
Translational Temperature of the Expansion to the  
Reservoir Temperature

---

$$T_i/T_0 = 1 + \left[ \frac{\gamma - 1}{2} \right] M_a^2 \quad (\text{A.2})$$

Where,  $M_a$  is the Mach number calculated by Equation A.1  
 $\gamma = 1.667$  as before

---

The Ratio of the Density of the  
Expansion to the Density of the Gas in  
the Reservoir

---

$$\rho_i/\rho_0 = [T_i/T_0]^{1/(\gamma-1)} \quad (\text{A.3})$$

Where,  $T_i/T_0$  is the temperature ratio calculated by Equation A.2  
 $\gamma = 1.667$  as before

---

Ratio of the Pressure in the Expansion  
to the Pressure in the Reservoir

---

$$P_i/P_0 = (\rho_i/\rho_0) \cdot (T_i/T_0) \quad (\text{A.4})$$

Where,  $\rho_i/\rho_0$  is calculated by Equation A.3  
 $T_i/T_0$  is calculated by Equation A.2

---

Expansion Density in moles/m<sup>3</sup>

---

$$\rho_i(\text{mol/m}^3) = [P_0/(T_0 \cdot R)] (\rho_i/\rho_0) \quad (\text{A.5})$$

Where,  $P_0$  = Reservoir pressure in atmospheres  
 $T_0$  = Reservoir temperature in K  
 $R$  = Gas constant =  $8.21 \times 10^{-5} \text{ m}^3 \cdot \text{atm} \cdot \text{mol}^{-1} \cdot \text{K}^{-1}$

---

Local Speed of Sound,  $a$ , in the Expansion

---

$$a \text{ (m/s)} = [ \gamma \cdot R \cdot T_{tr} / M ]^{\frac{1}{2}} \quad (\text{A.6})$$

Where,  $\gamma = 1.667$  as before

$T_{tr}$  = Translational Temperature in K  $\approx T_i$  calculated from the product of  $T_i/T_0$  and the reservoir temperature,  $T_0$

$R$  = Gas constant =  $8314 \text{ m}^2 \cdot \text{s}^{-2} \cdot \text{g} \cdot \text{mol}^{-1} \cdot \text{K}^{-1}$

$M$  = Molecular weight of the expanding gas

---

Velocity,  $u$ , of the Expanding Gas

---

$$u \text{ (m/s)} = M_a \cdot a \quad (\text{A.7})$$

Where,  $M_a$  = Mach number from Equation A.1

$a$  = The local speed of sound from Equation A.6

---

Collision Frequency,  $\nu$ , of the Gas Particles in the Expansion

---

$$\nu \text{ (s}^{-1}\text{)} = 4\rho\pi\sigma^2 [ (R \cdot T_{tr}) / (M \cdot \pi) ]^{\frac{1}{2}} \cdot 6.02 \times 10^{23} \quad (\text{A.8})$$

Where,  $\rho$  = Gas density in  $\text{mol/m}^3$  from Equation A.5

$\sigma$  = Hard sphere diameter =  $2.58 \times 10^{-10} \text{ m}$  for He

$T_{tr} \approx T_i$  in K

$M$  = Molecular weight of the gas

$R$  = Gas Constant =  $8314 \text{ m}^2 \cdot \text{s}^{-2} \cdot \text{g} \cdot \text{mol}^{-1} \cdot \text{K}^{-1}$

---

Mach Disk Location,  $X_m$ 


---

$$X_m = 0.667 D^* [ P_0/P_1 ]^{\frac{1}{2}} \quad (A.9)$$

Where,  $D^*$  = Nozzle orifice diameter

$P_0$  = Reservoir Pressure

$P_1$  = Vacuum chamber pressure

---

Mach Disk Diameter,  $X_d$ 


---

$$X_d = 0.45 \cdot X_m \quad (A.10)$$

Where,  $X_m$  = Mach disk location from Equation A.9.

## B Compiling and Assembling Research Programs and Subroutines

The assembly language subroutines developed to enhance the high level BASIC control programs used in this research are all combined into two library files with the common name, RESEARCH. One of these libraries, which has a file extension of .QLB (Quick LiBrary), is loaded at the command line when QuickBASIC (QB4) is started from DOS. This provides a means by which programs that require the subroutines can be run from within the QuickBASIC programming environment. The Microsoft LINK utility (version 3.61 or later) is used to produce the quick library using the following syntax.

```
Link /Q SUB1 SUB2 SUB3 . . . SUBn, RESEARCH.QLB,, BQLB40.LIB;
```

where the SUBs are the previously compiled object files (.OBJ extension) of each of the assembly language subroutines, RESEARCH.QLB is the name of the library to be created, and BQLB40.LIB is a library provided with QB4 that must be linked into the research library. Due to the nature of the link process, each time one of the subroutines is changed, the entire set of subroutine object files must be re-linked.

The second library containing the research subroutines is a conventional Microsoft library (.LIB extension) created by the utility LIB (version 3.08). This is the library used to link the various subroutines into the compiled BASIC research programs to produce a DOS executable program (.EXE extension). The syntax for creation and maintenance of the library is:

```
LIB RESEARCH.LIB, -+SUB1 -+SUB2 -+SUB3 . . . -+SUBn;
```

where RESEARCH.LIB is the name of the library to create, and the

-+SUB causes the current version of the subroutine to be inserted in the library, replacing any previous subroutine with the same name regardless of the file date and time. In contrast to the quick library, individual subroutines can be installed or replaced without requiring all other subroutines to also be reinstalled. The syntax for replacing an individual subroutine is:

```
LIB RESEARCH.LIB, -+SUBn;
```

It is clear from this discussion that when a subroutine is changed or a new subroutine is created, a fair amount of work is required to produce a version of both libraries that includes the new routine; the routine must first be assembled, a quick library must be created and finally, a conventional library must be created. Only then can the subroutine be called from a BASIC program. Currently, there are 14 subroutines included in the RESEARCH libraries. Thus, a fair amount of bookkeeping is required to ensure that the correct version of each subroutine is used in creation of the libraries. Fortunately, a utility is provided with the Microsoft Macro Assembler that aids in the management and assembly of the various files and the creation of the libraries. The MAKE utility (version 4.06) operates in a fashion similar to conventional batch files; the commands necessary to compile and link the various routines are placed on individual lines of a MAKE file. In addition, MAKE has the ability to execute the desired compiling commands only if the source file has been changed since the last time an operation was performed. A sample, one-subroutine MAKE file that might be used to create the desired research libraries from a single source code file is illustrated below.

```
DELAY.OBJ:    DELAY.ASM
             MASM DELAY;
             LIB RESEARCH.LIB -+DELAY;

RESEARCH.QLB: DELAY.OBJ
             LINK /Q DELAY.OBJ;
```

When MAKE processes this file it reads in the first line which indicates that the object file DELAY.OBJ is produced from the source file DELAY.ASM. MAKE then checks the file creation date and time of each of these files and if the source file (on the right) was created after the destination file (in this case the object file on the left), the commands indented under the first line are executed until a blank line is reached. In this case, if DELAY.ASM was created after DELAY.OBJ, the source file, DELAY.ASM, is compiled by the Microsoft Macro assembler (MASM) and the resulting object file is placed in the research library. If however, the two file creation dates are the same, or if the object file was created after the source file, MAKE ignores all statements to the next blank line where it begins processing the next pair of files. The second pair of files in this example are the research quick library (destination) and the object file just produced (source). This results in the automatic production of the quick library.

Thus, if the subroutine DELAY had just been written or modified, and a MAKE file, DELAY.MAK, had also been created, the programmer would simply type

```
MAKE RESEARCH.MAK
```

to assemble the routine and create both libraries. The actual MAKE file used in this research to maintain all 14 subroutines is listed at the end of this appendix.

Once the subroutines have been combined into the two libraries, they can be used by any BASIC program. If it is desired to execute a program that uses one of these subroutines from within the QB4 environment, the quick library must be loaded from the command line:

```
QB PROGNAME /1 RESEARCH
```

In addition, the subroutine must be declared at the beginning of the program prior to any executable program lines, specifying the exact number of variables and their type. In the current example the

subroutine DELAY would be declared in the following manner.

```

        DECLARE SUB DELAY (A%)
or
        DECLARE SUB DELAY (A AS INTEGER)

```

Once declared, the subroutine can be called from anywhere within the program using the following syntax:

```

        CALL DELAY(DelayTime%)
        CALL DELAY(5)
or
        DELAY DelayTime%
        DELAY 5

```

where DelayTime% is an integer variable containing the number of seconds to delay. It is important that the programmer NOT mix the the two calling formats described above and use the following incorrect syntax.

```

        DELAY (DelayTime%)
or
        CALL DELAY DelayTime%

```

These two examples will not execute properly and the first example will not be caught as an error by the compiler.

Finally, when the program has been debugged from within the environment and it becomes necessary to produce a DOS executable file, it is recommended that the program be compiled and linked from the command line, NOT from within QuickBASIC. The reason for this recommendation lies in the way that QB4 calls the linker. If a program is compiled to a .EXE file from within the environment, QB4 shells to DOS and executes the following two commands:

```

BC PROGNAME;      (The BASIC compiler, BC)
LINK /EX /NOE PROGNAME+RESEARCH.LIB, PROGNAME.EXE,NUL,;

```



The problem arises from the way that QB4 links the research library to the program; QB4 treats the library as an object file, not as a library. This means that the entire library will be linked with the program even though only one of the subroutines was used. If the library contains a large number of subroutines, the size of the resulting EXE file will be excessively large since it contains a great deal of useless "excess baggage". In addition, since the library is treated as an object file, not a library, the DOS environment variable LIB, which allows library files to all be placed in a single subdirectory, does not apply, and the research library must always be located in the same subdirectory as the source file.

To solve this problem, the program can be compiled and linked outside of the QB4 environment using the following batch file statements:

```
BC /d/x %1;  
LINK /EX /NOE %1,%1.exe,nul,RESEARCH.LIB;
```

where %1 is a variable containing the filename passed from the batch file command line. In this case the research library is linked as a true library, and only the routines that are used in the BASIC program will be linked.

RESEARCH.MAK

Monday, August 1, 1988

Page 1

File Created: Saturday, May 7, 1988 at 10:28 am

```

MSDELAY.OBJ:  MSDELAY.ASM
              MASM MSDELAY;
              LIB \PROG\LIB\RESEARCH.LIB --MSDELAY;

DELAY.OBJ:    DELAY.ASM
              MASM DELAY;
              LIB \PROG\LIB\RESEARCH.LIB --DELAY;

PULSE.OBJ:    PULSE.ASM
              MASM PULSE;
              LIB \PROG\LIB\RESEARCH.LIB --PULSE;

TRAIN.OBJ:    TRAIN.ASM
              MASM TRAIN;
              LIB \PROG\LIB\RESEARCH.LIB --TRAIN;

TIMERBAS.OBJ:  TIMERBAS.ASM
              MASM TIMERBAS;
              LIB \PROG\LIB\RESEARCH.LIB --TIMERBAS;

INCREMNT.OBJ:  INCREMNT.ASM
              MASM INCREMNT;
              LIB \PROG\LIB\RESEARCH.LIB --INCREMENT;

DECREMNT.OBJ:  DECREMNT.ASM
              MASM DECREMNT;
              LIB \PROG\LIB\RESEARCH.LIB --DECREMENT;

A2D.OBJ:      A2D.ASM
              MASM A2D;
              LIB \PROG\LIB\RESEARCH.LIB --A2D;

DATAQ.OBJ:    DATAQ.ASM
              MASM DATAQ;
              LIB \PROG\LIB\RESEARCH.LIB --DATAQ;

VIDEO.OBJ:    VIDEO.ASM
              MASM VIDEO;
              LIB \PROG\LIB\RESEARCH.LIB --VIDEO;

ACTMODE.OBJ:  ACTMODE.ASM
              MASM ACTMODE;
              LIB \PROG\LIB\RESEARCH.LIB --ACTMODE;

INPUTS.OBJ:    \PROG\QB4\INPUTS.BAS
              BC /d \PROG\QB4\INPUTS;
              LIB \PROG\LIB\RESEARCH.LIB --INPUTS;

VIDINFO.OBJ:  VIDINFO.ASM
              MASM VIDINFO;
              LIB \PROG\LIB\RESEARCH.LIB --VIDINFO;

PRNTSCRN.OBJ:  PRNTSCRN.ASM
              MASM PRNTSCRN;
              LIB \PROG\LIB\RESEARCH.LIB --PRNTSCRN;

\PROG\LIB\RESEARCH.QLB: DELAY.OBJ PULSE.OBJ TRAIN.OBJ INPUTS.OBJ INCREMNT.OBJ\
                        MSDELAY.OBJ TIMERBAS.OBJ DECREMNT.OBJ A2D.OBJ\
                        DATAQ.OBJ VIDEO.OBJ VIDINFO.OBJ \PROG\LIB\BQLB40.LIB\
                        ACTMODE.OBJ PRNTSCRN.OBJ
LINK /Q @RESEARCH.LNK
COPY \PROG\LIB\RESEARCH.LIB \RESEARCH\PROG

```

### C. Program and Subroutine Listings

This appendix contains the listings of all important assembly language subroutines used in this research as well as the BASIC source listings of representative data acquisition and control programs. Due to space constraints, only a representative set of the BASIC programs that were used in this project are listed. However, the programs that are left out are, in most cases, similar in nature to one of the programs that is listed below. For example, SPECTRUM and CHROM are modified versions of the same program, as are PEAK and UVCAL. In addition, the important subroutines of BIFIT have been published elsewhere [82]. Finally, the calibration program CMX4CAL uses acquisition routines and follows a program flow that is similar in nature to CHROM.

The six assembly language subroutines are listed first in alphabetical order:

A2D.ASM  
DATAQ.ASM  
DELAY.ASM  
MSDELAY.ASM  
PULSE.ASM  
TRAIN.ASM

The BASIC programs are listed next, also in alphabetical order.

CHROM.BAS  
GPMENU.BAS  
PEAK.BAS  
REPLOT.BAS

A2D.ASM

Monday, August 1, 1988  
 File Created: Tuesday, March 22, 1988 at 12:35 pm

Page 1

COMMENT @

=====

Program: A2D

An assembly language subroutine which performs the necessary instructions to cause an analog-to-digital conversion on a desired multiplexer channel. The result of the ADC is passed back to the calling program in the form of a low byte integer, and a high byte integer, which must be recombined by the high-level program.

USAGE:

CALL A2D (Channel%, LoByte%, HiByte%)  
 A2D Channel%, LoByte%, HiByte%

Where Channel% is the multiplexer channel on which the ADC will be performed, LoByte% is the Low Byte of the data being returned, and HiByte% is the High Byte of the data being returned.

COMMENTS:

Make sure to declare A2D before calling it from QB4:

DECLARE SUB A2D(a%,b%,c%)

The two return bytes can be recombined in QB4 as follows:

$X = \text{HiByte\%} * 16 + \text{LoByte\%} / 16$

This subroutine assumes you have a MetraByte DASH-8 board installed a base address of 816.

REVISIONS:

Written by,

Scott J. Hein  
 Dept. of Chemistry  
 Oregon State University  
 Corvallis, OR 97331

-----  
 | Version 1.00 |  
20 January 1988

@

.MODEL Medium

.DATA

base\_add equ 816  
 adc\_reg equ base\_add + 1  
 stat\_reg equ base\_add + 2

Lo\_byte\_add dw 0  
 Hi\_byte\_add dw 0  
 mpx\_channel db 0

.CODE

A2D public A2D  
 proc

push bp ;Set new BP  
 mov bp,sp  
 push dx ;Save callers registers  
 push cx  
 push bx  
 push ax

mov bx, [bp+10] ;Get first parameter  
 mov cx, [bx]  
 mov mpx\_channel, cl ;save multiplexer channel

A2D.ASM

Monday, August 1, 1988  
 File Created: Tuesday, March 22, 1988 at 12:35 pm

Page 2

```

      mov     bx,[bp+8]           ;Get address of second param
      mov     Lo_byte_add,bx     ;save address of Low Byte

      mov     bx,[bp+6]           ;Get address of third param
      mov     Hi_byte_add,bx     ;save address of High Byte

      ;point mpx to the correct channel

      mov     al,mpx_channel
      mov     dx,stat_reg
      out     dx,al

      ;Start ADC on mpc_channel

      mov     dx,adc_reg
      xor     ax,ax              ;set ax = 0
      out     dx,al

      ;poll for end-of-conversion

      mov     dx,stat_reg
EOC:   in      al,dx
      test    al,10000000b       ;Test bit 7, if 1 then ADC
      jnz     EOC                ;hasnit finished, so loop back

      ;Read and return Lo-byte

      mov     dx,base_add
      mov     bx,lo_byte_add
      in      al,dx
      mov     [bx],al

      ;read and return Hi-byte

      mov     dx,adc_reg
      mov     bx,hi_byte_add
      in      al,dx
      mov     [bx],al

      ;return

      pop     ax                  ;restore registers
      pop     bx
      pop     cx
      pop     dx
      pop     bp

      ret     6                  ;far return: 3 parameters*2 = 6

A2D   endp
      end

```

DATAQ.ASM

Monday, August 1, 1988  
 File Created: Tuesday, March 22, 1988 at 11:22 am

Page 1

COMMENT @

=====

Program: DATAQ

An assembly language subroutine which performs the necessary instructions to fire the cmx-4 laser, as well as a pulsed valve, or hollow cathode lamp. In addition, an analog-to-digital conversion is performed on a desired multiplexer channel to obtain the desired signal. The result of the ADC is passed back to the calling program in the form of a low byte integer, and a high byte integer, which must be recombined by the high-level program.

USAGE:

CALL DATAQ (TrigByte%, Channel%, LoByte%, HiByte%)  
 DATAQ TrigByte%, Channel%, LoByte%, HiByte%

Where Channel% is the multiplexer channel on which the ADC will be performed, LoByte% is the Low Byte of the data being returned, and HiByte% is the High Byte of the data being returned.

COMMENTS:

Make sure to declare DATAQ before calling it from QB4:

DECLARE SUB DATAQ(a%,b%,c%,d%)

The two return bytes can be recombined in QB4 as follows:

X = HiByte% \* 16 + LoByte% / 16

This subroutine assumes you have a MetraByte DASH-8 board installed a base address of 816.

REVISIONS:

Written by,

Scott J. Hein  
 Dept. of Chemistry  
 Oregon State University  
 Corvallis, OR 97331

-----  
 | Version 1.00 |  
28 January 1988

=====

.MODEL Medium

.DATA

base\_add equ 816  
 adc\_reg equ base\_add + 1  
 stat\_reg equ base\_add + 2

Lo\_byte\_add dw 0  
 Hi\_byte\_add dw 0  
 mpx\_channel db 0  
 trig\_byte db 0

.CODE

public DATAQ  
 proc

push bp ;Set new BP  
 mov bp,sp  
 push dx ;Save callers registers  
 push cx  
 push bx  
 push ax  
 mov bx, [bp+12] ;Get first parameter

DATAQ.ASM

Monday, August 1, 1988  
 File Created: Tuesday, March 22, 1988 at 11:22 am

Page 2

```

      mov     cx,[bx]
      mov     trig_byte,cl

      mov     bx,[bp+10]
      mov     cx,[bx]
      mov     mpx_channel,cl           ;save multiplexer channel

      mov     bx,[bp+8]               ;Get address of second param
      mov     lo_byte_add,bx         ;save address of Low Byte

      mov     bx,[bp+6]               ;Get address of third param
      mov     hi_byte_add,bx         ;save address of High Byte

      ;=====
      ;Wait for Delay 1b indicating it's
      ;ok to fire the laser (1 on bit 4
      ;of statreg)
      ;=====

D1B:  mov     dx,stat_reg
      in      al,dx
      test    al,00010000b
      jz      D1B

      ;=====
      ;Fire Pulsed Valve (or HCL) and
      ;trigger Delay 2b to fire laser
      ;=====

      mov     al,trig_byte
      out     dx,al

      ;=====
      ;Now check to see if the gated
      ;integrator has been gated yet
      ;indicating that an ADC can be
      ;performed (1 on bit 5 of stat_reg)
      ;=====

GATE: nop
      in      al,dx
      test    al,00100000b
      jz      gate

      ;=====
      ;Point MPX to mpx_channel in
      ;preparation for an ADC
      ;=====

      mov     al,mpx_channel
      mov     dx,stat_reg
      out     dx,al

      ;=====
      ;Now Start the ADC on mpx_channel
      ;by writing any value to adc_reg
      ;=====

      mov     dx,adc_reg
      xor     ax,ax                   ;set ax = 0
      out     dx,al

      ;=====
      ;poll for end-of-conversion.
      ;conversion is done when bit 7 of
      ;statreg is 0.

```

DATAQ.ASM

Monday, August 1, 1988  
 File Created: Tuesday, March 22, 1988 at 11:22 am

Page 3

```

;=====
EOC:  mov     dx,stat_reg
      in      al,dx
      test    al,10000000b      ;Test bit 7, if 1 then ADC
      jnz     EOC               ;has not finished, so loop back

;=====
;conversion is done so data is available
;at adc_reg, and base_add. First,
;read and return Lo-byte from base_add.
;=====

      mov     dx,base_add
      mov     bx,lo_byte_add
      in      al,dx
      mov     [bx],al           ;store lobyte of data
                                   ;at the address of LoByte%

;=====
;now, read and return Hi-byte from
;adc_reg.
;=====

      mov     dx,adc_reg
      mov     bx,hi_byte_add
      in      al,dx
      mov     [bx],al           ;store hibyte of data
                                   ;at the address of HiByte%

;=====
;data acquisition is finished, so
;restore the registers and return
;=====

      pop     ax                ;restore registers
      pop     bx
      pop     cx
      pop     dx
      pop     bp

      ret     8                 ;far return: 4 parameters @ 2bytes = 8

DATAQ  endp
      end

```



DELAY.ASM

Monday, August 1, 1988  
 File Created: Tuesday, March 22, 1988 at 10:04 am

Page 1

```

=====
;TITLE: Delay.ASM
;DESCRIPTION:
;   An assembly language subroutine to be called from QuickBASIC 4.0,
;   or QuickC 1.0. Designed to allow higher resolution time delays
;   to be generated than are possible using BASICs TIMER function.
;   Programs the 8253 (8254 in the AT) programmable timer to count in
;   one millisecond increments. Control is returned to the calling
;   program after the desired number of milliseconds have passed. The
;   desired delay should be correct to within 0.1% if the correct
;   compensated counts have been placed in first_msec and one_msec.
;PARAMETERS:
;
;       delay_time      integer: Number of milliseconds to delay
;       first_msec      integer: Compensated timer count for 1st msec
;       one_msec        integer: Compensated count for remaining msec
;
;   DELAY calls the assembly language procedure n_msec_delay located
;   in the file MSDELAY.ASM which must be linked to delay. n_msec_delay
;   does the actual counting, based on the public variable delay_time.
;
;USE WITH QB4:
;   MAKE file format (DELAY.MAK):
;-----
;MSDELAY.OBJ:  MSDELAY.ASM
;             MASM MSDELAY;
;
;DELAY.OBJ:   DELAY.ASM
;            MASM DELAY;
;
;\PROG\LIB\DELAY.QLB:  DELAY.OBJ MSDELAY.OBJ \PROG\LIB\BQLB40.LIB
;                     LINK /Q MSDELAY.OBJ DELAY PULSE.OBJ,\PROG\LIB\DELAY.QLB,,BQLB40.LIB;
;
;\PROG\LIB\DELAY.LIB:  MSDELAY.OBJ
;                     LIB \PROG\LIB\DELAY.LIB-+DELAY.OBJ-+MSDELAY.OBJ-+PULSE.OBJ;
;                     COPY \PROG\LIB\DELAY.LIB \PROG\QB4
;
;-----
;
;   1. Create the Quick Library DELAY.QLB using the make file shown above.
;   2. Load the Quick Library from the QB4 command line:
;       QB /L DELAY
;   3. DECLARE the procedure as a SUB PROGRAM:
;       DECLARE SUB msdelay (msec%)
;   4. msdelay can be called with or without a CALL:
;       CALL delay(msec%)
;       or
;       delay msec%
;
;=====

.MODEL MEDIUM

.DATA
PUBLIC delay_time      ;Passed from QB
PUBLIC first_msec      ;Compensated count for 1st millisecond
PUBLIC one_msec        ;Compensated count for remaining milliseconds
delay_time            dw      0
one_msec              dw      0
first_msec            dw      0

.CODE

EXTRN n_msec_delay:proc
public delay
delay proc

```

DELAY.ASM

Monday, August 1, 1988  
 File Created: Tuesday, March 22, 1988 at 10:04 am

Page 2

```

      push    bp          ;save base pointer
      mov     bp,sp      ;
      push    ax          ;save registers
      push    bx
      push    cx
      push    dx
      push    ds          ;save callers data segment

      mov     ax,@data    ;get location of the data segment
      mov     ds,ax       ;point ds to this subs data segment

      mov     bx,[bp+6]   ;get parameter passed from QB4
      mov     cx,[bx]     ;Parm 1 = # milliseconds to delay
      mov     delay_time,cx ;put parameter into public var delay_time

      cmp     cx,0        ;Check to see if delay is zero
      je      exit        ;if so, no delay so exit

      mov     ax,0432h    ;# counts = 1 msec, compensated for initial
      mov     first_msec,ax ;code overhead
      mov     ax,0494h    ;# counts = 1 msec, compensted for remaining
      mov     one_msec,ax ;code overhead

      call    n_msec_delay ;call msdelay.asm

exit:  pop     ds          ;restore callers data segment
      pop     dx
      pop     cx
      pop     bx
      pop     ax
      pop     bp          ;restore registers, etc.
      ret     2           ;far return (1 parameter)

delay endp
      end

```

MSDELAY.ASM

Monday, August 1, 1988  
 File Created: Saturday, December 26, 1987 at 9:55 am

Page 1

```

=====
;TITLE: MSDelay.ASM (n_msec_delay)
;DESCRIPTION:
;
;  An assembly language procedure to be called from other procedures
;  which require delays with 1 millisecond resolution.
;  This procedure is designed to allow higher resolution time delays
;  to be generated than are possible using BASICs TIMER function.
;  Programs the 8253 (8254 in the AT) programmable timer to count in
;  one millisecond increments. Control is returned to the calling
;  program after the desired number of milliseconds have passed.
;
;  Millisecond period can be fine tuned to take code overhead (jitter)
;  into account by adjusting the value of first_msec, and one_msec.
;  Since the first millisecond period will include the overhead related
;  to the time required to transfer control from the calling program, as
;  well as the time required to set up Timer 2, this period must be
;  compensated differently than the remaining milliseconds which only
;  must compensate for the code in the msec loop (loop2)
;PARAMETERS:
;
;  delay_time      integer:    Number of milliseconds to delay
;  first_msec      integer:    Number of timer counts = 1 msec
;                               taking initial code overhead into
;                               account
;  one_msec        integer:    Number of timer counts = 1 msec
;                               taking msec loop overhead into
;                               account
;ADDITIONAL INFORMATION:
;
;  -----
;  8253 Programmable IntervalTimer:
;  -----
;
;  the timer is programmed by writing a mode command to its control port
;  at address 43h. The control port bits are arranged as follows:
;
;  -----
;  | SC1 | SC0 | RL1 | RL0 | M2 | M1 | M0 | BCD |
;  -----
;  | 7   | 6   | 5   | 4   | 3   | 2   | 1   | 0   |
;
;  SC = Select Counter:  0 0 : counter 0
;                        0 1 : counter 1
;                        1 0 : counter 2
;                        1 1 : illegal counter #
;
;  RL = Read/Load:      0 0 : Latch counter
;                        1 0 : Read/Load MSB only
;                        0 1 : Read/Load LSB only
;                        1 1 : Read/load LSB followed by MSB
;
;  M = Mode:            0 0 0 : Mode 0
;                        0 0 1 : Mode 1
;                        x 1 0 : Mode 2
;                        x 1 1 : Mode 3
;                        1 0 0 : Mode 4
;                        1 0 1 : Mode 5
;
;  BCD:                 0 : Count down in binary (16 bits)
;                       1 : Count down in BCD (4 decades)
;
;  The three counters, 0, 1, & 2 are located at 40h, 41h, & 42h,
;  respectively. Data can be written to these counters a byte at a time,
;  and the current count value can be read by latching the contents with
;  the latch counter command, and then reading the data a byte at a time.
;

```

```

;-----
; 8255 Programmable Peripheral Interface (PPI)
;-----
; Note:  this method of polling the output of counter 2 in the PPI
;        works on the Corona PC, but appears not to work on the
;        AST Premium 286.  This will have to be examined in more detail.
;
; The PPI has three Ports, A,B, & C located at 60h, 61h, & 62h,
; respectively.  The ports which are of interest in using the 8253
; timer, are ports B & C:
;
; Port B (61h)  | 7 | 6 | 5 | 4 | 3 | 2 | 1 | 0 |
;               -----
;               ^
;               |
; Speaker data ( 0 for this app) _|
; Timer 2 gate (rising edge) _____
;
; Port C (62h)  | 7 | 6 | 5 | 4 | 3 | 2 | 1 | 0 |
;               -----
;               ^
;               |
; Timer 2 output _|
;
; This information can be examined in greater detail in the INTEL
; Microprocessors and peripherals handbook, Vol 2, 1984.
;
;-----
; Calculating Count Value
;-----
;
; The programmable interval timer in both the PC & AT run at a base
; frequency of 1/4 the PCs 4.77 MHz clock frequency, or 1.19318 MHz.
; This means that there are 1,193,180 counts per second.  Therefore, to
; get the counter to count in 1 msec increments, the counter must be
; loaded with 0.001 sec x 1,193,180 = 1193 counts.  The actual value
; which gets loaded will be less than this since there is some code
; overhead associated with calling this procedure and setting up the
; timer.
;=====

```

# .MODEL MEDIUM

## .DATA

```

        EXTRN  delay_time:word
        EXTRN  first_msec:word
        EXTRN  one_msec:word
timer_con    equ    43h          ; 8253A control port
timer2       equ    42h          ; timer two r/w port
timer_gate   equ    61h          ; timer gate controlled by 8255
timer_out    equ    62h          ; timer 2 output bit in PPI Port C
timer_mode   equ    0b2h         ; 8253 control byte:
                                   ; timer 2, mode 1, lo/hi load, binary

```

## .CODE

```

        public n_msec_delay
n_msec_delay proc
;
        push    ax                ;save registers
        push    cx
        push    dx
;
prep:    mov     al,timer_mode
        out     timer_con,al      ;Set up timer 2 (mode 1, lo/hi, bin)
        mov     dx,first_msec     ;put # of ticks = 1 msec into the

```

MSDELAY.ASM

Monday, August 1, 1988

Page 3

File Created: Saturday, December 26, 1987 at 9:55 am

```

        mov     al,dl                ;counter: first_msec compensates
        out     timer2,al           ;for initial code overhead.
        mov     al,dh
        out     timer2,al

        in      al,timer_gate       ;read 8255 value (whatever it is)
        or      al,1               ;turn on bit 0 (gate for timer 2)
        out     timer_gate,al      ;relaod & restart timer
        mov     cl,al              ;save trigger byte for later trigger
        xor     al,1               ;turn off bit 0
        out     timer_gate,al      ;next trigger requires rising gate edge

        mov     dx,one_msec        ;change the value of count to reflect
        mov     al,dl              ;code overhead after the 1st msec
        out     timer2,al
        mov     al,dh              ;This new count will be used with
        out     timer2,al          ;subsequent gates

;-----
;Counter Polling loop
;determines when 1 ms
;has elapsed
;-----
loop2:   in      al,timer_out       ;get PPI Port 2 byte value
        test    al,00100000b      ;test bit 5 (counter 2 out)
        jz      loop2             ;if 0 then C2 output is low ==>
                                   ;terminal count hasn't been reached
        mov     al,cl              ;mov trigger byte into al
        out     timer_gate,al     ;quickly relaod & restart timer
        xor     al,1               ;set timer_gate bit to 0 for next trig
        out     timer_gate,al

;-----
;Loop to check the
;length of the delay
;-----
        dec     delay_time        ; downcount # cycles which give one second
        jnz     loop2             ; if less than one second, keep reading

exit:    pop     dx
        pop     cx
        pop     ax

        ret

n_msec_delay    endp

        end

```

PULSE.ASM

Monday, August 1, 1988  
 File Created: Thursday, December 24, 1987 at 10:00 am

Page 1

```

=====
;TITLE: pulse.ASM
;DESCRIPTION:
;   An assembly language subroutine to be called from QuickBASIC 4.0,
;   or QuickC 1.0. Designed to allow higher resolution pulses to ports
;   to be generated than are possible using BASICs TIMER & out function.
;   The assembly language timer control subroutine, n_msec_delay, takes the
;   number of milliseconds stored in the public variable delay_time and
;   programs the 8253 (8254 in the AT) programmable timer to count in
;   one millisecond increments.
;PARAMETERS:
;   The number of milliseconds to delay is passed from the calling program
;   and is placed in the public variable delay_time.
;
;   1.    delay_time    integer: Desired output pulse width
;   2.    output_port   integer: Output Port address
;   3.    out_byte_on   integer: Byte which will be output to turn
;                               on the desired bits of the port
;   4.    out_byte_off  integer: Byte which will be output to turn
;                               off the desired bits of the port
;   5.    first_msec    integer: Compensated timer count for 1st msec
;   6.    one_msec      integer: Compensated count for remaining msec
;
;USE WITH QB4:
;
;MAKE file format:
-----
;MSDELAY.OBJ:  MSDELAY.ASM
;             MASM MSDELAY;
;
;PULSE.OBJ:   PULSE.ASM
;             MASM PULSE;
;
;\PROG\LIB\DELAY.QLB:  PULSE.OBJ MSDELAY.OBJ \PROG\LIB\BQLB40.LIB
;                     LINK /Q PULSE MSDELAY,\PROG\LIB\DELAY.QLB,,BQLB40.LIB;
;
;\PROG\LIB\DELAY.LIB:  PULSE.OBJ MSDELAY.OBJ
;                     LIB \PROG\LIB\DELAY.LIB-+MSDELAY.OBJ-+PULSE.OBJ
;                     COPY \PROG\LIB\DELAY.LIB \PROG\QB4
;
-----
;
;   1. Create the Quick Library DELAY.QLB using the make file shown above.
;   2. Load the Quick Library from the QB4 command line:
;       QB /L DELAY
;   3. DECLARE the procedures as a SUB PROGRAM:
;       DECLARE SUB pulse (msec%, port%, on%, off%)
;   4. procedures can be called with or without a CALL:
;       CALL pulse (msec%, port%, on%, off%)
;       or
;       pulse msec%, port%, on%, off%
;
=====

.MODEL MEDIUM

.DATA
EXTRN  delay_time:WORD
EXTRN  one_msec:WORD
EXTRN  first_msec:WORD
output_port  dw  0          ;Address of port to send pulse to
out_byte_on  db  0          ;Byte to pulse to Port on
out_byte_off db  0          ;Byte to pulse port off

.CODE
EXTRN n_msec_delay:proc

```

PULSE.ASM

Monday, August 1, 1988  
 File Created: Thursday, December 24, 1987 at 10:00 am

Page 2

```

pulse    public pulse
proc
    push    bp                ;save base pointer
    mov     bp,sp            ;
    push    ax                ;save registers
    push    dx
    push    bx
    push    cx
    push    ds                ;save callers data segment

    mov     ax,@data
    mov     ds,ax            ;point ds to our data segment

    mov     bx,[bp+12]        ;get parameter passed from QB4
    mov     cx,[bx]
    mov     delay_time,cx    ;Parm 1 = Pulse width in Msec (integer)

    mov     bx,[bp+10]        ;Get second param
    mov     cx,[bx]
    mov     output_port,cx   ;Parm 2 = Output Port Address (integer)

    mov     bx,[bp+8]         ;Get third Parm
    mov     cx,[bx]
    mov     out_byte_on,cl    ;Parm 3 = Byte to turn on  output_port (int)

    mov     bx,[bp+6]         ;Get fourth (last) parameter
    mov     cx,[bx]
    mov     out_byte_off,cl   ;Parm 4 = Byte to turn off output_ port

    mov     ax,0432h          ;take code overhead into account: overhead is
    mov     first_msec,ax      ;greater for the 1st msec than the remaining
    mov     ax,0491h          ;set up number of ticks = 1 msec
    mov     one_msec,ax

    mov     dx,output_port
    mov     al,out_byte_on
    out     dx,al             ;Pulse desired output port bits high

    call    n_msec_delay      ;Delay delay_time (pulse width)

    mov     dx,output_port
    mov     al,out_byte_off
    out     dx,al             ;Turn off desired output port bits

    pop     ds                ;Restore callers data segment
    pop     cx                ;restore registers
    pop     bx
    pop     dx
    pop     ax
    pop     bp
    ret     8                 ;far return: 2 * 4 params = 8
pulse    endp
end

```

TRAIN.ASM

Monday, August 1, 1988  
 File Created: Thursday, December 24, 1987 at 9:57 am

Page 1

```

=====
;TITLE: train.ASM
;DESCRIPTION:
;   An assembly language subroutine to be called from QuickBASIC 4.0,
;   or QuickC 1.0. Designed to allow higher resolution pulse trains
;   to be generated than are possible using BASICs TIMER & Out function.
;   Programs the 8253 (8254 in the AT) programmable timer to count in
;   one millisecond increments. Control is returned to the calling
;   program after the desired number of milliseconds have passed.
;PARAMETERS:
;   The number of milliseconds to delay is passed from the calling program
;   and is placed in the variable delay_time.
;
;   1.    delay_time    integer: Desired output pulse width + delay
;   2.    output_port   integer: Output Port address
;   3.    out_byte_on   integer: Byte which will be output to turn
;                               on the desired bits of the port
;   4.    out_byte_off  integer: Byte which will be output to turn
;                               off the desired bits of the port
;   5.    train_length  integer: Number of pulses which will be sent
;                               to the port
;   6.    first_msec    integer: compensated timer count for 1st msec
;   7.    one_msec      integer: compensted count for remaining msec
;
;USE WITH QB4:
;MAKE file format:
-----
;MSDELAY.OBJ:  MSDELAY.ASM
;             MASM MSDELAY;
;
;TRAIN.OBJ:   TRAIN.ASM
;            MASM TRAIN;
;
;\PROG\LIB\DELAY.QLB:  TRAIN.OBJ MSDELAY.OBJ \PROG\LIB\BQLB40.LIB
;                     LINK /Q TRAIN MSDELAY,\PROG\LIB\DELAY.QLB,,BQLB40.LIB;
;
;\PROG\LIB\DELAY.LIB:  TRAIN.OBJ MSDELAY.OBJ
;                     LIB \PROG\LIB\DELAY.LIB-+MSDELAY.OBJ-+TRAIN.OBJ
;                     COPY \PROG\LIB\DELAY.LIB \PROG\QB4
;
-----
;
;   1. Create the Quick Library DELAY.QLB using the make file shown above.
;   2. Load the Quick Library from the QB4 command line:
;       QB /L DELAY
;   3. DECLARE the procedures as a SUB PROGRAM:
;       DECLARE SUB TRAIN (msec%, port%, on%, off%)
;   4. procedures can be called with or without a CALL:
;       CALL TRAIN (pw%, delay%, length%, port%, on%, off%)
;       or
;       TRAIN pw%, delay%, length%, port%, on%, off%
;
=====

.MODEL MEDIUM

.DATA
EXTRN  delay_time:WORD
EXTRN  one_msec:WORD
EXTRN  first_msec:WORD
output_port    dw  0          ;Address of port to send pulse to
out_byte_on    db  0          ;Byte to pulse to Port on
out_byte_off   db  0          ;Byte to pulse off port off
pulse_width    dw  0          ;pulse width
pulse_delay    dw  0          ;delay between pulses

```



TRAIN.ASM

Monday, August 1, 1988  
 File Created: Thursday, December 24, 1987 at 9:57 am

Page 2

```

train_length    dw      0                ;Number of pulses in train

        .CODE
        EXTRN n_msec_delay:proc
        public train
train        proc

        push    bp                ;save base pointer
        mov     bp,sp              ;
        push    ax                ;save registers
        push    dx
        push    bx
        push    cx
        push    ds                ;save callers data segment

        mov     ax,@data
        mov     ds,ax              ;point ds to our data segment

        mov     bx,[bp+16]         ;get parameter passed from QB4
        mov     cx,[bx]            ;Parm 1 = Pulse width in Msec (integer)
        mov     pulse_width,cx

        mov     bx,[bp+14]
        mov     cx,[bx]
        mov     pulse_delay,cx    ;parm 2 = Delay between pulses in Msec

        mov     bx,[bp+12]
        mov     cx,[bx]
        mov     train_length,cx  ;parm 3 = Number of pulses to send

        mov     bx,[bp+10]
        mov     cx,[bx]
        mov     output_port,cx   ;Parm 4 = Output Port Address (integer)

        mov     bx,[bp+8]
        mov     cx,[bx]
        mov     out_byte_on,cl   ;Parm 5 = Byte to turn on output_port (int)

        mov     bx,[bp+6]
        mov     cx,[bx]
        mov     out_byte_off,cl  ;Parm 6 = Byte to turn off output_port

here:     mov     cx,pulse_width   ;set up pulse width
        mov     delay_time,cx

        mov     ax,0432h
        mov     first_msec,ax
        mov     ax,0491h         ;set up number of ticks = 1 msec
        mov     one_msec,ax

        mov     dx,output_port
        mov     al,out_byte_on
        out     dx,al            ;Pulse desired output port bits high

        call    n_msec_delay      ;Delay delay_time (pulse width)

        mov     dx,output_port
        mov     al,out_byte_off
        out     dx,al            ;Turn off desired output port bits

        mov     cx,pulse_delay
        mov     delay_time,cx    ;set up delay between pulses
        mov     ax,03e8h
        mov     first_msec,ax
        mov     ax,0491h         ;set up number of ticks = 1 msec

```

TRAIN.ASM

Monday, August 1, 1988  
File Created: Thursday, December 24, 1987 at 9:57 am

Page 3

```
    mov     one_msec,ax
    call    n_msec_delay    ;Delay delay_time (pulse delay)
    dec     train_length
    jnz     here            ;Done with train?
    pop     ds              ;Restore callers data segment
    pop     cx              ;restore registers
    pop     bx
    pop     dx
    pop     ax
    pop     bp
    ret     12              ;far return: 2 * 6 params = 12
train     endp
end
```

CHROM.BAS

Monday, August 1, 1988  
 File Created: Thursday, June 9, 1988 at 2:37 pm

Page 1

```

DECLARE SUB WaveProgram ()
DECLARE SUB Video.Mode ()
DECLARE SUB InjDelay ()
DECLARE SUB AcquireDelay ()
DECLARE SUB ChromDef ()
DECLARE SUB PlotData ()
DECLARE FUNCTION exist% (File.Name$)
DECLARE FUNCTION GetBFX! (B0!, B1!, B2!, Lambda!)
DECLARE FUNCTION GetUVX! (U0!, U1!, U2!, Lambda!)
DECLARE SUB Step.UV.Motor (a%, B%)
DECLARE SUB UVHyst ()
DECLARE SUB VideoMode ()
DECLARE SUB INITIALIZE ()
DECLARE SUB PREAQ ()
DECLARE SUB ScanParam ()
DECLARE SUB WRITEDATA ()
DECLARE SUB CalcXet ()
DECLARE SUB eraseline (a%)
DECLARE SUB StepMotors ()
DECLARE SUB CMX4DAT ()
DECLARE SUB FRAME ()
DECLARE SUB PeakPower ()
DECLARE SUB Acquire ()
DECLARE SUB SCALEDATA ()
DECLARE SUB TIMERINIT ()
DECLARE SUB DISPLAYX ()
DECLARE SUB ViewLower ()
DECLARE SUB Yscale ()
DECLARE SUB Frame2 ()
DECLARE SUB QUANTIZE (a!)
DECLARE SUB ViewUpper ()
DECLARE SUB Step.UV.Motors (a%, B%)
DECLARE SUB Input$ (a$)
DECLARE SUB Pulse (a%, B%, C%, D%)
      'Syntax: Pulse PulseWidth, Port, ByteOn, ByteOff
DECLARE SUB delay (a%)
      'Syntax: Delay DLY (in msec)
DECLARE SUB A2D (a%, B%, C%)
      'Syntax: A2D MPXChan, LoByte, HiByte
DECLARE SUB dataq (a%, B%, C%, D%)
      'Syntax: Dataq TrigByte, MPXChan, LoByte, HiByte

'=====
'Program CHROM.BAS:   Program to control and synchronize CMX-4 Laser, Evans
'                   Associates Gated Int., and MB Dash8 I/O Board
'                   to produce high-resolution Rotationally Cooled
'                   Laser-excited fluorescence excitation
'                   chromatograms.
'
'   Written By,
'
'                   Scott J. Hein
'                   Dept. of Chemistry
'                   Oregon State University
'                   Corvallis, OR 97331
'
'                   21 April 1988
'                   Version 1.00
'
'Program Written using the Microsoft QuickBASIC Compiler, Version 4.0.
'Assembly language subroutines written using the Microsoft Macro Assembler
'Version 5.0
'
'NOTES:
'   CHROM requires the following input files:
'
'       (1)   CMX4CAL.DAT, a sequential ASCII file containing
'             calibration variables.
'
'       (2)   CMX4DAT.DAT, a sequential ASCII file containing
'             default variables which relate to the CMX4.

```

CHROM.BAS

Monday, August 1, 1988  
 File Created: Thursday, June 9, 1988 at 2:37 pm

Page 2

```

'      (3)      CHROM.DEF, a sequential ASCII file containing
'               the current defaults for this programs variables
'
'External Subprograms Required:
'
'      InputS(a$)      located in:      INPUTS.BAS
'      Pulse (A%,B%,C%,D%)      PULSE.ASM
'      DELAY (A%)      DELAY.ASM
'      A2D (A%,B%,C%)      A2D.ASM
'      DATAQ (A%, B%, C%, D%)      DATAQ.ASM
'
'      These subroutines have been compiled and linked into the libraries
'      RESEARCH.QLB and RESEARCH.LIB.
'      In order to compile and run this program, this library must be
'      loaded from the command line.
'      QB CHROM /L RESEARCH
'      Note that the Library RESEARCH.LIB must also be available in order to
'      make an EXE file.
'
'-----
'Initials      Date      Revision History      Lines      Comments
'=====
'      SJH      4/21/88      Chrom converted from Spectrum 4.00
'
'=====Begin Main Program=====
DEFINT A-Z
COMMON FromGPMENU AS INTEGER
'DYNAMIC Declare arrays dynamic

CONST Dly1 = 40, Dly2 = 10
CONST TRUE = -1, FALSE = 0
CONST VERSION = 1.01
CONST Forward = -1      'Boolean direction constants for stepping
CONST Reverse = 0      'UV Crystal stepper motor
CONST Pwidth = 5      'msec Output pulsewidth for stepper motors
CONST BaseAdd = 816      'DASH-8 Base Address
CONST ADCReg = BaseAdd + 1      '2nd ADC register (BaseAdd is 1st ADC reg)
CONST StatReg = BaseAdd + 2      'DASH-8 Status & control register
CONST Counter2 = BaseAdd + 3      'Counter 2 data port
CONST TimeReg = BaseAdd + 7      'DASH-8 8253 timer control port
CONST portadd = 632      'Address of Parallel I/O port
                           'Possible Addresses:
                           ' LPT1: 3BC (HEX) = 956 (DEC)
                           ' LPT2: 378 = 888
                           ' LPT3: 278 = 632

DIM SHARED Program!(20, 20) 'Retention time, wavelength array
DIM SHARED XETProg!(20)

OUT portadd, 0      'Zero Parallel I/O Port

'Video.Mode 'Make sure mode bw80 is active

CALL INITIALIZE      'Initialize Constants & Calibration Data
CALL PREAQ      'Input Initial X's and Pressure

'-----
'      Begin Main Data Acquisition Loop
'-----

DO
  START = FALSE
  SCREEN 0
  CALL ScanParam

```

CHROM.BAS

Monday, August 1, 1988  
 File Created: Thursday, June 9, 1988 at 2:37 pm

Page 3

```

'-----Dimension PTX dependent Variables-----

REDIM SHARED AvgSignal!(DataPts + 50), RetTime!(DataPts + 50)

'-----
'Set up Data Files
'-----

CLS

File.Name.OK = FALSE
DO

PRINT "Enter Filename to Write Data to (no extension): ";
  Input$ filename$
  PRINT

IF exist(filename$ + ".Dat") THEN
  BEEP
  INPUT "File Already Exists: Overwrite? ", Resp$
  IF Resp$ = "Y" OR Resp$ = "y" THEN
    File.Name.OK = TRUE
  END IF
ELSE
  File.Name.OK = TRUE
END IF

LOOP UNTIL File.Name.OK

CALL ChromDef

OPEN filename$ + ".DAT" FOR OUTPUT AS #1
OPEN filename$ + ".OUT" FOR OUTPUT AS #2

CALL WRITEDATA      'Record Experimental Parameters & write to file
CLOSE

'-----
'Set up array of etalon positions for scan,
'and step to initial position, to begin scan.
'-----

IF HighRes THEN
  CALL CalcXet      'Calculate Xet's for Lambda's
END IF

StepNum = 0

eraseline 25: PRINT "Press Any Key to Step Motors to Excitation Wavelength. . .";
WHILE INKEY$ = "": WEND
eraseline 25

Lambda! = Program!(1, 2)
IF HighRes THEN
  XET! = XETProg!(1)
END IF

CALL StepMotors      'Step Motors to Initial X's

CALL CMX4DAT      'Update X's

'-----

```

CHROM.BAS

 Monday, August 1, 1988  
 File Created: Thursday, June 9, 1988 at 2:37 pm

Page 4

```

'Set up Graphics screen and configure
'Plotting frame
'-----

      MaxX! = 600 * RepRate / PTX '10 minutes in points @ RepRate
      MaxY! = 15DD!
      MinY! = 80D!
      CALL FRAME

'-----
'Peak laser power initially then
'Begin Data Acquisition loop
'-----

eraseline 25
PRINT "Peak Laser Power for data collection <SPACE to cont.>";
CALL PeakPower
CALL Acquire      'Collect Data

'-----
'Continue to pulse valve until the
'GC Vent is opened
'-----

eraseline 25
PRINT "Open the GC vent, then press any key to continue. . . ";

WHILE INKEY$ = ""
      WAIT StatReg, 16
      OUT StatReg, 16
      OUT StatReg, D
WEND

'-----
'Examine the data set & determine what
'to do with data
'-----

CALL CMX4DAT      'Update X's
CALL SCALEDATA    'Rescale/Replot Data
eraseline 25: PRINT "Does Data Appear OK <Y or N> ? ";

DOK$ = ""
WHILE DOK$ = "": DOK$ = INKEY$: WEND
IF DOK$ = "N" OR DOK$ = "n" THEN
      CLOSE
      START = TRUE 'Restart from Beginning
END IF

'-----
'If spectrum was OK then write data to
'Data files, and enter peaks into the
'peak list
'-----

IF NOT START THEN

      'Write final scan info to ".out"

      OPEN filename$ + ".OUT" FOR APPEND AS #4

      PRINT #4, "": PRINT #4, "Run Information:": PRINT #4, "=====
      PRINT #4, "Pulses per Averaged Data Point"; PTX, TAB(25); , "Total Data Points: "; S
      tepNum
      PRINT #4, "": PRINT #4, "Experimental Parameters": PRINT #4, "-----"

```

CHROM.BAS

Monday, August 1, 1988  
 File Created: Thursday, June 9, 1988 at 2:37 pm

Page 5

```

PRINT #4, "Valve Pulsewidth (ms): "; PW!
PRINT #4, "Delay 2B: "; Delay2B!
PRINT #4, "Delay 4A: "; Delay4A!
PRINT #4, "Backing Pressure (psi): "; BackPress!
PRINT #4, "PMT Voltage (V): "; PMTVolt
PRINT #4, "X: Beam to Nozzle Distance (mm): "; XBeam!
PRINT #4, "Emission Filter Used: "; Filter$
PRINT #4,
PRINT #4, "Chromatographic Parameters:"
PRINT #4, "=====
PRINT #4,
PRINT #4, "Injection Port Temperature: "; InjTemp!
PRINT #4, "Transfer Line Temperature: "; TransTemp!
PRINT #4, "Valve Temperature: "; ValveTemp!
PRINT #4, "Acquisition Length: "; AcqLength!; " minutes"
PRINT #4, "Acquisition Delay: "; AcqDelay!; " minutes"
PRINT #4, "Oven Temperature Program: "; TempProg$
PRINT #4,
PRINT #4, "Retention Time/Wavelength Program:"
PRINT #4, "=====
PRINT #4, " #      Ret. Time (min)      Wavelength (A)"
PRINT #4, "=====
FOR i = 1 TO NumProgs
    PRINT #4, USING "##      ###.##      ###.###"; i, Program!(i, 1), Pr
ogram!(i, 2)
NEXT i
PRINT #4, "=====
CLOSE #4

'Write Averaged Data to File.DAT

OPEN filename$ + ".DAT" FOR APPEND AS #2
FOR i = 1 TO StepNum
    PRINT #2, USING "###.###, #####.##"; RetTime!(i), AvgSignal!(i)
NEXT i
CLOSE #2

eraseline 25: PRINT "Obtain Another Chromatogram? ";
NewSpec$ = ""
WHILE NewSpec$ = "": NewSpec$ = INKEY$: WEND

IF NewSpec$ = "Y" OR NewSpec$ = "y" THEN CLOSE : START = TRUE

END IF

LOOP WHILE START

SCREEN 0
CLS
CLOSE
IF FromGPMENU THEN
    CHAIN "GPMENU"
ELSE
    END
END IF

Error.Handler:
ErrNum = ERR
RESUME NEXT

'=====END OF MAIN LOOP=====

*****
SUB Acquire STATIC

```

CHROM.BAS

Monday, August 1, 1988  
 File Created: Thursday, June 9, 1988 at 2:37 pm

Page 6

\*\*\*\*\*

SHARED XET!, AvgSignal!(), XOET!, XOB!!, XOUV!, AcqDelay!, AcqLength!  
 SHARED PTX, Lambda!, StepNum, PtNum  
 SHARED MaxX!, MaxY!, filename\$, TimeStart!, NumProgs

```

-----
'   PTNUM:    Keeps track of the number of points taken since the last
'             screen clear (Currently set for every 10 min).
'   STEPNUM   Keeps track of the cumulative number of steps
'             taken: is used to determine lambda!.
-----

```

```

PtNum = 0
StepNum = 1
ProgNum = 2 'ProgNum= 1 is the Initial Wavelength

```

'=====Begin Main Data Transfer Loop=====

```
CALL TIMERINIT          'Set up DASH8 Timer and Registers
```

```

eraseline 25
PRINT "Press a key to start the valve pulsing, then close the GC Vent";
WHILE INKEY$ = "": WEND

```

```

-----
'Begin acquisition of the spectrum
-----

```

```
acq = TRUE
```

```

eraseline 25
PRINT "Press any key to start the 20 second injection delay. . .";
WHILE INKEY$ = ""
    WAIT StatReg, 16
    OUT StatReg, 16
    OUT StatReg, 0
WEND
eraseline 25

```

```
InjDelay          'Visual Delay Countdown for Injection Synch
```

```
TimeStart! = TIMER / 60 'Assume Injection Starts here
```

```
AcquireDelay
```

```
DO
```

```

    IF PtNum THEN
        PSET (PtNum - 1, AvgSignal!(StepNum - 1))
    ELSE
        CALL ViewLower
        CLS
        PSET (0, 0)    'If PtNum =0 (False) point to origin
    END IF

```

```

-----
'Fire laser PTX times and collect G.I. signal.
-----

```

```

FOR i = 1 TO PTX
    dataq 48, 0, xl, xh          'Fire Laser & valve
    Datum = xh * 16 + xl / 16

    A2D 1, xl, xh

```



CHROM.BAS

Monday, August 1, 1988  
 File Created: Thursday, June 9, 1988 at 2:37 pm

Page 7

```

      Power = xh * 16 + xl / 16
      AvgSignal!(StepNum) = AvgSignal!(StepNum) + Datum / Power
NEXT i

RetTime!(StepNum) = TIMER / 60 - TimeStart!
AvgSignal!(StepNum) = 1000 * AvgSignal!(StepNum) / PTX'Corrected Signal

LINE -(Ptnum, AvgSignal!(StepNum))
LOCATE 24, 12: PRINT USING "Laser Power = ###"; Power;
LOCATE 24, 55: PRINT USING "Ret Time = ##.## min"; RetTime!(StepNum);

'-----
'Check to see if the scan is finished, or
'if data needs to be written to disk
'-----

IF TIMER / 60 - TimeStart! >= AcqLength! THEN acq = FALSE
IF Ptnum >= MaxX! THEN 'Clear the Chromatogram if >= 10 min
  CLS 0
  Ptnum = 0
END IF

'-----
'Check to see if the excitation wavelength
'needs to be changed to the next value
'during wavelength programs.
'-----

IF TIMER / 60 - TimeStart! >= Program!(ProgNum, 1) THEN
  Lambda! = Program!(ProgNum, 2)
  IF HighRes THEN
    XET! = XETProg!(ProgNum)
  END IF
  StepMotors
  ProgNum = ProgNum + 1
END IF

'-----
'See if any command were entered
'-----

Quit$ = INKEY$
IF Quit$ <> "" THEN
  IF Quit$ = CHR$(27) THEN acq = FALSE      'ESC to Quit
  IF Quit$ = "+" THEN                      '+ increases plot scale
    MaxY! = MaxY! + .2 * MaxY!
    CALL ViewLower
  END IF
  IF Quit$ = "-" THEN                      '- decreases plot scale
    MaxY! = MaxY! - .2 * MaxY!
    CALL ViewLower
  END IF
  IF Quit$ = "p" OR Quit$ = "P" THEN      'Look at laser power
    CALL PeakPower                        'w/o acquisition
  END IF
  IF Quit$ = "c" OR Quit$ = "C" THEN      'Change to next wavelength
    IF ProgNum < NumProgs THEN
      Program!(ProgNum, 1) = TIMER / 60 - TimeStart!
    END IF
  END IF
END IF

'-----
'If another step is to be taken, increment
'the counters, and step to the next wavelength

```

CHROM.BAS

Monday, August 1, 1988  
 File Created: Thursday, June 9, 1988 at 2:37 pm

Page 8

```

-----
      IF acq THEN
          Ptnum = Ptnum + 1          'Inc Write-to-Disk Counter
          StepNum = StepNum + 1      'Inc Overall point Counter
      END IF

  LOOP WHILE acq

  AcqLength! = TIMER / 60 - TimeStart! 'Correct if scan stopped early

  END SUB 'Acquire

  REM $STATIC
  DEFSNG A-Z
  *****
      SUB AcquireDelay STATIC
  *****
  SHARED AcqDelay!, TimeStart!

  BitPatt = 16
  CTime! = 0

  IF AcqDelay! > TIMER / 60 - TimeStart! THEN
      LOCATE 14, 21
      PRINT "Acquisition Delay, Time Remaining: ";
      WHILE AcqDelay! > CTime!

          IF CTime! > AcqDelay! - .2 THEN
              BitPatt = 48
          END IF

          WAIT StatReg, 16
          OUT StatReg, BitPatt
          OUT StatReg, 0

          CTime! = TIMER / 60 - TimeStart!
          LOCATE 14, 56
          PRINT USING "##.##"; AcqDelay! - CTime!;

          abort$ = INKEY$
          IF abort$ = CHR$(27) THEN CTime! = AcqDelay!

      WEND
  END IF

  END SUB

  REM $DYNAMIC
  DEFINT A-Z
  *****
      SUB CalcXet STATIC
  *****

  SHARED Lambda!, Eighty!, T#, Cos2Phi!, DeltaX!
  SHARED SSize!, WaveFactor, Press!, XET!

  '
  '=====Calculate X's for Lambda=====
  PRINT "Calculating Look-Up Table for X(etalon). . . "
  ' Define Constants
  K1# = 1.633746278#: K2# = -4180802.917#
  K3# = 6.4328E+11: K4# = 5993.220751#
  K5# = -18711275260#: K6# = 1E+16
  Temp! = 35: X1! = 5! 'estimate of x for calc of m
  Lambda! = Lambda! * WaveFactor

```

CHROM.BAS

Monday, August 1, 1988  
 File Created: Thursday, June 9, 1988 at 2:37 pm

Page 9

'Calculate Refractive index

```

N1A# = (K1# * Lambda! ^ 4 + K2# * Lambda! ^ 2 + K3#) / (K4# * Lambda! ^ 4 + K5# * Lambda! ^ 2 + K6#)
N1B# = (Press! / 760) * (288.2 / (273.2 + Temp!))
N1# = N1A# * N1B# + 1
N2# = 1.44587 + 554453! * ((1 / Lambda!) ^ 2) - 5.45094E+12 * ((1 / Lambda!) ^ 4) +
4.76638E+19 * ((1 / Lambda!) ^ 6)

```

' CALCULATE M FOR DESIRED LAMBDA

```

M0# = (Eighty! ^ 2 * Cos2Phi!) / ((X1! + DeltaX!) ^ 2 + Eighty! ^ 2)
M1# = SQR(N2# ^ 2 - N1# ^ 2 * (1 - M0#))
M = INT(((2 * T# * M1#) / (N1# * Lambda!)) + .5)

```

' Calculate X (Etalon)

```

D1# = (M * Lambda!) / (2 * T#): D2# = (N2# / N1#)
XET! = (Eighty! * SQR((Cos2Phi! / (D1# ^ 2 - D2# ^ 2 + 1)) - 1)) - DeltaX!
CALL QUANTIZE(XET!)

```

END SUB 'CALCXET

\*\*\*\*\*

SUB ChromDef STATIC

\*\*\*\*\*

SHARED BackPress!, PMTVolt, XBeam!, Lambda!

SHARED Filter\$, filename\$, PW!, Title\$, PTX, NumProgs

SHARED InjTemp!, TransTemp!, ValveTemp!, TempProg\$, AcqLength!, AcqDelay!

OPEN "Chrom.Def" FOR OUTPUT AS #6

```

PRINT #6, Lambda!
PRINT #6, BackPress!
PRINT #6, PMTVolt
PRINT #6, XBeam!
PRINT #6, Filter$
PRINT #6, filename$
PRINT #6, PW!
PRINT #6, Title$
PRINT #6, PTX
PRINT #6, InjTemp!
PRINT #6, TransTemp!
PRINT #6, ValveTemp!
PRINT #6, TempProg$
PRINT #6, AcqLength!
PRINT #6, AcqDelay!
PRINT #6, NumProgs
FOR i = 1 TO NumProgs
  PRINT #6, Program!(i, 1), Program!(i, 2)
NEXT i

```

CLOSE #6

END SUB 'ChromDef

\*\*\*\*\*

SUB CMX4DAT STATIC

\*\*\*\*\*

SHARED XOET!, XOBI!, Delay2B!, Delay4A!, Press!, LabTemp!, XOUV!

```

OPEN "CMX4DAT.DAT" FOR OUTPUT AS #5 'Write Current conditions to file
PRINT #5, XOET!
PRINT #5, XOBI!
PRINT #5, Delay2B!

```

[illegible]

```
ON ERROR GOTO 0

END FUNCTION

REM $DYNAMIC
*****
      SUB FRAME STATIC
*****

'=====Draw Plot Frame=====

SCREEN 2
'Draw upper window frame
LINE (72, 3)-(639, 50), , B
'Draw lower window frame
LINE (72, 51)-(639, 181), , B
'Place Tick Marks on Y-axis of lower window

FOR y = 52 TO 180 STEP 32
    LINE (68, y)-(72, y)
NEXT y
CALL Yscale

END SUB 'FRAME

*****
      SUB Frame2 STATIC
*****

SHARED MaxY!, MinY!, LenTitle, Range!, Title$

' Frame for Replot of data set
CLS 0
VIEW
WINDOW

Range! = MaxY! - MinY!
LINE (72, 12)-(639, 172), , B
LOCATE 1, (10 + (70 - LenTitle) / 2)
PRINT Title$
FOR y = 12 TO 172 STEP 40
    LINE (68, y)-(72, y)
NEXT y
FOR i = 0 TO 4
    LOCATE (22 - (i * 5)), 1
    PRINT USING "####.##"; Range! * (.25 * i) + MinY!
NEXT i

END SUB 'FRAME2

REM $STATIC
'>>>>>>>>>>>>>>>>>>>>>>>>>>>>>>>>>>>
FUNCTION GetBFX! (B0!, B1!, B2!, Lambda!)
'>>>>>>>>>>>>>>>>>>>>>>>>>>>>>>>>>>>

GetBFX! = (-B1! + SQR(B1! ^ 2 - 4 * B2! * (B0! - Lambda!))) / (2 * B2!)

END FUNCTION

'>>>>>>>>>>>>>>>>>>>>>>>>>>>>>>>>>>>
FUNCTION GetUVX! (U0!, U1!, U2!, Lambda!) STATIC
'>>>>>>>>>>>>>>>>>>>>>>>>>>>>>>>>>>>

GetUVX! = U0! + U1! * Lambda! + U2! * ((Lambda!) ^ 2)
```

CHROM.BAS

Monday, August 1, 1988  
 File Created: Thursday, June 9, 1988 at 2:37 pm

Page 12

END FUNCTION

REM \$DYNAMIC

\*\*\*\*\*

SUB INITIALIZE STATIC

\*\*\*\*\*

SHARED T#, Eighty!, Cos2Phi!, DeltaX!, B0!, B1!, B2!, U0!, U1!, U2!

SHARED NDFBeam\$, RepRate, NDFLPM\$, scale!, X0ET!, X0BI!, X0UV!

SHARED Delay2B!, Delay4A!, Press!, LabTemp!

SHARED BackPress!, PMTVolt, XBeam!, Lambda!

SHARED Filter\$, filename\$, PW!, Title\$, PTX, NumProgs

SHARED InjTemp!, TransTemp!, ValveTemp!, TempProg\$, AcqLength!, AcqDelay!

'=====Read in Calibration Parameters=====

OPEN "CMX4CAL.DAT" FOR INPUT AS #1

INPUT #1, T#

INPUT #1, Eighty!

INPUT #1, Cos2Phi!

INPUT #1, DeltaX!

INPUT #1, B0!

INPUT #1, B1!

INPUT #1, B2!

INPUT #1, U0!

INPUT #1, U1!

INPUT #1, U2!

CLOSE #1

'Set Default Parameters

NDFBeam\$ = "None"

RepRate = 5

NDFLPM\$ = "None"

scale! = 4095

'Read in additional defaults from disk file

OPEN "CMX4DAT.DAT" FOR INPUT AS #5 'Read Current conditions From file

INPUT #5, X0ET!

INPUT #5, X0BI!

INPUT #5, Delay2B!

INPUT #5, Delay4A!

INPUT #5, Press!

INPUT #5, LabTemp!

INPUT #5, X0UV!

CLOSE #5

OPEN "CHROM.DEF" FOR INPUT AS #6

INPUT #6, Lambda!

INPUT #6, BackPress!

INPUT #6, PMTVolt

INPUT #6, XBeam!

INPUT #6, Filter\$

INPUT #6, filename\$

INPUT #6, PW!

LINE INPUT #6, Title\$

INPUT #6, PTX

INPUT #6, InjTemp!

INPUT #6, TransTemp!

INPUT #6, ValveTemp!

LINE INPUT #6, TempProg\$

INPUT #6, AcqLength!

INPUT #6, AcqDelay!

INPUT #6, NumProgs

FOR i = 1 TO NumProgs

INPUT #6, Program!(i, 1), Program!(i, 2)

NEXT i

CHROM.BAS

Monday, August 1, 1988  
File Created: Thursday, June 9, 1988 at 2:37 pm

Page 13

```

        Program!(NumProgs + 1, 1) = -1
    CLOSE #6

END SUB 'INITIALIZE

REM $STATIC
*****
    SUB InjDelay STATIC
*****

        VIEW (73, 52)-(639, 180)
        WINDOW (1, 6)-(22, 1)
        FOR i = 2 TO 20 STEP 2
            LINE (i, 3)-(i + 1, 4), , BF
        NEXT i
        Block = 20

        WHILE Block > 0
            InjStart! = TIMER
            WHILE TIMER - InjStart! < 2
                WAIT StatReg, 16
                OUT StatReg, 16
                OUT StatReg, 0
            WEND
            LINE (Block, 3)-(Block + 1, 4), 0, BF
            Block = Block - 2
        WEND

END SUB

REM $DYNAMIC
*****
    SUB PeakPower STATIC
*****
    SHARED scale!, acq

    'Initialize Variables
    Quit = 0
    marker = 0
    redraw = -1
    Largest = 2055
    scale! = 2500
    IF acq THEN
        TrigByte = 48
    ELSE
        TrigByte = 32
    END IF

    eraseline 24

DO
    IF redraw THEN

        CALL ViewUpper
        CLS 1
        LOCATE 24, 30: PRINT USING "Y-max = ####"; scale!;
        Xpos = 0
        marker = -1
        redraw = 0
    END IF

    dataq 32, 1, xl, xh          'Fire Laser
    Lpower = xh * 16 + xl / 16   'Combine

    LINE (Xpos, 2048)-(Xpos + 2, Lpower), , BF      'draw histogram

```

CHROM.BAS

Monday, August 1, 1988  
 File Created: Thursday, June 9, 1988 at 2:37 pm

Page 14

```

LOCATE 24, 5: PRINT USING "Laser Power = ####"; Lpower;

Xpos = Xpos + 3
IF Lpower > Largest THEN marker = -1

IF marker THEN
  LINE (2, Largest)-(198, Largest + 3), 0, BF
  IF Lpower > Largest THEN Largest = Lpower
  LINE (2, Largest)-(198, Largest + 3), , BF
  marker = 0
  LOCATE 24, 50
  PRINT "Max = "; Largest;
  PRINT USING "(#.### V)"; (Largest - 2048) * .00244;
END IF

IF Xpos >= 200 THEN redraw = -1

Quit$ = INKEY$
IF Quit$ <> "" THEN
  IF Quit$ = CHR$(32) THEN Quit = -1
  IF Quit$ = "+" THEN scale! = scale! + 250
  IF Quit$ = "-" THEN scale! = scale! - 250
  IF Quit$ = "H" OR Quit$ = "h" THEN
    CALL UVHyst
  END IF
  redraw = -1
END IF

LOOP UNTIL Quit

CALL ViewLower

eraseline 24
eraseline 25

END SUB 'PEAKPOWER

REM $STATIC
*****
SUB PlotData STATIC
*****

SHARED StepNum, MinY!, MaxX!, MaxY!, AvgSignal!()

'=====Plot Current Data Set=====

VIEW (73, 13)-(638, 171)
WINDOW (0, MinY!)-(MaxX!, MaxY!)
PSET (0, MinY!)
FOR i = 1 TO StepNum
  LINE -(i, AvgSignal!(i))
NEXT

END SUB 'PlotData

REM $DYNAMIC
*****
SUB PREAQ STATIC
*****

SHARED Press!, LabTemp!, XOET!, XOBI!, XOUV!, RepRate, NDFLPM$

'=====Pre Acquisition Functions=====
CLS

```



CHROM.BAS

Monday, August 1, 1988  
 File Created: Thursday, June 9, 1988 at 2:37 pm

Page 15

```

PRINT "CHROM "; VERSION
PRINT "High-Resolution LIF/Chromatographic Data Acquisition Program"
PRINT "(C) 1986, 87, 88 Scott J. Hein"
PRINT
PRINT "Input Pressure of air surrounding etalon (; Press!; " TORR) ";
  INPUT TPRESS$
  IF TPRESS$ <> "" THEN Press! = VAL(TPRESS$)
PRINT "What is the Current Lab Temperature (; LabTemp!; " C) ";
  INPUT TLABTEMP$
  IF TLABTEMP$ <> "" THEN LabTemp! = VAL(TLABTEMP$)
PRINT "Current Etalon Turns # (; XOET!; "); ";
  INPUT TXET$
  IF TXET$ <> "" THEN XOET! = VAL(TXET$)
PRINT "Birefringent Filter Micrometer Setting (; XOB!; "); ";
  INPUT TXBI$
  IF TXBI$ <> "" THEN XOB! = VAL(TXBI$)
PRINT "UV Doubling Crystal Dial Setting (; XOUV!; "); ";
  INPUT TXUV$
  IF TXUV$ <> "" THEN XOUV! = VAL(TXUV$)
PRINT "Input Laser Rep Rate (; RepRate; " Hz) ";
  INPUT TREP$
  IF TREP$ <> "" THEN RepRate = VAL(TREP$)
PRINT "Neutral Density Filter for Laser Power Monitor (; NDFLPM$; "); ";
  INPUT tndf$
  IF tndf$ <> "" THEN NDFLPM$ = tndf$
CALL CMX4DAT 'Write any changed parameters to CMX4DAT

END SUB 'PREAQ

*****
SUB QUANTIZE (XET!) STATIC
*****

'=====Quantize XET=====

  XLEFT = INT(CDBL(XET!))
  XRIGHT# = CDBL(XET!) - XLEFT
  R1# = 100 * XRIGHT#
  R2 = INT(R1#)
  R3# = R1# - R2
  IF R3# < .25 THEN R3# = 0
  IF R3# >= .25 AND R3# < .75 THEN R3# = .5
  IF R3# >= .75 THEN R3# = 0: R2 = R2 + 1
  XRIGHT# = (R2 + R3#) / 100
  XET! = XLEFT + XRIGHT#

END SUB 'QUANTIZE

*****
SUB SCALEDATA STATIC
*****

SHARED Largest!, Smallest!, StepNum, AvgSignal!(), MaxX!, MaxY!, MinY!
SHARED CurrentX, XLargest!

'=====Determine Largest data Point & Scale Factor=====
eraseline 25: PRINT "Sorting Data and Determining New Scale Factor. . .";
Largest! = AvgSignal!(1): XLargest = 0
Smallest! = AvgSignal!(1)
FOR i = 1 TO StepNum
  IF Largest! < AvgSignal!(i) THEN
    Largest! = AvgSignal!(i)
    XLargest = i
  END IF
  IF Smallest! > AvgSignal!(i) THEN

```

CHROM.BAS

Monday, August 1, 1988  
 File Created: Thursday, June 9, 1988 at 2:37 pm

Page 16

```

      Smallest! = AvgSignal!(i)
    END IF
  NEXT i

  MaxX! = StepNum
  MaxY! = Largest!
  MinY! = Smallest!
  CLS
  CALL Frame2 'Draw Axes
  CALL PlotData

END SUB 'SCALEDATA

*****
      SUB ScanParam STATIC
*****

  SHARED Title$, LenTitle, IDNum$, WaveFactor, HighRes, UV.Scan
  SHARED NLSteps, PTX, Delay2B!, Delay4A!, BackPress!, AcqDelay!
  SHARED DGas$, PMTVolt, LampVolt!, XBeam!, Filter$, PW!, Lambda!, DataPts
  SHARED RepRate, InjTemp!, TransTemp!, ValveTemp!, TempProg$, AcqLength!

  ScanInfo = FALSE
  DO
    CLS
    PRINT "Enter Short (< 80 Chars.) title for this Data Set:"
    Input$ Title$
    PRINT
    IF LEN(Title$) > 80 THEN
      Title$ = MID$(Title$, 1, 80)
    END IF
    LenTitle = LEN(Title$)

    PRINT
    PRINT "Spectroscopic Parameters:"
    PRINT "=====
    PRINT

    INPUT "Is this a UV Scan <Y or N> ", TWaveFactor$

      IF TWaveFactor$ = "n" OR TWaveFactor$ = "N" THEN
        WaveFactor = 1
        UV.Scan = FALSE
      ELSE
        WaveFactor = 2
        UV.Scan = TRUE
      END IF

    INPUT "Is this a (H)igh or (L)ow Resolution Scan ", Tres$
    IF Tres$ = "H" OR Tres$ = "h" THEN
      HighRes = TRUE
    ELSE
      HighRes = FALSE
    END IF

    PRINT "Enter # of Pulses (Shots) to Average for each Data Point (; PTX; ");
    INPUT "", TPTX
    IF TPTX <> 0 THEN PTX = TPTX

    PRINT "Enter Desired Valve Pulse Width (; PW!; " mS): ";
    INPUT "", TPW$
    IF TPW$ <> "" THEN PW! = VAL(TPW$)

    PRINT "What is DELAY 2B (; Delay2B!; ");
    INPUT "", TDELAY2B$
    IF TDELAY2B$ <> "" THEN Delay2B! = VAL(TDELAY2B$)
  
```

CHROM.BAS

Monday, August 1, 1988  
 File Created: Thursday, June 9, 1988 at 2:37 pm

Page 17

```

PRINT "What is DELAY 4A ("; Delay4A!; ")": ";
      INPUT "", TDELAY4A$
      IF TDELAY4A$ <> "" THEN Delay4A! = VAL(TDELAY4A$)
PRINT "Backing Pressure ("; BackPress!; " psi): ";
      INPUT "", TBACK!
      IF TBACK! <> 0 THEN BackPress! = TBACK!
PRINT "PMT Voltage ("; PMTVolt; " V): ";
      INPUT "", TPMTVOLT
      IF TPMTVOLT <> 0 THEN PMTVolt = TPMTVOLT
PRINT "X: Beam to Nozzle Distance ("; XBeam!; " mm): ";
      INPUT "", TXBEAM!
      IF TXBEAM! <> 0 THEN XBeam! = TXBEAM!
PRINT "Emission Filter Used ("; Filter$; ")": ";
      INPUT "", TFILTER$
      IF TFILTER$ <> "" THEN Filter$ = TFILTER$

PRINT
PRINT "Chromatographic Parameters:"
PRINT "=====
PRINT

PRINT "Injection Port Temperature ("; InjTemp!; ")": ";
      INPUT "", Tinj!
      IF Tinj! <> 0 THEN InjTemp! = Tinj!
PRINT "Transfer Line Temperature ("; TransTemp!; ")": ";
      INPUT "", TTrans!
      IF TTrans! <> 0 THEN TransTemp! = TTrans!
PRINT "Valve Temperature ("; ValveTemp!; ")": ";
      INPUT "", TValve!
      IF TValve! <> 0 THEN ValveTemp! = TValve!
PRINT "Oven Temperature Program: ";
      Input$ TempProg$
      PRINT
PRINT "Data Acquisition/Chromatogram Length ("; AcqLength!; " min): ";
      INPUT "", TAcq!
      IF TAcq! <> 0 THEN AcqLength! = TAcq!
PRINT "Acquisition Delay After Injection ("; AcqDelay!; "min): ";
      INPUT "", Tdel$
      IF Tdel$ <> "" THEN AcqDelay! = VAL(Tdel$)
      RunLen! = AcqLength! - AcqDelay!
      DataPts = RepRate * 60 * (AcqLength! - AcqDelay!) / PTX

PRINT
PRINT "The Total Acquisition Time will Be "; RunLen!; " minutes"
PRINT "Which, at "; RepRate; " Hz will require "; RunLen! * RepRate * 60; " laser shots."
PRINT "Averaging "; PTX; " shots for each point will result in"
PRINT DataPts; " total averaged data points for the run."

PRINT : PRINT "Are These Parameters Satisfactory? <Y or N> ";
POK$ = ""
WHILE POK$ = "": POK$ = INKEY$: WEND

IF POK$ = "N" OR POK$ = "n" THEN
  ScanInfo = TRUE
ELSE
  ScanInfo = FALSE
END IF

LOOP WHILE ScanInfo

WaveProgram

CALL CMX4DAT
CALL ChromDef

END SUB 'ScanParam

```

CHROM.BAS

Monday, August 1, 1988  
File Created: Thursday, June 9, 1988 at 2:37 pm

Page 18

```

REM $STATIC
*****
      SUB Step.UV.Motor (NumSteps, direction)
*****

Dly = Dly1
IF direction THEN          'If direction is forward (<> 0)
      OUT portadd, 16      'Preset direction
      FOR i = 1 TO NumSteps
          Pulse 5, portadd, 48, 16
          delay Dly
          IF Dly > Dly2 THEN Dly = Dly - 1
      NEXT i
      XOUV! = XOUV! + NumSteps * .1
ELSE
      OUT portadd, 0       'Preset direction
      FOR i = 1 TO NumSteps
          Pulse 5, portadd, 32, 0
          delay Dly
          IF Dly > Dly2 THEN Dly = Dly - 1
      NEXT i
      XOUV! = XOUV! - NumSteps * .1
END IF

END SUB

REM $DYNAMIC
*****
      SUB StepMotors STATIC
*****

SHARED Lambda!, HighRes, UV.Scan, XET!, XOET!, XOB!!, XOUV!
SHARED B0!, B1!, B2!, U0!, U1!, U2!, StepNum, XBI!, XUV!, WaveFactor

REDIM NSteps(3), BitPat(3)

'This subprogram
'First, Determine the Number of steps each tuning element will have to
'be stepped by calculating the delta X and converting it to steps.

      'Calculate Desired B.F. Position
      'Note BF is calibrated with visible wavelengths & thus the desired
      'UV wavelength must be multiplied by wavefactor (2) to get the correct
      'X value.

      XBI! = GetBFX!(B0!, B1!, B2!, Lambda! * WaveFactor)
      DXBI# = XBI! - XOB!!          'DXET!/DXBI# = # of units to step

      IF HighRes THEN
          DXET! = XET! - XOET! 'XET = DESIRED X, XOET = CURRENT X
      ELSE
          DXET! = 0
      END IF

      IF UV.Scan THEN
          XUV! = GetUVX!(U0!, U1!, U2!, Lambda!)
          DXUV# = XUV! - XOUV!
      ELSE
          DXUV# = 0
      END IF

      CALL DISPLAYX 'Display Lambda,Xet,Xbi,Xuv 'Display Desired X's

      NSteps(1) = INT((1111.65 * DXBI#) + .5)      'BF:1111.65 STEPS/DIAL UNIT

```

CHROM.BAS

Monday, August 1, 1988  
 File Created: Thursday, June 9, 1988 at 2:37 pm

Page 19

```

    NXBI = NSteps(1)           'Save for later
    NSteps(2) = INT((200 * DXET!) + .5) 'ET:200 STEPS/DIAL UNIT
    NXET = NSteps(2)           'Save for later
    NSteps(3) = INT(10 * DXUV# + .5) 'UV:10 steps/dial unit
    NXUV = NSteps(3)

'Assign Birefringent Filter Step Parameters

    IF NSteps(1) < 0 THEN
        BitPat(1) = 8           'Bit Pattern to Step B.F. (-)
    ELSEIF NSteps(1) > 0 THEN
        BitPat(1) = 4           'Bit Pattern to Step B.F. (+)
    ELSE
        BitPat(1) = 0
    END IF

'Set up Etalon stepping Parameters

    IF NSteps(2) < 0 THEN
        BitPat(2) = 1           'Bit Pattern to step Etalon (-)
    ELSEIF NSteps(2) > 0 THEN
        BitPat(2) = 2           'Bit Pattern to step Etalon (+)
    ELSE
        BitPat(2) = 0
    END IF

'Set up UV Crystal Stepping parameters

    IF NSteps(3) < 0 THEN
        BitPat(3) = 32
        ByteOff = 0
        AddSteps = 200
        NSteps(3) = NSteps(3) - AddSteps
    ELSEIF NSteps(3) > 0 THEN
        BitPat(3) = 48
        ByteOff = 16
        AddSteps = 0
    ELSE
        BitPat(3) = 0
        ByteOff = 0
        AddSteps = 0
    END IF

'Make NSteps() an absolute number of steps since the stepping direction is
'already encoded in the Bit Pattern.

    FOR i = 1 TO 3
        NSteps(i) = ABS(NSteps(i))
    NEXT i

'Now, sort the stepping parameters on NSteps using a simple bubble sort

    DO
        Swapped = FALSE
        FOR i = 1 TO 2
            IF NSteps(i) > NSteps(i + 1) THEN
                SWAP NSteps(i), NSteps(i + 1)
                SWAP BitPat(i), BitPat(i + 1)
                Swapped = TRUE
            END IF
        NEXT i
    LOOP WHILE Swapped

'Now, set up BitPat, & NSteps for the loop: They are now sorted from
'lowest number of steps to highest. This means that All 3 will be stepped

```

CHROM.BAS

Monday, August 1, 1988  
 File Created: Thursday, June 9, 1988 at 2:37 pm

Page 20

'together for NSteps(1), using a Bit Pattern which is the sum of all 3  
 'individual bit patterns. Next, the elements with the middle and largest  
 'number of steps will be stepped together for the additional steps required  
 'to reach NSteps(2) using the Bit Pattern which is the sum of these two  
 'individual patterns. Finally, The element with the largest number of steps  
 'will be stepped the remaining amount needed to reach its desired NSteps(3)  
 'using only its own Bit Pattern.

NSteps(3) = NSteps(3) - NSteps(2)  
 NSteps(2) = NSteps(2) - NSteps(1)

BitPat(1) = BitPat(1) + BitPat(2) + BitPat(3)  
 BitPat(2) = BitPat(2) + BitPat(3)

' Loop for Stepping Both Motors at the same time

Dly = Dly1

OUT portadd, ByteOff 'Set stepper motor direction

FOR k = 1 TO 3

FOR i = 1 TO NSteps(k)

Pulse Pwidth, portadd, BitPat(k), ByteOff

delay Dly

IF Dly > Dly2 THEN Dly = Dly - 1

NEXT i

NEXT k

'Compensate for UV Hysterisis Addsteps

IF AddSteps THEN

Step.UV.Motor AddSteps, Forward

END IF

'If any Steps were taken, adjust X0BI for the actual distance in X-units.

'This helps eliminate rounding error which occurs when very high resolution

'scans are attempted where the B.F. is only stepped every few data points.

'Also reset the current etalon position, X0ET! and X0UV! to the new position.

IF NXBI <> 0 THEN X0BI! = X0BI! + NXBI \* (.000899564#)  
 ' .0008996 units/step

IF NXET <> 0 THEN X0ET! = XET!

IF NXUV <> 0 THEN X0UV! = X0UV! + NXUV \* .1

END SUB 'STEPMOTORS

SUB TIMERINIT STATIC

\*\*\*\*\*

'=====Set up Dash8 Timer=====

SHARED PW!

COUNT = INT((PW! \* .001 \* 2386400!) + .5)

HIBYTE = FIX(COUNT / 256)

LOBYTE = (COUNT / 256 - HIBYTE) \* 256

OUT TimeReg, 178 'Set up Register

OUT Counter2, LOBYTE 'Low Byte to Counter

OUT Counter2, HIBYTE 'High Byte to Counter

END SUB 'TIMERINIT

REM \$STATIC

\*\*\*\*\*

CHROM.BAS

Monday, August 1, 1988  
 File Created: Thursday, June 9, 1988 at 2:37 pm

Page 21

```

      SUB UVHyst STATIC
      *****

      'Subroutine to step UV stepper motor back 100 steps and forward 100 steps
      'to remove hysteresis effects

      Step.UV.Motor 100, Reverse
      Step.UV.Motor 100, Forward

      END SUB 'UVHyst

      *****
      SUB Video.Mode STATIC
      *****

      SHARED FromGPMENU AS INTEGER

      '-----
      '          Check to see if Display Adaptor is OK for Graphics

      DEF SEG = 0 'Set the segment to look in low memory
      V.Mode = PEEK(&H449) 'Byte 449 hex is the video mode byte
      DEF SEG      'Reset the default segment just to be safe

      IF V.Mode = 7 THEN 'Mode 7 is monochrome mode which cannot display
                        'graphics on this Corona Computer.
          CLS
          PRINT "A CGA, or EGA graphics adaptor is required by this program."
          PRINT "Remember to put the computer in MODE BW80, or C080."
          PRINT
          PRINT "Press any key to continue . . . .";
          WHILE INKEY$ = "": WEND
          CLS
          IF FromGPMENU THEN
              CHAIN "GPMENU"
          ELSE
              END
          END IF
      END IF

      '-----

      END SUB

      REM $DYNAMIC
      *****
      SUB ViewLower STATIC
      *****

      SHARED MaxX!, MaxY!, MinY!

      'Switch Graphics Window to lower view for data acquisition

          VIEW (73, 52)-(638, 179)
          WINDOW (0, MinY!)-(MaxX!, MaxY!)
          CALL Yscale

      END SUB 'ViewLower

      *****
      SUB ViewUpper STATIC
      *****

      SHARED scale!
  
```

CHROM.BAS

Monday, August 1, 1988  
File Created: Thursday, June 9, 1988 at 2:37 pm

Page 22

'Switch graphics window to upper view, for laser power adjustment

VIEW (73, 4)-(638, 48)  
WINDOW (0, 2048)-(200, scale!)

END SUB 'ViewUpper

REM \$STATIC

\*\*\*\*\*

SUB WaveProgram STATIC

\*\*\*\*\*

SHARED NumProgs, AcqLength!, Lambda!, XET!

ProgOK = FALSE

Program!(NumProgs + 1, 1) = -1

DO

CLS

PRINT "Enter the desired Retention times and wavelength pairs for this scan."

PRINT "Entering -1 for a retention time will terminate data entry"

PRINT

TRet\$ = ""

n = 0

WHILE (TRet\$ &lt;&gt; "-1") AND (n &lt; 10)

n = n + 1

PRINT "Ret. Time "; n; " in minutes ("; Program!(n, 1); "): ";

INPUT "", TRet\$

IF TRet\$ &lt;&gt; "" THEN

Program!(n, 1) = VAL(TRet\$)

ELSE

TRet\$ = STR\$(Program!(n, 1))

END IF

IF VAL(TRet\$) &gt;= 0 THEN

PRINT "Wavelength "; n; " in "; CHR\$(143); " ("; Program!(n, 2); "):

";

INPUT "", TWave!

IF TWave! &lt;&gt; 0 THEN Program!(n, 2) = TWave!

END IF

PRINT

WEND

NumProgs = n - 1

CLS

PRINT " # Ret Time Wavelength"

PRINT "=== ======"

FOR i = 1 TO NumProgs

PRINT USING "###.###.###"; i, Program!(i, 1), Program!(i,

2)

NEXT i

PRINT "=== ======"

PRINT

PRINT "Is this wavelength program OK? &lt;Y or N&gt; ";

Resp\$ = ""

WHILE Resp\$ = "": Resp\$ = INKEY\$: WEND

IF Resp\$ = "Y" OR Resp\$ = "y" THEN

ProgOK = TRUE

ELSE

ProgOK = FALSE

END IF



CHROM.BAS

Monday, August 1, 1988  
 File Created: Thursday, June 9, 1988 at 2:37 pm

Page 23

```
LOOP UNTIL ProgOK
```

```
'Set the upper limit for the wavelength program to the
'length of the run and the last wavelength
```

```
Program!(NumProgs + 1, 1) = AcqLength! + 1
Program!(NumProgs + 1, 2) = Program!(NumProgs, 2)
```

```
'Calculate XET for each of the program wavelengths if needed
IF HighRes THEN
```

```
  FOR i = 1 TO NumProgs
    Lambda! = Program!(i, 2)
    CalcXet
    XETProg!(i) = XET!
```

```
  NEXT i
```

```
END IF
```

```
END SUB
```

```
REM $DYNAMIC
```

```
*****
      SUB WRITEDATA STATIC
*****
```

```
SHARED IDNum$, Title$, UV.Scan, Raw.Data
```

```
'=====Write Info to Data File=====
```

```
FOR i = 1 TO 2
```

```
  PRINT #i, "Fluorescence Excitation Chromatogram Data"
```

```
  PRINT #i, "-----"
```

```
  PRINT #i,
```

```
  IF UV.Scan THEN
```

```
    PRINT #i, "UV doubled excitation laser beam with"
```

```
  ELSE
```

```
    PRINT #i, "Fundamental excitation laser beam with"
```

```
  END IF
```

```
  IF HighRes THEN
```

```
    PRINT #i, "High-resolution wavelength selection using etalon and B.F."
```

```
  ELSE
```

```
    PRINT #i, "Low-resolution wavelength selection using only the B.F."
```

```
  END IF
```

```
  PRINT #i, ""
```

```
  PRINT #i, DATE$, TIME$
```

```
  PRINT #i, "": PRINT #i, Title$
```

```
NEXT i
```

```
END SUB 'WRITEDATA
```

```
*****
      SUB Yscale STATIC
*****
```

```
SHARED MaxY!, MinY!
```

```
  Range! = MaxY! - MinY!
```

```
  FOR i = 0 TO 4
```

```
    LOCATE (23 - (i * 4)), 2
```

```
    PRINT USING "###.##"; Range! * (.25 * i) + MinY!
```

```
  NEXT i
```

CHROM.BAS

Monday, August 1, 1988

Page 24

File Created: Thursday, June 9, 1988 at 2:37 pm

END SUB 'YScale

GPMENU.BAS

Monday, August 1, 1988  
 File Created: Thursday, June 9, 1988 at 2:21 pm

Page 1

```
DECLARE SUB ParseDate (Day$, Month$, Year$)
```

```
'=====
```

```
'Program GPMENU.BAS      Master menu program to coordinate control,  
'                        calibration, and data acquisition of the CMX-4  
'                        laser system.
```

```
'Written by:  Scott J. Hein      -----  
'            Dept. of Chemistry      Ver 3.20  
'            Oregon State University  5 May 1988  
'            Corvallis, OR 97331      -----
```

```
'Written in BASIC for use with the QuickBasic Compiler, Version 4.0. Can  
'be compiled within the editor or from the command line (externally).
```

```
'-----  
'                        Revision List  
'Initials      Date      Lines      Comments  
'=====
```

Initials	Date	Lines	Comments
SJH	7-17-87	--	Completed version 2.0, 8087 numeric coprocessor now required.
SJH	7-31-87	Several	PEAK added as option 9. Menu rewritten using SELECT CASE
SJH	8-28-87		UVCAL Replaces ACQ as Option 8
SJH	9-9-87		Menu Outline Code improved, CHAIN replaces RUN, COMMON FromGPMENU added, recompiled with QB4.
SJH	5-5-88		Chrom option added (C)

```
'=====
```

```
COMMON FromGPMENU AS INTEGER
```

```
FromGPMENU = 1
```

```
CONST Version = 3.2
```

```
Quit = 0
```

```
DO
```

```
CLS  

SelColl = 8      'Left Column of Selection Numbers  

OptColl = SelColl + 5      'Left Column of Corresponding Options  

SelColR = 46     'Right Column of Selection Numbers  

OptColR = SelColR + 5      'Right Column of Corresponding Options  

OutT = 3         'Outline Top Y (Vertical) Coordinate  

OutL = 2         'Outline Left X (Horizontal) Coordinate  

OutR = 78        'Outline Right X (Horizontal) Coordinate  

OutB = OutT + 19  'Outline Bottom Y (Vertical) Coordinate  

OutDiv = OutT + 4 'Y coordinate of first Horizontal division  

Outdiv2 = OutT + 6 'Y coordinate of Second Horizontal division
```

```
'-----  
'Draw Menu Outline  
'-----
```

```
top$ = CHR$(218) + STRING$(OutR - OutL - 1, CHR$(196)) + CHR$(191)  

Sides$ = CHR$(179) + SPACES$(OutR - OutL - 1) + CHR$(179)  

cross$ = CHR$(195) + STRING$(OutR - OutL - 1, CHR$(196)) + CHR$(180)  

Bottom$ = CHR$(192) + STRING$(OutR - OutL - 1, CHR$(196)) + CHR$(217)
```

```
Ypos = OutT  

LOCATE Ypos, OutL  

PRINT top$;
```

```
DO
```

```
Ypos = Ypos + 1  

LOCATE Ypos, OutL
```

GPMENU.BAS

Monday, August 1, 1988  
 File Created: Thursday, June 9, 1988 at 2:21 pm

Page 2

```

    PRINT Sides$;

    LOOP UNTIL Ypos = OutDiv - 1

    Ypos = Ypos + 1
    Xpos = OutL
    LOCATE Ypos, Xpos
    PRINT cross$;

    DO
        Ypos = Ypos + 1
        LOCATE Ypos, OutL
        PRINT Sides$

    LOOP UNTIL Ypos = Outdiv2 - 1

    Ypos = Ypos + 1
    Xpos = OutL
    LOCATE Ypos, Xpos
    PRINT cross$;
    DO
        Ypos = Ypos + 1
        LOCATE Ypos, OutL
        PRINT Sides$
    LOOP UNTIL Ypos = OutB

    Ypos = Ypos + 1
    Xpos = OutL
    LOCATE Ypos, Xpos
    PRINT Bottom$;

'-----
'Heading
'-----

LOCATE OutT + 1, 20: PRINT "Data Acquisition and Control Software";
LOCATE OutT + 2, 17
    PRINT USING "for the Chromatix CMX-4 Dye Laser: Ver #.##"; Version;
LOCATE OutT + 3, 23: PRINT "(C) 1986, 87, 88  Scott J. Hein ";
LOCATE OutT + 5, 34: PRINT "MENU OPTIONS";

    CALL ParseDate(Day$, Month$, Year$)
    LOCATE OutT + 5, 10
    PRINT Day$; " "; Month$; " "; Year$;

'-----
'Menu Options
'-----

LOCATE OutT + 8, SelColl: COLOR 0, 7: PRINT " 1 "; : COLOR 7, 0
LOCATE OutT + 8, OptColl: PRINT "Calibrate CMX-4";
LOCATE OutT + 10, SelColl: COLOR 0, 7: PRINT " 2 "; : COLOR 7, 0
LOCATE OutT + 10, OptColl: PRINT "Simplex Optimization";
LOCATE OutT + 12, SelColl: COLOR 0, 7: PRINT " 3 "; : COLOR 7, 0
LOCATE OutT + 12, OptColl: PRINT "Poly Fit of B.F. & UV Data";
LOCATE OutT + 14, SelColl: COLOR 0, 7: PRINT " 4 "; : COLOR 7, 0
LOCATE OutT + 14, OptColl: PRINT "Acquire Fluorescence Spectra";
LOCATE OutT + 16, SelColl: COLOR 0, 7: PRINT " 5 "; : COLOR 7, 0
LOCATE OutT + 16, OptColl: PRINT "Edit (NE) BIFILTER.DAT";
LOCATE OutT + 18, SelColl: COLOR 0, 7: PRINT " C "; : COLOR 7, 0
LOCATE OutT + 18, OptColl: PRINT "Chromatographic Acquisition";

LOCATE OutT + 8, SelColR: COLOR 0, 7: PRINT " 6 "; : COLOR 7, 0
LOCATE OutT + 8, OptColR: PRINT "Edit (NE) ETALON.DAT";
LOCATE OutT + 10, SelColR: COLOR 0, 7: PRINT " 7 "; : COLOR 7, 0

```

GPMENU.BAS

Monday, August 1, 1988  
File Created: Thursday, June 9, 1988 at 2:21 pm

Page 3

```

LOCATE OutT + 10, OptColR: PRINT "DOS Shell (Return via EXIT)";
LOCATE OutT + 12, SelColR: COLOR 0, 7: PRINT " 8 "; : COLOR 7, 0
LOCATE OutT + 12, OptColR: PRINT "Calibrate Doubling Crystal";
LOCATE OutT + 14, SelColR: COLOR 0, 7: PRINT " 9 "; : COLOR 7, 0
LOCATE OutT + 14, OptColR: PRINT "Peak Laser Power";
LOCATE OutT + 16, SelColR: COLOR 0, 7: PRINT " P "; : COLOR 7, 0
LOCATE OutT + 16, OptColR: PRINT "Plot Fluor. or Chrom. Data";
LOCATE OutT + 18, SelColR: COLOR 0, 7: PRINT " Q "; : COLOR 7, 0
LOCATE OutT + 18, OptColR: PRINT "Quit and Return to DOS";

```

```

done = 0
ESC$ = CHR$(27)

```

DO

```

RESP$ = INKEY$
SELECT CASE RESP$
  CASE ""
    LOCATE OutT + 5, 65
    PRINT TIMES$;
  CASE "1"
    CHAIN "CMX4CAL"
  CASE "2"
    CHAIN "SIMPLEX"
  CASE "3"
    CHAIN "BIFIT"
  CASE "4"
    CHAIN "SPECTRUM"
  CASE "5"
    SHELL "ne bifilter.dat"
    done = -1
  CASE "6"
    SHELL "ne etalon.dat"
    done = -1
  CASE "7"
    CLS
    PRINT "          IMPORTANT NOTES"
    PRINT
    PRINT "1. Type Exit to Return to th CMX-4 Menu."
    PRINT "2. Do not load any Memory Resident Programs (TSRs)."
    PRINT "3. Make sure to change back to the desired default"
    PRINT "   subdirectory before EXITing (QB does not keep"
    PRINT "   track of where you were)."
    SHELL
    done = -1
  CASE "8"
    CHAIN "UVCAL"
  CASE "9"
    CHAIN "PEAK"
  CASE "P", "p"
    CHAIN "REPLOTT"
  CASE "C", "c"
    CHAIN "CHROM"
  CASE "Q", "q"
    done = -1: Quit = -1
  CASE CHR$(27)
    done = -1: Quit = -1
  CASE ELSE
    END SELECT

```

LOOP UNTIL done

LOOP UNTIL Quit

GPMENU.BAS

Monday, August 1, 1988  
File Created: Thursday, June 9, 1988 at 2:21 pm

Page 4

CLS

END

SUB ParseDate (Day\$, Month\$, Year\$)

Month\$ = MID\$(DATE\$, 1, 2)

Day\$ = MID\$(DATE\$, 4, 2)

IF MID\$(Day\$, 1, 1) = "0" THEN Day\$ = MID\$(Day\$, 2, 1)

Year\$ = MID\$(DATE\$, 7, 4)

SELECT CASE Month\$

CASE "01"

Month\$ = "January"

CASE "02"

Month\$ = "February"

CASE "03"

Month\$ = "March"

CASE "04"

Month\$ = "April"

CASE "05"

Month\$ = "May"

CASE "06"

Month\$ = "June"

CASE "07"

Month\$ = "July"

CASE "08"

Month\$ = "August"

CASE "09"

Month\$ = "September"

CASE "10"

Month\$ = "October"

CASE "11"

Month\$ = "November"

CASE "12"

Month\$ = "December"

END SELECT

END SUB

PEAK.BAS

Monday, August 1, 1988

Page 1

File Created: Thursday, June 9, 1988 at 2:25 pm

```

DECLARE SUB VideoMode1 ()
DECLARE SUB Acquire ()
DECLARE SUB DisplayMenu ()
DECLARE SUB VideoMode ()
DECLARE SUB EraseLine (A%)
DECLARE SUB FunctionSelect (outbit%, LABEL$, Y0Val%, Flag1%, PWset%, OPT$)
DECLARE SUB TimerInit (PWset%)
DECLARE SUB A2D (A%, B%, C%)
DECLARE SUB dataq (A%, B%, C%, D%)
DECLARE SUB PlotWindow (A%, B%, C%, D%)
DECLARE SUB Pulse (A%, B%, C%, D%)

```

```

=====
'Program: PEAK.BAS  Program designed to aid in adjustment of laser mirrors,
'                  and doubling crystal position. Laser power is acquired
'                  from an ADC of CH1, and displayed in real time as a
'                  running histogram on the graphics screen. The largest
'                  power level obtained is displayed as a line for reference.
'                  The display can be scaled by pressing <+>, or <->.
'                  Also, the Following Commands have been added:
'                  <1> Display G.I. Raw Signal
'                  <2> Display L.P. Raw Signal
'                  <3> Display Corrected Signal
'                  <4> Toggle Valve on and off
'                  <5> Set new valve pulsewidth
'                  <S> Auto Scale
'                  <D> Acquire data and save to disk
'                  <V> Toggle Laser on and off:
'                      (V)alve pulses continuously
'                  <B> Toggle the Beam Blocker open
'                      and closed
'                  <SPC> Pause
'

```

```

'Written by,      Scott J. Hein
'                Department of Chemistry
'                Oregon State University
'                Corvallis, OR 97331

```

```

-----
28 February 87
Version 3.20
-----

```

```

'Written in Microsoft QuickBasic Ver 4.0. An 8087 coprocessor, and a CGA card
'are required for operation. In order to successfully compile PEAK, the
'RESEARCH quick library must have been loaded from the command line.

```

```

-----
'                  Revision History
'


| Initials | Date    | Lines | Comments                                                                                      |
|----------|---------|-------|-----------------------------------------------------------------------------------------------|
| SJH      | 7-31-87 | --    | Version 1.00 Completed                                                                        |
| SJH      | 8-11-87 | n/a   | Scaling selected via WINDOW command<br>version 1.10                                           |
| SJH      | 9-17-87 |       | Peaking of G.I. CH0 added as an<br>option, Ver. 2.00                                          |
| SJH      | 9-28-87 |       | Additional commands added, Ver 2.10                                                           |
| SJH      | 10-7-87 |       | Option 5 Added, Screen format changed                                                         |
| SJH      | 12-8-87 | --    | Command Line checking added,<br>recompiled with QB4: Ver 3.00                                 |
| SJH      | 2-28-88 |       | Data acquisition and auto-scaling<br>options added, other minor<br>modifications: Version 3.2 |


```

```

'DASH-8 Register Addresses

```

```

COMMON FromGPMENU AS INTEGER 'Added to Check Whether Peak was Called from

```

PEAK.BAS

Monday, August 1, 1988  
 File Created: Thursday, June 9, 1988 at 2:25 pm

Page 2

```

'DOS or GPMENU: if Peak was called from GPMENU
'then FromGPMENU = TRUE

COMMON SHARED Y0 AS INTEGER
COMMON SHARED Npts AS INTEGER
COMMON SHARED Datum() AS SINGLE

DEFINT A-Z

CONST BASEADD = 816, ADCREG = BASEADD + 1, StatReg = BASEADD + 2
CONST COUNTER = BASEADD + 6, TIMEREG = BASEADD + 7, Portadd = 632
CONST Version = 3.2, TRUE = -1, FALSE = 0
CONST X0Main = 64, Y0Main = 20, X1Main = 639, Y1Main = 188

```

CLS

```

'-----
'Display Program Heading
'-----

```

```

PRINT "PEAK "; Version; ": CMX-4 Laser Peaking Utility"
PRINT "(C) 1987, Scott J. Hein"
PRINT
PRINT "Press Key to Begin . . . .";
WHILE INKEY$ = "": WEND

```

```

OUT Portadd, 0 'Zero Stepper Motor Lines

```

```

VideoMode1 'Check to see if graphics can be displayed

```

```

'-----
'      Begin Main Loop
'-----

```

```

MainLoop = TRUE
DO

```

CLS

```

'Initialize Variables
  Scale! = 4095 'This is Ymax for the Window
  Largest = Y0Val 'The Largest Value
  Quit = FALSE 'If Quit is TRUE the data acquisition loop is exited
  Marker = FALSE 'If Marker is TRUE the horizontal max line is redrawn
  Redraw = TRUE 'If Redraw is TRUE, the Graphics viewport is reset
  PWset = FALSE 'Keeps Track of whether PW! Has been set
  outbit = 32
  Avg! = 0
  AvgPts = 0
  Acq = FALSE
  AutoScale = TRUE
  ValveOnly = FALSE
  block = 0

```

```

PRINT "Select Signal to Monitor:"
PRINT "  [1] Raw Gated Integrator Signal (CH0)"
PRINT "  [2] Laser Power (CH1)"
PRINT "  [3] Corrected Signal (CH0/CH1*1000)"

```

```

INPUT " ", OPT$

```

```

CALL FunctionSelect(outbit, LABEL$, Y0Val, Flag1, PWset, OPT$)

```

SCREEN 2



PEAK.BAS

Monday, August 1, 1988

Page 3

File Created: Thursday, June 9, 1988 at 2:25 pm

Y0 = Y0Main

PlotWindow X0Main, Y0, X1Main, Y1Main

DisplayMenu

DO

IF Redraw THEN

WINDOW (0, Y0Val)-(200, Scale!)

CLS 1

LOCATE (Y0 + 4) / 8, 2

PRINT USING "####"; Scale!;

XPOS = 0

Marker = TRUE

Redraw = FALSE

END IF

```

'-----
'   Data Acquisition Code
'-----

```

IF ValveOnly THEN

WAIT StatReg, 16

Pulse 5, StatReg, 16, 0

A2D 0, xl, xh

GISignal = xh \* 16 + xl / 16 'Combine

A2D 1, xl, xh 'Get LP Signal from ADC CH1

Power = xh \* 16 + xl / 16 'Combine

ELSE

dataq outbit + block, block, xl, xh 'Pulse StatReg and get CH0 Data

GISignal = xh \* 16 + xl / 16 'Combine

A2D 1 + block, xl, xh 'Get LP Signal from ADC CH1

Power = xh \* 16 + xl / 16 'Combine

END IF

```

'-----

```

'Set Y1, the magnitude (Height) of the Histogram, to the desired Signal

IF Flag1 = 1 THEN Y1 = GISignal

IF Flag1 = 2 THEN Y1 = Power

IF Flag1 = 3 THEN Y1 = GISignal / Power \* 1000

IF AutoScale THEN

Scale! = 1.1 \* Y1

Redraw = TRUE

AutoScale = FALSE

END IF

IF Acq THEN

IF Ptnum &lt;= Npts THEN

Datum(Ptnum) = Y1

Ptnum = Ptnum + 1

IF Ptnum &gt; Npts THEN

PRINT #1, xval!

FOR i = 1 TO Npts

PRINT #1, Datum(i)

NEXT i

PRINT #1,

EraseLine 4

END IF

END IF

END IF

'Loop for writing

'Npts consecutive data points

PEAK.BAS

Monday, August 1, 1988

Page 4

File Created: Thursday, June 9, 1988 at 2:25 pm

'Update Variables for display of running average

```

Avg! = Avg! + Y1
AvgPts = AvgPts + 1
LOCATE ((Y0 + 4) / 8 + 1), 68
PRINT USING "####: ####"; AvgPts, Avg! / AvgPts

```

'Draw Signal Power Histogram

```

LINE (XPOS, YOVal)-(XPOS + 2, Y1), , BF
LOCATE 25, 5: PRINT LABEL$, Y1;
XPOS = XPOS + 3
IF Y1 > Largest THEN Marker = TRUE

```

'Redraw the horizontal maximum marker line if the new Y1 &gt; the old Largest.

```

IF Marker THEN
    LINE (2, Largest)-(198, Largest), 0 'Erase the old line
    IF Y1 > Largest THEN Largest = Y1
    LINE (2, Largest)-(198, Largest) 'Draw the new one
    Marker = FALSE
    LOCATE 25, 50
    PRINT "Max = "; Largest; 'Print out Largest
    PRINT USING "(#.### V)"; (Largest - 2048) * .00244;
END IF

```

IF XPOS &gt;= 200 THEN Redraw = TRUE

Quit\$ = INKEY\$

IF Quit\$ &lt;&gt; "" THEN

```

    SELECT CASE Quit$
        CASE CHR$(27)
            Quit = TRUE
        CASE "+"
            'Manual Scale +
            Scale! = Scale! + 250
            Redraw = TRUE
        CASE "-"
            'Manual Scale -
            Scale! = Scale! - 250
            Redraw = TRUE
        CASE "1", "2", "3", "5"
            FunctionSelect outbit, LABEL$, YOVal, Flag1, PWset, Quit$
            Marker = TRUE
            Largest = YOVal
            'Redraw = TRUE
            AutoScale = TRUE
        CASE "4"
            'Turn valve off and on
            IF PWset THEN
                IF outbit = 32 THEN
                    outbit = 48
                ELSE
                    outbit = 32
                END IF
            END IF
        CASE " "
            'Pause Acquisition
            EraseLine 1
            PRINT "Acquisition Paused: Press any Key to Continue";
            WHILE INKEY$ = "": WEND
            DisplayMenu
            Avg! = 0 'Reset running average
            AvgPts = 0
        CASE "S", "s"
            'Auto Scale
            Scale! = 1.1 * Y1
            Redraw = TRUE
        CASE "D", "d"
            'Acquire Data, Save to Disk
            IF Acq = FALSE THEN

```

PEAK.BAS

Monday, August 1, 1988  
 File Created: Thursday, June 9, 1988 at 2:25 pm

Page 5

```

        Acq = TRUE
    ELSE
        Acq = FALSE
    END IF
    IF Acq THEN
        Acquire
        Redraw = TRUE
        DisplayMenu
        Ptrum = Npts + 1
    ELSE
        CLOSE #1
        CLS 0
        Y0 = Y0Main
        PlotWindow X0Main, Y0, X1Main, Y1Main
        Redraw = TRUE
        DisplayMenu
    END IF
CASE CHR$(13)
    IF Acq THEN
        EraseLine 4
        INPUT "Enter X value for these Points: ", xval!
        Ptrum = 1
        Avg! = 0
        AvgPts = 0
    END IF
CASE "v", "V"
    IF ValveOnly THEN
        ValveOnly = FALSE
    ELSE
        ValveOnly = TRUE
    END IF
CASE "B", "b"
    IF block THEN
        block = 0
    ELSE
        block = 64
    END IF

CASE ELSE
END SELECT

END IF

LOOP UNTIL Quit

CLS
SCREEN 0

EraseLine 1
PRINT "(C)ontinue, or (Q)uit and Return to the System";
INPUT ; Quit$

IF Quit$ = "Q" OR Quit$ = "q" THEN MainLoop = FALSE

LOOP WHILE MainLoop

IF FromGPMENU THEN
    CHAIN "GPMENU"
ELSE
    END
END IF

DEFSNG A-Z
*****
    SUB Acquire

```

PEAK.BAS

Monday, August 1, 1988  
 File Created: Thursday, June 9, 1988 at 2:25 pm

Page 6

```

*****
      CLS 0
      YO = 36
      PlotWindow XOMain, YO, X1Main, Y1Main
      EraseLine 1
      INPUT ; "Enter a Filename to Write Data to (No Ext.): ", DataFile$
      DataFile$ = DataFile$ + ".SIG"
      OPEN DataFile$ FOR OUTPUT AS #1
      EraseLine 2
      INPUT "How Many Shots to Acquire for each Point: ", Npts
      REDIM Datum(Npts) AS SINGLE
      EraseLine 3
      PRINT "Press <CR> To Collect Each data Set, <D> to Stop Acquisition";
      WIDTH #1, 255
END SUB 'Acquire

*****
      SUB DisplayMenu
*****

EraseLine 1
PRINT "[1] Raw G.I. [2] Raw L.P. [3] Corr. Sig. [4] Valve on/off [5] Set PW"
EraseLine 2
PRINT "[SPC] Pause [ESC] Quit [S] Auto Scale [+/-] Man Scale [D] Disk"

END SUB 'DisplayMenu

DEFINT A-Z
*****
      SUB EraseLine (LineNumber) STATIC
*****

LOCATE LineNumber, 1
PRINT SPACES(80);
LOCATE LineNumber, 9

END SUB 'EraseLine

*****
      SUB FunctionSelect (outbit, LABEL$, YOVal, Flag1, PWset, OPT$) STATIC
*****

SELECT CASE OPT$
  CASE "1"
    LABEL$ = "G.I. Signal = "
    CALL EraseLine(1)
    IF NOT PWset THEN
      INPUT ; "Fire Pulsed Valve (Y or N) ", RESP$
      IF RESP$ = "Y" OR RESP$ = "y" THEN
        CALL TimerInit(PWset)
      END IF
    END IF
    YOVal = 2049
    Flag1 = 1
    outbit = 48

  CASE "2"
    outbit = 32
    LABEL$ = "Laser Power = "
    YOVal = 2048
    Flag1 = 2

  CASE "3"
    outbit = 48
    LABEL$ = "Corr Signal = "

```

PEAK.BAS

Monday, August 1, 1988  
 File Created: Thursday, June 9, 1988 at 2:25 pm

Page 7

```

    IF NOT PWset THEN CALL TimerInit(PWset)
    YOVal = 500
    Flag1 = 3

    CASE "5"
        CALL TimerInit(PWset)

CASE ELSE
END SELECT

DisplayMenu

END SUB 'FunctionSelect

*****
SUB PlotWindow (X0, Y0, X1, Y1)
*****

'Set up Plot Outline

    WINDOW
    VIEW
    LINE (X0, Y0)-(X1, Y1), , B
    VIEW (X0 + 1, Y0 + 1)-(X1 - 1, Y1 - 1)

END SUB 'PlotWindow

*****
SUB TimerInit (PWset) STATIC
*****

    CALL EraseLine(1)
    INPUT ; "Enter Desired Pulse Width (ms) ", PW!

    'Set up Dash8 Timer

    COUNT = INT((PW! * .001 * 2386400!) + .5)
    HIBYTE = FIX(COUNT / 256)
    LOBYTE = (COUNT / 256 - HIBYTE) * 256
    OUT TIMREG, 178          'Set up Register
    OUT COUNTER, LOBYTE      'Low Byte to Counter
    OUT COUNTER, HIBYTE      'High Byte to Counter
    PWset = TRUE

END SUB 'TimerInit

*****
SUB VideoMode1 STATIC
*****

DEF SEG = 0
Video.Mode = PEEK(&H449)
DEF SEG

IF Video.Mode = 7 THEN
    PRINT
    PRINT "A Color Graphics (CGA), or Enhanced Graphics Display (EGA) is "
    PRINT "required by this program (remember to set MODE BW80).\"
    PRINT
    PRINT "Press any key to continue. . . .";
    WHILE INKEY$ = "": WEND
    IF FromGPMENU THEN
        CHAIN "GPMENU"
    ELSE
        END

```

PEAK.BAS

Monday, August 1, 1988

Page 8

File Created: Thursday, June 9, 1988 at 2:25 pm

END IF

END IF

END SUB 'VideoMode



RELOT.BAS

Monday, August 1, 1988  
 File Created: Monday, August 1, 1988 at 1:14 pm

Page 2

```

=====

DEFINT A-Z
COMMON FromGPMENU AS INTEGER

CONST Version! = 2.1
CONST TRUE = -1, FALSE = 0

DIM SHARED Lambda!(4000), Anal.Signal!(4000)
DIM SHARED Peak!(10), Inten!(10), PeakDesc$(10), PeakArea!(10, 10), tw!(10, 10)
DIM SHARED Number$(0 TO 10), PeakBkg!(10, 10)

CLS
PRINT USING "Replot Version ##.##"; Version!
PRINT "Quick Replot of Chromatographic and Spectral Data"
PRINT "(c) Scott J. Hein, 1988."
PRINT

Chk.Video.Mode

FileName$ = COMMAND$      'Get Filename from the command line
IF FileName$ = "" THEN    'Otherwise check in the environment
    FileName$ = ENVIRON$("RELOT")
END IF

DO

DO
    PRINT "What data file to plot (No Extension): ";
    Input$ FileName$
    PRINT
    IF exist(FileName$ + ".DAT") THEN
        File.OK = TRUE
    ELSE
        File.OK = FALSE
    END IF
LOOP UNTIL File.OK

PRINT "Reading Data Pairs from "; FileName$; ".DAT"
OPEN FileName$ + ".DAT" FOR INPUT AS #1
'First Read in the 9 lines of text which are present
FOR i = 1 TO 8
    LINE INPUT #1, dummy$
NEXT i
LINE INPUT #1, Title$

i = 0
DO WHILE NOT EOF(1)
    INPUT #1, Lambda!(i), Anal.Signal!(i)
    i = i + 1
LOOP
CLOSE

StepNum = i - 1 ' since i gets incremented after the last read
PRINT StepNum; " Data pairs were input from "; FileName$; ".DAT"
PRINT
  
```



RELOT.BAS

Monday, August 1, 1988  
 File Created: Monday, August 1, 1988 at 1:14 pm

Page 3

```

INPUT "(C)hromatogram or (S)pectrum: ", FileType$

IF FileType$ = "C" OR FileType$ = "c" THEN
    Spectrum = FALSE
ELSE
    Spectrum = TRUE
END IF

PRINT
PRINT "Press Any Key to Plot Data. . ."
WHILE INKEY$ = "": WEND

Scale.Data
Frame.Window
Plot.Data
Plot.Point
Find.Peaks

Erase.Line 25
PRINT "Press <P> to print this graphics screen (GRAPHICS must be installed)";
GrphPrnt$ = ""

WHILE GrphPrnt$ = "": GrphPrnt$ = INKEY$: WEND
IF GrphPrnt$ = "P" OR GrphPrnt$ = "p" THEN
    Erase.Line 25
    PrntScrn
END IF

Erase.Line 25
PRINT "Write Peak list to (P)rinter, or (A)ppend to the Output (.OUT) File: ";
HardCopy$ = ""
WHILE HardCopy$ = "": HardCopy$ = INKEY$: WEND

IF HardCopy$ = "A" OR HardCopy$ = "a" THEN
    IF exist(FileName$ + ".out") THEN
        OPEN FileName$ + ".OUT" FOR APPEND AS #1
        Print.Report
        CLOSE #1
    ELSE
        Erase.Line 25
        PRINT "The Output data file doesn't exist: Send list to Printer?";
        Resp$ = ""
        WHILE Resp$ = "": Resp$ = INKEY$: WEND
        IF Resp$ = "Y" OR Resp$ = "y" THEN HardCopy$ = "P"
    END IF
ELSEIF HardCopy$ = "P" OR HardCopy$ = "p" THEN
    OPEN "PRN" FOR OUTPUT AS #1
    Print.Report
    CLOSE #1
END IF

Erase.Line 25
PRINT "Replot another Data File <Y or N>: ";
Another$ = ""
WHILE Another$ = "": Another$ = INKEY$: WEND
IF Another$ = "Y" OR Another$ = "y" THEN
    MainLoop = TRUE
ELSE
    MainLoop = FALSE
END IF
SCREEN 0
CLS

LOOP WHILE MainLoop

```

RELOT.BAS

Monday, August 1, 1988  
 File Created: Monday, August 1, 1988 at 1:14 pm

Page 4

```

IF FromGPMENU THEN
    CHAIN "GPMENU"
ELSE
    END
END IF

Error.Handler:
    ErrNum = ERR
    RESUME NEXT

*****
    SUB Chk.Video.Mode STATIC
*****
    SHARED CGA, EGA, HGC, FromGPMENU AS INTEGER

    VidInfo MDA, CGA, EGA, HGC, ActiveMode

    PRINT "The following display adaptors are installed:"
    IF MDA THEN PRINT "    Monochrome Display Adaptor (MDA)"
    IF CGA THEN PRINT "    Color Graphics Adaptor (CGA)"
    IF EGA THEN PRINT "    Enhanced Graphics Adaptor (EGA)"
    IF HGC THEN PRINT "    Hercules Graphics Adaptor (HGC)"
    PRINT

    IF (MDA AND ActiveMode = 7) AND NOT (EGA OR CGA OR HGC) THEN

        PRINT "A CGA, EGA or Hercules graphics adaptor is required by this"
        PRINT "Program."
        PRINT
        PRINT "Press any key to return to DOS . . . .";
        WHILE INKEY$ = "": WEND
        CLS
        IF FromGPMENU THEN
            CHAIN "GPMENU"
        ELSE
            END
        END IF
    ELSEIF ActiveMode = 7 AND HGC THEN
        PRINT "Remember to Run QBHERC to Display Hercules Graphics"
    ELSEIF ActiveMode = 7 AND (EGA OR CGA) THEN
        PRINT "Although a CGA or EGA adaptor is present, the current video"
        PRINT "mode is monochrome text (mode 7):"
        PRINT "Please put the computer in MODE BW80 or C080 to display graphics"
        PRINT
        PRINT "Press any key to continue. . . ."
        WHILE INKEY$ = "": WEND
        CLS
        IF FromGPMENU THEN
            CHAIN "GPMENU"
        ELSE
            END
        END IF
    END IF
END IF
END SUB 'Video.Mode

*****
    SUB Erase.Line (Line.Num) STATIC
*****

    LOCATE Line.Num, 1
    PRINT SPACES(80);
    LOCATE Line.Num, 12

END SUB 'Erase.Line

```

REPLLOT.BAS

Monday, August 1, 1988  
 File Created: Monday, August 1, 1988 at 1:14 pm

Page 5

SUB Erase.Point STATIC

SHARED Anal.Signal!(), Currentx, YVal!, LastX, StepNum

'=====Erase X at Current Location=====

```

    YVal! = Anal.Signal!(Currentx)
    Xpos = Currentx
    PSET (Xpos, YVal!)
    DRAW "S5CONU3ND3NL4NR4C1"
    Xpos = Xpos - 4
    IF Xpos < 0 THEN Xpos = 0
    IF Xpos > StepNum THEN Xpos = StepNum
    PSET (Xpos, Anal.Signal!(Xpos))
    FOR i = 1 TO 8
      LINE -(Xpos + i, Anal.Signal!(Xpos + i))
    NEXT i

```

END SUB

FUNCTION exist (File.Name\$) STATIC

SHARED ErrNum

ErrNum = 0

ON ERROR GOTO Error.Handler

OPEN File.Name\$ FOR INPUT AS #8

IF ErrNum = 0 THEN

exist = TRUE

CLOSE #8

ELSEIF ErrNum = 53 THEN

exist = FALSE

ELSEIF ErrNum = 52 THEN

exist = FALSE

PRINT "Bad File Name or Number"

ELSEIF ErrNum = 76 THEN

exist = FALSE

PRINT "Path Not Found"

ELSE

PRINT "Bad File Mode, Error Number "; ErrNum

END IF

ON ERROR GOTO 0

END FUNCTION

\*\*\*\*\*

SUB Find.Peaks STATIC

\*\*\*\*\*

SHARED num, Peak!(), Inten!(), PeakDesc\$(), Currentx, StepNum, YVal!, XVal!

SHARED Maxy!, Anal.Signal!(), MinY!, Spectrum, Lambda!(), PeakBkg!()

num = 0

Numbers 'Set up Numbers Drawing array

Erase.Line 25

PRINT "Use Arrow Keys to Position + at Maximum of Peak: Hit &lt;CR&gt; to Mark";

Menu = TRUE

DO

Max\$ = ""

RELOT.BAS

Monday, August 1, 1988  
 File Created: Monday, August 1, 1988 at 1:14 pm

Page 6

```

WHILE Max$ = "": Max$ = INKEY$: WEND
  IF MID$(Max$, 1, 1) = CHR$(0) THEN
    Max$ = MID$(Max$, 2, 1)
    Max = 1000 + ASC(Max$)
  ELSE
    Max = ASC(Max$)
  END IF

SELECT CASE Max
CASE 27
  Menu = FALSE
CASE 13
  CALL Plot.Point
  AreaNum = 1
  num = num + 1
  Peak!(num) = XVal!
  Inten!(num) = YVal!
  PSET (Currentx + .01 * StepNum, YVal! + .01 * Maxy!), 0
  DRAW "S8" + "C1" + Number$(num)
  PSET (Currentx, YVal!)
  Erase.Line 25
  PRINT "Short (One Line) Description: ";
  LINE INPUT ; ""; PeakDesc$(num)
  IF num = 10 THEN Menu = FALSE
  IF Menu THEN
    Erase.Line 25
    PRINT "Calc Area via <L> & <R>, Next Peak with <CR>, or <ESC>
    > to Quit";
  END IF
CASE 1077 'Right Arrow
  CALL Erase.Point
  Currentx = Currentx + 1
  IF Currentx > StepNum THEN Currentx = 0
  CALL Plot.Point
CASE 1075 'Left Arrow
  CALL Erase.Point
  Currentx = Currentx - 1
  IF Currentx < 0 THEN Currentx = StepNum
  CALL Plot.Point
CASE 1115 'Ctrl-LftArrow
  CALL Erase.Point
  Currentx = Currentx - 10
  IF Currentx < 0 THEN Currentx = StepNum + Currentx
  CALL Plot.Point
CASE 1116 'Ctrl-RtArrow
  CALL Erase.Point
  Currentx = Currentx + 10
  IF Currentx > StepNum THEN
    Currentx = Currentx - StepNum
  END IF
  CALL Plot.Point
CASE 76, 108 'Left Side of Integration range
  LL = Currentx
  LB! = Anal.Signal!(LL) 'Left Background
  LINE (LL, LB!)-(LL, MinY!)
CASE 82, 114 'Right side of integration
  Area! = 0
  RL = Currentx
  RB! = Anal.Signal!(RL)
  slope! = (RB! - LB!) / (RL - LL)
  tw!(num, AreaNum) = Lambda!(RL) - Lambda!(LL)
  PeakBkg!(num, AreaNum) = (RB! + LB!) / 2

```

REPLOT.BAS

Monday, August 1, 1988

Page 7

File Created: Monday, August 1, 1988 at 1:14 pm

```

LINE (RL, RBI)-(RL, MinY!)
LINE (LL, LBI)-(RL, RBI)

FOR i = LL TO RL
    WidthLeft! = (Lambda!(i) - Lambda!(i - 1)) / 2
    WidthRight! = (Lambda!(i + 1) - Lambda!(i)) / 2
    'Minutes --> Seconds
    PointWidth! = (WidthLeft! + WidthRight!) * 60
    bkg! = LBI + (i - LL) * slope!
    Area! = Area! + (Anal.Signal!(i) - bkg!) * PointWidth!
    LINE (i, bkg!)-(i, Anal.Signal!(i))
NEXT
LOCATE 4, 60
PRINT USING "Area ##:## = #####"; num; AreaNum; Area!;
PeakArea!(num, AreaNum) = Area!
AreaNum = AreaNum + 1

CASE 67, 99 'C: Clear the screen and redraw
CLS
Plot.Data
Plot.Point

CASE ELSE
END SELECT

LOOP WHILE Menu

END SUB

*****
      SUB Frame.Window STATIC
*****

SHARED MaxY!, MinY!, Range!, FileName$, Lambda!(), StepNum, Y1, Y2, X2, Title$
SHARED EGA, CGA, HGC, Spectrum

' Frame for Replot of data set

IF EGA THEN
    SCREEN 9
    Y1 = 35
    Y2 = 300
    X2 = 639
ELSEIF CGA THEN
    SCREEN 2
    Y1 = 20
    Y2 = 172
    X2 = 639
ELSEIF HGC THEN
    SCREEN 3
    Y1 = 35
    Y2 = 300
    X2 = 719
END IF

Title1$ = "Replot of Data in: " + FileName$ + ".DAT"
LenTitle1 = LEN(Title1$)
Title2$ = Title$
LenTitle2 = LEN(Title2$)

Range! = MaxY! - MinY!
LINE (72, Y1)-(X2, Y2), , B
LOCATE 1, (10 + (70 - LenTitle1) / 2)
PRINT Title1$;
LOCATE 2, (10 + (70 - LenTitle2) / 2)

```

RELOT.BAS

Monday, August 1, 1988

Page 8

File Created: Monday, August 1, 1988 at 1:14 pm

```

PRINT Title2$;

FOR y = Y1 TO Y2 STEP (Y2 - Y1) / 4
  LINE (68, y)-(72, y)
NEXT y
FOR i = 0 TO 4
  LOCATE (22 - INT(i * 19 / 4 + .5)), 1
  PRINT USING "####.###"; Range! * (.25 * i) + MinY!
NEXT i

LOCATE 23, 8
PRINT USING "####.###"; Lambda!(0);
LOCATE 23, 73
PRINT USING "####.###"; Lambda!(StepNum);
LOCATE 23, 34
IF Spectrum THEN
  PRINT "Wavelength (Angstroms)";
ELSE
  PRINT "Retention Time (min.)"
END IF
END SUB

*****
SUB Numbers STATIC
*****

'These are the draw commands to create numbers for labeling peaks
'Number$(1) contains the commands to draw a 1, etc.

Number$(0) = "E4BDHL2GD2FR2EU2BF2BD"
Number$(1) = "BRR2LU4GBF3BR2"
Number$(2) = "BU3ER2FGLG2R4BR2"
Number$(3) = "BU3ER2FGLBL8GFR2EHBF2BR"
Number$(4) = "BR3U4G3R4BRBF"
Number$(5) = "R3EHL3U2R3BF3BD"
Number$(6) = "BU2R3FGL2HU2ER2BF3BD"
Number$(7) = "BU4R4G2D2BR4"
Number$(8) = "BRHEHER2FGL2R2FGL2BR5"
Number$(9) = "BRR2EU2HL2GFR3BF2"
Number$(10) = "BRR2LU4GBF3BR2BR1E4BDHL2GD2FR2EU2BF2BD"

END SUB ' Numbers

*****
SUB Plot.Data
*****
SHARED StepNum, MinY!, MaxX!, MaxY!, Anal.Signal!(), Lambda!(), Y1, Y2, X2

'=====Plot Current Data Set=====

VIEW (73, Y1 + 1)-(X2 - 1, Y2 - 1)
WINDOW (0, MinY!)-(MaxX!, MaxY!)
PSET (0, MinY!)
FOR i = 0 TO StepNum
  LINE -(i, Anal.Signal!(i))
NEXT
END SUB

SUB Plot.Point STATIC

SHARED Anal.Signal!(), Lambda!(), Currentx, XVal!, YVal!, Spectrum

```

RELOT.BAS

Monday, August 1, 1988  
File Created: Monday, August 1, 1988 at 1:14 pm

Page 9

```
'=====Plot X at Current Graph Location=====
YVal! = Anal.Signal!(Currentx)
Xpos = Currentx
PSET (Xpos, YVal!)
DRAW "S5NU3ND3NL4NR4"
XVal! = Lambda!(Currentx)

IF Spectrum THEN
    LOCATE 24, 17: PRINT USING "Lambda= ####.### "; XVal!;
ELSE
    LOCATE 24, 17: PRINT USING "Time = ####.### "; XVal!;
END IF

LOCATE 24, 57: PRINT USING "Signal= ####.### "; YVal!;

END SUB

*****
SUB Print.Report
*****

SHARED num, Spectrum, FileName$

PRINT #1, "Data Compiled From: "; FileName$; ".DAT"

IF Spectrum THEN

    PRINT #1, ""
    PRINT #1, "Peak #", "Wavelength", "Intensity", "Description"
    PRINT #1, "=====", "=====", "=====", "====="
    FOR i = 1 TO num
        PRINT #1, i, Peak!(i), Inten!(i), PeakDesc$(i)
    NEXT i
ELSE
    PRINT #1, ""
    PRINT #1, "Peak #   Ret. Time   Peak Hgt   Peak Area   Bkg   tw   Description"
    PRINT #1, "====   =====   =====   =====   =====   =====   ====="
    FOR i = 1 TO num
        PRINT #1, USING " ##      ##.##      ###.###      #####.##      ###.##      ##.## "; i; Peak!(
i); Inten!(i), PeakArea!(i, 1), PeakBkg!(i, 1), tw!(i, 1);
        PRINT #1, PeakDesc$(i)
        FOR j = 2 TO UBOUND(PeakArea!, num)
            IF PeakArea!(i, j) <> 0 THEN
                PRINT #1, USING " #####.##      ###.##      ##.###"; PeakArea!(
i, j), PeakBkg!(i, j), tw!(i, j)
            END IF
        NEXT j
    NEXT i
END IF

END SUB

*****
SUB Scale.Data STATIC
*****

SHARED Largest!, Smallest!, StepNum, Anal.Signal!(), MaxX!, MaxY!, MinY!
SHARED XLargest!, Currentx

'=====Determine Largest data Point & Scale Factor=====

PRINT "Sorting Data and Determining New Scale Factor. . .";

Largest! = Anal.Signal!(0): XLargest = 0
Smallest! = Anal.Signal!(0)
```

REPLOT.BAS

Monday, August 1, 1988

Page 10

File Created: Monday, August 1, 1988 at 1:14 pm

```
FOR i = 0 TO StepNum
  IF Largest! < Anal.Signal!(i) THEN
    Largest! = Anal.Signal!(i)
    XLargest = i
  END IF
  IF Smallest! > Anal.Signal!(i) THEN
    Smallest! = Anal.Signal!(i)
  END IF
NEXT i

MaxX! = StepNum
MaxY! = Largest! + .05 * Largest!
MinY! = Smallest!

Currentx = XLargest

END SUB 'ScaleData
```